Group Report

71G-1
Part IV

Distortions and Stresses of Paraboloidal Surface Structures

J. W. Mar
F. Y. M. Wan

29 April 1964

Prepared under Electronic Systems Division Contract AF 19(628)-500 by

Lincoln Laboratory
MASSACHUSETTS INSTITUTE OF TECHNOLOGY
Lexington, Massachusetts

The work reported in this document was performed at Lincoln Laboratory, a center for research operated by Massachusetts Institute of Technology, with the support of the U.S. Air Force under Contract AF 19(628)-500.

MASSACHUSETTS INSTITUTE OF TECHNOLOGY

LINCOLN LABORATORY

DISTORTIONS AND STRESSES OF PARABOLOIDAL SURFACE STRUCTURES

J. W. MAR

F. Y. M. WAN

Group 71

GROUP REPORT 71G-1, PART IV

29 APRIL 1964

LEXINGTON MASSACHUSETTS

ABSTRACT

The present report is the fourth part of a series bearing the general title of "Distortions and Stresses of Paraboloidal Surface Structures." Asymptotic integration methods are used to obtain solutions for shells which are deeper than those treated in Part III. A large number of specifie configurations has been analyzed and the numerieal results are presented in the form of dimensionless plots. The discussion is focused on the deformation behavior under gravity loads as it is affeeted by the span of the shell, the direetion of the gravity vector, and the boundary eonditions. There are also contour plots of deflections relative to the face-up positicn which depiet the change in the shapes of the paraboloidal surface as the directicn of the gravity vector is changed.

Accepted for the Air Force
Franklin C. Hudson, Deputy Chief
Air Force Lincoln Laboratory Office

TABLE OF CONTENTS

TABLE OF CONTENTS (Cont'd)

NOMENCLATURE, SYMBOLS, AND ASSORTED MARKS

y^1, y^2, y^3 - rectangular Cartesian coordinates

x^1, x^2, x^3 - general curvilinear coordinates

ξ^1, ξ^2 - general coordinates on middle surface of undeformed shell

ζ - coordinate normal to middle surface of undeformed shell

γ, θ - polar parameters on middle surface of undeformed shell

x, y - cartesian parameters on middle surface of undeformed shell

r - radius of revolution of middle surface of undeformed paraboloid

θ - angular coordinate of middle surface of undeformed paraboloid

$\gamma = \frac{r}{2f}$ - slope of meridian tangent to middle surface of paraboloid

ϕ - angle which meridianal tangent makes with tangent plane to apex of paraboloid (see figure 2.1.3)

f - focal length of middle surface of paraboloid

$\bar{r}_o$ - radius vector to point on middle surface of undeformed shell

$\bar{r}$ - radius vector to point in undeformed shell

$\bar{R}_o$ - radius vector to point on middle surface of deformed shell

$\bar{R}$ - radius vector to point in deformed shell

$\bar{a}_1, \bar{a}_2$ - covariant base vectors of middle surface of undeformed shell

$\bar{a}^1, \bar{a}^2$ - contravariant base vectors of middle surface of undeformed shell

$\bar{n}$ - unit normal to middle surface of undeformed shell

$\bar{g}_1, \bar{g}_2, \bar{g}_3$ - covariant base vectors of undeformed body

$\bar{g}^1, \bar{g}^2, \bar{g}^3$ - contravariant base vectors of undeformed body

g_{mn} - covariant metric tensor of undeformed body

g^{mn} - contravariant metric tensor of undeformed body

a_{mn} - covariant metric tensor of middle surface of undeformed shell

a^{mn} - contravariant metric tensor of middle surface of undeformed shell

$\bar{G}_1, \bar{G}_2, \bar{G}_3$ - covariant base vectors of deformed body

$\bar{G}^1, \bar{G}^2, \bar{G}^3$ - contravariant base vectors of deformed body

$\bar{A}_1, \bar{A}_2$ - covariant base vectors of deformed middle surface of shell

$\bar{A}^1, \bar{A}^2$ - contravariant base vectors of deformed middle surface of shell

$\bar{N}$ - unit normal vector to deformed middle surface

R_1, R_2 - principal radii of curvature of middle surface of undeformed shell

b_{11}, b_{12}, b_{22} - second fundamental quadratic covariant tensor of undeformed middle surface of shell

$b_1^1, b_2^2, b_2^1, b_1^2$ - second fundamental quadratic mixed tensor of undeformed middle surface of shell

$\gamma_{mn}, \gamma_n^m, \gamma^{mn}$ - strain tensors

$\sigma^{mn}, \sigma_{mn}, \sigma_n^m$ - stress tensors

$\ell^{\alpha\beta}$ - stress resultant tensor of shell

$m^{\alpha\beta}$ - moment resultant tensor of shell

q^{α} - transverse shear resultant tensor of shell

$N\alpha\beta$ - physical components of force resultants tensors referred to ξ^1, ξ^2 coordinate system (units of force per unit length)

$M_{\alpha\beta}$ - physical components of moment resultants tensors ξ^1, ξ^2 coordinate system (units of force-length per unit length)

Q_{α} - physical components of transverse shear tensor ξ^1, ξ^2 coordinate system (units of force per unit length)

$\bar{i}_1, \bar{i}_2, \bar{i}_3$ - unit base vectors associated with y^1, y^2, y^3

$\varepsilon_{\alpha\beta}$ - covariant permutation surface tensor

$\varepsilon^{\alpha\beta}$ - contravariant permutation surface tensor

$N_r, N_\theta, N_{r\theta}$ - force-resultants referred to r, θ coordinate system (units of force per unit length)

$M_r, M_\theta, M_{r\theta}$ - moment-resultants referred to r, θ coordinate system (units of force-length per unit length)

Q_r, Q_θ - transverse shear resultant referred to r, θ coordinate system (units of force per unit length)

f - focal length of parabola

f^2, f^3, f^4, f^5 - powers of f, the focal length

u^σ, u_σ - displacement tensors of middle surface

w^σ, w_σ - rotation tensors of middle surface

w - displacement of middle surface along ζ (units of length)

u_r^o - displacement of middle surface along tangent to meridian (units of length)

u_θ^o - displacement of middle surface along tangent to latitude (units of length)

$\gamma_{\alpha\beta}^o$ - strain tensor of middle surface

$k_{\alpha\beta}$ - strain-curvature tensor of middle surface

ϵ_r - extensional strain along meridian (dimensionless)

ϵ_θ - extensional strain along latitude (dimensionless)

$\epsilon_{r\theta}$ - shear strain (dimensionless)

ϵ_r° - extensional strain of middle surface along meridian (dimensionless)

ϵ_θ° - extensional strain of middle surface along latitude (dimensionless)

$\epsilon_{r\theta}^\circ$ - shear strain of middle surface (dimensionless)

K_r - extensional strain-curvature of middle surface along meridian (units of $(\text{length})^{-1}$)

K_θ - extensional strain-curvature of middle surface along latitude (units $(\text{length})^{-1}$)

$K_{r\theta}$ - shear strain-curvature of middle surface (units of $(\text{length})^{-1}$)

h - thickness of undeformed shell (units of length)

E - Youngs modulus (units of force per unit area)

$\mu = \frac{E}{2(1+\nu)}$ - shear modulus (units of force per unit area)

ν - Poissons ratio (dimensionless)

ρ_o - weight-density (units of force per unit volume)

ν^2 - powers of ν , Poissons ratio

ζ^* - coordinate normal to middle surface of deformed shell

h^* - thickness of deformed shell (units of length)

$\bar{\ell}^1, \bar{\ell}^2$ - force-resultant vectors (units of force per unit length)

$\bar{m}^1, \bar{m}^2$ - moment-resultant vectors (units of force-length per unit length)

F^α, F^3 - tensor components of body force vector

$\bar{P}$ - body force vector (units of force per unit area)

p_r, p_θ, p_n - physical components of body force vector (units of force per unit area)

N_x, N_y, N_{xy} - force-resultants referred to cartesian parameters (units of force per unit length)

M_x, M_y, M_{xy} - moment resultants referred to cartesian parameters (units of force-length per unit length)

Q_x, Q_y - transverse shear resultant referred to cartesian parameters (units of force per unit length)

γ_1, γ_2 - bounding latitudes of paraboloidal shell

$(\bar{\ })$ - signifies quantity under bar is a vector

$|_d$ or $|_m$ - vertical slash before subscript signifies covariant differentiation with respect to metric of deformed body

$,_\alpha$ or $,_m$ - comma before subscript signifies covariant differentiation with respect to metric of undeformed body

$\left\{ {m \atop n\ p} \right\}_o$ - Christoffel symbols of second kind of undeformed body

$\left\{ {\alpha \atop \beta\ \gamma} \right\}_o$ - Christoffel symbols of second kind of the middle surface of undeformed body

$\left\{ {m \atop n\ p} \right\}$ - Christoffel symbols of second kind of deformed body

$\left\{ {\alpha \atop \beta\ \gamma} \right\}$ - Christoffel symbols of second kind of the middle surface of deformed body

$\cdot$ - dot between two vectors signifies scalar product

$\times$ - cross between two vectors signifies vector product

$B_{\alpha\beta}, B_\beta^\sigma$ - second fundamental tensors of deformed middle surface

$b_{\alpha\beta}, b_\beta^\sigma$ - second fundamental tensors of undeformed middle surface

$u_{rn}(\gamma)$, $u_{\theta n}(\gamma)$, $w_n(\gamma)$ - n^{th} Fournier components of displacement of u_r°, u_θ° and w, respectively

n - Fourier integer in sin n θ , cos n θ

L_{ij} - Differential operators associated with momentless behavior (i,j = 1,2,3)

L_{ij}^* - Differential operators associated with edge zone behavior (i,j = 1, 2, 3)

$p_{in}(\gamma)$ - n^{th} Fourier expansion for surface loads p_i (γ, θ)

a_{ij}, b_{ij}, c_{ij}, $a_{ij}^\circ, b_{ij}^\circ, c_{ij}^\circ$ - coefficients of differential operators

$k^4 = 12 \left(\frac{2f}{h} \right)^2 \approx \frac{\text{extensional stiffness}}{\text{bending stiffness}} \times (R)^2$; large parameter

$\beta_i(\gamma)$ - Auxiliary functions

λ_i - Roots of characteristic equation; i = 1, 2, --8

ω_i - Fourth roots of -1; i = 1, 2, 3, 4

$m = \sqrt[4]{1 - \nu^2}$ - inconvenient constant

$\tau = \frac{km}{\sqrt{2}} \int^{\gamma} \sqrt{1 + \gamma^2}\, d\gamma$ - exponent of e

c_i - Constants (real) of integration i = 1, 2, 3,-- 8

$g_i(\gamma)$ - Auxiliary functions (i = 1, ..,10)

$f_i(\gamma)$ - Auxiliary functions (i = 1, 2, 3)

Superscript e signifies edge zone portion of solution.

Subscript 0 signifies axi-symmetric solution (n = 0).

Subscript 1 signifies anti-symmetric solution (n = 1).

8.1 INTRODUCTION

Since an exact solution to the set of shell equations developed in Chapters I through V [32] does not seem possible, recourse must be taken to solutions which will adequately describe the behavior of a shell under suitably restricted conditions. In Chapter VI [33], the shell was assumed to carry the applied loads by a momentless or membrane type of action. In Chapter VII [34], the shallow shell theory, while including the bending actions, restricts application to shells whose middle surface slope is small. Unlike these earlier efforts, the present chapter will attack the entire set of shell equations. Thus, although the solution to be obtained is approximate, the restrictions inherent in the membrane and shallow shell analyses have been removed.

Let us write the equations of static equilibrium of forces (4.4.1.14), (4.4.1.15) and (4.4.1.16) in terms of the middle surface displacements. For a complete shell of revolution, all quantities involved must be periodic in the circumferential direction, and Fourier series expansions of these quantities in θ are in order.

$$u_r^o = \sum_{n=0}^{\infty} u_{rn}(\gamma)\begin{Bmatrix}\sin n\theta\\ \cos n\theta\end{Bmatrix} \qquad 8.1.1$$

$$u_\theta^o = \sum_{n=0}^{\infty} u_{\theta n}(\gamma)\begin{Bmatrix}\cos n\theta\\ \sin n\theta\end{Bmatrix} \qquad 8.1.2$$

$$w = \sum_{n=0}^{\infty} w_n(\gamma)\begin{Bmatrix}\sin n\theta\\ \cos n\theta\end{Bmatrix} \qquad 8.1.3$$

The set of three partial differential equations of force equilibrium can then be reduced to a system of 3n ordinary differential equations. For the n^{th} harmonic of the expansions, the equilibrium equations

read as follows.

$$\left\{\left[L_{11}(u_{rn})+L_{12}(u_{\theta n})+L_{13}(w_n)\right] + k^{-4}\left[L^*_{11}(u_{rn})+L^*_{12}(u_{\theta n})+L^*_{13}(w_n)\right]\right\} = \frac{(1-\nu^2)}{Eh}P_{1n} \qquad 8.1.4$$

$$\left\{\left[L_{21}(u_{rn})+L_{22}(u_{\theta n})+L_{23}(w_n)\right] + k^{-4}\left[L^*_{21}(u_{rn})+L^*_{22}(u_{\theta n})+L^*_{23}(w_n)\right]\right\} = \frac{(1-\nu^2)}{Eh}P_{2n} \qquad 8.1.5$$

$$\left\{\left[L_{31}(u_{rn})+L_{32}(u_{\theta n})+L_{33}(w_n)\right] + k^{-4}\left[L^*_{31}(u_{rn})+L^*_{32}(u_{\theta n})+L^*_{33}(w_n)\right]\right\} = \frac{(1-\nu^2)}{Eh}P_{3n} \qquad 3.1.6$$

where

$$k^4 = 12\left(\frac{2f}{h}\right)^2 \qquad 8.1.7$$

$$P_{in}(\gamma) = -4f^2\gamma\sqrt{1+\gamma^2}\;\; p_{in}(\gamma) \qquad 8.1.8$$

$p_{in}(\gamma)$ being the n^{th} coefficient of the Fourier expansion for the surface loads $p_i(\gamma,\theta)$, i.e.,

$$p_1(\gamma,\theta) = \sum_{n=0}^{\infty} p_{1n}(\gamma)\begin{Bmatrix}\sin n\theta\\ \cos n\theta\end{Bmatrix}$$
$$p_2(\gamma,\theta) = \sum_{n=0}^{\infty} p_{2n}(\gamma)\begin{Bmatrix}\cos n\theta\\ \sin n\theta\end{Bmatrix}$$
$$p_3(\gamma,\theta) = \sum_{n=0}^{\infty} p_{3n}(\gamma)\begin{Bmatrix}\sin n\theta\\ \cos n\theta\end{Bmatrix} \qquad 8.1.9$$

The linear operators L_{ij} and L^*_{ij} are

$$L_{11} = c^\circ_{12}\frac{d^2}{d\gamma^2} + c^\circ_{11}\frac{d}{d\gamma} + c^\circ_{10}$$
$$L_{12} = b^\circ_{11}\frac{d}{d\gamma} + b^\circ_{10}$$
$$L_{13} = a^\circ_{11}\frac{d}{d\gamma} + a^\circ_{10}$$
$$L^*_{11} = c_{12}\frac{d^2}{d\gamma^2} + c_{11}\frac{d}{d\gamma} + c_{10}$$
$$L^*_{12} = b_{11}\frac{d}{d\gamma} + b_{10}$$
$$L^*_{13} = a_{13}\frac{d^3}{d\gamma^3} + a_{12}\frac{d^2}{d\gamma^2} + a_{11}\frac{d}{d\gamma} + a_{10}$$

$$L_{21} = c_{21}^{\circ}\frac{d}{d\gamma} + c_{20}^{\circ}$$

$$L_{22} = b_{22}^{\circ}\frac{d^2}{d\gamma^2} + b_{21}^{\circ}\frac{d}{d\gamma} + b_{20}^{\circ}$$

$$L_{23} = a_{20}^{\circ}$$

$$L_{21}^{*} = c_{21}\frac{d}{d\gamma} + c_{20}$$

$$L_{22}^{*} = b_{22}\frac{d^2}{d\gamma^2} + b_{21}\frac{d}{d\gamma} + b_{20}$$

$$L_{23}^{*} = a_{22}\frac{d^2}{d\gamma^2} + a_{21}\frac{d}{d\gamma} + a_{20}$$

$$L_{31} = c_{31}^{\circ}\frac{d}{d\gamma} + c_{30}^{\circ}$$

$$L_{32} = b_{30}^{\circ}$$

$$L_{33} = a_{30}^{\circ}$$

$$L_{31}^{*} = c_{33}\frac{d^3}{d\gamma^3} + c_{32}\frac{d^2}{d\gamma^2} + c_{31}\frac{d}{d\gamma} + c_{30}$$

$$L_{32}^{*} = b_{32}\frac{d^2}{d\gamma^2} + b_{31}\frac{d}{d\gamma} + b_{30}$$

and

$$L_{33}^{*} = a_{34}\frac{d^4}{d\gamma^4} + a_{33}\frac{d^3}{d\gamma^3} + a_{32}\frac{d^2}{d\gamma^2} + a_{31}\frac{d}{d\gamma} + a_{30}$$

The coefficients a_{ij}, b_{ij}, c_{ij}, a_{ij}°, b_{ij}°, c_{ij}° (i, j = 1, 2 and 3) of the above linear differential operators are all analytic functions of γ ($0<\gamma<\infty$) and contain in them the parameter n from the Fourier expansions. In what follows, attention will be restricted to $n \ll k$. Only those coefficients needed in the subsequent development are given here. The remaining ones can be found in the appendix.

$$a_{10}^{\circ} = \frac{\gamma^2(4+\gamma^2)}{(1+\gamma^2)^{5/2}}$$

$$a_{11}^{\circ} = \frac{-\gamma(1+\nu+\nu\gamma^2)}{(1+\gamma^2)^{3/2}}$$

$$a_{20}^{\circ} = \frac{\mp n(1+\nu+\gamma^2)}{(1+\gamma^2)}$$

$$a_{30}^{\circ} = -\frac{\gamma(2(1+\nu)(1+\gamma^2)+\gamma^4)}{(1+\gamma^2)^{5/2}}$$

$$a_{33} = \frac{2(1-2\gamma^2)}{(1+\gamma^2)^{5/2}}$$

$$a_{34} = \frac{-\gamma}{(1+\gamma^2)^{3/2}}$$

$$b_{21}^{\circ} = \frac{1+\nu}{2(1+\gamma^2)^{3/2}}$$

$$b_{22}^{\circ} = \frac{\gamma(1-\nu)}{2\sqrt{1+\gamma^2}}$$

$$c_{11}^{\circ} = \frac{1}{(1+\gamma^2)^{3/2}}$$

$$c_{12}^{\circ} = \frac{\gamma}{\sqrt{1+\gamma^2}}$$

$$c_{20}^{\circ} = \frac{\pm n(3-\nu)}{2\gamma}$$

$$c_{21}^{\circ} = \frac{\pm n(1+\nu)}{2}$$

$$c_{30}^{\circ} = \frac{(1+\nu+\gamma^2)}{(1+\gamma^2)^{3/2}}$$

$$c_{31}^{\circ} = \frac{\gamma(1+\nu+\nu\gamma^2)}{(1+\gamma^2)^{3/2}}$$

It is seen that the left hand sides of equations (8.1.4), (8.1.5) and (8.1.6) are divided into two groups of terms. One group which is multiplied by k^{-4} is associated with the bending behavior while the other is associated with momentless or membrane behavior. The fourth power of the parameter k is in reality proportional to the ratio of extensional stiffness to bending stiffness multiplied by a factor porportional to the square of a representative magnitude, R, of the radii of curvature, i.e.,

$$k^4 \propto \frac{\text{extensional stiffness}}{\text{bending stiffness}} \times (R)^2$$

In a homogeneous shell of thickness h, the ratio of the stiffnesses is inversely proportional to the square of the thickness while the radii of curvature for a paraboloid is proportional to 2f. For a thin shell the parameter k is therefore larger than unity since by definition (see Section 4.2) the ratio of 2f/h is larger than 10. In general, large antennae have ratios of 2f/h larger than 200 which leads to a value of k greater than 25.

The magnitude of k (for sufficiently thin shells) and the form of the differential equations makes appropriate an asymptotic analysis of the solution to the differential equations. The asymptotic behavior of a linear system such as given by equations (8.1.1), (8.1.2), and (8.1.3) has been investigated by H. L. Turrittin [35] and the results of his study form the basis of the present investigation.

8.2 THE ASYMPTOTIC BEHAVIOR OF A LINEAR SYSTEM CONTAINING A LARGE PARAMETER

Consider a real function $g(k)$ of a real variable k defined over some interval including infinity. A formal power series in k^{-1} (denoted by $P_g(k)$)

$$P_g(k) = \sum_{i=0}^{\infty} p_i k^{-i} \qquad 8.2.1$$

with partial sum $S_m(k)$

$$S_m(k) = \sum_{i=0}^{m} p_i k^{-i} \qquad (m = 0, 1, 2, \cdots) \qquad 8.2.2$$

is said to be an asymptotic expansion for g (in the given interval of k) as $|k| \to \infty$ (denoted by $g \sim P_g$) if for every $m = 0, 1, 2, \cdots$ there exists some constant K_m such that

$$|g(k) - S_m(k)| \leq \frac{K_m}{|k|^{m+1}} \qquad 8.2.3$$

as $|k| \to \infty$ uniformly. Note that if the series P_g converges to g, then it is the usual Laurent series representation of g; but in general $P_g(k)$ is not necessarily a convergent series.

If

$$g(k) = \frac{g_1(k)}{g_2(k)} \qquad 8.2.4$$

and if

$$g(k) \sim P_g(k) = \sum_{i=0}^{\infty} p_i k^{-i} \qquad 8.2.5$$

then we write

$$g_1(k) \sim g_2(k) P_g(k) = g_2(k) \sum_{i=0}^{\infty} p_i k^{-i} \qquad 8.2.6$$

whether or not g_1 and g_2 have their own asymptotic expansions. In the event that g_2 (and therefore g_1) does not have an asymptotic expansion, (8.2.6) is to be interpreted as

$$g(k) = \frac{g_1(k)}{g_2(k)} \sim P_g(k)$$

It is not difficult to see from the preceding definition that if g has an asymptotic expansion, then the expansion is unique. For if g has two different asymptotic expansions $P_1(k)$ and $P_2(k)$,

$$P_1(k) = \sum_{i=0}^{\infty} p_{1i} k^{-i} \qquad 8.2.7$$

$$P_2(k) = \sum_{i=0}^{\infty} p_{2i} k^{-i} \qquad 8.2.8$$

then
$$|k|^m |S_{1m}(k) - S_{2m}(k)| = |k|^m \left| (p_{10} - p_{20}) + \frac{1}{k}(p_{11} - p_{21}) + \cdots + \frac{1}{k^m}(p_{1m} - p_{2m}) \right| \qquad 8.2.9$$

where S_{1m} and S_{2m} are the partial sums of P_1 and P_2, respectively. But by (8.2.3), we have

$$|k|^m |S_{1m}(k) - S_{2m}(k)| \leq |k|^m \left[|S_{1m} - g| + |S_{2m} - g| \right] \leq \frac{K_m}{|k|} \qquad 8.2.10$$

Therewith

$$|k|^m \left| (p_{10} - p_{20}) + (p_{11} - p_{21}) k^{-1} + \cdots + (p_{1m} - p_{2m}) k^{-m} \right| \leq \frac{K_m}{|k|} \qquad 8.2.11$$

Taking m = 0, 1, 2 ---- (in that order) and letting k go to infinity for each m, we get $p_{1m} = p_{2m}$ for all m.

On the other hand, two functions g_1 and g_2 which are not identical in a given interval of k may have the same asymptotic expansion. For instance, if equation (8.2.5) holds, then $g(k) + e^{-k} \sim P_g(k)$ since

$$\lim_{|k| \to \infty} |k|^m e^{-|k|} = 0 \qquad 8.2.13$$

for m = 0, 1, 2, 3, ----.

It can also be shown that (cf. [36], [37])

(1) If $g_i(k)$, $i = 1, 2, \cdots, m$ are functions of k which all have asymptotic expansions, $g_i \sim P_i$, in the same interval of k, and $f_p(x_1, \cdots, x_m)$ is a polynomial in m variables, then F(k), defined by

$$F(k) = f_p(g_1(k), \cdots, g_m(k)) \qquad 8.2.14$$

i.e., replacing x_i in f_p by $g_i(k)$ has an asymptotic expansion in the given interval and is calculated as if all the expansions were convergent series.

(2) If g (k) is continuous for $k \geq k_o$ and possesses an asymptotic expansion,

$$g(k) \sim \sum_{i=0}^{\infty} p_i k^{-i} \qquad 8.2.15$$

then

$$G(k) = \int_k^{\infty} \left[g(\tau) - p_0 - p_1 \tau^{-1} \right] d\tau \sim \sum_{i=1}^{\infty} \frac{p_{i+1}}{i} k^{-i} \qquad 8.2.16$$

(3) If the derivative of g exists and is continuous and if g' has an asymptotic expansion, equation 8.2.15, then

$$g' = \frac{dg}{dk} \sim -\sum_{i=2}^{\infty} (i-1) p_{i-1} k^{-i} \qquad 8.2.17$$

In the subsequent analysis, these results will be used frequently and tacitly.

Next, let us consider the second order differential equation

$$\frac{d^2x}{dt^2} + \left\{ k^2 \phi^2(t) + q(t) \right\} x = 0 \qquad 8.2.18$$

where $\phi^2(t)$ is either positive or negative for all t, $a \leq t \leq b$, and

k^2 is a large parameter such that

$$|q(t)| \leq |k^2 \phi^2(t)| \qquad 8.2.19$$

for all t in the given interval. Intuitively, the first two terms in (8.2.18) constitute the most significant portion of the differential equation as the third term is negligible by definition. The above observation naturally suggests a solution of the form

$$x(t) \sim e^{\pm i k f(t)} \sum_{j=0}^{\infty} Y_j(t) k^{-j} \qquad 8.2.20$$

where

$$f(t) = \int^t \phi(t)\, dt \qquad 8.2.21$$

and $Y_j(t)$ can be computed from a recurrence relation derivable from (8.2.18) and (8.2.20). Since the series on the right hand side of (8.2.20) is not necessarily a convergent series in k for $a \leq t \leq b$, it is therefore (formally) an asymptotic representation of x(t). For discussions of the asymptotic behavior of (8.2.18), readers are referred to [38], [39], [40] and [41].

As a natural extension of the results obtained for the single ordinary differential equation (8.2.18), Turrittin investigated the asymptotic behavior of a set of simultaneous linear (real) ordinary differential equations

$$x' = \frac{dx}{dt} = k^{m_o} A(t,k)\, x \qquad 8.2.22$$

where $m_o \geq 1$ is an integer; x' and x are m x 1 column matrices; A is an m x m square matrix; k is a real number which is large relative to unity. Each element $\alpha_{ij}(t,k)$ of the matrix A (t,k) is assumed to have an asymptotic expansion in k

$$\alpha_{ij}(t) \sim \sum_{\ell=0}^{\infty} k^{-\ell} \alpha_{ij}^{\ell}(t) \qquad 8.2.23$$

where the $\alpha_{ij}^{\ell}(t)$'s are infinitely differentiable in t. Denote the matrix whose elements are $\alpha_{ij}^{\circ}(t)$ by $A_o(t)$, i.e.,

$$A_o(t) = \left[\alpha_{ij}^{\circ}(t)\right] \qquad 8.2.24$$

and the characteristic roots of $A_o(t)$ by $\lambda_q(t)$, q = 1, 2, ---, m. For a system for which $A_o(t)$ has the same number of distinct characteristic roots for all t, $a \leq t \leq b$ (i.e., if $\lambda_i(t)$ and $\lambda_j(t)$ are two roots, then either

$$\lambda_i(t) \equiv \lambda_j(t) \qquad 8.2.25$$

or

$$\lambda_i(t) \neq \lambda_j(t) \qquad 8.2.26$$

for all t, $b \leq t \leq a$). Turrittin showed that there exists a solution $x^{(j)}(t)$ ($x^{(j)}$ is a column matrix) of the system (8.2.22) such that each of its elements, $x_i^{(j)}(t)$, has an asymptotic expansion of the form

$$x_i^{(j)}(t) \sim e^{q^{(j)}(t,k)} \sum_{r=0}^{\infty} p_{ir}^{(j)}(t) k^{-r} \qquad 8.2.27$$

for $|k| \gg 1$, where

$$\frac{dq^{(j)}}{dt} = k^{m_o}\left[\lambda_j(t) + \bar{q}_1^{(j)}(t) k^{-1} + \cdots + \bar{q}_{m_o}^{(j)}(t) k^{-m_o}\right] \qquad 8.2.28$$

$p_{ir}^{(j)}(t)$ and $\bar{q}_r^{(j)}(t)$ are computed by a certain algorithm. As j varies from 1 to m (to account for all the m characteristic roots), we will have the desired asymptotic expansions of the m linearly independent solutions to the given system of differential equations.

8.3 THE EIGENVALUES OF $A_c(t)$

As the first step in the application of the results of Section 8.2 to our shell problem, we must find the characteristic roots of the matrix corresponding to A_o for the system of equations 8.1.4, 8.1.5, and 8.1.6. In order to do this, we will convert our system of differential equations into the form of (8.2.18). With no loss in generality, we may write

$$u_{rn} = \frac{\beta_1}{k} \qquad 8.3.1$$

$$u_{\theta n} = \frac{\beta_2}{k^2} \qquad 8.3.2$$

$$w_n = \beta_3 \qquad 8.3.3$$

$$\frac{du_{rn}}{d\gamma} = \beta_4 \qquad 8.3.4$$

$$\frac{du_{\theta n}}{d\gamma} = \frac{\beta_5}{k} \qquad 8.3.5$$

$$\frac{dw_n}{d\gamma} = k\beta_6 \qquad 8.3.6$$

$$\frac{d^2w_n}{d\gamma^2} = k^2\beta_7 \qquad 8.3.7$$

$$\frac{d^3w_n}{d\gamma^3} = k^3\beta_8 \qquad 8.3.8$$

where the k in these equations is the shell parameter defined by equation (8.1.7), and the β_i's take on the role played by x_i in section 8.2. We then have the following system of homogeneous first order differential equations which is equivalent to the set of shell equations.

$$\frac{d\beta_1}{d\gamma} = k\beta_4 \qquad 8.3.9$$

$$\frac{d\beta_2}{d\gamma} = k\beta_5 \qquad 8.3.10$$

$$\frac{d\beta_3}{d\gamma} = k\beta_6 \qquad 8.3.11$$

$$\frac{d\beta_4}{d\gamma} = -k\left\{\frac{a_{11}^{\circ}}{c_{12}^{\circ}} + O\left(\frac{1}{k}\right)\right\}\beta_6 \qquad 8.3.12$$

$$\frac{d\beta_5}{d\gamma} = -k\left\{\left[\frac{a_{20}^{\circ}}{b_{22}^{\circ}} + O\left(\frac{1}{k}\right)\right]\beta_3 + \left[\frac{c_{21}^{\circ}}{b_{22}^{\circ}} + O\left(\frac{1}{k}\right)\right]\beta_4\right\} \qquad 8.3.13$$

$$\frac{d\beta_6}{d\gamma} = k\beta_7 \qquad 8.3.14$$

$$\frac{d\beta_7}{d\gamma} = k\beta_8 \qquad 8.3.15$$

$$\frac{d\beta_8}{d\gamma} = -k\left\{\left[\frac{a_{30}^{\circ}}{a_{34}} + O\left(\frac{1}{k}\right)\right]\beta_3 + \left[\frac{c_{31}^{\circ}}{a_{34}} + O\left(\frac{1}{k}\right)\right]\beta_4\right\} \qquad 8.3.16$$

more concisely,

$$\frac{d\beta}{d\gamma} = \{\beta_i\} = kA\beta = k[\alpha_{ij}]\{\beta_j\} \qquad 8.3.17$$

where

$$A_o(t,k) = \begin{bmatrix} 0 & 0 & 0 & 1 & 0 & 0 & 0 & 0 \\ 0 & 0 & 0 & 0 & 1 & 0 & 0 & 0 \\ 0 & 0 & 0 & 0 & 0 & 1 & 0 & 0 \\ 0 & 0 & 0 & 0 & 0 & \frac{-a_{11}^{\circ}}{c_{12}^{\circ}} & 0 & 0 \\ 0 & 0 & \frac{-a_{20}^{\circ}}{b_{22}^{\circ}} & \frac{-c_{21}^{\circ}}{b_{22}^{\circ}} & 0 & 0 & 0 & 0 \\ 0 & 0 & 0 & 0 & 0 & 0 & 1 & 0 \\ 0 & 0 & 0 & 0 & 0 & 0 & 0 & 1 \\ 0 & 0 & \frac{-a_{30}^{\circ}}{a_{34}} & \frac{-c_{31}^{\circ}}{a_{34}} & 0 & 0 & 0 & 0 \end{bmatrix} \qquad 8.3.18$$

$$\beta = \begin{Bmatrix} \beta_1 \\ \beta_2 \\ \vdots \\ \beta_8 \end{Bmatrix} \qquad 8.3.19$$

The eight characteristic roots of this matrix are

$$\lambda_1(\gamma) \equiv \lambda_2(\gamma) \equiv \lambda_3(\gamma) \equiv \lambda_4(\gamma) \equiv 0 \qquad 8.3.20$$

and $\lambda_5(\gamma)$, $\lambda_6(\gamma)$, $\lambda_7(\gamma)$, and $\lambda_8(\gamma)$ which are the four roots of

$$\lambda^4 - \left\{ \frac{a_{11}^{\circ} c_{31}^{\circ}}{a_{34} c_{12}^{\circ}} - \frac{a_{30}^{\circ}}{a_{34}} \right\} = 0 \qquad 8.3.21$$

Note that these roots satisfy the conditions (8.2.25 and 8.2.26). Moreover, they are independent of n, the parameter from the Fourier expansions. With these characteristic roots, we may proceed to compute the asymptotic solutions to our system of differential equations in accordance with an algorithm outlined in [35]. Inasmuch as this algorithm is rather involved, we shall adopt a simpler procedure which is possible because of the nature of our system of equations.

Observe that for our problem, $m_o = 1$ (cf. (8.3.17)); the equation corresponding to (8.2.28) is therefore reduced to

$$\frac{dq_j^{(j)}}{d\gamma} = k\lambda_j(\gamma) + \bar{q}_1^{(j)}(\gamma) \qquad 8.3.22$$

for all j. With no loss in generality, we set $\bar{q}_1^{(j)}(\gamma) = 0$ because it does not involve k; therewith

$$\frac{dq_j^{(j)}}{d\gamma} = k\lambda_j(\gamma) \qquad 8.3.23$$

(8.2.27), and (8.2.28) for the case at hand then combine to yield

$$\beta_i^{(j)}(\gamma, k) \sim e^{k\int^{\gamma} \lambda_j \, d\gamma} \sum_{r=0}^{\infty} \beta_{ir}^{(j)}(\gamma) k^{-r} \qquad 8.3.24$$

for i, j = 1, 2, ---, 8 and $\beta_{ir}^{(j)}$ take on the role of $p_{ir}^{(j)}$. In other words, the work of Turrittin assures us that there exist solutions to (8.1.4), (8.1.5), and (8.1.6) having (8.3.24) as their asymptotic

expansions. We will see later that these asymptotic solutions divide themselves into two groups. The leading terms of the expansions associated with the four zero roots (8.3.20) will identify themselves with the membrane and inextensional solutions (i.e., displacements associated with the homogeneous solutions to the membrane force equilibrium equations and to the strain-displacement equations). The second group of the asymptotic solutions associated with the non-zero roots (8.3.21) will be shown to be significant only in a region near the edge(s) of the shell since their magnitudes decay rapidly with distance from the edge(s) and is thus referred to as the edge zone solutions. Consequently, the membrane and inextensional solutions dominate the behavior of the shell interior and together they are referred to as the interior solutions. We will discuss separately these two groups of solutions in the following two sections.

8.4 THE INTERIOR SOLUTIONS

For $\lambda_i(\gamma)$, i = 1, 2, 3 and 4, i.e., the zero eigenvalues, (8.3.24) becomes

$$\beta_j(\gamma,k) \sim \sum_{s=0}^{\infty} \beta_{js}(\gamma) k^{-s} \qquad 8.4.1$$

or

$$u_{rn}(\gamma,k) \sim \sum_{s=0}^{\infty} \beta_{1s}(\gamma) k^{-s-1} \qquad 8.4.2$$

$$u_{\theta n}(\gamma,k) \sim \sum_{s=0}^{\infty} \beta_{2s}(\gamma) k^{-s-2} \qquad 8.4.3$$

and

$$w_n(\gamma,k) \sim \sum_{s=0}^{\infty} \beta_{3s}(\gamma) k^{-s} \qquad 8.4.4$$

To find the asymptotic homogeneous solution to the given system of shell equations, we substitute (8.4.2), (8.4.3) and (8.4.4) into (8.1.4), (8.1.5) and (8.1.6) with the forcing terms (i.e., the right hand side) suppressed and collect coefficients of the same power of k. Equating these coefficients to zero, we get

$$L_{m3}(\beta_{30}) = 0 \qquad 8.4.5$$

$$L_{m3}(\beta_{31}) + L_{m1}(\beta_{10}) = 0 \qquad 8.4.6$$

$$L_{m3}(\beta_{32}) + L_{m2}(\beta_{20}) + L_{m1}(\beta_{11}) = 0 \qquad 8.4.7$$

and for $s \geq 3$

$$L_{m3}(\beta_{3s}) + L_{m2}(\beta_{2s-2}) + L_{m1}(\beta_{1s-1}) =$$
$$-\left\{L^*_{m3}(\beta_{3s-4}) + L^*_{m2}(\beta_{2s-6}) + L^*_{m1}(\beta_{1s-5})\right\} \qquad 8.4.8$$

where m = 1, 2 and 3. Quantities with a negative subscript should be taken as zeros. In general, β_{30} can not satisfy the three equations

given by (8.4.5). Therefore, we must have

$$\beta_{30}(\gamma) \equiv 0 \qquad 8.4.9$$

Similarly, β_{31} and β_{10} in general can not satisfy the three equations given by (8.4.6); therefore

$$\beta_{31}(\gamma) \equiv \beta_{10}(\gamma) \equiv 0 \qquad 8.4.10$$

In view of (8.4.8), (8.4.9) and (8.4.10), we may now (with no loss in generality) rewrite (8.4.2), (8.4.3) and (8.4.4) in the form of

$$u_{rn}(\gamma, k) \sim \sum_{s=0}^{\infty} \beta_{1s}(\gamma)\, k^{-4s} \qquad 8.4.11$$

$$u_{\theta n}(\gamma, k) \sim \sum_{s=0}^{\infty} \beta_{2s}(\gamma)\, k^{-4s} \qquad 8.4.12$$

and

$$w_{n}(\gamma, k) \sim \sum_{s=0}^{\infty} \beta_{3s}(\gamma)\, k^{-4s} \qquad 8.4.13$$

so that (8.4.7) and (8.4.8) become

$$\sum_{\ell=1}^{3} L_{m\ell}(\beta_{\ell 0}) = 0 \qquad 8.4.14$$

and

$$\sum_{\ell=1}^{3} L_{m\ell}(\beta_{\ell s}) = -\sum_{\ell=1}^{3} L^{*}_{m\ell}(\beta_{\ell s-1}), \quad (s \geq 1) \qquad 8.4.15$$

for m = 1, 2 and 3. The set of equations given by (8.4.14) upon comparison with the complete set of shell equations (8.1.4), (8.1.5) and (8.1.6) can be recognized as the membrane equations (written in terms of the middle surface displacement components by way of the strain-displacement relations) since the terms containing k are not present. The four linearly independent solutions to these equations (corresponding to the fact that zero is a quadruple root) are the same as those previously obtained in Chapter VI. Since two of these linearly independent solutions are the homogeneous solutions of the

strain-displacement equations while the other two are associated with the homogeneous solutions to the membrane force equilibrium equations, they are often referred to as the inextensional and membrane solutions, respectively. While in principle the higher order terms in the expansions can be obtained by way of (8.4.15), the calculations are, in general, tedious. Since the additional terms are of order $1/k^4$ and higher, we will only be interested in the leading term of each expansion in the subsequent development, i.e., we will only be concerned with the above described solutions to (8.4.14).

8.5 THE EDGE ZONE SOLUTIONS

For $\lambda_i(\gamma)$, i = 5, 6, 7 and 8, i.e., the non-zero eigenvalues (8.3.25), we have

$$u_{rn}^{(i)} \sim e^{k\int \lambda_i d\gamma} \sum_{j=0}^{\infty} \beta_{1j}^{(i)}(\gamma) k^{-j-1} \qquad 8.5.1$$

$$u_{\theta n}^{(i)} \sim e^{k\int \lambda_i d\gamma} \sum_{j=0}^{\infty} \beta_{2j}^{(i)}(\gamma) k^{-j-2} \qquad 8.5.2$$

and

$$w_n^{(i)} \sim e^{k\int \lambda_i d\gamma} \sum_{j=0}^{\infty} \beta_{3j}^{(i)}(\gamma) k^{-j} \qquad 8.5.3$$

Again we substitute these expressions into (8.1.4), (8.1.5) and (8.1.6) and collect the coefficients of the same power of k. Equating each of these coefficients to zero, we have the following recurrence relations:

$$\phi_j^{17} + \phi_{j-1}^{16} + \phi_{j-2}^{15} + \phi_{j-3}^{14} + \phi_{j-4}^{13} + \phi_{j-5}^{12} + \phi_{j-6}^{11} + \phi_{j-7}^{10} = 0 \qquad 8.5.4$$

$$\phi_j^{26} + \phi_{j-1}^{25} + \phi_{j-2}^{24} + \phi_{j-3}^{23} + \phi_{j-4}^{22} + \phi_{j-5}^{21} + \phi_{j-6}^{20} = 0 \qquad 8.5.5$$

$$\phi_j^{36} + \phi_{j-1}^{35} + \phi_{j-2}^{34} + \phi_{j-3}^{33} + \phi_{j-4}^{32} + \phi_{j-5}^{31} + \phi_{j-6}^{30} = 0 \qquad 8.5.6$$

where

$$\phi_j^{17} = a_{11}^{\circ} f' \beta_{3j}^{(i)} + c_{12}^{\circ} (f')^2 \beta_{1j}^{(i)} \qquad 8.5.7$$

$$\phi_{j-1}^{16} = a_{11}^{\circ} \beta_{3j}^{(i)\prime} + a_{10}^{\circ} \beta_{3j}^{(i)} + 2 f' c_{12}^{\circ} \beta_{1j}^{(i)\prime} + (c_{11}^{\circ} f' + c_{12}^{\circ} f'') \beta_{1j}^{(i)} \qquad 8.5.8$$

$$\phi_{j-2}^{15} = a_{13} (f')^3 \beta_{3j}^{(i)} + b_{11}^{\circ} f' \beta_{2j}^{(i)} + c_{12}^{\circ} \beta_{1j}^{(i)\prime\prime} + c_{11}^{\circ} \beta_{1j}^{(i)\prime} + c_{10}^{\circ} \beta_{1j}^{(i)} \qquad 8.5.9$$

$$\phi_{j-6}^{20} = b_{22}\beta_{2j}^{(i)''} + b_{21}\beta_{2j}^{(i)'} + b_{20}\beta_{2j}^{(i)} \qquad 8.5.21$$

$$\phi_{j}^{36} = \left[a_{34}(f')^4 + a_{30}^{\circ}\right]\beta_{3j}^{(i)} + c_{31}^{\circ} f'\beta_{1j}^{(i)} \qquad 8.5.22$$

$$\phi_{j-1}^{35} = 4a_{34}(f')^3\beta_{3j}^{(i)'} + \left[6a_{34}f''(f')^2 + a_{33}(f')^3\right]\beta_{3j}^{(i)} + c_{31}^{\circ}\beta_{1j}^{(i)'} + c_{30}^{\circ}\beta_{1j}^{(i)} \qquad 8.5.23$$

$$\phi_{j-2}^{34} = 6a_{34}(f')^2\beta_{3j}^{(i)''} + 3f'\left[4a_{34}f'' + a_{33}f'\right]\beta_{3j}^{(i)'} + \left[(4f'f''' + 3(f'')^2)a_{34} + 3a_{33}f'f'' + a_{32}(f')^2\right]\beta_{3j}^{(i)} + b_{30}^{\circ}\beta_{2j}^{(i)} + c_{33}(f')^3\beta_{1j}^{(i)} \qquad 8.5.24$$

$$\phi_{j-3}^{33} = 4a_{34}f'\beta_{3j}^{(i)'''} + 3\left[2a_{34}f'' + a_{33}f'\right]\beta_{3j}^{(i)''} + \left[4a_{34}f''' + 3a_{33}f'' + 2a_{32}f'\right]\beta_{3j}^{(i)'} + \left[a_{34}f'''' + a_{33}f''' + a_{32}f'' + a_{31}f'\right]\beta_{3j}^{(i)} + 3(f')^2c_{33}\beta_{1j}^{(i)'} + \left[3c_{33}f'f'' + c_{32}(f')^2\right]\beta_{1j}^{(i)} \qquad 8.5.25$$

$$\phi_{j-4}^{32} = a_{34}\beta_{3j}^{(i)''''} + a_{33}\beta_{3j}^{(i)'''} + a_{32}\beta_{3j}^{(i)''} + a_{31}\beta_{3j}^{(i)'} + a_{30}\beta_{3j}^{(i)} + b_{32}(f')^2\beta_{2j}^{(i)} + 3c_{33}f'\beta_{1j}^{(i)''} + \left[3f''c_{33} + 2f'c_{32}\right]\beta_{1j}^{(i)'} + \left[c_{33}f''' + c_{32}f'' + c_{31}f'\right]\beta_{1j}^{(i)} \qquad 8.5.26$$

$$\phi_{j-5}^{31} = 2b_{32}f'\beta_{2j}^{(i)'} + \left[b_{32}f'' + b_{31}f'\right]\beta_{2j}^{(i)} + c_{33}\beta_{1j}^{(i)'''} + c_{32}\beta_{1j}^{(i)''} + c_{31}\beta_{1j}^{(i)'} + c_{30}\beta_{1j}^{(i)} \qquad 8.5.27$$

$$\phi_{j-3}^{14} = 3a_{13}(f')^2\beta_{3j}^{(i)\prime} + \left[3f'f''a_{13} + a_{12}(f')^2\right]\beta_{3j}^{(i)} + b_{11}^{\circ}\beta_{2j}^{(i)\prime} + b_{10}^{\circ}\beta_{2j}^{(i)} \qquad 8.5.10$$

$$\phi_{j-4}^{13} = 3a_{13}f'\beta_{3j}^{(i)\prime\prime} + \left[3f''a_{13} + 2a_{12}f'\right]\beta_{3j}^{(i)\prime} + \left[a_{13}f''' + a_{12}f'' + a_{12}f'\right]\beta_{3j}^{(i)} + c_{12}(f')^2\beta_{1j}^{(i)} \qquad 8.5.11$$

$$\phi_{j-5}^{12} = a_{13}\beta_{3j}^{(i)\prime\prime\prime} + a_{12}\beta_{3j}^{(i)\prime\prime} + a_{11}\beta_{3j}^{(i)\prime} + a_{10}\beta_{3j}^{(i)} + 2c_{12}f'\beta_{1j}^{(i)\prime} + \left[c_{12}f'' + c_{11}f'\right]\beta_{1j}^{(i)} \qquad 8.5.12$$

$$\phi_{j-6}^{11} = b_{11}f'\beta_{2j}^{(i)} + c_{12}\beta_{1j}^{(i)\prime\prime} + c_{11}\beta_{1j}^{(i)\prime} + c_{10}\beta_{1j}^{(i)} \qquad 8.5.13$$

$$\phi_{j-7}^{10} = b_{11}\beta_{2j}^{(i)\prime} + b_{10}\beta_{2j}^{(i)} \qquad 8.5.14$$

$$\phi_{j}^{26} = a_{20}^{\circ}\beta_{3j}^{(i)} + b_{22}^{\circ}(f')^2\beta_{2j}^{(i)} + c_{21}^{\circ}f'\beta_{1j}^{(i)} \qquad 8.5.15$$

$$\phi_{j-1}^{25} = 2b_{22}^{\circ}f'\beta_{2j}^{(i)\prime} + \left[b_{22}^{\circ}f'' + b_{21}^{\circ}f'\right]\beta_{2j}^{(i)} + c_{21}^{\circ}\beta_{1j}^{(i)\prime} + c_{20}^{\circ}\beta_{1j}^{(i)} \qquad 8.5.16$$

$$\phi_{j-2}^{24} = a_{22}(f')^2\beta_{3j}^{(i)} + b_{22}^{\circ}\beta_{2j}^{(i)\prime\prime} + b_{21}^{\circ}\beta_{2j}^{(i)\prime} + b_{20}^{\circ}\beta_{2j}^{(i)} \qquad 8.5.17$$

$$\phi_{j-3}^{23} = a_{22}f'\beta_{3j}^{(i)\prime} + \left[a_{22} + a_{21}f'\right]\beta_{3j}^{(i)} \qquad 8.5.18$$

$$\phi_{j-4}^{22} = a_{22}\beta_{3j}^{(i)\prime\prime} + a_{21}\beta_{3j}^{(i)\prime} + a_{20}\beta_{3j}^{(i)} + b_{22}(f')^2\beta_{2j}^{(i)} + c_{21}f'\beta_{1j}^{(i)} \qquad 8.5.19$$

$$\phi_{j-5}^{21} = 2b_{22}f'\beta_{2j}^{(i)\prime} + \left[b_{22}f'' + b_{21}f'\right]\beta_{2j}^{(i)} + c_{21}\beta_{1j}^{(i)\prime} + c_{20}\beta_{1j}^{(i)} \qquad 8.5.20$$

$$\phi^{30}_{j-6} = b_{32}\,\beta^{(i)\prime\prime}_{2j} + b_{31}\,\beta^{(i)\prime}_{2j} + b_{30}\,\beta^{(i)}_{2j} \qquad 8.5.28$$

where

$$\mathcal{J} = \int \lambda_i \, d\gamma \qquad 8.5.29$$

Quantities with negative subscripts are again to be taken as zeros.

For j = 0, equations (8.5.7), (8.5.8), and (8.5.9) become

$$\lambda_i\left(a^{\circ}_{11}\,\beta_{30} + c^{\circ}_{12}\lambda_i\,\beta_{10}\right) = 0 \qquad 8.5.30$$

$$a^{\circ}_{20}\,\beta_{30} + \lambda_i\left(\lambda_i\, b^{\circ}_{22}\,\beta_{20} + c^{\circ}_{21}\,\beta_{10}\right) = 0 \qquad 8.5.31$$

and

$$\left[a_{34}(\lambda_i)^4 + a^{\circ}_{30}\right]\beta_{30} + c^{\circ}_{31}\lambda_i\,\beta_{10} = 0 \qquad 8.5.32$$

respectively. (8.5.30), (8.5.31), and (8.5.32) have nontrivial solutions for β_{10}, β_{20}, and β_{30} because the determinant of the coefficients vanishes:

$$\lambda_i^4\left(\lambda_i^4(\gamma) - \left[\frac{c^{\circ}_{31}\,a^{\circ}_{11}}{a_{34}\,c^{\circ}_{12}} - \frac{a^{\circ}_{30}}{a_{34}}\right]\right) = 0 \qquad 8.5.33$$

which is assured by (8.3.21).

For j = 1, (8.5.7), (8.5.8), and (8.5.9) become

$$\left[a^{\circ}_{11}\,\beta_{31} + c^{\circ}_{12}\,\lambda_i\,\beta_{11}\right]\lambda_i + a^{\circ}_{11}\,\beta'_{30} + a^{\circ}_{10}\,\beta_{30}$$
$$+ 2\lambda_i\, c^{\circ}_{12}\,\beta'_{10} + \left[c^{\circ}_{11}\lambda_i + c^{\circ}_{12}\,\lambda'_i\right] = 0 \qquad 8.5.34$$

$$a_{20}^{\circ}\beta_{31} + b_{22}^{\circ}(\lambda_i)^2\beta_{21} + c_{21}^{\circ}\lambda_i\beta_{11} + 2b_{22}^{\circ}\lambda_i\beta_{20}' + \left[b_{22}^{\circ}\lambda_i' + b_{21}^{\circ}\lambda_i\right]\beta_{20} + c_{21}^{\circ}\beta_{10}' + c_{20}^{\circ}\beta_{10} = 0 \qquad 8.5.35$$

and

$$\left[a_{34}\lambda_i^4 + a_{30}^{\circ}\right]\beta_{31} + c_{31}^{\circ}\lambda_i\beta_{11} + 4a_{34}\lambda_i^3\beta_{30}' + \left[6a_{34}\lambda_i'\lambda_i^2 + a_{33}\lambda_i^3\right]\beta_{30} + c_{31}^{\circ}\beta_{10}' + c_{30}^{\circ}\beta_{10} = 0 \qquad 8.5.36$$

where $(\,)' = \dfrac{d(\,)}{d\gamma}$

The first and third equations yield (keeping in mind the results for j = 0)

$$\beta_{30}(\gamma) = \exp\left\{-\frac{1}{4}\int\left[\frac{6\lambda_i'}{\lambda_i} + \frac{a_{33}}{a_{44}} - \frac{(c_{31}^{\circ}a_{10}^{\circ} + a_{11}^{\circ}c_{30}^{\circ})}{c_{12}^{\circ}a_{34}\lambda_i^4} + \frac{c_{31}^{\circ}a_{11}^{\circ\prime}}{c_{12}^{\circ}a_{34}\lambda_i^4} + \frac{a_{11}^{\circ}c_{31}^{\circ}(c_{11}^{\circ} - c_{12}^{\circ\prime})}{(c_{12}^{\circ})^2 a_{34}\lambda_i^4}\right]d\gamma\right\} \qquad 8.5.37$$

From (8.5.30) and (8.5.31), we have

$$\beta_{10}(\gamma) = -\frac{a_{11}^{\circ}}{c_{12}\lambda_i}\beta_{30} \qquad 8.5.38$$

and

$$\beta_{20}(\gamma) = -\frac{1}{b_{22}^{\circ}\lambda_i^2}\left(a_{20}^{\circ}\beta_{30} + c_{21}^{\circ}\lambda_i\beta_{10}\right) \qquad 8.5.39$$

Terms associated with higher powers of $(k)^{-1}$ to each expansion can again be computed by way of the recurrence relations (8.5.4) through (8.5.6), although the computations are not only tedious but may be very difficult because new sets of differential equations arise. Since k is large, these higher order terms are negligibly small in comparison with the leading term and therefore will not be considered in the subsequent development, i.e., we will consider only β_{10}, β_{20}, and β_{30}.

8.6 THE PARTICULAR SOLUTION

For a shell under gravity loading, the components of the load intensity vector are [cf. [33])

$$p_1 = p_r = \frac{\rho_0 h}{\sqrt{1+\gamma^2}}\left[\sin\Psi \sin\theta - \gamma\cos\Psi\right] \qquad 8.6.1$$

$$p_2 = p_\theta = \rho_0 h \sin\Psi \cos\theta \qquad 8.6.2$$

and

$$p_3 = p_n = \frac{\rho_0 h}{\sqrt{1+\gamma^2}}\left[-\gamma \sin\Psi \sin\theta - \cos\Psi\right] \qquad 8.6.3$$

The form of the corresponding $P_{in}(\gamma)$ (i = 1, 2, 3) suggests that any particular integral of the dependent variables cannot contain a factor $e^{kf(\gamma)}$ for any $f(\gamma)$ which is not identically zero. Thus we will seek particular asymptotic solutions of the form

$$u_{rnp}(\gamma,k) \sim \sum_{j=0}^{\infty} \delta_{n1j}(\gamma)\, k^{-4j} \qquad (n = 0, 1) \qquad 8.6.4$$

$$u_{\theta np}(\gamma,k) \sim \sum_{j=0}^{\infty} \delta_{n2j}(\gamma)\, k^{-4j} \qquad (n = 1) \qquad 8.6.5$$

$$w_{np}(\gamma,k) \sim \sum_{j=0}^{\infty} \delta_{n3j}(\gamma)\, k^{-4j} \qquad (n = 0, 1) \qquad 8.6.6$$

Substituting (8.6.4), (8.6.5), and (8.6.6) into (8.1.4), (8.1.5), and (8.1.6), collecting coefficients of the same power of k and equating them to zero, we get for n = 0

$$L_{13}(\delta_{030}) + L_{11}(\delta_{010}) = \frac{4f^2(1-\nu^2)}{Eh}\cos\Psi\, \rho_0 h\, \gamma^2 \qquad 8.6.7$$

$$L_{33}(\delta_{030}) + L_{31}(\delta_{030}) = \frac{4f^2(1-\nu^2)}{Eh}\cos\Psi\, \rho_0 h\, \gamma \qquad 8.6.8$$

and

$$L_{m3}(\delta_{03s})+L_{m1}(\delta_{01s})=-\left[L^{*}_{m3}(\delta_{03s-1})+L^{*}_{m1}(\delta_{01s-1})\right] \quad (s\geq 1) \qquad 8.6.9$$

where m = 1 and 3; and for n = 1

$$L_{13}(\delta_{130})+L_{12}(\delta_{120})+L_{11}(\delta_{110})=-\frac{4f^{2}(1-\nu^{2})\rho_{o}h\sin\psi}{Eh}\left[\gamma^{2}\right] \qquad 8.6.10$$

$$L_{23}(\delta_{130})+L_{22}(\delta_{120})+L_{21}(\delta_{110})=-\frac{4f^{2}(1-\nu^{2})\rho_{o}h\sin\psi}{Eh}\left[\gamma\sqrt{1+\gamma^{2}}\right] \qquad 8.6.11$$

$$L_{33}(\delta_{130})+L_{32}(\delta_{120})+L_{31}(\delta_{110})=\frac{4f^{2}(1-\nu^{2})\rho_{o}h\sin\psi}{Eh}\left[\gamma^{2}\right] \qquad 8.6.12$$

and

$$\sum_{i=1}^{3} L_{mi}(\delta_{1is})=-\sum_{i=1}^{3} L^{*}_{mi}(\delta_{1is-1}) \qquad (s\geq 1) \qquad 8.6.13$$

where m = 1, 2, and 3.

Clearly, the leading term of the expansions given by (8.6.4), (8.6.5), and (8.6.6) can be identified as the particular solution to the corresponding middle surface displacement in the membrane analysis of a shell loaded by gravity. Higher order terms of these expansions can be obtained from (8.6.9) and (8.6.13). However, since these additional terms are of order $\frac{1}{k^{4}}$ or higher, (small in comparison with the leading term) they are therefore omitted from further considerations.

8.7 SOME RELEVANT RELATIONS

Some of the relations derived in Chapters I through V will be recapitulated here in a form suitable for the purpose of asymptotic solutions.

$$N_r = \frac{Eh}{(1-\nu^2)}\left\{-\left[\frac{1}{2f(1+\gamma^2)^{3/2}} + \frac{\nu}{2f\sqrt{1+\gamma^2}}\right]w + \frac{\nu}{2f\gamma\sqrt{1+\gamma^2}}\,u_r + \frac{1}{2f\sqrt{1+\gamma^2}}\,\frac{\partial u_r}{\partial\gamma} + \frac{\nu}{2f\gamma}\,\frac{\partial u_\theta}{\partial\theta}\right\} \qquad 8.7.1$$

$$N_\theta = \frac{Eh}{(1-\nu^2)}\left\{-\left[\frac{\nu}{2f(1+\gamma^2)^{3/2}} + \frac{1}{2f\sqrt{1+\gamma^2}}\right]w + \frac{1}{2f\gamma\sqrt{1+\gamma^2}}\,u_r + \frac{\nu}{2f\sqrt{1+\gamma^2}}\,\frac{\partial u_r}{\partial\gamma} + \frac{1}{2f\gamma}\,\frac{\partial u_\theta}{\partial\theta}\right\} \qquad 8.7.2$$

$$N_{r\theta} = \frac{Eh}{2(1+\nu)}\left\{\frac{1}{2f\gamma}\,\frac{\partial u_r}{\partial\theta} - \frac{u_\theta}{2f\gamma\sqrt{1+\gamma^2}} + \frac{1}{2f\sqrt{1+\gamma^2}}\,\frac{\partial u_\theta}{\partial\gamma}\right\} \qquad 8.7.3$$

$$M_r = \frac{-D}{4f^2}\left\{\frac{1}{(1+\gamma^2)}\,\frac{\partial^2 w}{\partial\gamma^2} + \frac{\nu}{\gamma^2}\,\frac{\partial^2 w}{\partial\theta^2} + \frac{[\nu-(1-\nu)\gamma^2]}{\gamma(1+\gamma^2)^2}\,\frac{\partial w}{\partial\gamma} + \frac{\nu}{\gamma\sqrt{1+\gamma^2}}\,\frac{\partial u_\theta}{\partial\theta} + \frac{1}{(1+\gamma^2)^2}\,\frac{\partial u_r}{\partial\gamma} + \frac{[\nu-(3-\nu)\gamma^2]}{\gamma(1+\gamma^2)^3}\,u_r\right\} \qquad 8.7.4$$

$$M_\theta = \frac{-D}{4f^2}\left\{\frac{\nu}{(1+\gamma^2)}\,\frac{\partial^2 w}{\partial\gamma^2} + \frac{1}{\gamma^2}\,\frac{\partial^2 w}{\partial\theta^2} + \frac{[1+(1-\nu)\gamma^2]}{\gamma(1+\gamma^2)^2}\,\frac{\partial w}{\partial\gamma} + \frac{1}{\gamma\sqrt{1+\gamma^2}}\,\frac{\partial u_\theta}{\partial\theta} + \frac{\nu}{(1+\gamma^2)^2}\,\frac{\partial u_r}{\partial\gamma} + \frac{[1+(1-3\nu)\gamma^2]}{\gamma(1+\gamma^2)^3}\,u_r\right\} \qquad 8.7.5$$

$$M_{r\theta} = \frac{-D(1-\nu)}{4f^2}\left\{\frac{1}{\gamma\sqrt{1+\gamma^2}}\,\frac{\partial^2 w}{\partial\gamma\partial\theta} - \frac{1}{\gamma^2\sqrt{1+\gamma^2}}\,\frac{\partial w}{\partial\theta} + \frac{1}{2(1+\gamma^2)}\,\frac{\partial u_\theta}{\partial\gamma} - \frac{(1+2\gamma^2)}{2\gamma(1+\gamma^2)^2}\,u_\theta + \frac{1}{2\gamma(1+\gamma^2)^{3/2}}\,\frac{\partial u_r}{\partial\theta}\right\} \qquad 8.7.6$$

$$Q_\theta = \frac{1}{4f^2\gamma\sqrt{1+\gamma^2}}\left\{\frac{\partial(2f\gamma M_{r\theta})}{\partial\gamma} + \frac{\partial(2f\sqrt{1+\gamma^2}M_\theta)}{\partial\theta} + 2fM_{r\theta}\right\} \quad 8.7.7$$

$$Q_r = \frac{1}{4f^2\gamma\sqrt{1+\gamma^2}}\left\{\frac{\partial(2f\gamma M_r)}{\partial\gamma} + \frac{\partial(2f\sqrt{1+\gamma^2}M_{r\theta})}{\partial\theta} - 2fM_\theta\right\} \quad 8.7.8$$

$$\omega_r = -\left\{\frac{u_r}{2f(1+\gamma^2)^{3/2}} + \frac{1}{2f\sqrt{1+\gamma^2}}\frac{\partial w}{\partial\gamma}\right\} \quad 8.7.9$$

$$\omega_\theta = -\left\{\frac{u_\theta}{2f\sqrt{1+\gamma^2}} + \frac{1}{2f\gamma}\frac{\partial w}{\partial\theta}\right\} \quad 8.7.10$$

where

$$D = \frac{Eh^3}{12(1-\nu^2)} \quad 8.7.11$$

8.8 THE LEADING TERM OF THE ASYMPTOTIC EXPANSION FOR THE EDGE ZONE SOLUTIONS

We shall consider in this section asymptotic solutions for a paraboloidal shell of revolution corresponding to the four characteristic roots $\lambda_i(\gamma)$ which are not identically zero.

$$\int^{\gamma} \lambda_i(\gamma)\, d\gamma = \omega_i m \int^{\gamma} \sqrt[4]{1+\gamma^2}\; d\gamma \qquad 8.8.1$$

where

$$m = \sqrt[4]{(1-\nu^2)} \qquad 8.8.2$$

and ω_i is the appropriate root of the equation

$$\omega^4 + 1 = 0 \qquad 8.8.3$$

For the n^{th} harmonic of the Fourier expansion, the leading terms of the expansions (8.5.1), (8.5.2) and 8.5.3) are

$$\beta_{30}^{(i)} = \left\{ \frac{(1+\gamma^2)^{3/8}}{\sqrt{\gamma}} \right\} C \qquad 8.8.4$$

$$\beta_{10}^{(i)} = \frac{\left[(1+\nu)+\nu\gamma^2\right]}{m\sqrt{\gamma}} \left[1+\gamma^2\right]^{-7/8} \left\{ \frac{C}{\omega_i} \right\} \qquad 8.8.5$$

and

$$\beta_{20}^{(i)} = \frac{\pm n\,(1+\gamma^2)^{-5/8}}{m^2(\gamma)^{3/2}} \left[(1+\nu)+(2+\nu)\gamma^2\right] \left\{ \frac{C}{\omega_i^2} \right\} \qquad 8.8.6$$

where C is a complex constant of integration. Retaining only the leading terms of the asymptotic solutions, the relevant edge zone stress resultants and bending moments can be obtained from the middle surface displacements by way of the relations listed in section 8.6. In what follows, the

superscript e attached to a dependent variable means the edge zone part of that dependent variable. Similarly the superscript i refers to the interior.

$$w_n^e \sim \frac{(1+\gamma^2)^{3/8}}{\sqrt{\gamma}}\left\{e^{\tau}\left[C_5\cos\tau + C_6\sin\tau\right] + e^{-\tau}\left[C_7\cos\tau + C_8\sin\tau\right]\right\}\begin{Bmatrix}\sin n\theta\\ \cos n\theta\end{Bmatrix}$$

8.8.7

$$u_{rn}^e \sim \frac{(1+\gamma^2)^{-7/8}\left[(1+\nu)+\nu\gamma^2\right]}{km\sqrt{\gamma}}\left\{e^{\tau}\left[C_5\cos(\tau-\tfrac{\pi}{4}) + C_6\sin(\tau-\tfrac{\pi}{4})\right]\right.$$
$$\left. -e^{-\tau}\left[C_7\cos(\tau+\tfrac{\pi}{4}) + C_8\sin(\tau+\tfrac{\pi}{4})\right]\right\}\begin{Bmatrix}\sin n\theta\\ \cos n\theta\end{Bmatrix}$$

8.8.8

$$u_{\theta n}^e \sim \frac{\pm n(1+\gamma^2)^{-5/8}\left[(1+\nu)+(2+\nu)\gamma^2\right]}{(m+k)^2\gamma^{3/2}}\left\{e^{\tau}\left[C_5\sin\tau - C_6\cos\tau\right]\right.$$
$$\left. -e^{-\tau}\left[C_7\sin\tau - C_8\cos\tau\right]\right\}\begin{Bmatrix}\cos n\theta\\ \sin n\theta\end{Bmatrix}$$

8.8.9

$$M_{rn}^e \sim \frac{D(m+k)^2}{4f^2\sqrt{\gamma}\,(1+\gamma^2)^{1/8}}\left\{e^{\tau}\left[C_5\sin\tau - C_6\cos\tau\right]\right.$$
$$\left. -e^{-\tau}\left[C_7\sin\tau - C_8\cos\tau\right]\right\}\begin{Bmatrix}\sin n\theta\\ \cos n\theta\end{Bmatrix}$$

8.8.10

$$M_{\theta n}^e \sim \nu M_{rn}^e$$

8.8.11

$$M_{r\theta n}^e \sim \frac{\mp nD(1-\nu)(m+k)(1+\gamma^2)^{1/8}}{4f^2(\gamma)^{3/2}}\left\{e^{\tau}\left[C_5\cos(\tau+\tfrac{\pi}{4}) + C_6\sin(\tau+\tfrac{\pi}{4})\right]\right.$$
$$\left. -e^{-\tau}\left[C_7\cos(\tau-\tfrac{\pi}{4}) + C_8\sin(\tau-\tfrac{\pi}{4})\right]\right\}\begin{Bmatrix}\cos n\theta\\ \sin n\theta\end{Bmatrix}$$

8.8.12

$$N_{rn}^e \sim O\left(\frac{1}{k}\right)N_{rn}^i$$

$$N_{\theta n}^e \sim \frac{-Eh}{2f\sqrt{\gamma}\,(1+\gamma^2)^{1/8}}\left\{e^{\tau}\left[C_5\cos\tau + C_6\sin\tau\right]\right.$$

8.8.13

$$\left. +e^{-\tau}\left[C_7\cos\tau + C_8\sin\tau\right]\right\}\begin{Bmatrix}\sin n\theta\\ \cos n\theta\end{Bmatrix}$$

8.8.14

$$N^{e}_{r\theta n} \sim \pm \frac{nEh(1+\gamma^2)^{1/8}}{2f(mk)\gamma^{3/2}} \left\{ e^{\tau}\left[c_5 \cos(\tau-\tfrac{\pi}{4}) + c_6 \sin(\tau-\tfrac{\pi}{4})\right] - e^{-\tau}\left[c_7 \cos(\tau+\tfrac{\pi}{4}) + c_8 \sin(\tau+\tfrac{\pi}{4})\right]\right\}\begin{Bmatrix}\cos n\theta \\ \sin n\theta\end{Bmatrix}$$

8.8.15

$$Q^{e}_{rn} \sim \frac{D(mk)^3}{8f^3\sqrt{\gamma}\,(1+\gamma^2)^{3/8}} \left\{ e^{\tau}\left[c_5 \cos(\tau-\tfrac{\pi}{4}) + c_6 \sin(\tau-\tfrac{\pi}{4})\right] - e^{-\tau}\left[c_7 \cos(\tau+\tfrac{\pi}{4}) + c_8 \sin(\tau+\tfrac{\pi}{4})\right]\right\}\begin{Bmatrix}\sin n\theta \\ \cos n\theta\end{Bmatrix}$$

8.8.16

$$Q^{e}_{\theta n} \sim \frac{\pm nD(mk)^2}{8f^3\gamma^{3/2}(1+\gamma^2)^{1/8}} \left\{ e^{\tau}\left[c_5 \sin\tau - c_6 \cos\tau\right] - e^{-\tau}\left[c_7 \sin\tau - c_8 \cos\tau\right]\right\}\begin{Bmatrix}\cos n\theta \\ \sin n\theta\end{Bmatrix}$$

8.8.17

$$\omega^{e}_{\theta n} \sim \frac{\mp n(1+\gamma^2)^{3/8}}{2f\gamma^{3/2}} \left\{ e^{\tau}\left[c_5 \cos\tau + c_6 \sin\tau\right] + e^{-\tau}\left[c_7 \cos\tau + c_8 \sin\tau\right]\right\}\begin{Bmatrix}\cos n\theta \\ \sin n\theta\end{Bmatrix}$$

8.8.18

$$\omega^{e}_{rn} \sim \frac{-(mk)(1+\gamma^2)^{1/8}}{2f\sqrt{\gamma}} \left\{ e^{\tau}\left[c_5 \cos(\tau+\tfrac{\pi}{4}) + c_6 \sin(\tau+\tfrac{\pi}{4})\right] - e^{-\tau}\left[c_7 \cos(\tau-\tfrac{\pi}{4}) + c_8 \sin(\tau-\tfrac{\pi}{4})\right]\right\}\begin{Bmatrix}\sin n\theta \\ \cos n\theta\end{Bmatrix}$$

8.8.19

where

$$\tau = \frac{km}{\sqrt{2}} \int^{\gamma} \sqrt[4]{1+\gamma^2}\, d\gamma = \sqrt{\frac{2f}{h}}\, \sqrt[4]{3(1-\nu^2)} \int^{\gamma} \sqrt[4]{1+\gamma^2}\, d\gamma \qquad 8.8.20$$

c_i, i = 5, 6, 7, 8 are constants of integrations.

The leading term of N^{e}_{r} is proportional to k^{-1}. Since we shall have no need for it, the explicit expression for N^{e}_{r} will not be given here. To compute the coefficient associated with this leading term would necessitate the derivation of the second term of the expansions (8.5.1) and (8.5.3). On the other hand, the error accrued to

the neglect of N_r^e is of the order (k^{-1}) in the presence of N_r^i, the interior solution corresponding to $\lambda_i \equiv 0$. Observe that the effects of the solutions obtained in this section due to the presence of $e^{\pm\tau}$ are of significance only in a region near the edges of the shell; hence, they are often referred to as the edge zone solutions. In many situations, the edge zone is only a small percentage of the span of the shell.

8.9 THE LEADING TERMS OF THE ASYMPTOTIC SOLUTIONS FOR AXI-SYMMETRIC GRAVITY LOADING

In this section the interior solution (section 8.4 and chapter VI), the edge zone solution (section 8.8),and the particular solution (section 8.6 and chapter VI) will be combined for a paraboloidal shell under axi-symmetric gravity loading. It should be recognized that the result represents only the leading terms (section 8.4 and 8.5) of the asymptotic solution to the shell equations 8.1.4, 8.1.5, and 8.1.6.

$$w_o \sim \frac{4f^2\rho_o}{3E\sqrt{1+\gamma^2}}\left\{(1+\nu)\left(\ln\gamma-\frac{1}{\gamma^2}\right)+\left(\frac{3-\nu}{2}\right)\gamma^2+\frac{1}{4}\gamma^4+(1+\gamma^2)\left[2(\nu-1)+\frac{1+\nu}{\gamma^2}+\nu\gamma^2\right]\right.$$
$$\left.+C_1\left[-(1+\nu)\ln\left(\frac{1+\sqrt{1+\gamma^2}}{\gamma}\right)+\sqrt{1+\gamma^2}\,(1+\nu)\right]+C_2\right\}$$
$$+\frac{(1+\gamma^2)^{3/8}}{\sqrt{\gamma}}\left\{e^{\tau}\left[C_5\cos\tau+C_6\sin\tau\right]+e^{-\tau}\left[C_7\cos\tau+C_8\sin\tau\right]\right\} \qquad 8.9.1$$

$$u_{ro} \sim \frac{4f^2\rho_o}{3E\sqrt{1+\gamma^2}}\left\{(1+\nu)\left[\gamma\ln\gamma-\frac{1}{\gamma}\right]+\left(\frac{3-\nu}{2}\right)\gamma^3+\frac{1}{4}\gamma^5\right.$$
$$\left.-C_1\gamma\left[(1+\nu)\ln\left(\frac{1+\sqrt{1+\gamma^2}}{\gamma}\right)+(1+\nu)\frac{\sqrt{1+\gamma^2}}{\gamma^2}-\sqrt{1+\gamma^2}\right]+C_2\gamma\right\} \qquad 8.9.2$$

$$N_{ro} \sim \frac{2f\rho_o h}{3}\,\frac{\sqrt{1+\gamma^2}}{\gamma^2}\left\{(1+\gamma^2)^{3/2}+C_1\right\} \qquad 8.9.3$$

$$N_{\theta o} \sim 2f\rho_o h\left\{1-\frac{1}{3\gamma^2\sqrt{1+\gamma^2}}\left[(1+\gamma^2)^{3/2}+C_1\right]\right\}$$
$$-\frac{Eh}{2f}\left\{\frac{1}{\sqrt{\gamma}\,(1+\gamma^2)^{1/8}}\right\}\left\{e^{\tau}\left[C_5\cos\tau+C_6\sin\tau\right]\right.$$
$$\left.+e^{-\tau}\left[C_7\cos\tau+C_8\sin\tau\right]\right\} \qquad 8.9.4$$

$$M_{ro} \sim \frac{D(m+k)^2}{4f^2\sqrt{\gamma}\,(1+\gamma^2)^{1/8}}\left\{e^{\tau}\left[C_5\sin\tau-C_6\cos\tau\right]\right.$$
$$\left.-e^{-\tau}\left[C_7\sin\tau-C_8\cos\tau\right]\right\} \qquad 8.9.5$$

$$M_{\theta o} \sim \frac{\nu D(mk)^2}{4f^2\sqrt{\gamma}\,(1+\gamma^2)^{1/8}} \left\{ e^{\tau}\left[C_5 \sin\tau - \cos\tau \right] - e^{-\tau}\left[C_7 \sin\tau - C_8 \cos\tau \right] \right\} \qquad 8.9.6$$

$$Q_{ro} \sim \frac{D(mk)^3}{8f^3\sqrt{\gamma}\,(1+\gamma^2)^{3/8}} \left\{ e^{\tau}\left[C_5 \cos(\tau-\tfrac{\pi}{4}) + C_6 \sin(\tau-\tfrac{\pi}{4}) \right] - e^{-\tau}\left[C_7 \cos(\tau+\tfrac{\pi}{4}) + C_8 \sin(\tau+\tfrac{\pi}{4}) \right] \right\} \qquad 8.9.7$$

In addition, we will also be interested in the rotation ω_r

$$\omega_{ro} \sim \frac{-\gamma km\,(1+\gamma^2)^{1/8}}{2f\sqrt{\gamma}} \left\{ e^{\tau}\left[C_5 \cos(\tau+\tfrac{\pi}{4}) + C_6 \sin(\tau+\tfrac{\pi}{4}) \right] - e^{-\tau}\left[C_7 \cos(\tau-\tfrac{\pi}{4}) + C_8 \sin(\tau-\tfrac{\pi}{4}) \right] \right\} \qquad 8.9.8$$

u_r^e and N_r^e have been omitted in the expressions (8.9.2) and (8.9.3) for u_r and N_r, respectively, because they are of the order k^{-1} in the presence of the interior solution (see equations (8.8.8) and (8.8.13)). In contrast, ω_r^i, M_r^i, M_θ^i, and Q_r^i which are of order k^{-1}, k^{-2}, k^{-2}, and k^{-3}, respectively, relative to the edge zone solutions, cannot be neglected on the relative order of magnitude basis because they are the dominant terms in the interior of the shell. Nevertheless, these same terms which represent the bending actions of the shell have been omitted since, relative to the membrane actions, they do not contribute significantly to the stresses and distortions of the shell. An alternate derivation of the above results can be found in [12].

The six real constants of integration C_1, C_2, C_5, C_6, C_7 and C_8 can be chosen in such a way that an admissible set of edge conditions is satisfied. Considered herein are boundary conditions

which are commonly called (a) simply supported, (b) clamped, and (c) free.

The simply-supported edge at a fixed value of γ requires the following:

$$u_r = 0 \qquad 8.9.9$$

$$w = 0 \qquad 8.9.10$$

$$M_r = 0 \qquad 8.9.11$$

The clamped edge at a fixed value of γ requires the following:

$$u_r = 0 \qquad 8.9.12$$

$$w = 0 \qquad 8.9.13$$

$$\omega_r = 0 \qquad 8.9.14$$

The free edge at a fixed value of γ requires the following:

$$N_r = 0 \qquad 8.9.15$$

$$M_r = 0 \qquad 8.9.16$$

$$Q_r = 0 \qquad 8.9.17$$

For a more detailed explanation of the boundary conditions, see Section 7.11.

8.10 THE LEADING TERMS OF THE ASYMPTOTIC SOLUTIONS FOR ASYMMETRIC GRAVITY LOADING ($\Psi = \frac{\pi}{2}$)

The leading terms of the asymptotic solutions of a shell whose axis of revolution is perpendicular to the gravity vector are

$$w_1 \sim \frac{8f^2\rho_0}{E}\left\{C_1 g_7(\gamma)+C_2 g_8(\gamma)+C_3 g_9(\gamma)+C_4 g_{10}(\gamma)+g_{11}(\gamma)\right\}\sin\theta$$
$$+\frac{(1+\gamma^2)^{3/8}}{\sqrt{\gamma}}\left\{e^{\tau}\left[C_5\cos\tau+C_6\sin\tau\right]+e^{-\tau}\left[C_7\cos\tau+C_8\sin\tau\right]\right\}\sin\theta \qquad 8.10.1$$

$$u_{r1} \sim \frac{8f^2\rho_0}{E}\left\{C_1 g_4(\gamma)+C_2 g_5(\gamma)-\frac{C_3\gamma^2}{2\sqrt{1+\gamma^2}}+\frac{C_4}{\sqrt{1+\gamma^2}}+g_6(\gamma)\right\}\sin\theta \qquad 8.10.2$$

$$u_{\theta 1} \sim \frac{8f^2\rho_0}{E}\left\{C_1 g_1(\gamma)+C_2 g_2(\gamma)+\frac{C_3\gamma^2}{2}+C_4+g_3(\gamma)\right\}\cos\theta \qquad 8.10.3$$

$$N_{r1} \sim -4f\rho_0 h\left\{\frac{(1+\gamma^2)^3}{15\gamma^3}+\frac{C_1\sqrt{1+\gamma^2}}{2\gamma}+\frac{C_2\sqrt{1+\gamma^2}}{\gamma^3}\right\}\sin\theta \qquad 8.10.4$$

$$N_{\theta 1} \sim 4f\rho_0 h\left\{\frac{\gamma}{2}+\frac{(1+\gamma^2)^2}{15\gamma^3}+\frac{C_1}{2\gamma\sqrt{1+\gamma^2}}+\frac{C_2}{\gamma^5\sqrt{1+\gamma^2}}\right\}\sin\theta$$
$$-\frac{Eh}{2f\sqrt{\gamma}(1+\gamma^2)^{1/8}}\left\{e^{\tau}\left[C_5\cos\tau+C_6\sin\tau\right]+e^{-\tau}\left[C_7\cos\tau+C_8\sin\tau\right]\right\}\sin\theta \qquad 8.10.5$$

$$N_{r\theta 1} \sim 4f\rho_0 h\left\{\frac{C_2}{\gamma^3}-\frac{C_1}{2\gamma}+\frac{(1-4\gamma^2)(1+\gamma^2)^{3/2}}{15}\right\}\cos\theta \qquad 8.10.6$$

$$M_{r1} \sim \frac{D(m+k)^2}{4f^2\sqrt{\gamma}(1+\gamma^2)^{1/8}}\left\{e^{\tau}\left[C_5\sin\tau-C_6\cos\tau\right]-e^{-\tau}\left[C_7\sin\tau-C_8\cos\tau\right]\right\}\sin\theta \qquad 8.10.7$$

$$M_{\theta 1} \sim \frac{\nu D(m+k)^2}{4f^2\sqrt{\gamma}(1+\gamma^2)^{1/8}}\left\{e^{\tau}\left[C_5\sin\tau-C_6\cos\tau\right]-e^{-\tau}\left[C_7\sin\tau-C_8\cos\tau\right]\right\}\sin\theta \qquad 8.10.8$$

$$M_{r\theta 1} \sim \frac{-D(1-\nu)(m+k)(1+\gamma^2)^{1/8}}{4f^2(\gamma)^{3/2}}\left\{e^{\tau}\left[C_5\cos(\tau+\tfrac{\pi}{4})+C_6\sin(\tau+\tfrac{\pi}{4})\right]\right.$$
$$\left.-e^{-\tau}\left[C_7\cos(\tau-\tfrac{\pi}{4})+C_8\sin(\tau-\tfrac{\pi}{4})\right]\right\}\cos\theta \qquad 8.10.9$$

$$Q_{r1} \sim \frac{D(m+k)^3}{8f^3\sqrt{\gamma}(1+\gamma^2)^{3/8}}\left\{e^{\tau}\left[C_5\cos(\tau-\tfrac{\pi}{4})+C_6\sin(\tau-\tfrac{\pi}{4})\right]\right.$$
$$\left.-e^{-\tau}\left[C_7\cos(\tau+\tfrac{\pi}{4})+C_8\sin(\tau+\tfrac{\pi}{4})\right]\right\}\sin\theta \qquad 8.10.10$$

$$Q_{\theta 1} \sim \frac{D(m+k)^2}{8f^3\gamma^{3/2}(1+\gamma^2)^{1/8}}\left\{e^{\tau}\left[C_5\sin\tau - C_6\cos\tau\right]\right.$$
$$\left. -e^{-\tau}\left[C_7\sin\tau - C_8\cos\tau\right]\right\}\cos\theta \qquad 8.10.11$$

$$\omega_{r1} \sim \frac{-(m+k)(1+\gamma^2)^{1/8}}{2f\sqrt{\gamma}}\left\{e^{\tau}\left[C_5\cos(\tau+\tfrac{\pi}{4}) + C_6\sin(\tau+\tfrac{\pi}{4})\right]\right.$$
$$\left. -e^{-\tau}\left[C_7\cos(\tau-\tfrac{\pi}{4}) + C_8\sin(\tau-\tfrac{\pi}{4})\right]\right\}\sin\theta \qquad 8.10.12$$

$$\omega_{\theta 1} \sim \frac{-8f^2\rho_0}{2f\gamma E}\left[C_1 g_1(\gamma) + C_2 g_8(\gamma) + C_3 g_9(\gamma) + C_4 g_{10}(\gamma) + g_{11}(\gamma)\right]$$
$$\left. + \frac{(1+\gamma^2)^{3/8}}{\sqrt{\gamma}}\left[e^{\tau}(C_5\cos\tau + C_6\sin\tau) + e^{-\tau}(C_7\cos\tau + C_8\sin\tau)\right]\right\}\cos\theta \qquad 8.10.13$$

where

$$g_1(\gamma) = \frac{(1+\gamma^2)^{3/2}}{6} - (1+\nu)\left[\sqrt{1+\gamma^2} + \ln(\sqrt{1+\gamma^2}-1) - \ln(\gamma)\right] \qquad 8.10.14$$

$$g_2(\gamma) = \frac{(1-\nu)\gamma^2}{4}\ln\left(\frac{\sqrt{1+\gamma^2}-1}{\gamma}\right) + \frac{(1-\nu)}{4}(1+\sqrt{1+\gamma^2}) - \frac{(1+\nu)(1+\gamma^2)^{3/2}}{2\gamma^2} \qquad 8.10.15$$

$$g_3(\gamma) = \frac{\gamma^6}{360} - \frac{(40+29\nu)}{240}\gamma^4 - \frac{(1+\nu)}{30\gamma^2} - \frac{(1-\nu)}{120}\gamma^2 + \ln\gamma\left[\frac{(1-\nu)}{60}\gamma^2 - \frac{(1+\nu)}{3}\right] \qquad 8.10.16$$

$$g_4(\gamma) = \frac{g_1(\gamma)}{\sqrt{1+\gamma^2}} - \frac{f_1(\gamma)\gamma}{\sqrt{1+\gamma^2}} - (1+\nu) \qquad 8.10.17$$

$$g_5(\gamma) = \frac{g_2(\gamma)}{\sqrt{1+\gamma^2}} - \frac{f_2(\gamma)\gamma}{\sqrt{1+\gamma^2}} + \frac{2(1+\nu)}{\gamma^2} \qquad 8.10.18$$

$$g_6(\gamma) = \frac{g_3(\gamma)}{\sqrt{1+\gamma^2}} - \frac{f_3(\gamma)\gamma}{\sqrt{1+\gamma^2}} + \frac{2(1+\nu)(1-4\gamma^2)(1+\gamma^2)^{3/2}}{15\gamma^2} \qquad 8.10.19$$

$$g_7(\gamma) = \frac{1}{\gamma}\left\{g_4(\gamma) - \sqrt{1+\gamma^2}\,g_1(\gamma) - \frac{(1+\nu)}{2} - \frac{\nu\gamma^2}{2}\right\} \qquad 8.10.20$$

$$g_8(\gamma) = \frac{1}{\gamma}\left\{g_5(\gamma) - \sqrt{1+\gamma^2}\,g_2(\gamma) - \frac{1}{\gamma^2}(1+\nu) - \nu\right\} \qquad 8.10.21$$

$$g_9(\gamma) = \frac{-\gamma}{\sqrt{1+\gamma^2}}\left\{1 + \frac{\gamma^2}{2}\right\} \qquad 8.10.22$$

$$q_{10}(\gamma) = \frac{-\gamma}{\sqrt{1+\gamma^2}} \qquad 8.10.23$$

$$q_{11}(\gamma) = \frac{1}{\gamma}\left\{ q_6(\gamma) - \sqrt{1+\gamma^2}\, q_3(\gamma) - \frac{\sqrt{1+\gamma^2}}{\gamma^2}\left[\frac{\gamma^4}{2} + \frac{(1+\gamma^2)^2}{15} + \frac{\nu(1+\gamma^2)^3}{15}\right]\right\} \qquad 8.10.24$$

$$f_1(\gamma) = \sqrt{1+\gamma^2}\left[\frac{\gamma}{2} - \frac{(1+\nu)}{\gamma}\right] \qquad 8.10.25$$

$$f_2(\gamma) = \frac{(1+\nu)\sqrt{1+\gamma^2}}{\gamma^3}\left[1 - \frac{\gamma^2}{2}\right] + \frac{(1-\nu)\gamma}{2}\left[\ln(\sqrt{1+\gamma^2}-1) - \ln(\gamma)\right] \qquad 8.10.26$$

$$f_3(\gamma) = \frac{(1-\nu)\gamma}{3}\ln(\gamma) + \frac{(1+\nu)}{15\gamma^3} - \frac{(1+\nu)}{3\gamma} - \frac{(40+29\nu)}{60}\gamma^3 + \frac{\gamma^5}{60} \qquad 8.10.27$$

In the derivation of the above results, terms of the order $(k)^{-m}$ $m \geq 1$ are again neglected in the presence of unity for the various reasons discussed in section (8.9). The eight constants of integration C_i, $i = 1, - - - - -, 8$, are to be determined by the boundary conditions which are commonly called (a) simply supported, (b) clamped, and (c) free.

The simply-supported edge at a fixed value of γ requires the following:

$$u_r = 0 \qquad 8.10.28$$

$$u_\theta = 0 \qquad 8.10.29$$

$$w = 0 \qquad 8.10.30$$

$$M_r = 0 \qquad 8.10.31$$

The clamped edge at a fixed value of γ requires the following:

$$u_r = 0 \qquad 8.10.32$$

$$u_\theta = 0 \qquad 8.10.33$$

$$w = 0 \qquad 8.10.34$$

$$\omega_r = 0 \qquad 8.10.35$$

The free edge at a fixed value of γ requires the following:

$$N_r = 0 \qquad 8.10.36$$

$$\frac{M_{r\theta}}{2f\sqrt{1+\gamma^2}} + N_{r\theta} = 0 \qquad 8.10.37$$

$$M_r = 0 \qquad 8.10.38$$

$$Q_r = 0 \qquad 8.10.39$$

8.11 THE LEADING TERMS OF THE ASYMPTOTIC SOLUTIONS FOR A SHELL UNDER UNIFORM PRESSURE

The membrane behavior of a paraboloidal shell of revolution under uniform pressure has been investigated in [33]. The results presented there coupled with the results given in section 8.7 (with n = 0) constitute the leading terms of the asymptotic expansions of the stress resultants, bending moments, and mid-surface displacements which describe the shell behavior under uniform pressure. If the intensity of the pressure is $-q_0$ with respect to the mid-surface of a shell whose normal is assigned to be positive when directed inward, we have

$$w \sim \frac{2f^2 q_0}{Eh}\left\{\left(\frac{5-\nu}{3}\right)(1+\gamma^2)+C_1(1+\nu)\left[1-\frac{1}{\gamma^2}-\frac{1}{\sqrt{1+\gamma^2}}\ln\left(\frac{1+\sqrt{1+\gamma^2}}{\gamma}\right)\right]+\frac{C_2}{\sqrt{1+\gamma^2}}\right\}+\frac{(1+\gamma^2)^{3/8}}{\sqrt{\gamma}}\left\{e^{\tau}\left[C_5\cos\tau+C_6\sin\tau\right]+e^{-\tau}\left[C_7\cos\tau+C_8\sin\tau\right]\right\} \tag{8.11.1}$$

$$u_r \sim \frac{2f^2 q_0}{Eh}\left\{\frac{(2\nu-1)}{3}\gamma^3+\frac{(2\nu+2)}{3}\gamma+C_1\left[\gamma-\frac{(1+\nu)}{\gamma}-\frac{(1+\nu)\gamma}{\sqrt{1+\gamma^2}}\ln\left(\frac{1+\sqrt{1+\gamma^2}}{\gamma}\right)\right]+\frac{C_2\gamma}{\sqrt{1+\gamma^2}}\right\} \tag{8.11.2}$$

$$N_r \sim q_0 f\left\{-\sqrt{1+\gamma^2}+C_1\left[\frac{\sqrt{1+\gamma^2}}{\gamma^2}\right]\right\} \tag{8.11.3}$$

$$N_\theta \sim -q_0 f\left\{\frac{1+2\gamma^2}{\sqrt{1+\gamma^2}}+\frac{C_1}{\gamma^2\sqrt{1+\gamma^2}}\right\}-\left\{\frac{Eh}{2f\sqrt{\gamma}\,(1+\gamma^2)^{1/8}}\right\}\left\{e^{\tau}\left[C_5\cos\tau+C_6\sin\tau\right]+e^{-\tau}\left[C_7\cos\tau+C_8\sin\tau\right]\right\} \tag{8.11.4}$$

$$M_r \sim \frac{D(m\bar{k})^2}{4f^2\sqrt{\gamma}\,(1+\gamma^2)^{1/8}}\left\{e^{\tau}\left[C_5\sin\tau-C_6\cos\tau\right]-e^{-\tau}\left[C_7\sin\tau+C_8\cos\tau\right]\right\} \tag{8.11.5}$$

$$M_\theta \sim \frac{\nu D(mk)^2}{4f^2\sqrt{\gamma}\,(1+\gamma^2)^{1/8}} \left\{ e^{\tau}\left[C_5 \sin\tau - C_6 \cos\tau\right] - e^{-\tau}\left[C_7 \sin\tau - C_8 \cos\tau\right] \right. \qquad 8.11.6$$

$$Q_r \sim \frac{D(mk)^3}{8f^3\sqrt{\gamma}\,(1+\gamma^2)^{3/8}} \left\{ e^{\tau}\left[C_5 \cos(\tau-\tfrac{\pi}{4}) + C_6 \sin(\tau-\tfrac{\pi}{4})\right] - e^{-\tau}\left[C_7 \cos(\tau+\tfrac{\pi}{4}) + C_8 \sin(\tau+\tfrac{\pi}{4})\right] \right\} \qquad 8.11.7$$

$$\omega_r \sim \frac{-(mk)(1+\gamma^2)^{1/8}}{2f\sqrt{\gamma}} \left\{ e^{\tau}\left[C_5 \cos(\tau+\tfrac{\pi}{4}) + C_6 \sin(\tau+\tfrac{\pi}{4})\right] - e^{-\tau}\left[C_7 \cos(\tau-\tfrac{\pi}{4}) + C_8 \sin(\tau-\tfrac{\pi}{4})\right] \right\} \qquad 8.11.8$$

where τ, k, and m are defined by (8.7.20), (8.1.25), and (8.7.2), respectively. C_i, i = 1, 2, ----8, are constants of integration.

8.12 THE SINGULARITY AT THE APEX

The presence of a large parameter k^4 has led to an asymptotic analysis of the solution to the shell equations. Implicit in this analysis is an assumption concerning the order of magnitude of the coefficients associated with the differential equations. Observe that if, in (8.2.18), $\phi^2(t)$ vanishes for some t_o, $a \leq t_o \leq b$, while $q_o(t_o) \neq 0$, then whatever the magnitude of k^2, the term $k^2\phi^2$ fails to remain significant relative to q at $t = t_o$. In fact, if ϕ^2 is continuous, then for a fixed finite k, however large, there exists a δ such that

$$|k^2\phi^2(t)| \leq |q(t)| \qquad 8.12.1$$

for $|t-t_o| < \delta$. Thus, for $|t-t_o| < \delta$, the formal asymptotic solution (8.2.20) would cease to be meaningful.

An examination of (8.1.4), (8.1.5), and (8.1.6) reveals that some of the a°_{ij}, b°_{ij}, and c°_{ij} vanish at $\gamma = 0$, i.e., the apex of the shell, while the corresponding a_{ij}, b_{ij}, and c_{ij} do not. Thus, there will be some neighborhood surrounding the apex in which the asymptotic solutions obtained in section 8.8 cannot be used to describe the behavior of the shell. A method of asymptotic integration has been developed by R. E. Langer, yielding a solution which is valid at the singularity $\gamma = 0$ (cf. [40], [41]). Using Langer's results, C. N. DeSilva investigated the axi-symmetric deformation (including the transverse shear deformations) of a paraboloidal shell of revolution and derived the leading terms of the asymptotic representations of the rotation, $\omega_r(\gamma)$, and the horizontal stress resultant, $H(\gamma)$, which are valid for $0 \leq a \leq \gamma \leq b \leq \infty$ [42]. The other stress resultants, bending

moments and middle surface displacements are derivable from ω_r and H. These quantities are all in the form of the appropriate Bessel functions with argument $k\,\Delta(\gamma)$ where $\Delta \to 0$ as $\gamma \to 0$. It is not difficult to verify that the results given in section 8.8 for $n = 0$ are just those obtained by DeSilva with the Bessel functions replaced by the first term of their asymptotic expansions and the transverse shear deformability suppressed. While the asymptotic representations of the Bessel functions cease to be meaningful as $\gamma \to 0$, the Bessel functions themselves remain unaffected.

An asymptotic solution to the shell equations which is valid at the apex and without the restriction of axi-symmetry has also been obtained by C. R. Steele (cf. [43]). But, since the region in which our asymptotic solutions (given in section 8.8) are erroneous is extremely small for a thin shell (see discussions of results) and since the exact behavior of the shell at the apex can be deduced from the differential equations, the behavior near the apex can be obtained to a good approximation by simple interpolations. For engineering purposes, it is not necessary to perform the proposed refined asymptotic analysis, although such an analysis would offer a better understanding of the behavior of the shell near and at the apex. For instance, it can be concluded from the results of this refined analysis that the condition of finiteness at $\gamma = 0$ requires the vanishing of the constants C_7 and C_8 in the results listed in section 8.7. The relatively large amount of computer time needed for the use of the double precision Bessel function subroutines was also a strong factor in our decision not to extend the present analysis.

INTRODUCTION TO NUMERICAL RESULTS

Numerical calculations are presented in curve form in the subsequent nine sections. It is, of course, impossible to anticipate all the configurations which may be of interest to the antenna designer. However, a fairly wide range of sizes are covered and, additionally, the results are presented in normalized form. These results can be used to determine the magnitude of displacements (and stresses) for purposes of preliminary design. A more detailed analysis of a specific configuration can be made by use of the digital computer programs which have been developed for this report.

The results, in addition to being used for numerical data, also illustrate the behavior of paraboloidal surface structures. Most of the text accompanying each of the nine groups discusses various aspects of the shell behavior which have been revealed by the numerical calculations. In general, the shells exhibit the same qualitative behavior as that given by a shallow shell analysis(reference Part III) but there are some significant differences.

An attempt has been made to present the results in a uniform manner but deviations will be noted to accommodate the specifics of each group. Dimensions and boundary conditions are presented in tables. Both the symmetric and anti-symmetric behavior under gravity loads are shown with the former corresponding to a pointing angle of $\psi = 0°$ and the latter to $\psi = 90°$. The curves, in addition to three groups of numbers, bear the letter s, meaning symmetric and a, meaning anti-symmetric, e.g., figure 8.13.1.1s and figure 8.13.5.1a. Some of the parameters such as

Q_r^* and M_r^* tend to overlap if plotted on the same scale. These have been separated in the interest of identifying each curve but there may be some confusion regarding the scales. However, a careful second examination of each figure should be sufficient to relate each curve with the proper ordinate and abscissa scales.

The normalizing factors are as follows (see section 7.12):

$$N_r^* = \frac{N_r}{2f\rho_o h}$$

$$N_\theta^* = \frac{N_\theta}{2f\rho_o h}$$

$$N_{r\theta}^* = \frac{N_{r\theta}}{2f\rho_o h}$$

$$M_r^* = \frac{M_r}{2f\rho_o h^2}$$

$$M_\theta^* = \frac{M_\theta}{2f\rho_o h^2}$$

$$M_{r\theta}^* = \frac{M_{r\theta}}{2f\rho_o h^2}$$

$$w^* = \frac{wE}{4f^2\rho_o}$$

$$u_r^* = \frac{u_r E}{4f^2\rho_o}$$

$$u_\theta^* = \frac{u_\theta E}{4f^2\rho_o}$$

$$Q_r^* = \frac{Q_r}{\rho_o h\sqrt{2fh}}$$

$$Q_\theta^* = \frac{Q_\theta}{\rho_o h\sqrt{2fh}}$$

$$\omega_r^* = \frac{\omega_r E}{2f\rho_o}\sqrt{\frac{h}{2f}}$$

$$\omega_\theta^* = \frac{\omega_\theta E}{2f\rho_o}\sqrt{\frac{h}{2f}}$$

8.13 Group I -- Four Closed Shells with Outer Edges of γ = .20, .40, .80, 1.20

The Group I results presented in this section illustrate the behavior of four shells, closed at the apex, which differ only in their outer radii. Dimensions and other pertinent data are presented in Table 8.13.1. The four outer radii are 230.4, 460.8, 921.6, and 1382.4 inches which, since the focal length is 576 inches, result in slopes at the outer edges of γ = .20, .40, .80, and 1.20, respectively.

An examination of figure 8.13.1s reveals the very interesting result that the maximum deflections are a somewhat unconventional function of the outer radius. A table of maximum deflection (w^*_{max}) for different shells under symmetric loading vs. the position where it takes place (γ_m) is shown below:

Table 8.13.2

γ_2	w^*_{max} Symmetric Loading w^*_{max}	γ_m
.20	-.417	.144
.40	-.411	.348
.80	-.609	0
1.20	-1.043	0

We observe that case 2s with the outer edge at γ_2 = .40 experiences a w^*_{max} which is actually less than that experienced by the smaller shell (case 1s). Furthermore, case 4s, which is a shell having a diameter three times that of case 2s, experiences deflections only 2.5 times that of case 2s. Generally speaking, with the same relative increase in length, the transverse deflections of beams and plates which vary as the square of the span length would yield deflections nine times greater. Hence, these results clearly illustrate the stiffness advantage of a shell

structure over that of beams or plates.

Note also that the edge zone behavior for the two smaller shells causes a hump in the deflection curve which places the maximum deflection near the outer boundary. The hump is more pronounced in case 1s than in 2s. The edge zone behavior is also clearly visible for the two larger shells although the hump is overshadowed by the interior behavior.

A better indication of the edge zone behavior is given by the plots of M_θ^*, M_r^*, and Q_r^*. We observe that d, the width of the edge zone, is approximately the same for all four sizes and agrees well with the result, $\frac{d}{2f} \approx .006°$ (see equation 7.12.1.1) given by

$$\frac{d}{2f} \approx 2\sqrt{\frac{h}{2f}} \qquad 8.13.1$$

The maximum values of these quantities which characterize the bending behavior occurring in the edge zone, i.e., M_θ^*, M_r^*, and Q_r^*, decrease as the outer radius increases. This means that the bending stresses will be larger for a smaller shell.

The manner in which the curves of N_r^* and N_θ^* coincide should also be noted. This, again, illustrates the membrane behavior of the shell. As has been previously described (see sections 7.12.1) the shell prefers to carry the applied loads by membrane action; bending action takes place near the edges in order to satisfy practical geometrical constraints. Hence, the interiors of shells will develop nearly the same values of N_r^* and N_θ^* providing the edge zone widths are not a major proportion of the total radii.

The anti-symmetric results are shown in figures 8.13.5 through 8.13.11. We note for all except the smallest shell that the displacements

for the anti-symmetric gravity loading are larger than for the symmetric situation. For the two larger shells, the maximum anti-symmetric deflections are more than twice as large. This can be attributed to the unfavorable orientation of the gravity vector relative to the surface of the shell resulting in appreciable components of loading in the radial and tangential directions (see equations 8.6.1, 8.6.2, and 8.6.3). These components cause larger membrane loads which, in turn, make more severe the bending action at the boundary. It should be borne in mind that the asymmetric shell behavior varies either as sin θ or cos θ (see section 8.10).

There are some additional interesting differences and similarities between the symmetric and anti-symmetric behavior to be observed. The force-results N_r^* , N_θ^* , and $N_{r\theta}^*$ again coincide for the four sizes. The widths of the edge zones as shown by the curves of M_r^* and M_θ^* and Q_r^* are essentially identical. However, unlike the symmetric case, the maximum values of the bending quantities increase significantly rather than decrease with the size of the shell. The maximum radial and tangential components of displacement are the same order of magnitude as the normal component. Thus, the calculation of the resultant deflection of a point on the shell must consider the vector addition of u^*, v^*, and w^*.

The quantities Q_θ^* and M_θ^* have not been displayed because of their small magnitudes. For example, for case 4s, the maximum value of Q_θ^* is -.0038 and for $M_{r\theta}^*$, the maximum value is -.00404. Both of these values are at least an order of magnitude smaller than the values for the other transverse shear and bending moments, respectively.

Table 8.13.1

Case	R_1 (inches)	R_2 (inches)	B.C. at R_1	B.C. at R_2	Loading
1s*	0	230.4	----	Simple support	Symmetric-gravity
2s	"	460.8	----	"	"
3s	"	921.6	----	"	"
4s	"	1382.4	----	"	"
1a	"	230.4	----	"	Anti-sym.-gravity
2a	"	460.8	----	"	"
3a	"	921.6	----	"	"
4a	"	1382.4	----	"	"

Note: Material properties are $E = 10^7$ p.s.i., $\nu = .3$, $\rho_o = .10$ lb. per cubic inch.

Focal length $f = 576$ inches, shell thickness $h = 1$ inch.

* Calculated from shallow shell routine (see Chapter 7).

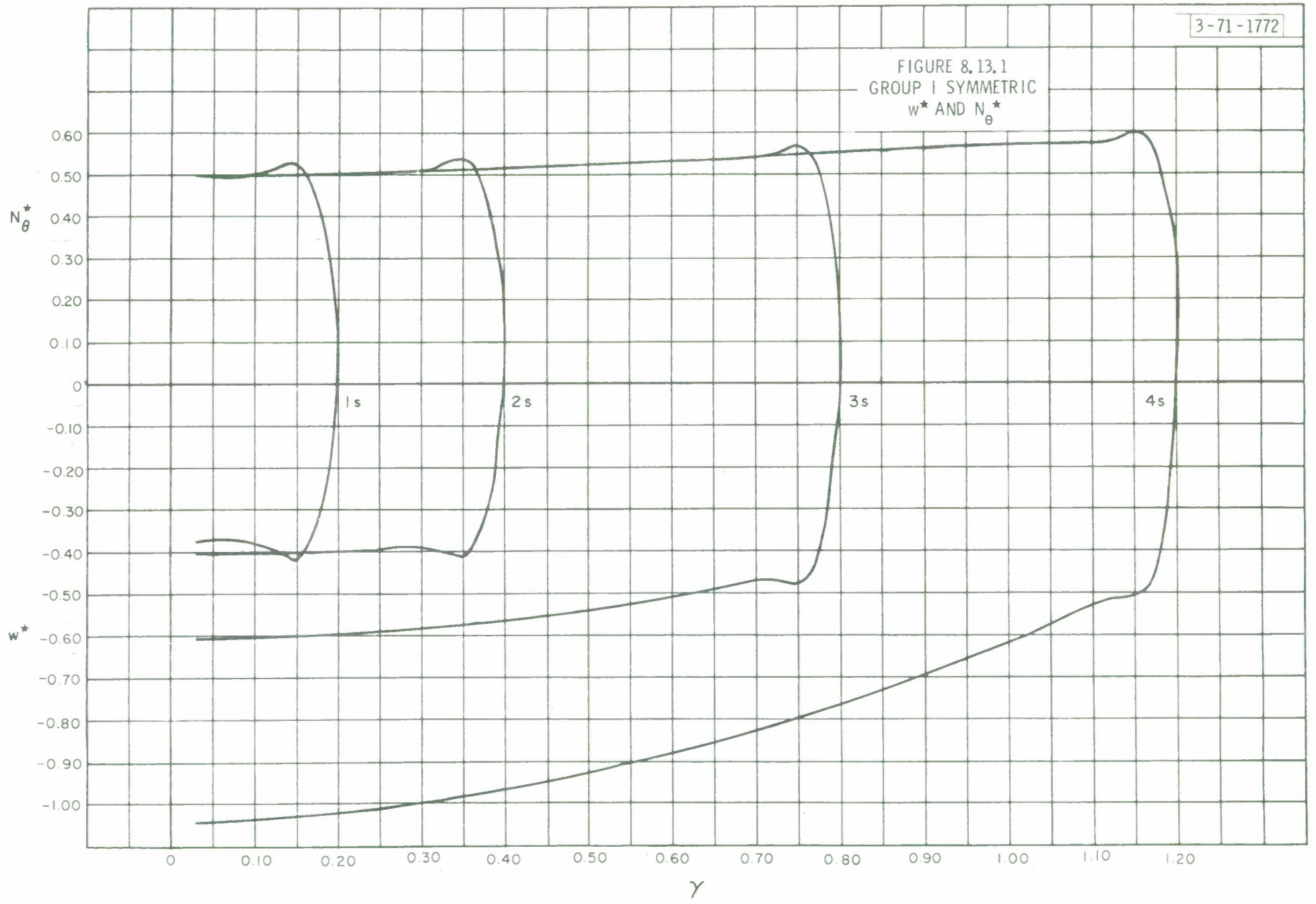
3-71-1772
FIGURE 8.13.1
GROUP I SYMMETRIC
w* AND N_θ*
N_θ^*
w*
0.60
0.50
0.40
0.30
0.20
0.10
0
-0.10
-0.20
-0.30
-0.40
-0.50
-0.60
-0.70
-0.80
-0.90
-1.00
1s
2s
3s
4s
0
0.10
0.20
0.30
0.40
0.50
0.60
0.70
0.80
0.90
1.00
1.10
1.20
γ

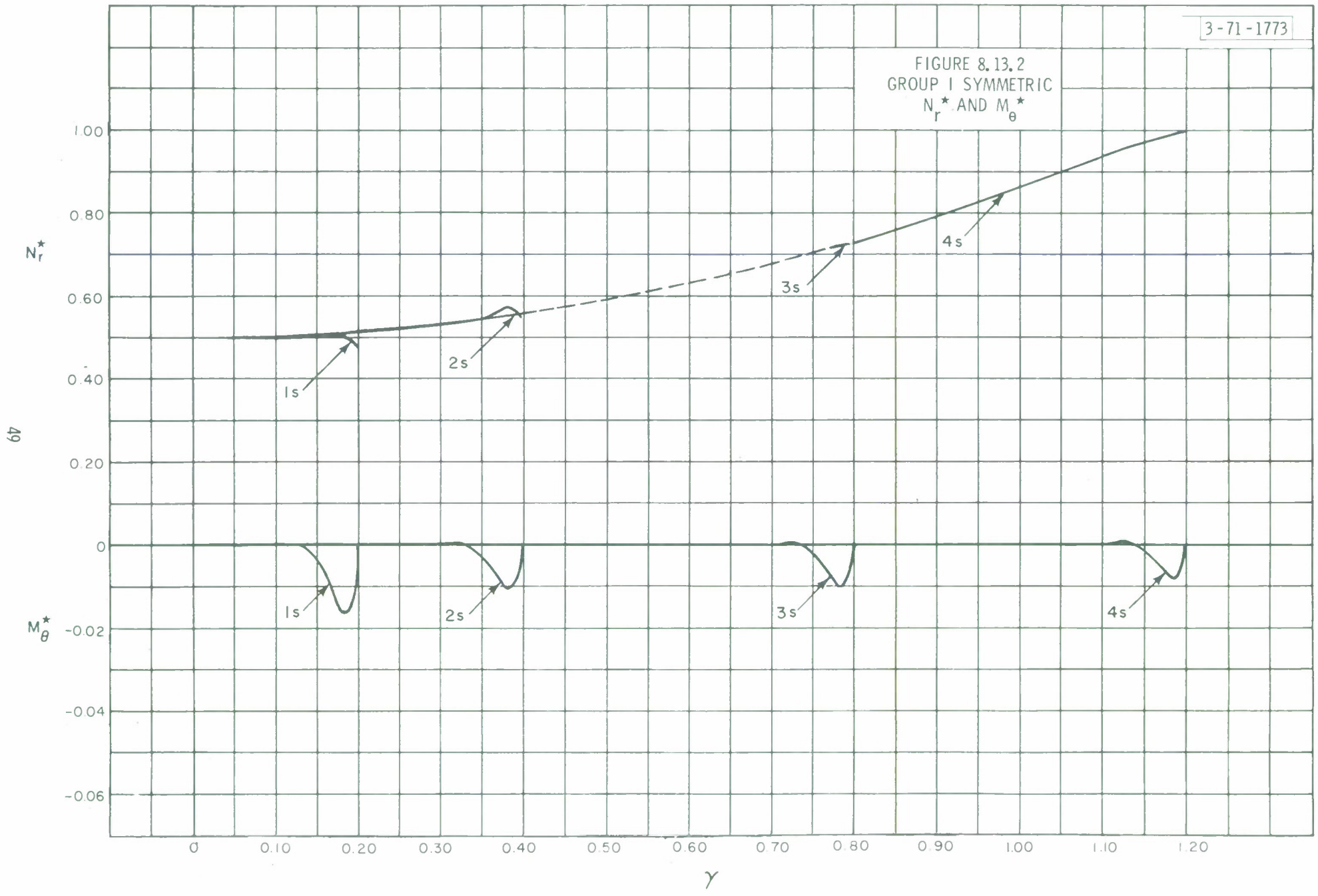
3-71-1773
FIGURE 8.13.2
GROUP I SYMMETRIC
N_r^* AND M_θ^*
N_r^*
M_θ^*
1.00
0.80
0.60
0.40
0.20
0
-0.02
-0.04
-0.06
1s
2s
3s
4s
1s
2s
3s
4s
0
0.10
0.20
0.30
0.40
0.50
0.60
0.70
0.80
0.90
1.00
1.10
1.20
γ

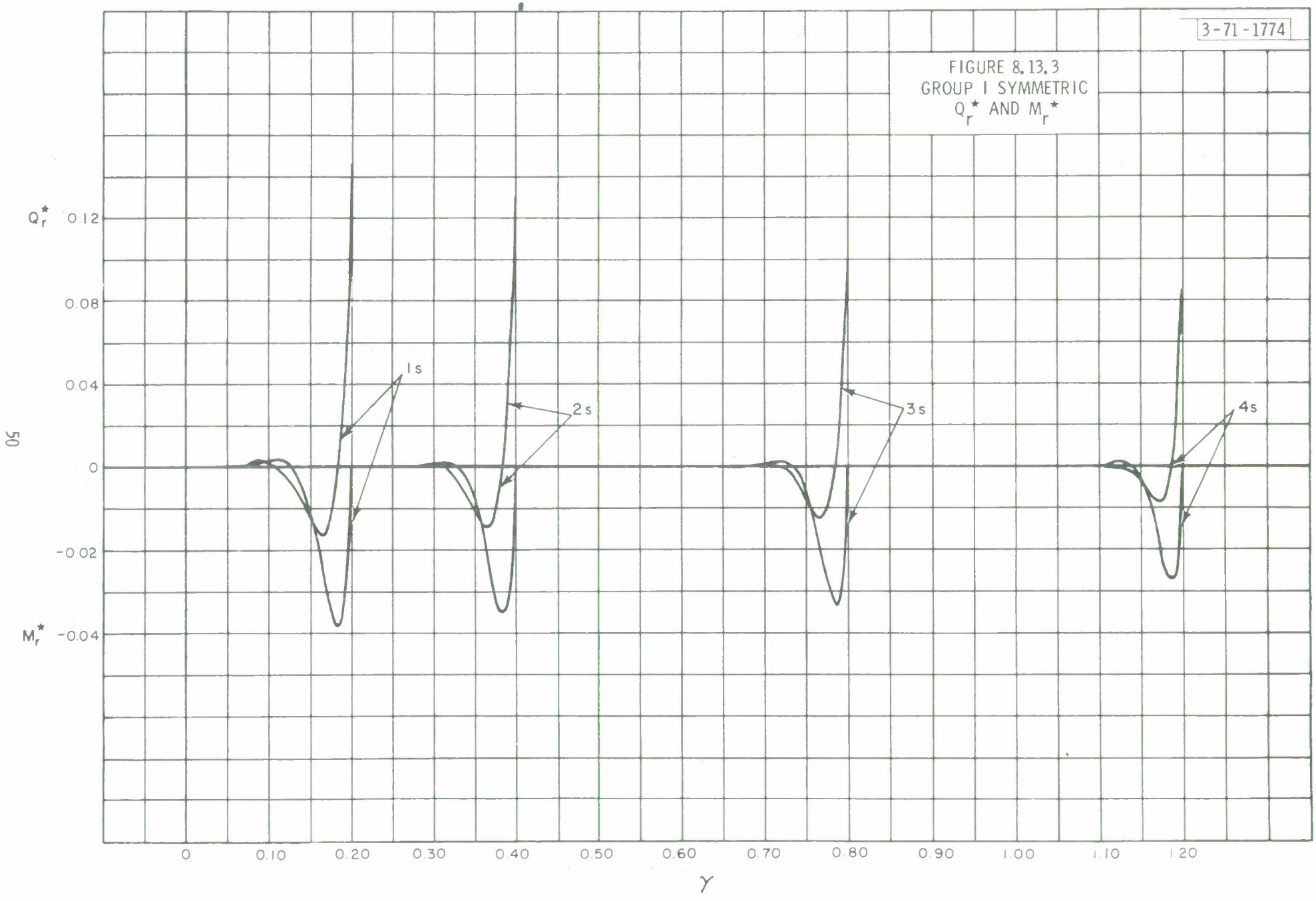
3-71-1774
FIGURE 8.13.3
GROUP I SYMMETRIC
Q_r^* AND M_r^*
Q_r^*
0.12
0.08
0.04
0
-0.02
M_r^*
-0.04
1s
2s
3s
4s
0
0.10
0.20
0.30
0.40
0.50
0.60
0.70
0.80
0.90
1.00
1.10
1.20
γ

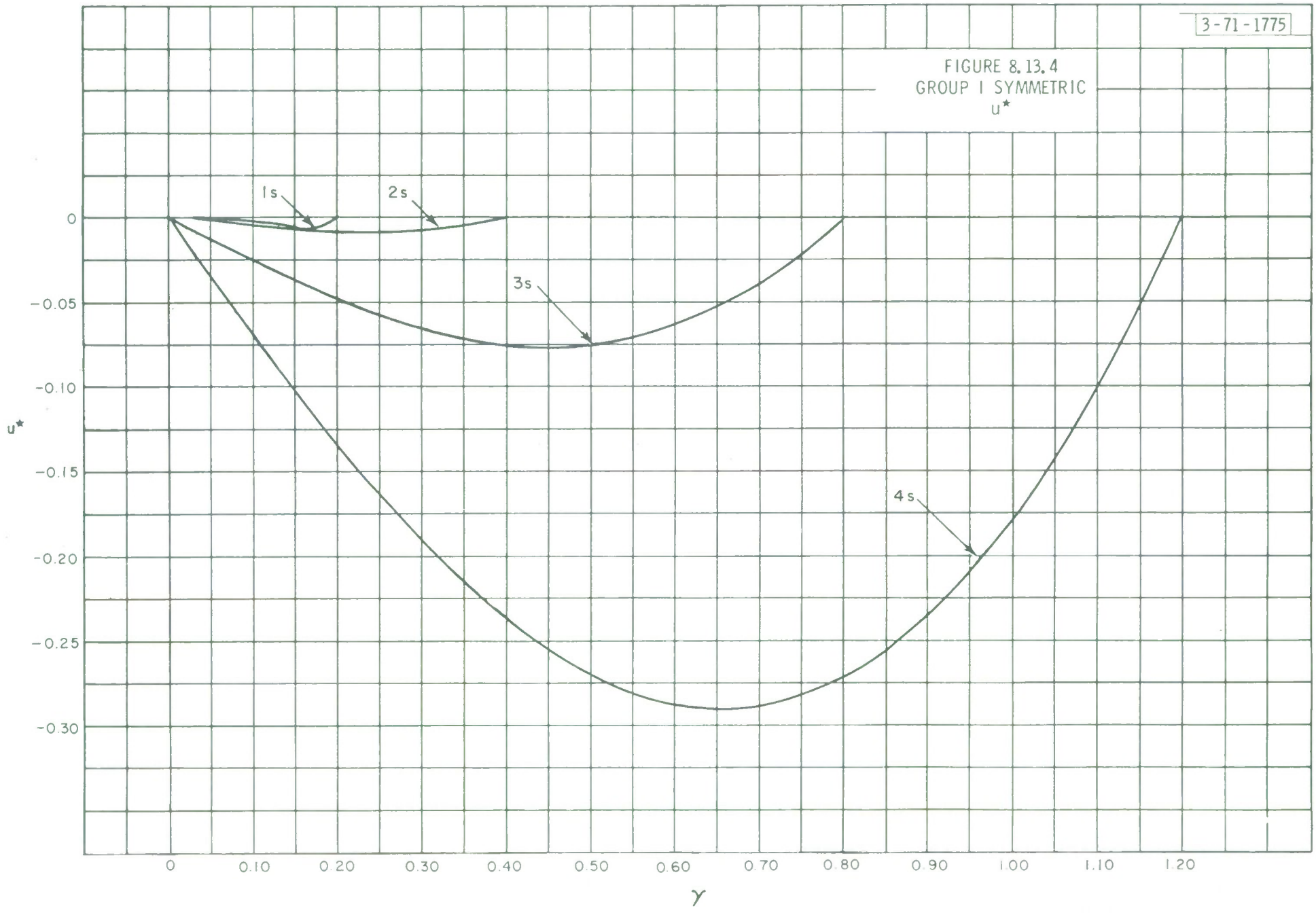
3-71-1775
FIGURE 8.13.4
GROUP I SYMMETRIC
u*
1s
2s
3s
4s
0
-0.05
-0.10
-0.15
-0.20
-0.25
-0.30
ε*
0
0.10
0.20
0.30
0.40
0.50
0.60
0.70
0.80
0.90
1.00
1.10
1.20
γ

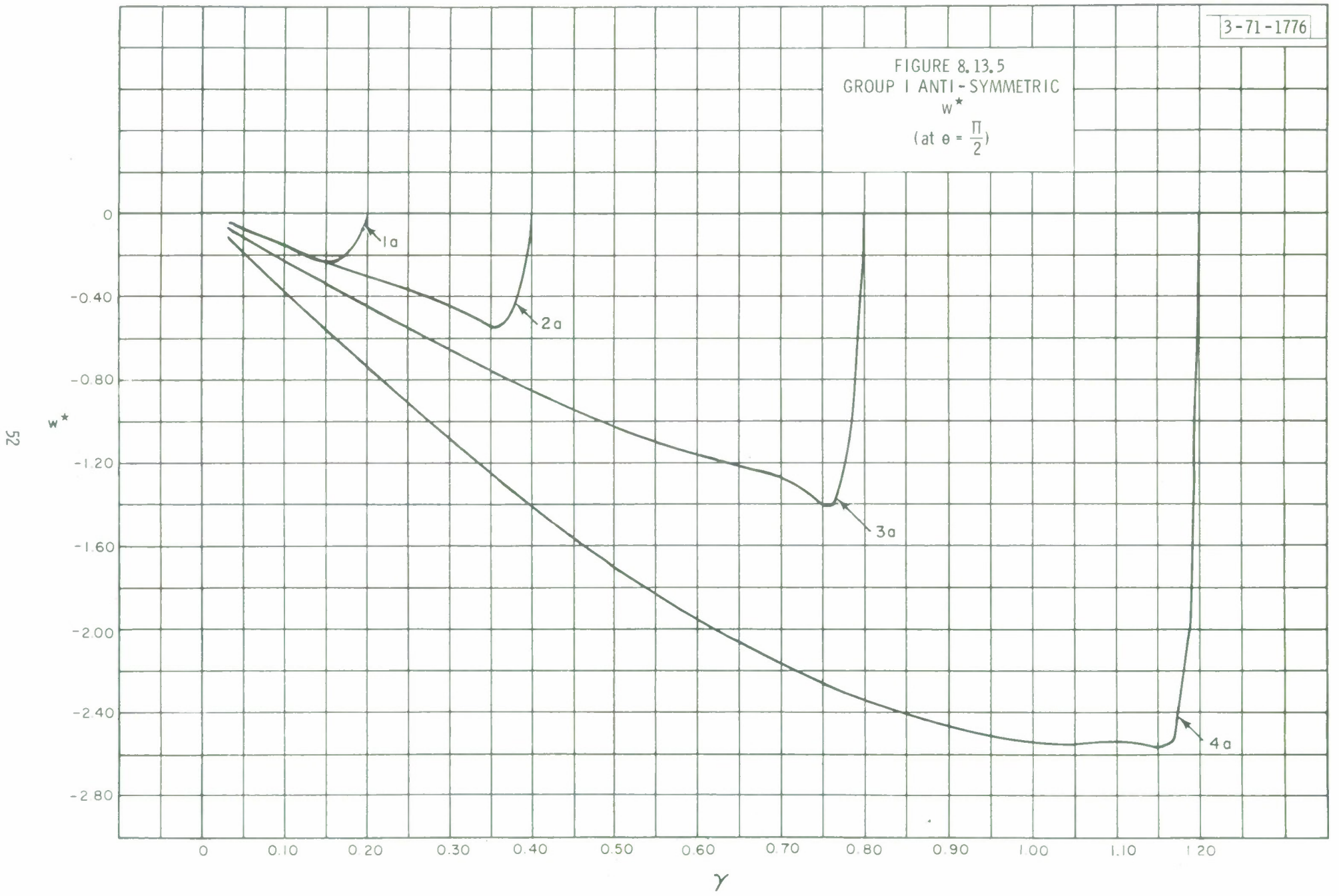
3-71-1776
FIGURE 8.13.5
GROUP I ANTI-SYMMETRIC
w*
(at θ = Π/2)
0
-0.40
-0.80
-1.20
-1.60
-2.00
-2.40
-2.80
w*
0
0.10
0.20
0.30
0.40
0.50
0.60
0.70
0.80
0.90
1.00
1.10
1.20
γ
1a
2a
3a
4a

FIGURE 8.13.6
GROUP I ANTI-SYMMETRIC
N_r^*
(at $\theta = \frac{\pi}{2}$)

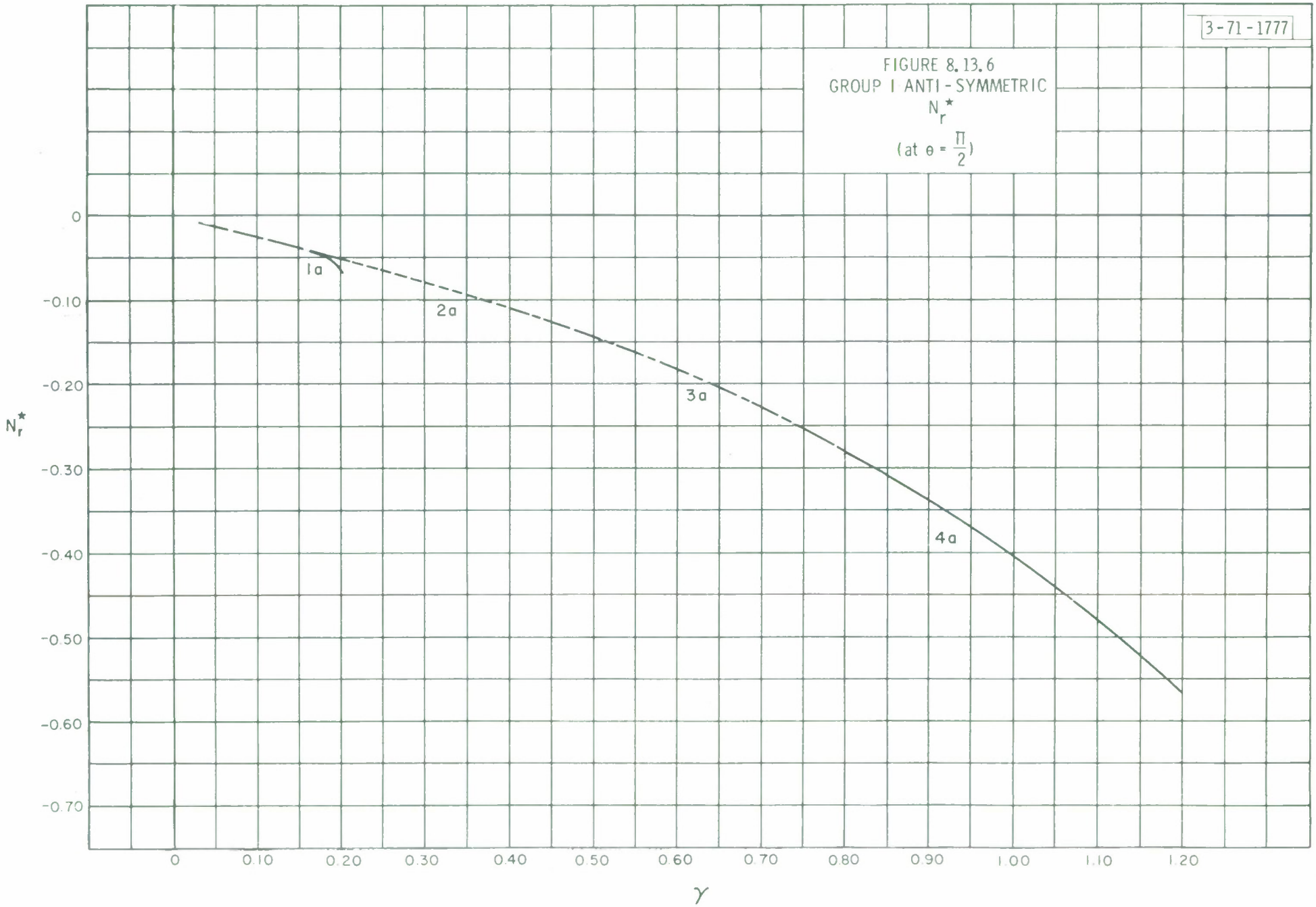

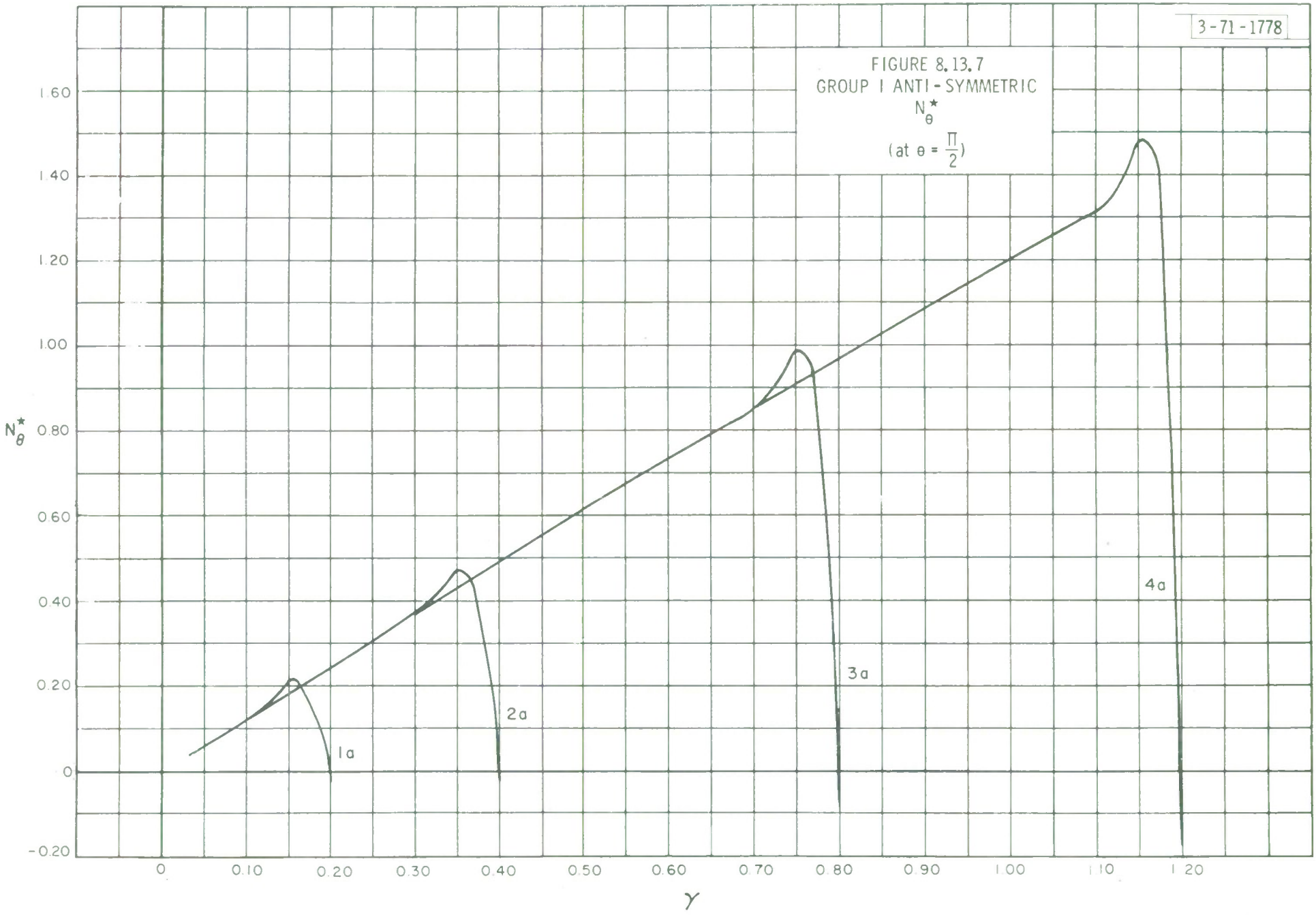
3-71-1778
FIGURE 8.13.7
GROUP I ANTI-SYMMETRIC
$N_\theta^\star$
(at $\theta = \frac{\pi}{2}$)
1.60
1.40
1.20
1.00
0.80
0.60
0.40
0.20
0
-0.20
$N_\theta^\star$
0
0.10
0.20
0.30
0.40
0.50
0.60
0.70
0.80
0.90
1.00
1.10
1.20
γ
1a
2a
3a
4a

3-71-1779

FIGURE 8.13.8
GROUP I ANTI-SYMMETRIC
$N^{\star}_{r\theta}$
(at $\theta = 0$)

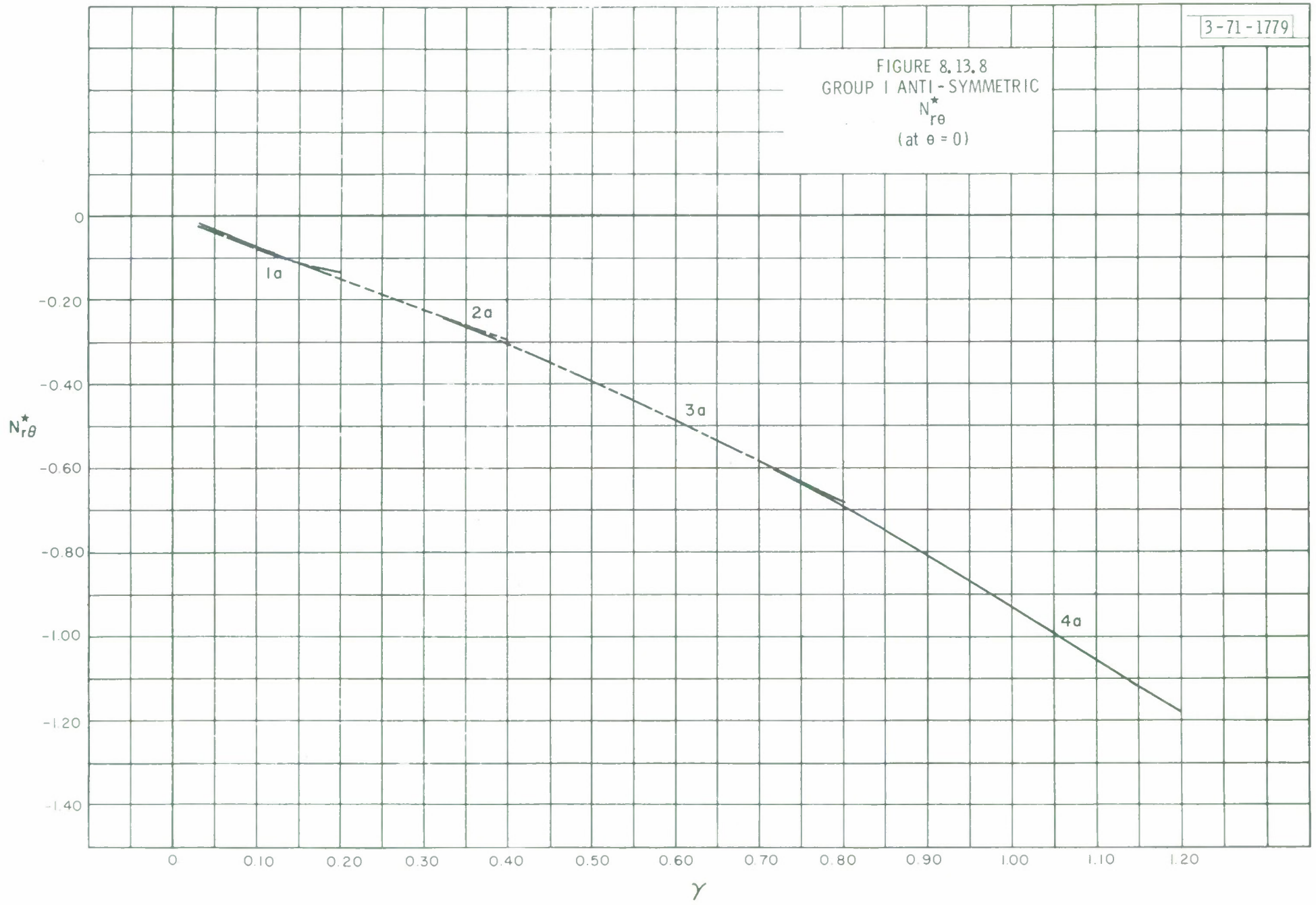

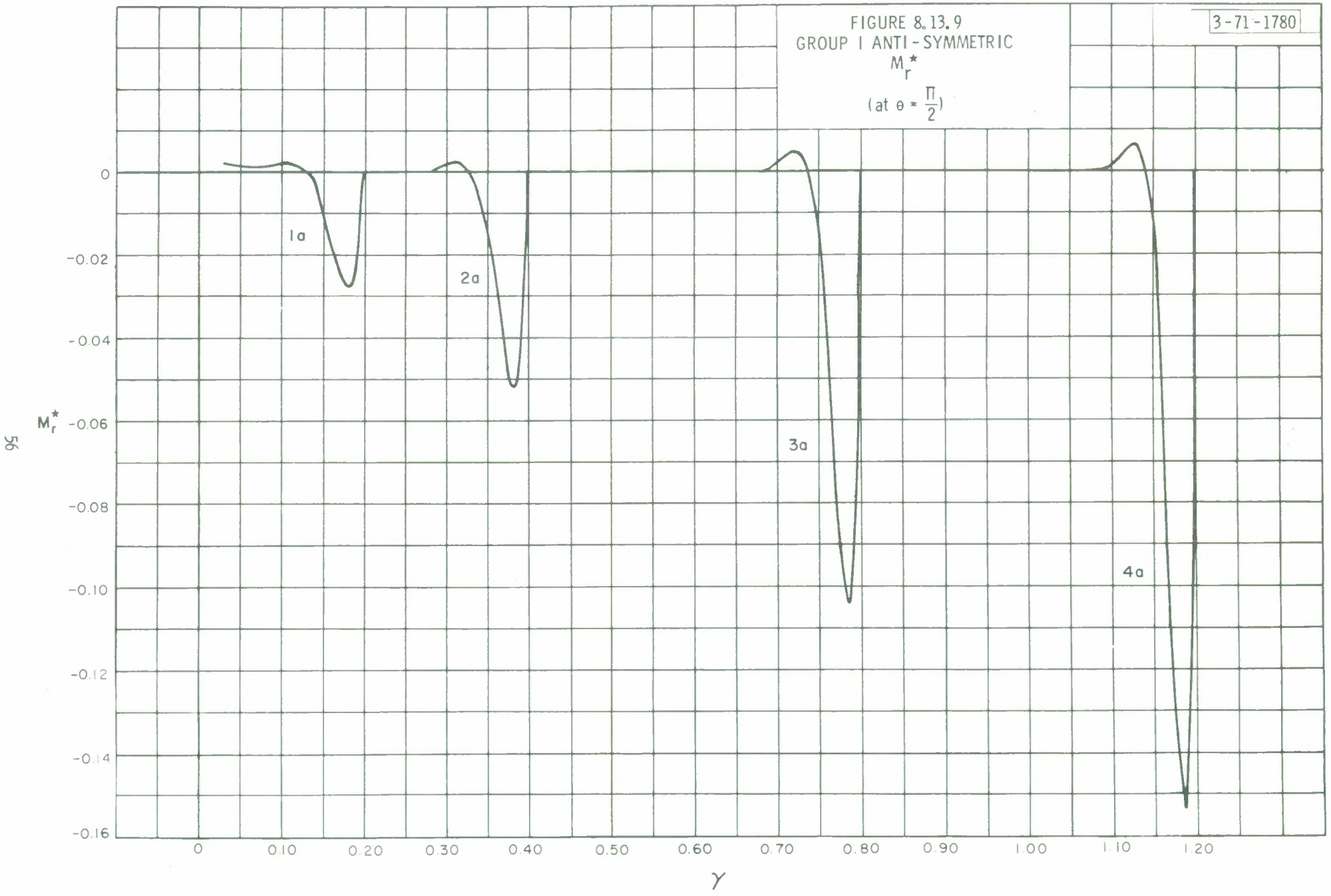
FIGURE 8.13.9
GROUP I ANTI-SYMMETRIC
M_r^*
(at $\theta = \frac{\pi}{2}$)
3-71-1780
0
-0.02
-0.04
-0.06
-0.08
-0.10
-0.12
-0.14
-0.16
M_r^*
1a
2a
3a
4a
0
0.10
0.20
0.30
0.40
0.50
0.60
0.70
0.80
0.90
1.00
1.10
1.20
γ


3-71-1781
FIGURE 8.13.10
GROUP I ANTI-SYMMETRIC
$M_\theta^\star$
(at $\theta = \frac{\pi}{2}$)
1a
2a
3a
4a
0
-0.01
-0.02
-0.03
-0.04
-0.05
-0.06
$M_\theta^\star$
0
0.10
0.20
0.30
0.40
0.50
0.60
0.70
0.80
0.90
1.00
1.10
1.20
γ

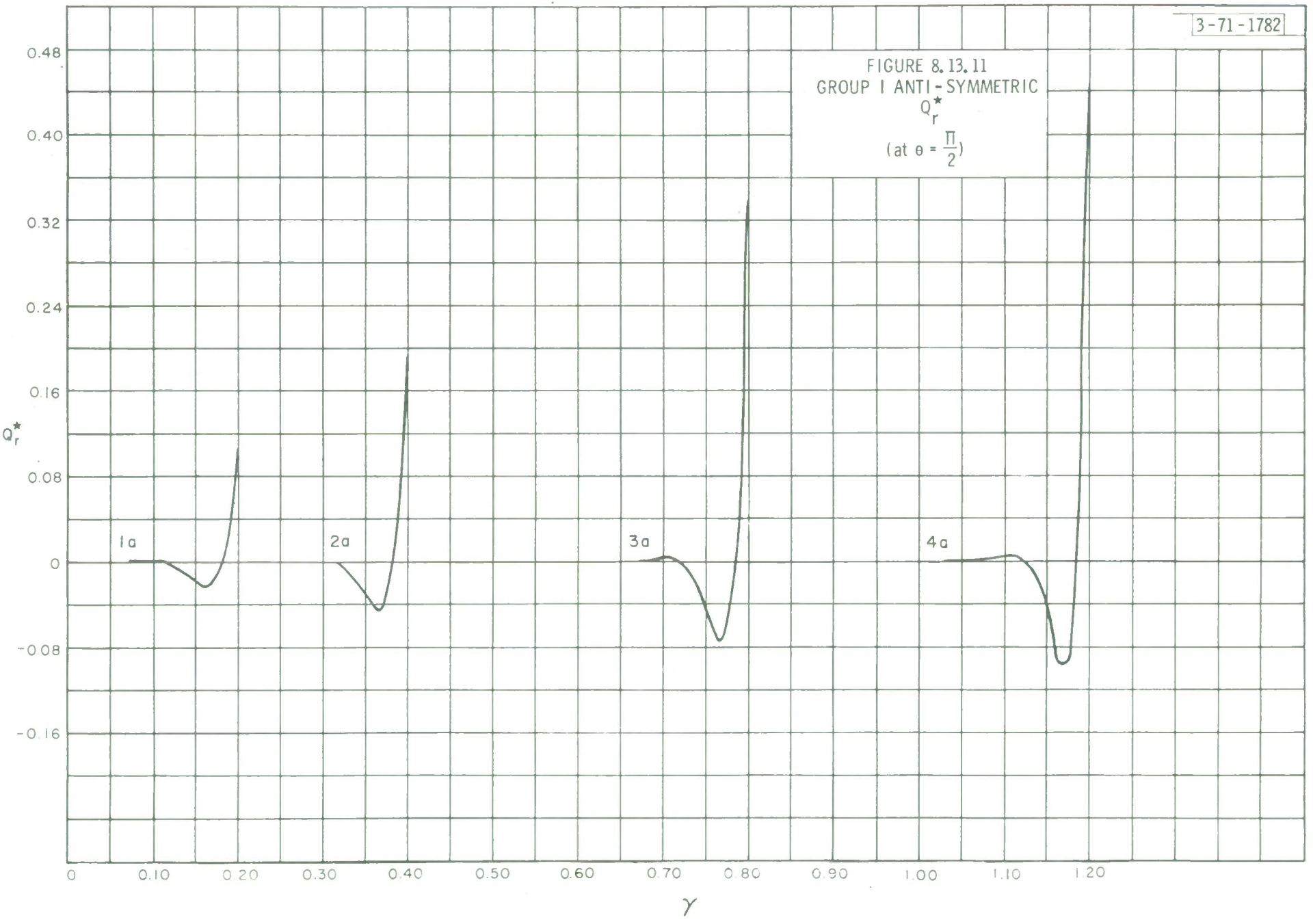
3-71-1782
FIGURE 8.13.11
GROUP I ANTI-SYMMETRIC
Q_r^*
(at $\theta = \frac{\pi}{2}$)
0.48
0.40
0.32
0.24
0.16
0.08
0
-0.08
-0.16
Q_r^*
1a
2a
3a
4a
0
0.10
0.20
0.30
0.40
0.50
0.60
0.70
0.80
0.90
1.00
1.10
1.20
γ

3-71-1783

FIGURE 8.13.12
GROUP I ANTI-SYMMETRIC
u_θ^*
(at $\theta = 0$)

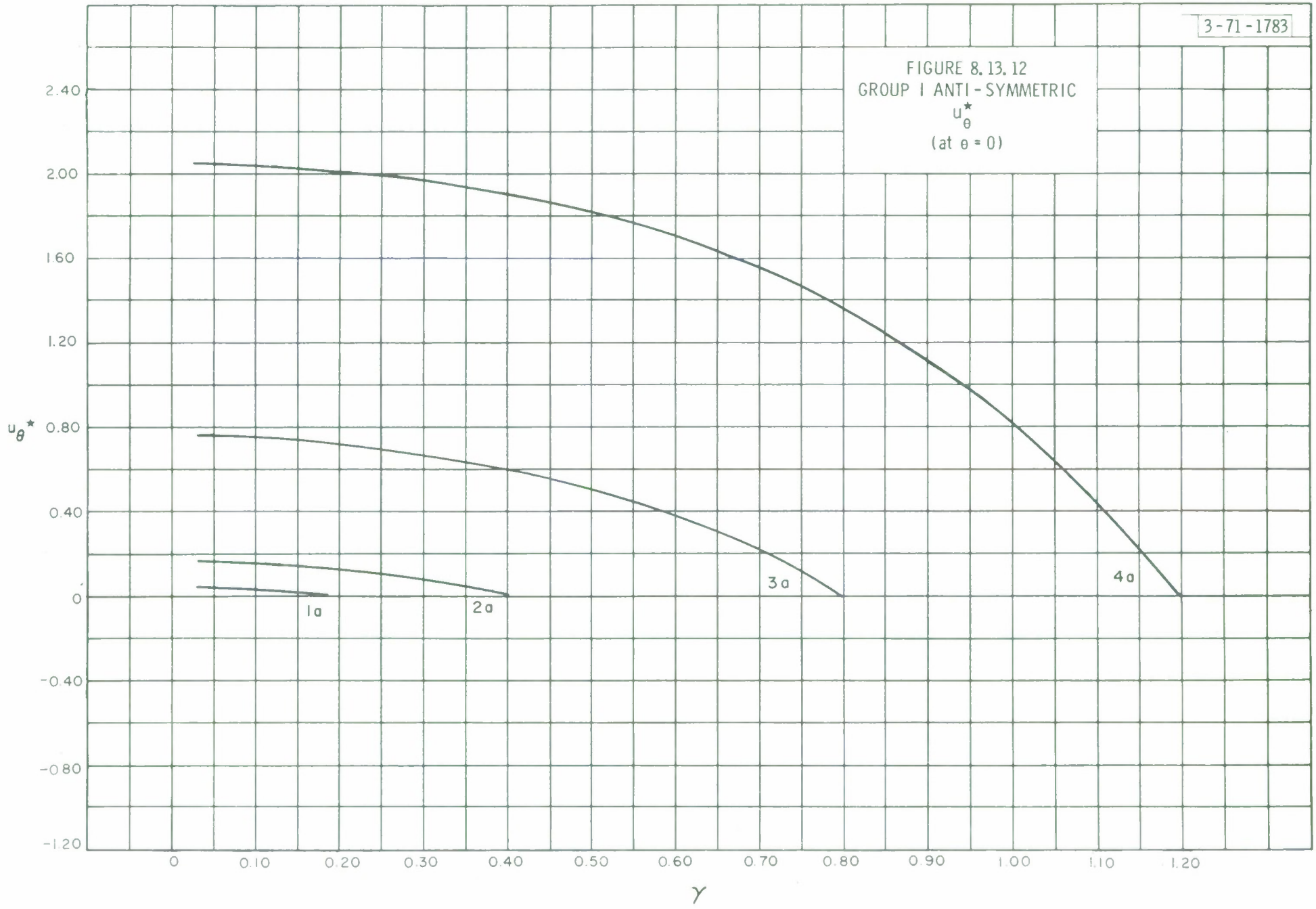

3-71-1784

FIGURE 8.13.13
GROUP I ANTI-SYMMETRIC
u_r^*
(at $\theta = \frac{\pi}{2}$)

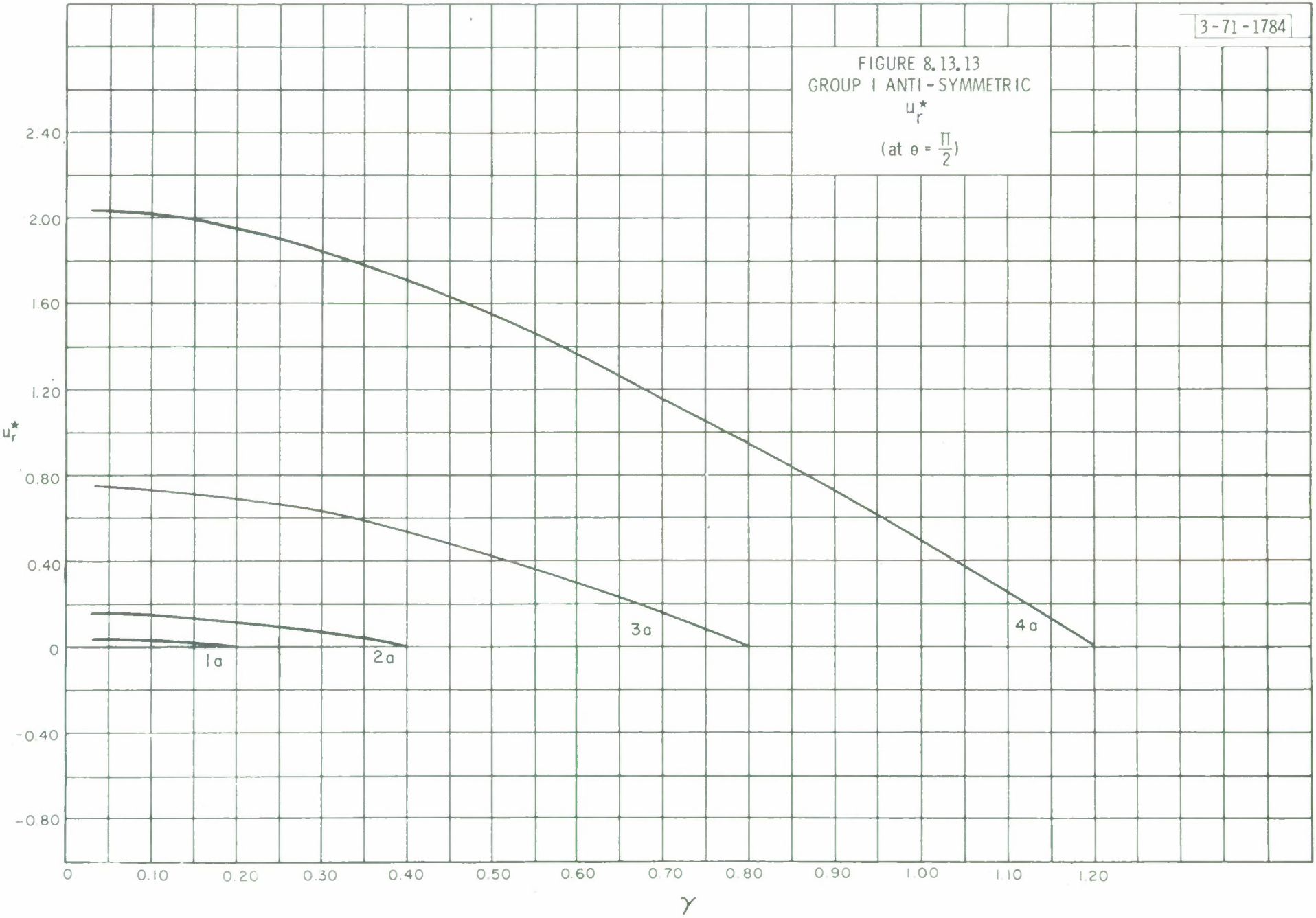

8.14 Group II - Five Shells with an Outer Radius of 460.8 Inches

The results in this section illustrate the behavior of five shells all open at the apex and with the same outer radius of 460.8 inches but terminating at various inner radii. All the shells are simply supported along both edges. Dimensions and other pertinent data are presented in Table 8.14.1. The outer radius is equivalent to a slope of $\gamma = .40$ while the inner radii correspond to $\gamma = .16, .20, .25, .30,$ and $.35$. Both the symmetric and anti-symmetric behavior under gravity loads are presented with the former corresponding to a pointing angle $\psi = 0°$ and the latter to $\psi = 90°$. The curves, in addition to the heading of three groups of numbers (e.g. 8.14.1), bear either the letter s, signifying symmetric behavior or a, signifying anti-symmetric behavior. Results are all in normalized form (see page 43 of this report).

The deflection results shown in figure 8.14.1 for the behavior under a symmetric gravity loading show the same trend as that exhibited by the shallow shells studied in section 7.12.3; namely, that the maximum deflections increase as the span of the shell (we shall define the span to be the difference between the outer and inner radius of the shell) gets smaller. This somewhat unexpected deformation behavior is due to the interaction of the membrane behavior in the interior of the shell and the bending behavior in the edge zones at the boundaries (see section 7.12.3). As can be seen from Table 8.14.2, the deflections for the purely membrane behavior increase with decreasing span. In order to correct the inherent shortcoming of the membrane solution, the asymptotic solution can be visualized as superimposing transverse shear, moments and in-plane forces at the boundaries onto the membrane solution so as to meet the requirement of

zero w^* displacement at the edges. These edge loads induce inextensional behavior (cf. references [44], [45]) in the interior of the shell and it is the inextensional behavior which causes the curves of w^* (see figure 8.14.1) to exhibit humps near the edges.

The curves of the bending moments M_r^* and M_θ^* shown in figures 8.14.3 and 8.14.4 give a clear illustration of the widths of the edge zone at the boundaries of the shell. It is interesting to note that the shapes and magnitudes of each set of the bending moment curves are essentially the same in the edge zone except for case 5s which does not have an edge zone. This latter case exhibits essentially "plate" behavior in that the deformation is predominantly bending. The curve of Q_r^* in figure 8.14.5 for case 5s also indicates "plate" behavior.

The curves for the anti-symmetric behavior in this section are self-explanatory. In all cases, the magnitudes of the various parameters are smaller than their counterparts under symmetric loading.

Table 8.14.1

Group II Examples

Case	R_1 (inches)	R_2 (inches)	B.C. at R_1	B.C. at R_2	Loading
1s	184.32	460.8	Simple support	Simple support	Symmetric-gravity
2s	230.4	"	"	"	"
3s	288.0	"	"	"	"
4s	345.6	"	"	"	"
5s	403.2	"	"	"	"
6s	---	"	---	"	"
1a	184.32	"	Simple support	"	Anti-sym.-gravity
2a	230.4	"	"	"	"
3a	288.0	"	"	"	"
4a	345.6	"	"	"	"
5a	403.2	"	"	"	"

Note: Material properties are $E = 10^7$ p.s.i., $\nu = .3$, $\rho_o = .10$ lb. per cubic inch.

Focal length $f = 576$ inches, shell thickness $h = 1$ inch.

Table 8.14.2

Membrane Solutions for Cases 1s, 2s, 3s and 4s

Case 1s	γ	u_r^*	w^*	N_r^*
	.16	0	-.411	.466
	.22	-.0040	-.407	.495
	.28	-.0054	-.402	.515
	.34	-.0041	-.395	.533
	.40	0	-.386	.552

Case 2s	γ	u_r^*	w^*	N_r^*
	.20	0	-.413	.472
	.25	-.0031	-.409	.495
	.30	-.0040	-.404	.514
	.35	-.0031	-.398	.531
	.40	0	-.391	.548

Case 3s	γ	u_r^*	w^*	N_r^*
	.250	0	-.417	.480
	.288	-.0019	-.414	.498
	.325	-.0025	-.409	.513
	.363	-.0019	-.405	.528
	.400	0	-.399	.542

Case 4s	γ	u_r^*	w^*	N_r^*
	.300	0	-.421	.489
	.325	-.0009	-.419	.502
	.350	-.0012	-.416	.513
	.375	-.0009	-.413	.523
	.400	0	-.409	.534

FIGURE 8.14.1
GROUP II SYMMETRIC
w^* AND N_θ^*

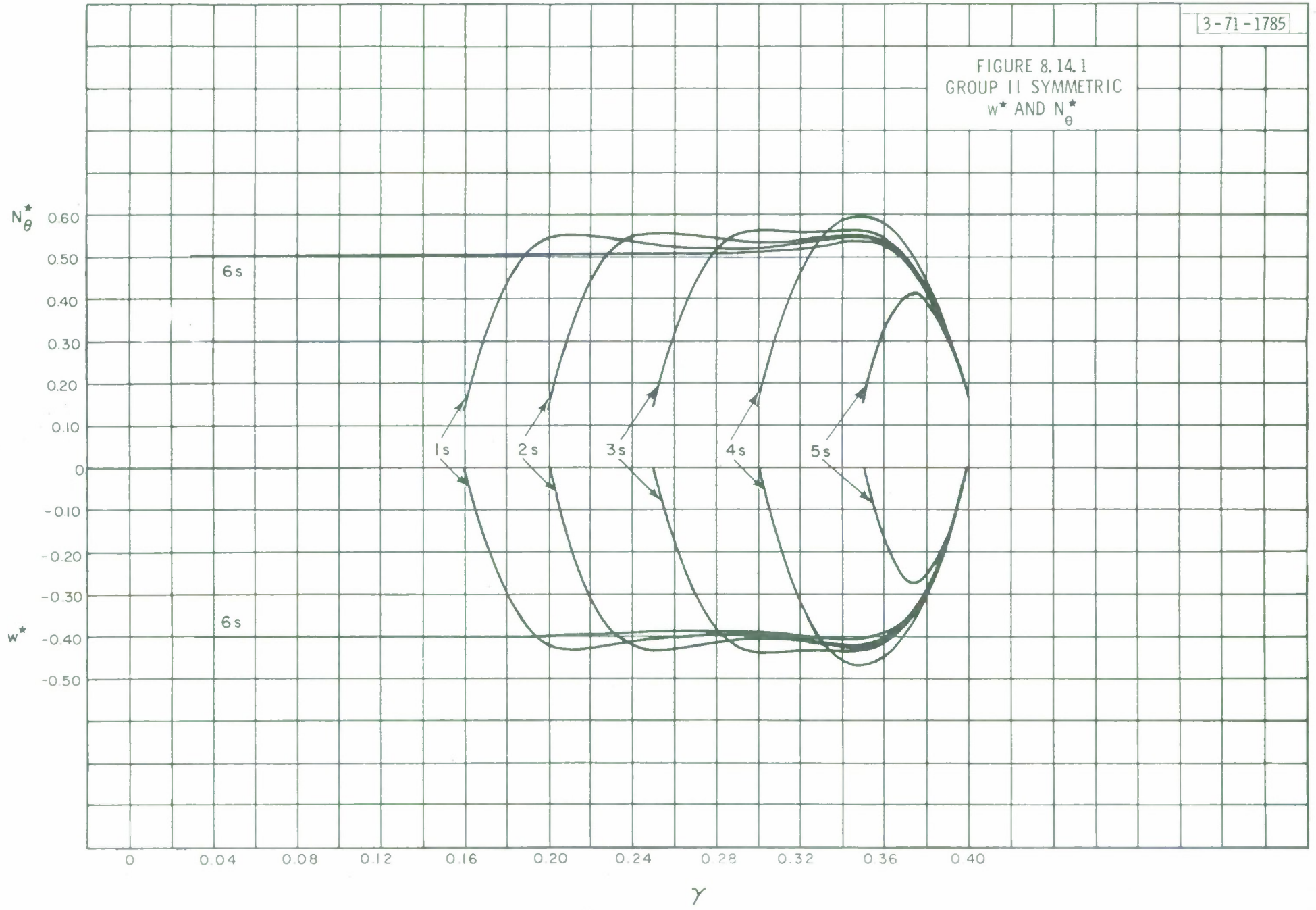

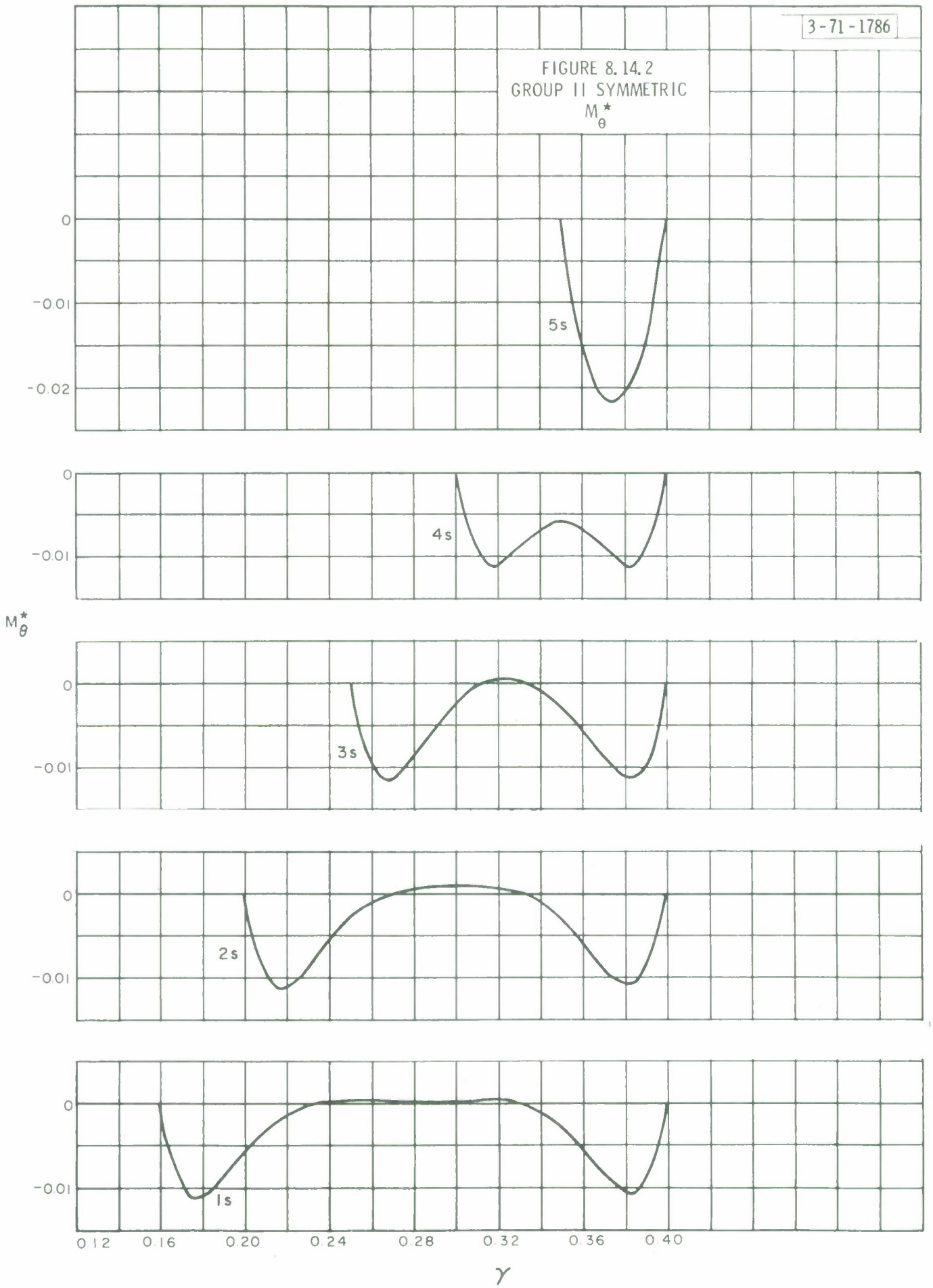
3-71-1786
FIGURE 8.14.2
GROUP II SYMMETRIC
M_θ^*
0
-0.01
-0.02
5s
0
-0.01
4s
M_θ^*
0
-0.01
3s
0
-0.01
2s
0
-0.01
1s
0.12
0.16
0.20
0.24
0.28
0.32
0.36
0.40
γ

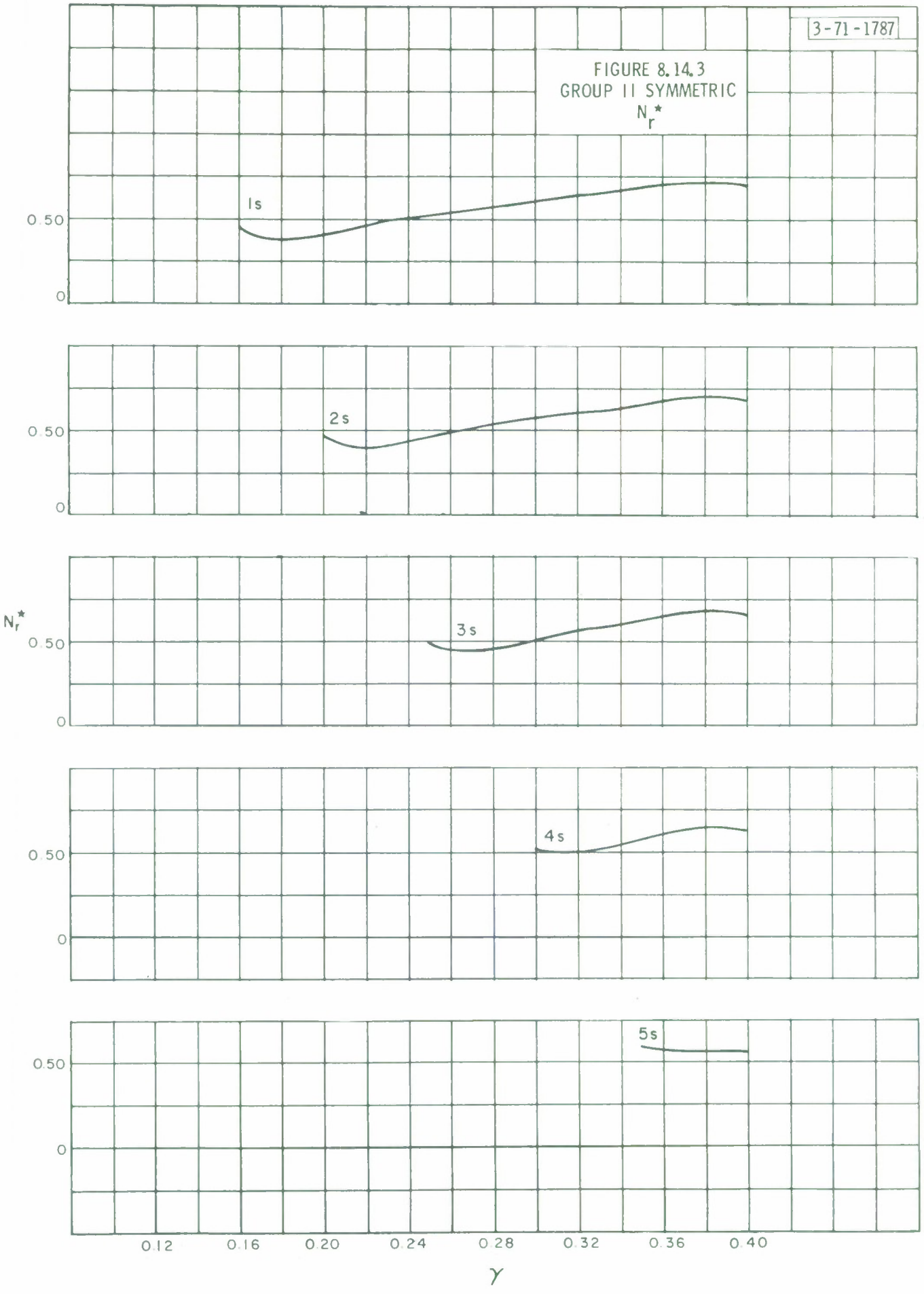
3-71-1787
FIGURE 8.14.3
GROUP II SYMMETRIC
N_r^*
1s
2s
3s
4s
5s
N_r^*
0.50
0
0.12
0.16
0.20
0.24
0.28
0.32
0.36
0.40
γ

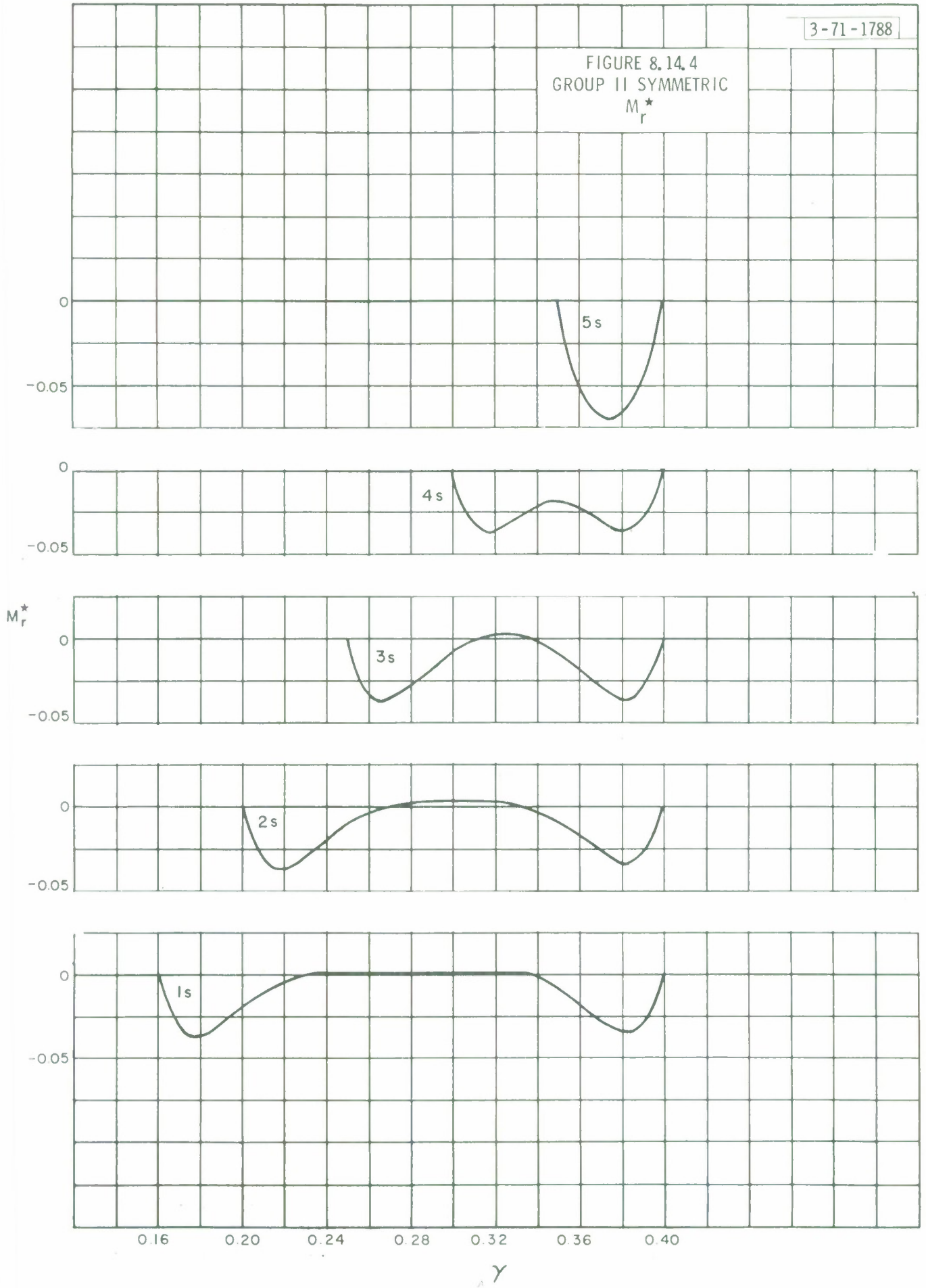
3-71-1788
FIGURE 8.14.4
GROUP II SYMMETRIC
M_r^*
5s
4s
3s
2s
1s
0
-0.05
M_r^*
0.16
0.20
0.24
0.28
0.32
0.36
0.40
γ

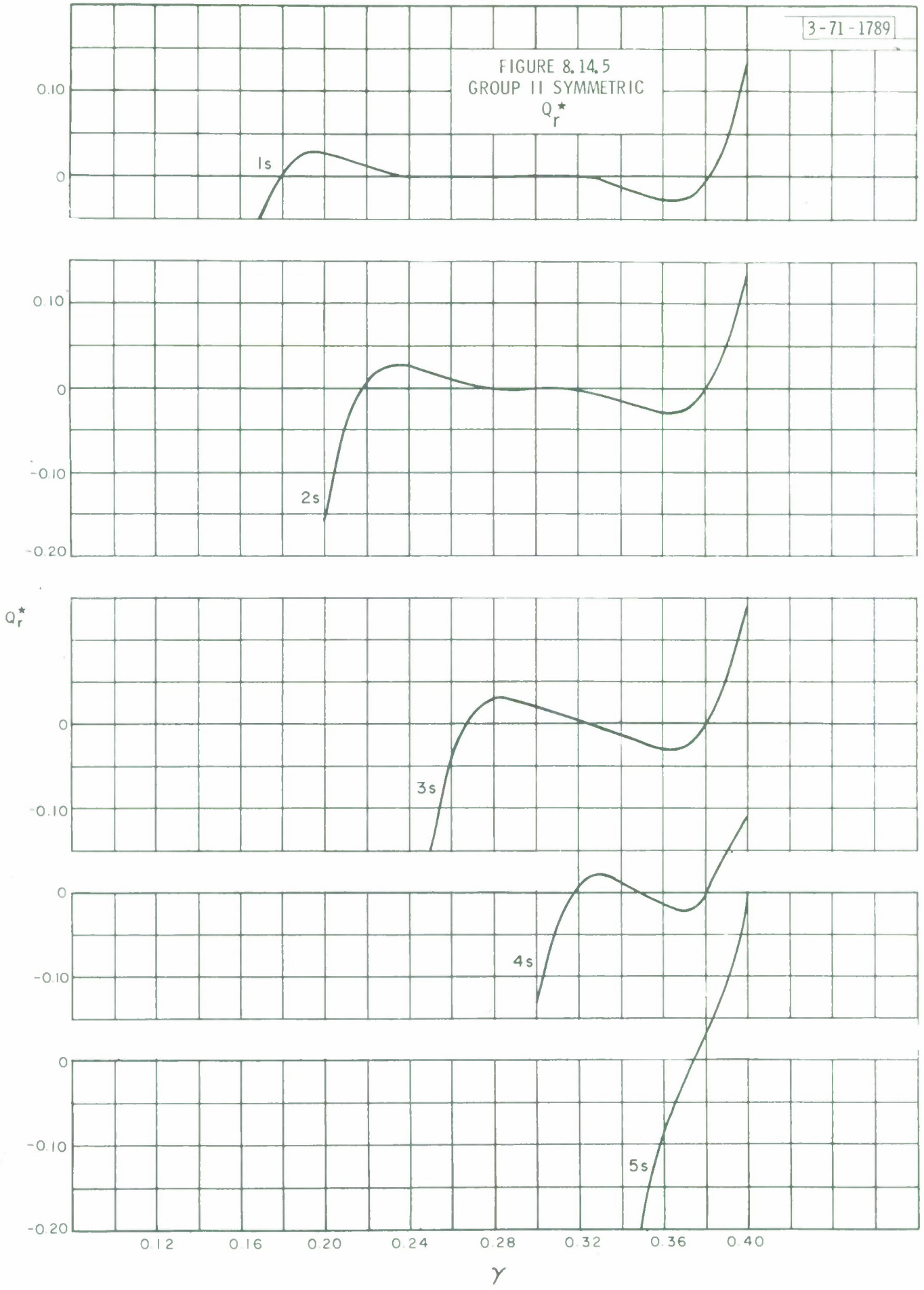
3-71-1789
FIGURE 8.14.5
GROUP II SYMMETRIC
Q_r^*
1s
2s
3s
4s
5s
0.10
0
-0.10
-0.20
Q_r^*
0.12
0.16
0.20
0.24
0.28
0.32
0.36
0.40
γ

3-71-1790

FIGURE 8.14.6
GROUP II ANTI-SYMMETRIC
w^*
(at $\theta = \frac{\pi}{2}$)

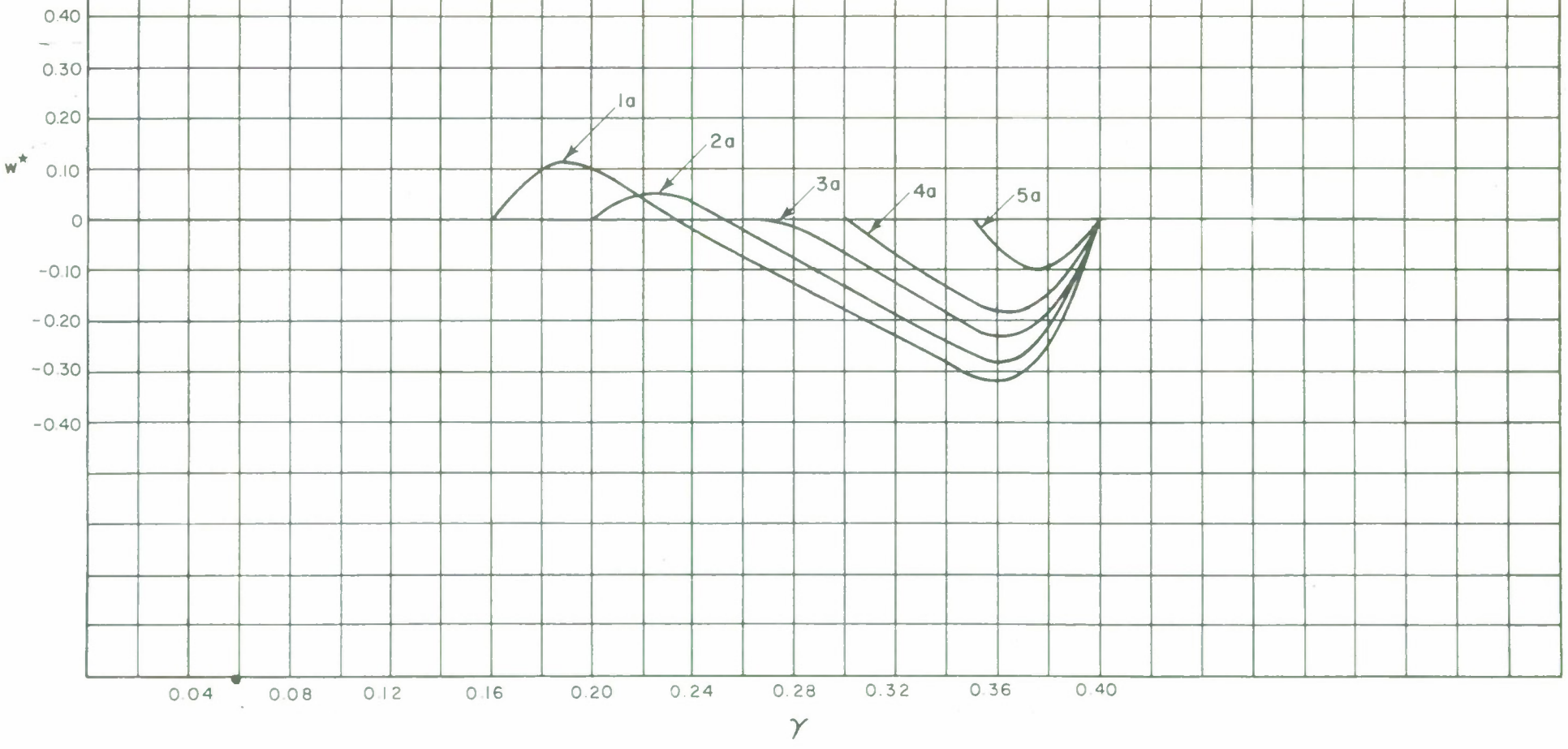

3-71-1791

FIGURE 8.14.7
GROUP II ANTI-SYMMETRIC
N_r^*
(at $\theta = \frac{\pi}{2}$)

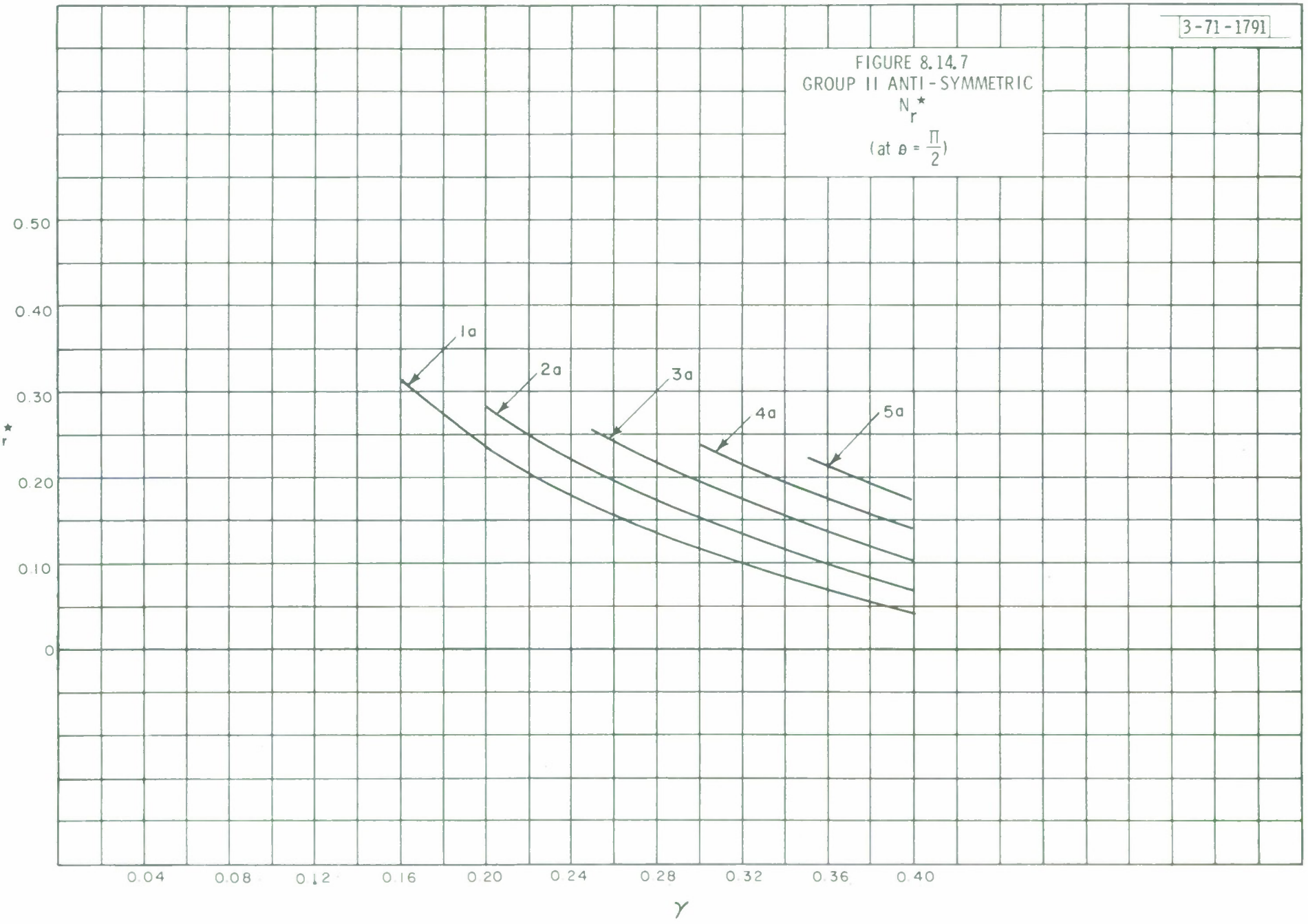

3-71-1792

FIGURE 8.14.8
GROUP II ANTI-SYMMETRIC
N_θ^*
(at $\theta = \frac{\pi}{2}$)

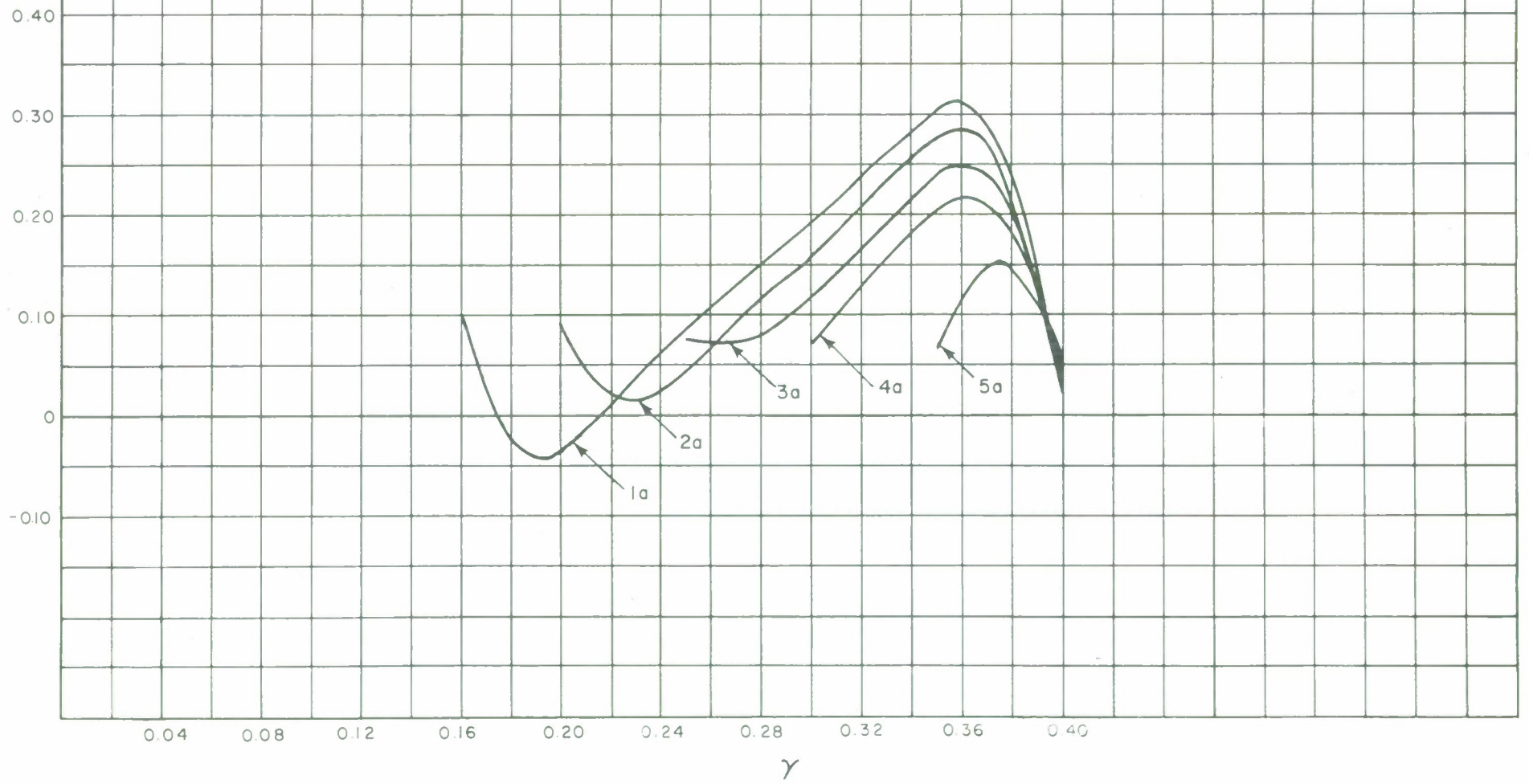

3-71-1793

FIGURE 8.14.9
GROUP II ANTI-SYMMETRIC
$N^{*}_{r\theta}$
(at $\theta = 0$)

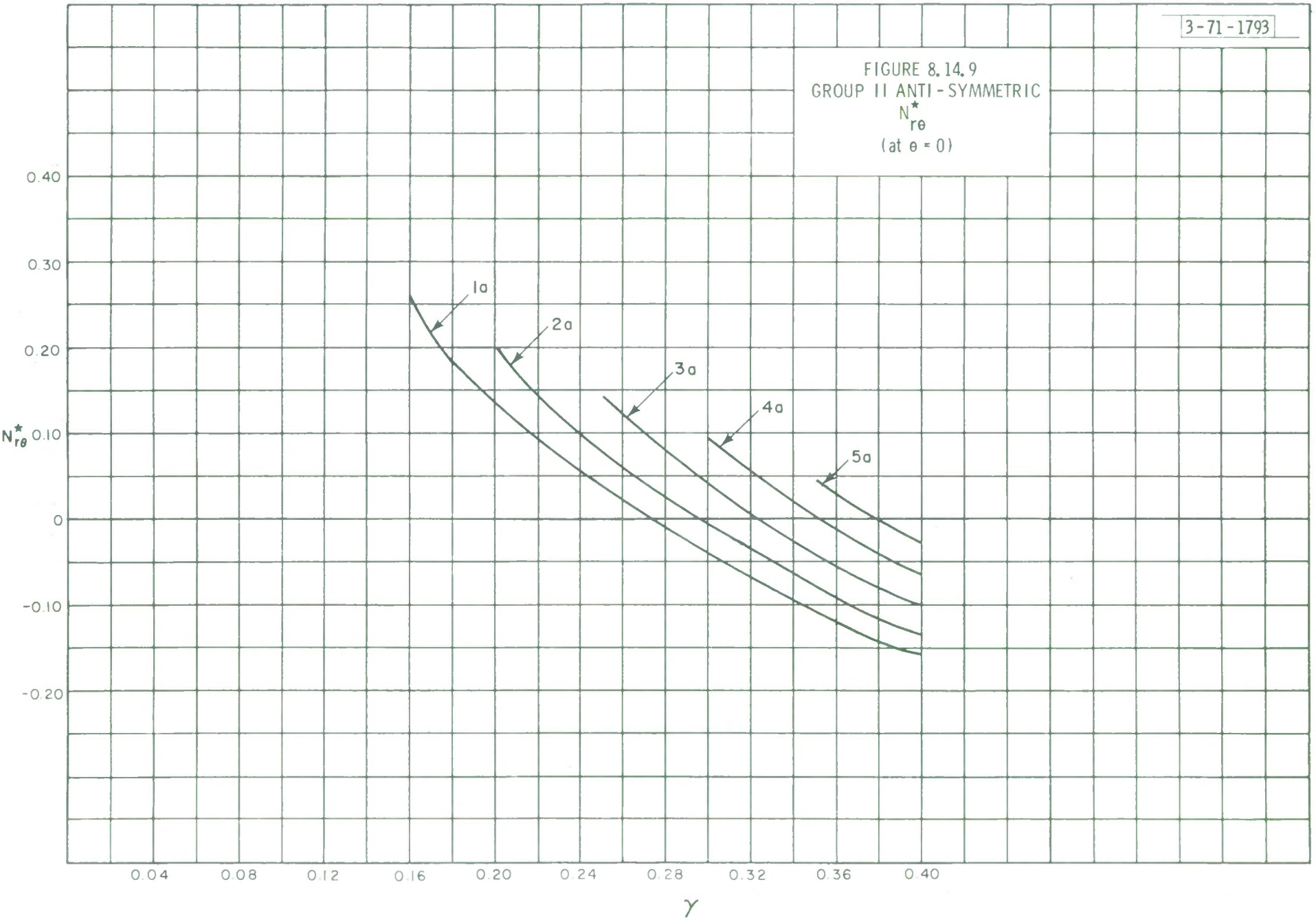

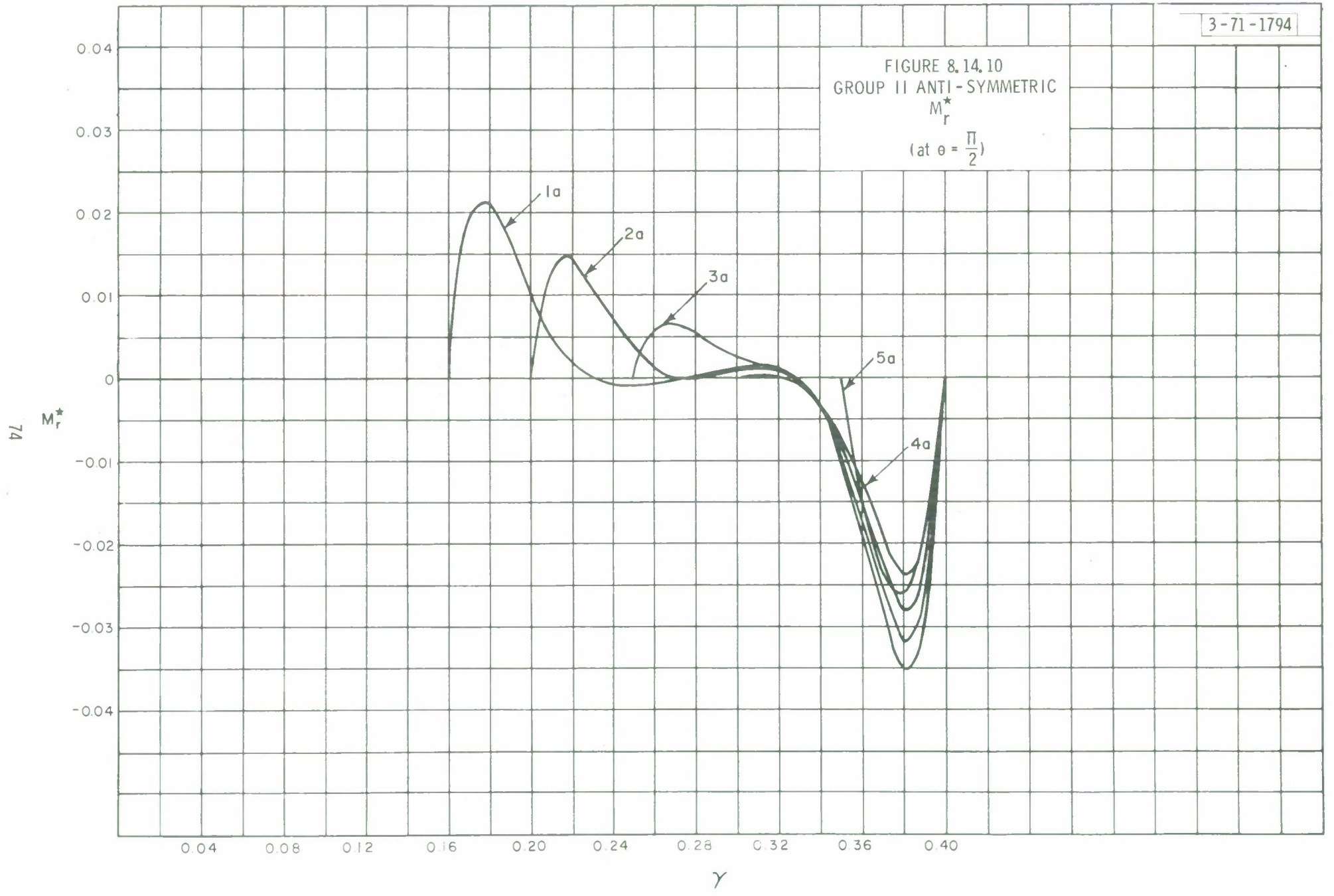
3-71-1794
FIGURE 8.14.10
GROUP II ANTI-SYMMETRIC
M_r^*
(at $\theta = \frac{\pi}{2}$)
1a
2a
3a
4a
5a
0.04
0.03
0.02
0.01
0
-0.01
-0.02
-0.03
-0.04
M_r^*
0.04
0.08
0.12
0.16
0.20
0.24
0.28
0.32
0.36
0.40
γ

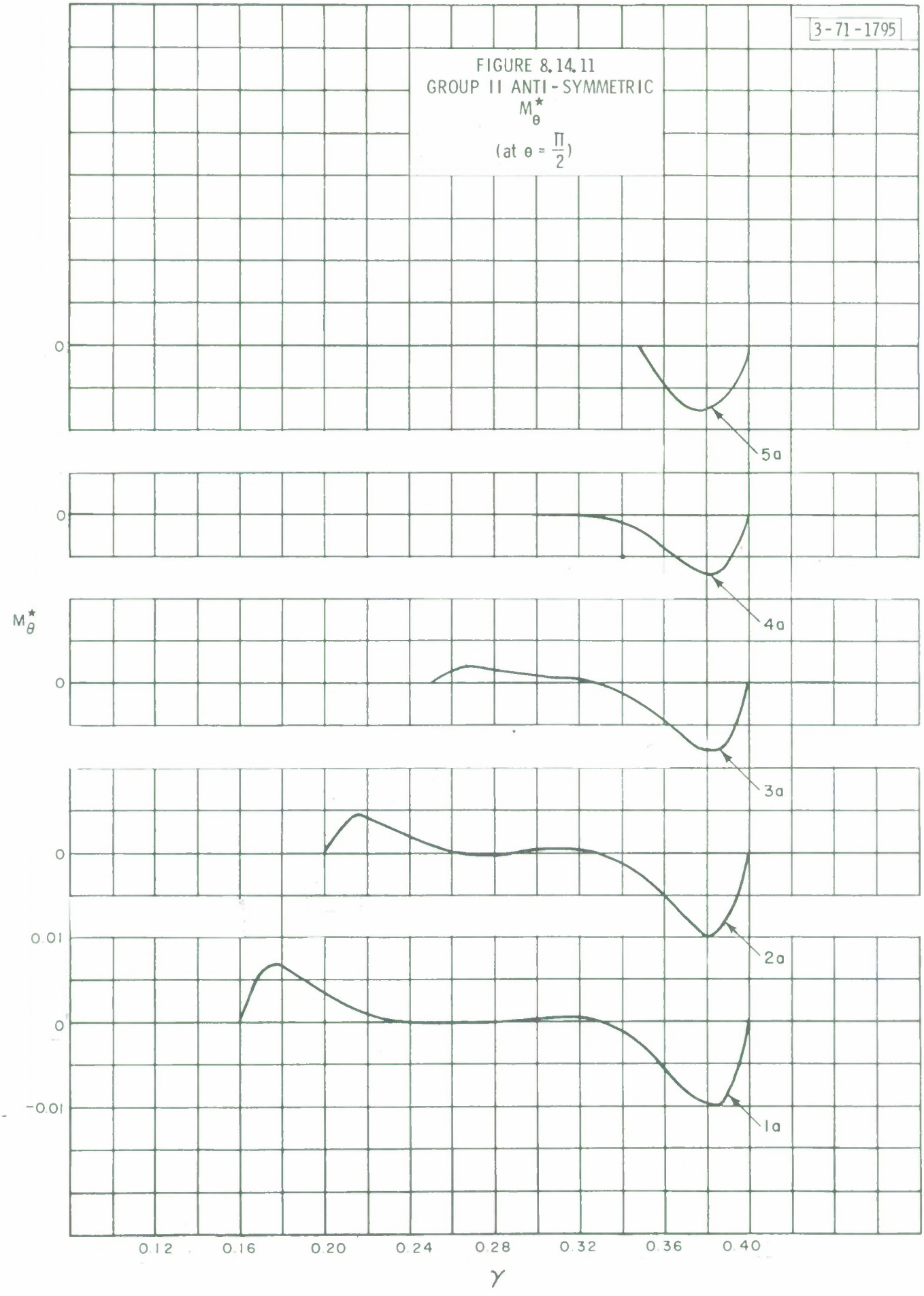
3-71-1795
FIGURE 8.14.11
GROUP II ANTI-SYMMETRIC
$M_\theta^\star$
(at $\theta = \frac{\Pi}{2}$)
$M_\theta^\star$
0
0
0
0
0.01
0
-0.01
5a
4a
3a
2a
1a
0.12
0.16
0.20
0.24
0.28
0.32
0.36
0.40
γ

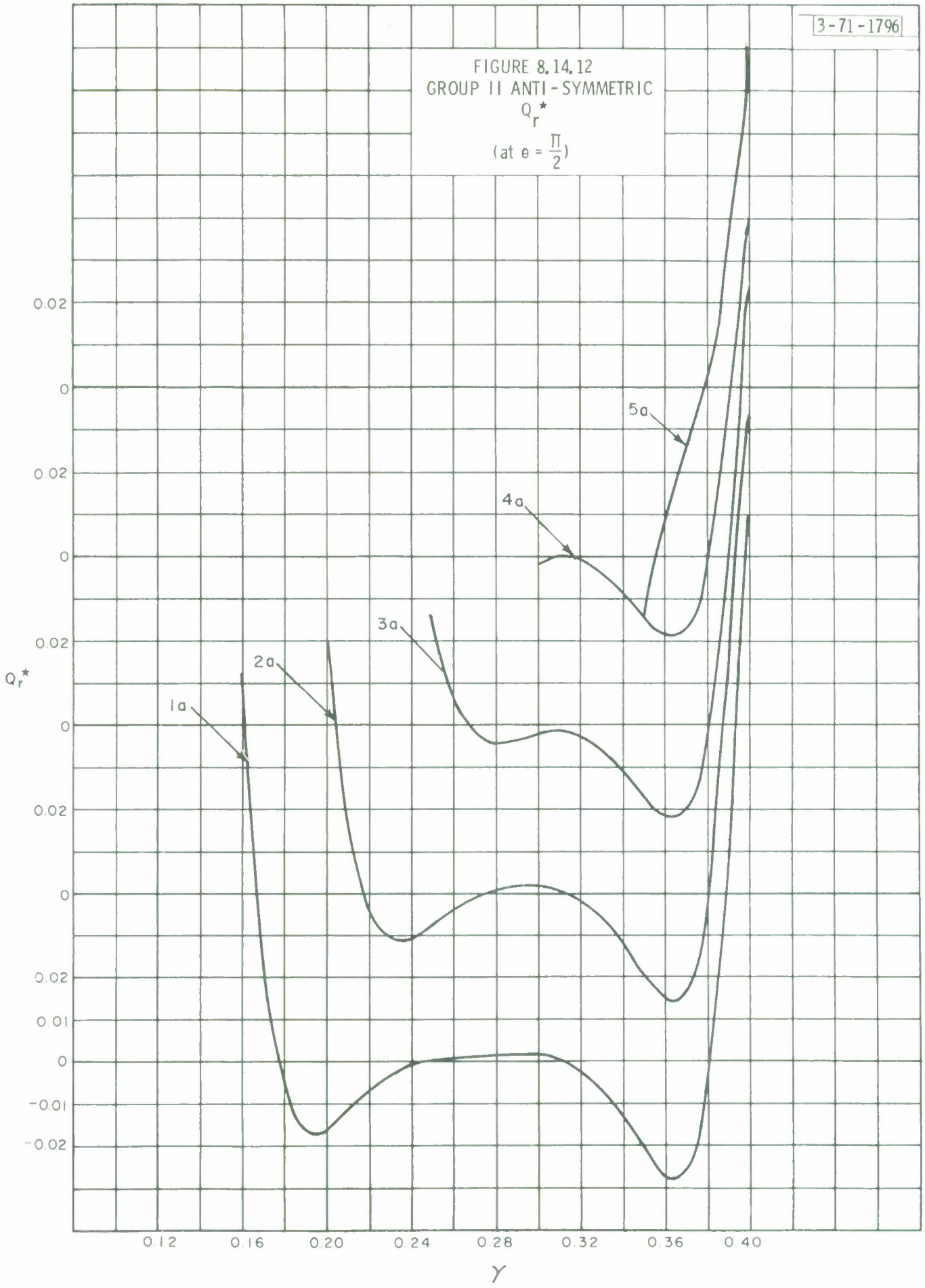
3-71-1796
FIGURE 8.14.12
GROUP II ANTI-SYMMETRIC
Q_r^*
(at $\theta = \frac{\pi}{2}$)
0.02
0
0.02
0
0.02
0
0.02
0
0.02
0.01
0
-0.01
-0.02
Q_r^*
1a
2a
3a
4a
5a
0.12
0.16
0.20
0.24
0.28
0.32
0.36
0.40
γ

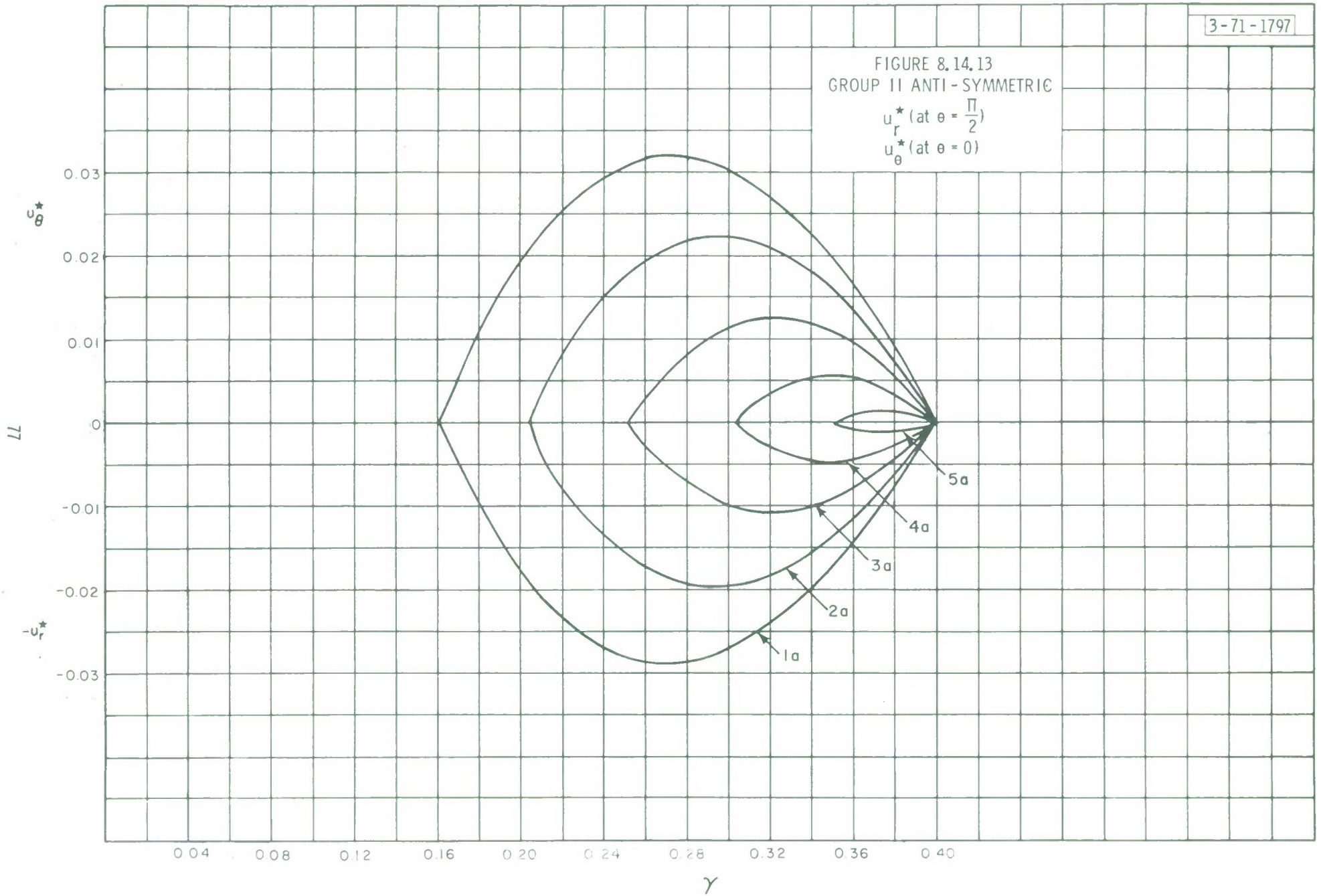
3-71-1797
FIGURE 8.14.13
GROUP II ANTI-SYMMETRIC
u_r^* (at $\theta = \frac{\pi}{2}$)
u_θ^* (at $\theta = 0$)
0.03
0.02
0.01
0
-0.01
-0.02
-0.03
v_θ^*
$-v_r^*$
0.04
0.08
0.12
0.16
0.20
0.24
0.28
0.32
0.36
0.40
γ
1a
2a
3a
4a
5a

8.15 Group III - Five Shells with an Outer Radius of 691.2 Inches

The results in this section illustrate the behavior of five shells with the same outer radius of 691.2 inches but terminating at various inner radii. Dimensions and other pertinent data are presented in Table 8.15.1. The outer radius is equivalent to $\gamma = .60$ while the inner radii correspond to a shell closed at the apex and to slopes of $\gamma = .20, .40, .50$ and $.55$. Both the symmetric and anti-symmetric behavior under gravity loads are presented with the former corresponding to a pointing angle of $\psi = 0°$ and the latter to $\psi = 90°$. The curves, in addition to the heading of three groups of numbers (e.g. 8.15.1), bear either the letter s, signifying symmetric behavior or a, signifying anti-symmetric behavior. Results are all in normalized form (see page 43 of this report).

In general, the results are comparable to those shown in section 8.14 and the same discussion is pertinent. However, unlike the results of the previous section, the anti-symmetric behavior for the larger span shells (cases 1 and 2) of this group results in larger values for the force resultants, moments, and deflections than for the symmetric behavior.

Table 8.15.1

Group III Examples

Case	R_1 (inches)	R_2 (inches)	B.C. at R_1	B.C. at R_2	Loading
1s	---	691.2	---	Simple support	Sym.-gravity
2s	230.4	"	Simple support	"	"
3s	460.8	"	"	"	"
4s	576	"	"	"	"
5s	633.6	"	"	"	"
1a	---	"	---	"	
2a	230.4	"	Simple support	"	Anti-sym.-gravity
3a	460.8	"	"	"	"
4a	576	"	"	"	"
5a	633.6	"	"	"	"

Note: Material properties are $E = 10^7$ p.s.i., $\nu = .3$, $\rho_o = .10$ lb. per cubic inch.

Focal length $f = 576$ inches, shell thickness $h = 1$ inch.

3-71-1798

FIGURE 8.15.1
GROUP III SYMMETRIC
w^* AND N_θ^*

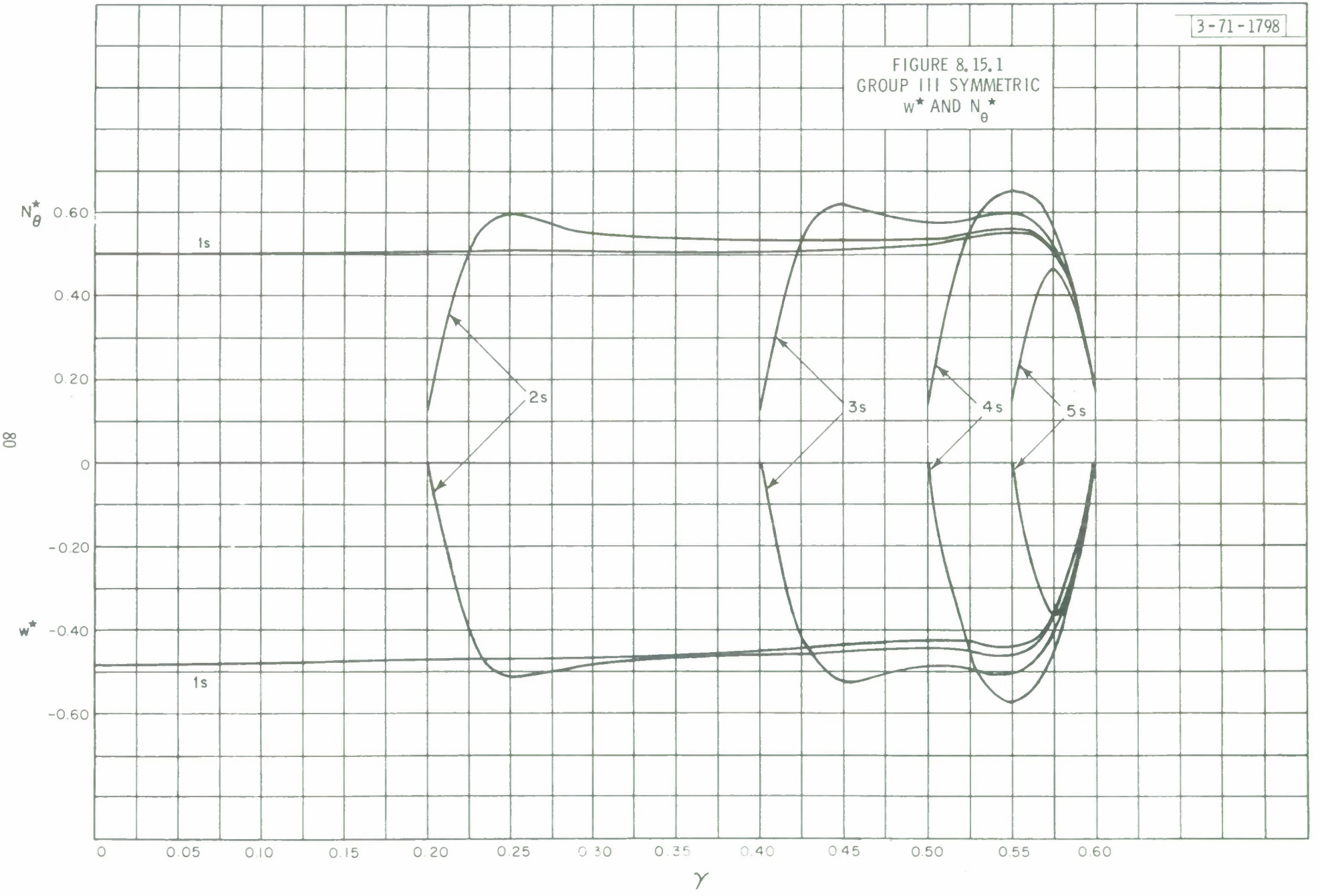

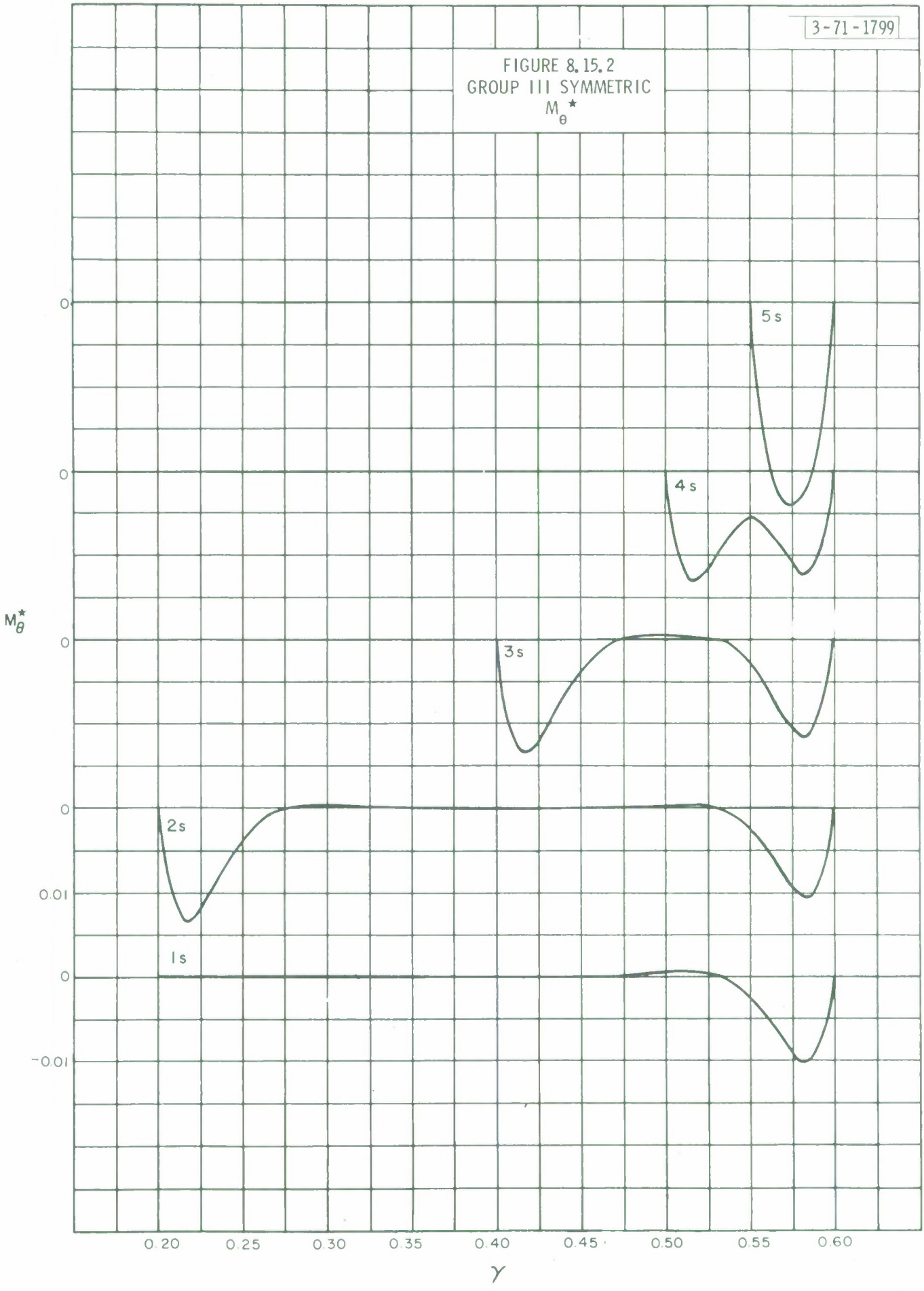
3-71-1799
FIGURE 8.15.2
GROUP III SYMMETRIC
M_θ^*
5s
4s
3s
2s
1s
M_θ^*
0
0
0
0
0.01
0
-0.01
0.20
0.25
0.30
0.35
0.40
0.45
0.50
0.55
0.60
γ

3-71-1800

FIGURE 8.15.3
GROUP III SYMMETRIC
N_r^*

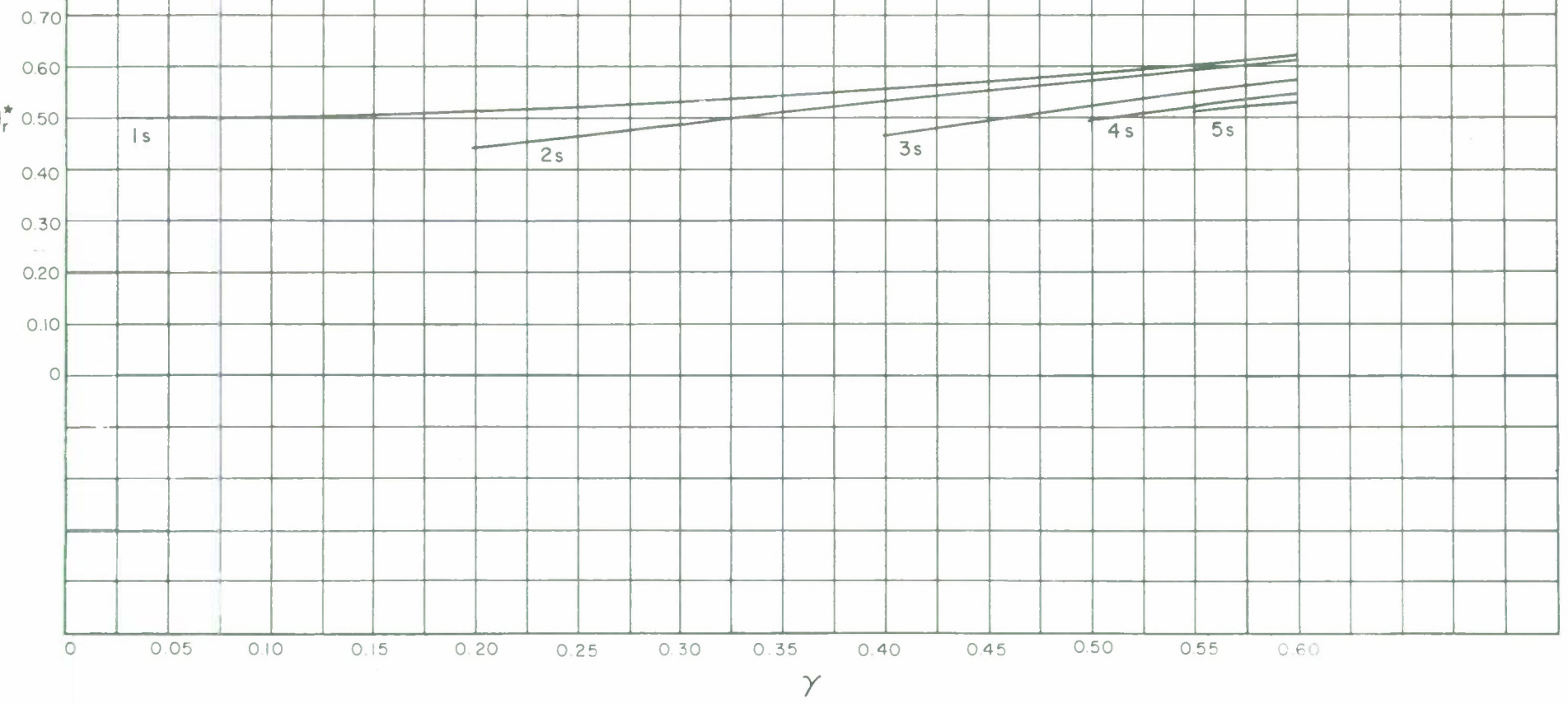

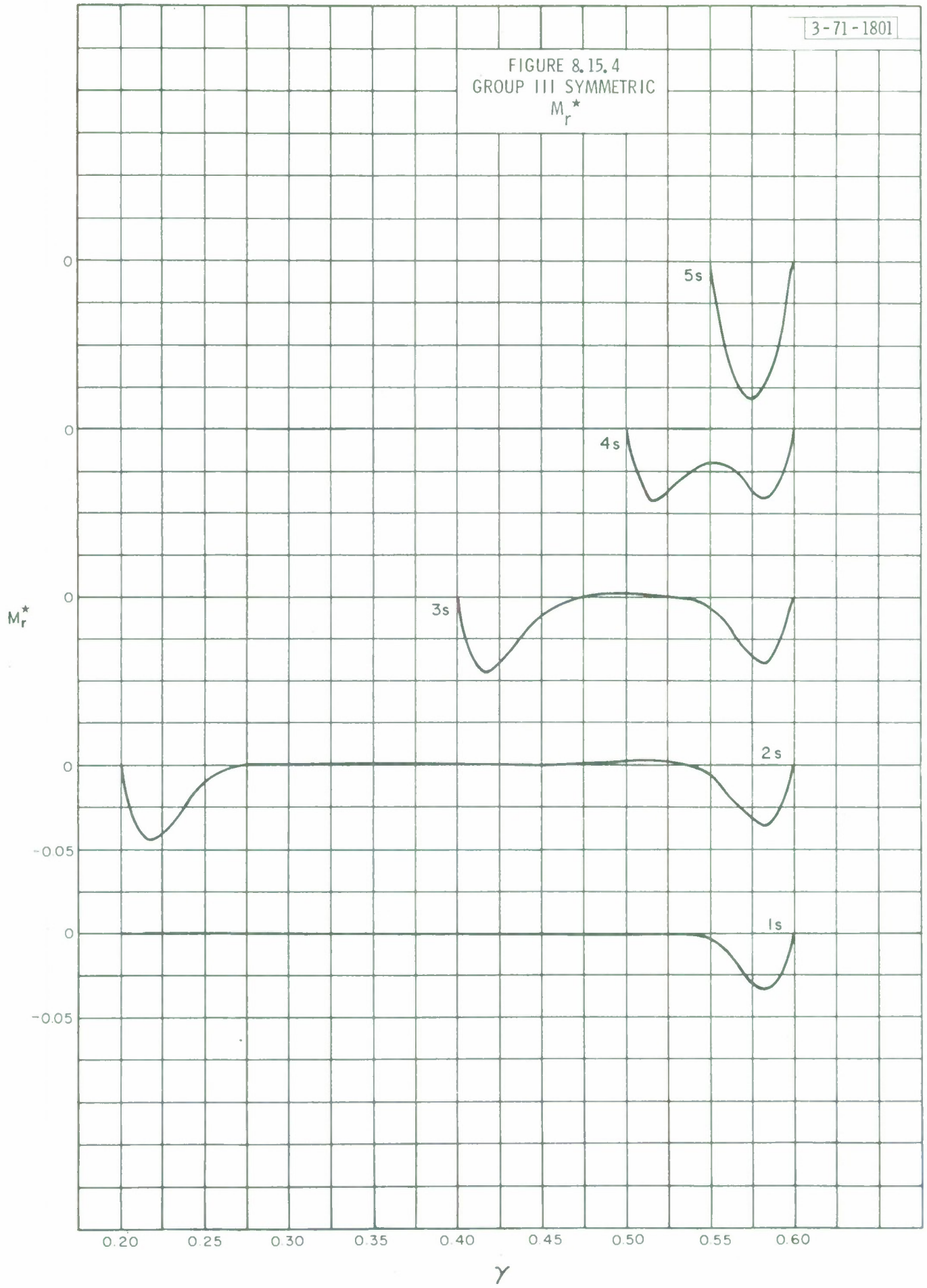
3-71-1801
FIGURE 8.15.4
GROUP III SYMMETRIC
M_r^*
5s
4s
3s
2s
1s
0
0
0
0
-0.05
0
-0.05
M_r^*
0.20
0.25
0.30
0.35
0.40
0.45
0.50
0.55
0.60
γ

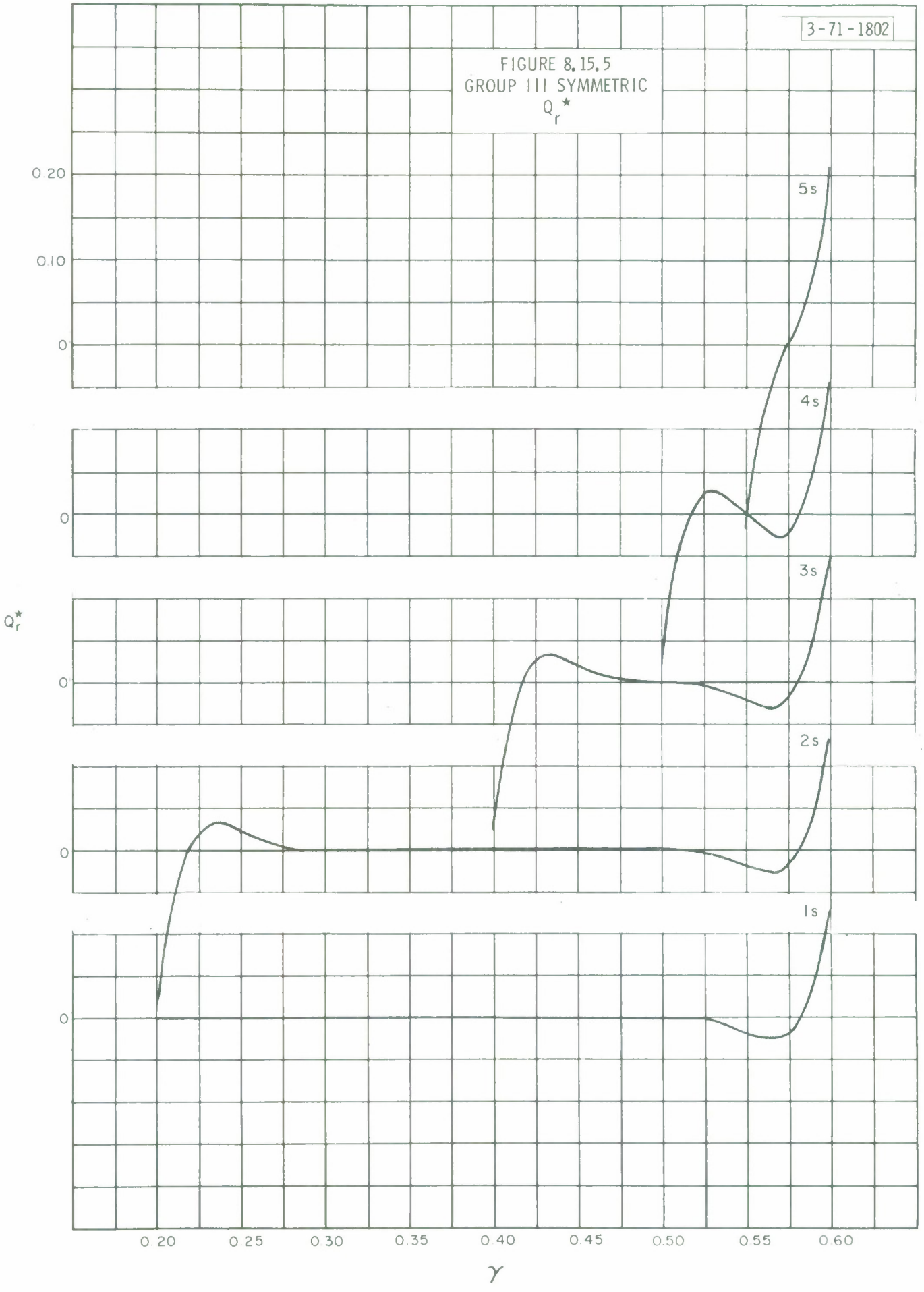
3-71-1802
FIGURE 8.15.5
GROUP III SYMMETRIC
Q_r^*
0.20
0.10
0
5s
4s
3s
2s
1s
Q_r^*
0.20
0.25
0.30
0.35
0.40
0.45
0.50
0.55
0.60
γ

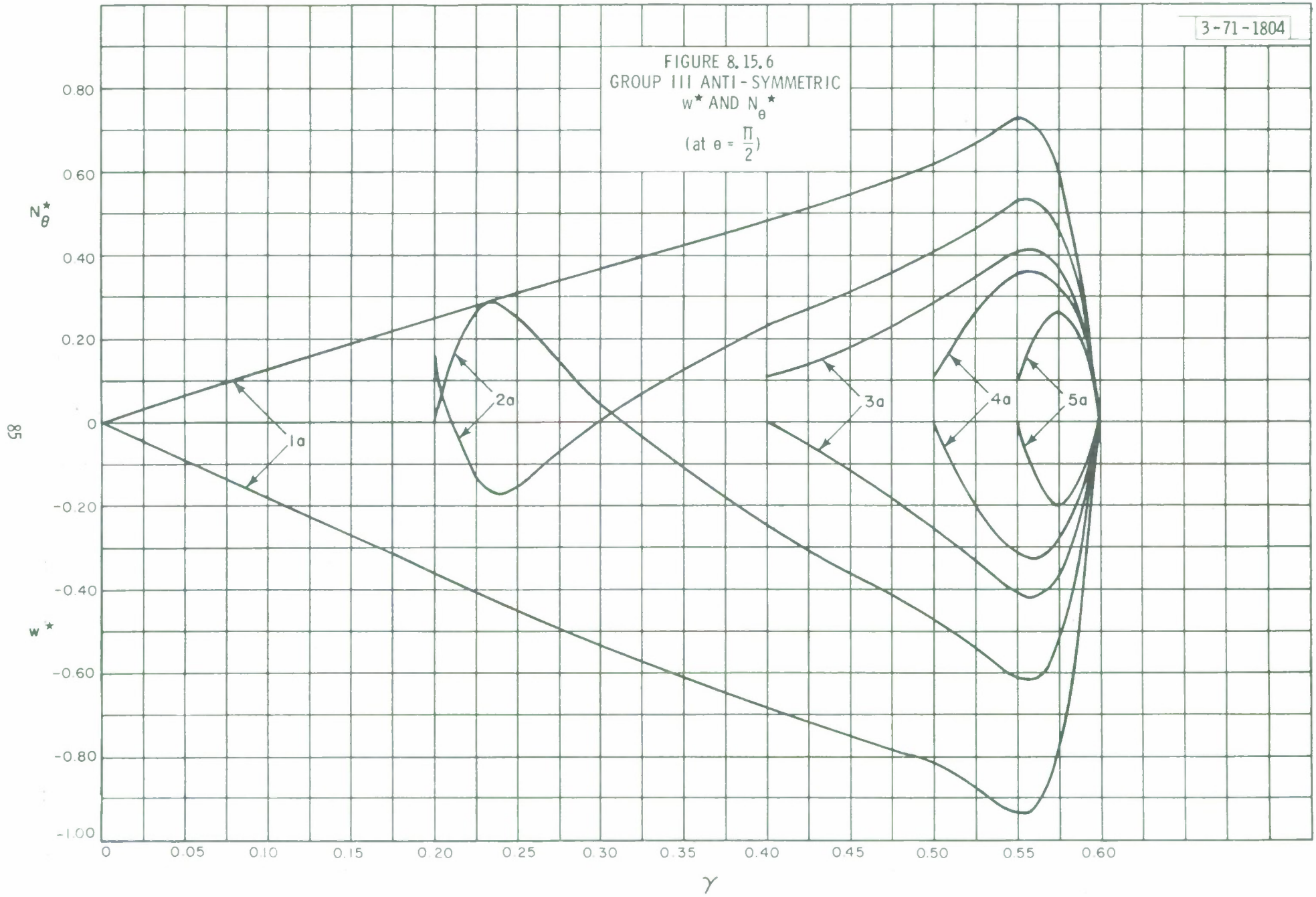
3-71-1804
FIGURE 8.15.6
GROUP III ANTI-SYMMETRIC
w* AND N_θ*
(at θ = π/2)
0.80
0.60
0.40
0.20
0
-0.20
-0.40
-0.60
-0.80
-1.00
N_θ*
w*
1a
2a
3a
4a
5a
0
0.05
0.10
0.15
0.20
0.25
0.30
0.35
0.40
0.45
0.50
0.55
0.60
γ

FIGURE 8.15.7
GROUP III ANTI-SYMMETRIC
N_r^*
(at $\theta = \frac{\pi}{2}$)

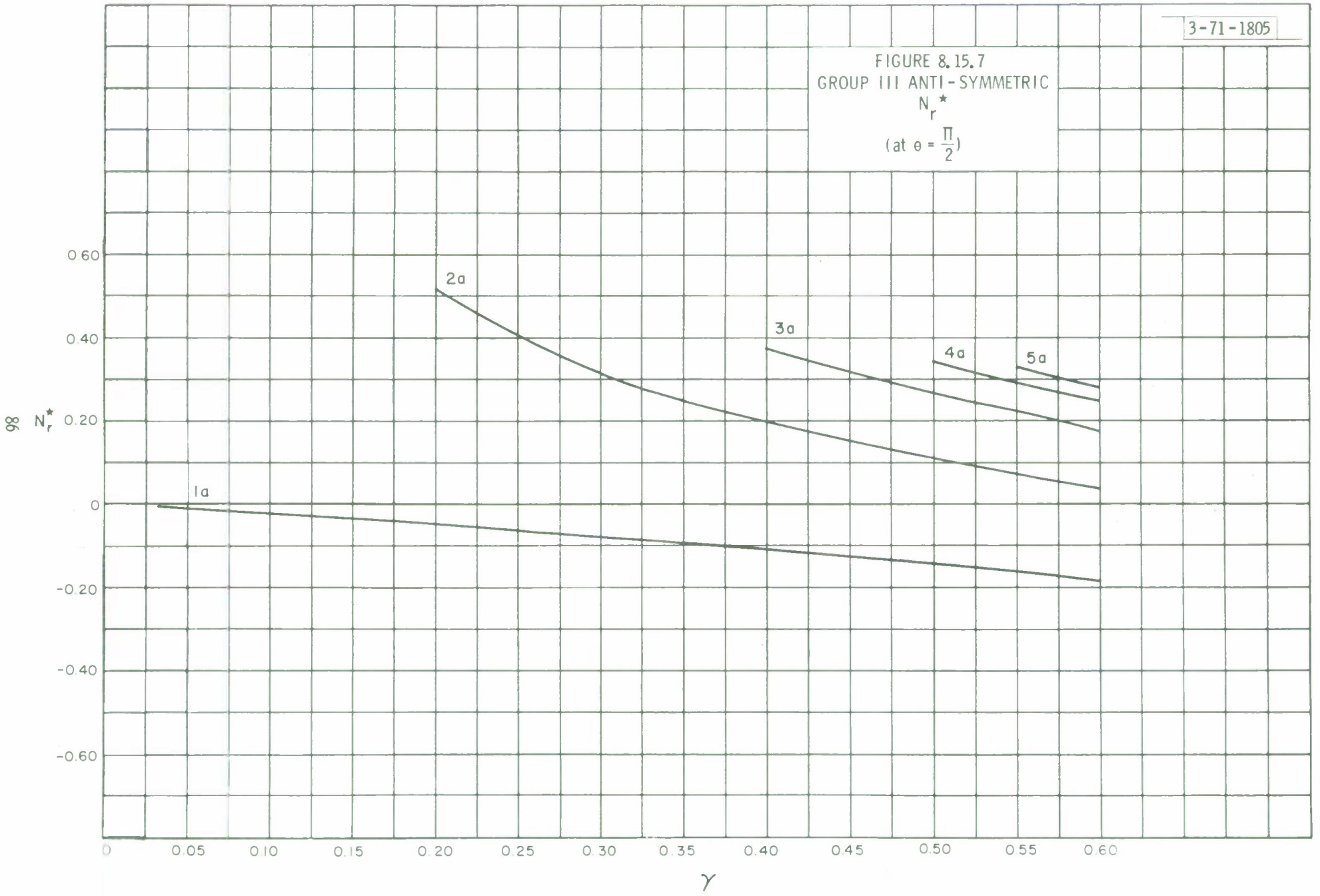

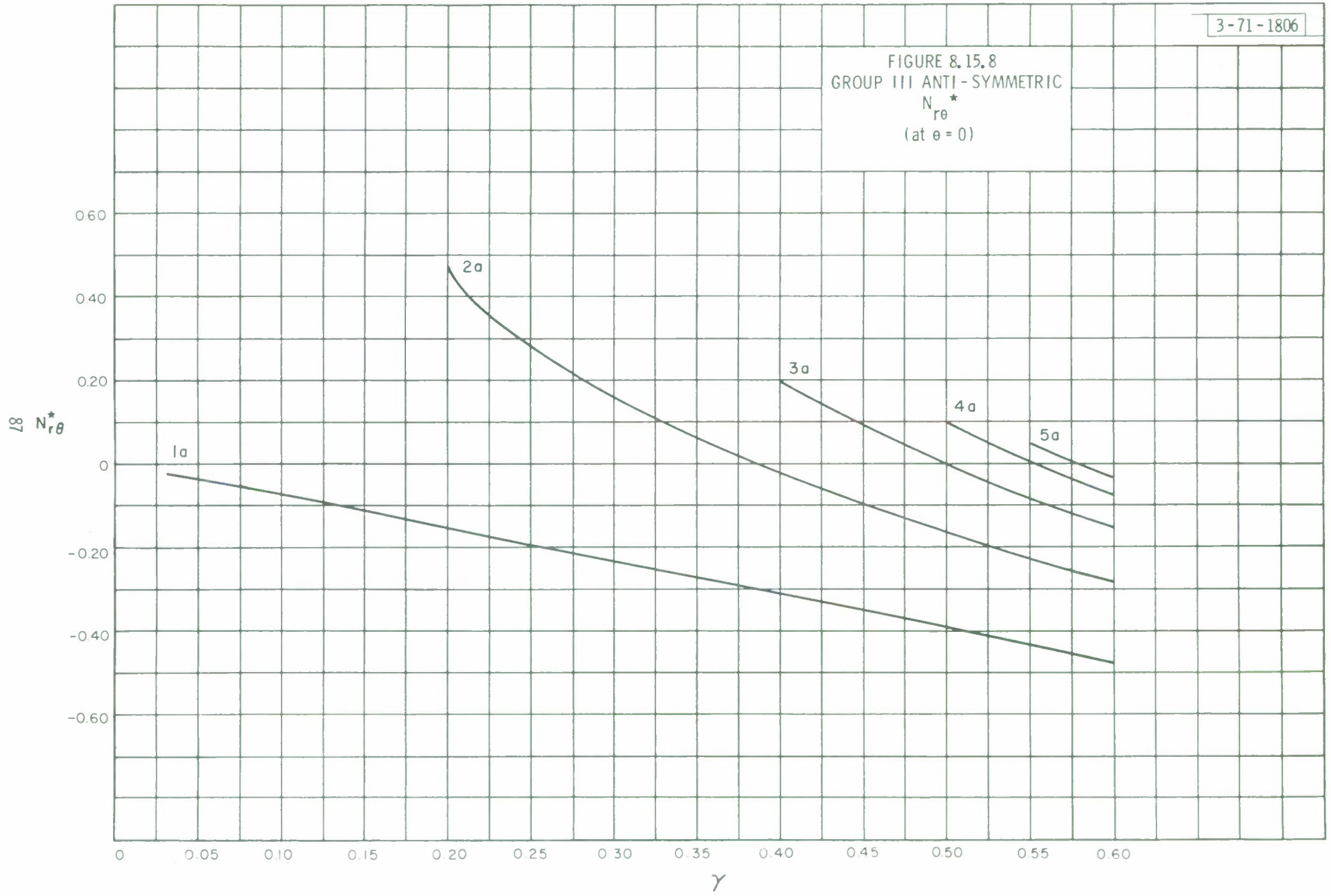
3-71-1806
FIGURE 8.15.8
GROUP III ANTI-SYMMETRIC
$N_{r\theta}^{\star}$
(at $\theta = 0$)
0.60
0.40
0.20
0
-0.20
-0.40
-0.60
$N_{r\theta}^{\star}$
1a
2a
3a
4a
5a
0
0.05
0.10
0.15
0.20
0.25
0.30
0.35
0.40
0.45
0.50
0.55
0.60
γ

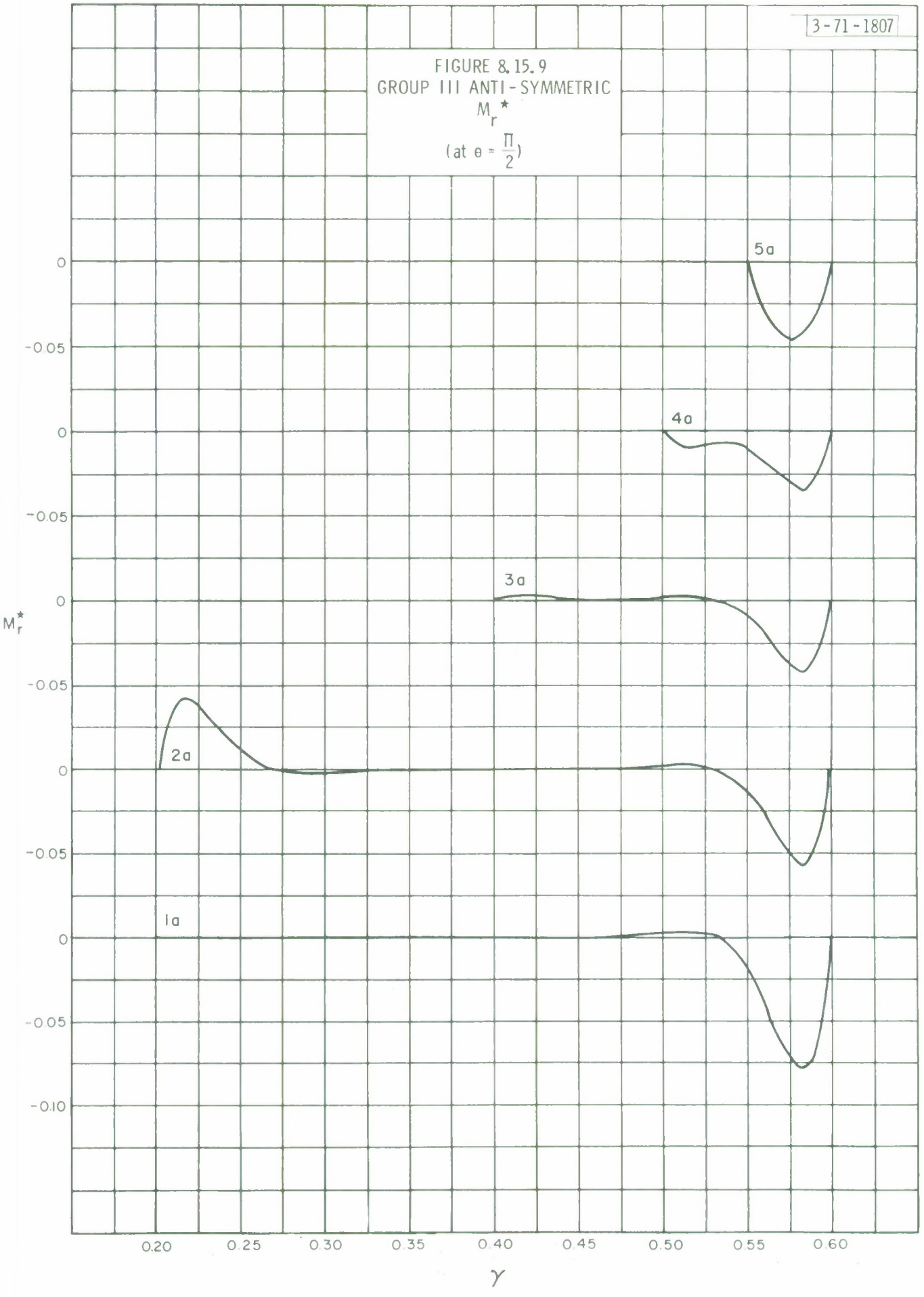
3-71-1807
FIGURE 8.15.9
GROUP III ANTI-SYMMETRIC
M_r^*
(at $\theta = \frac{\pi}{2}$)
5a
4a
3a
2a
1a
0
-0.05
0
-0.05
0
-0.05
0
-0.05
0
-0.10
M_r^*
0.20
0.25
0.30
0.35
0.40
0.45
0.50
0.55
0.60
γ

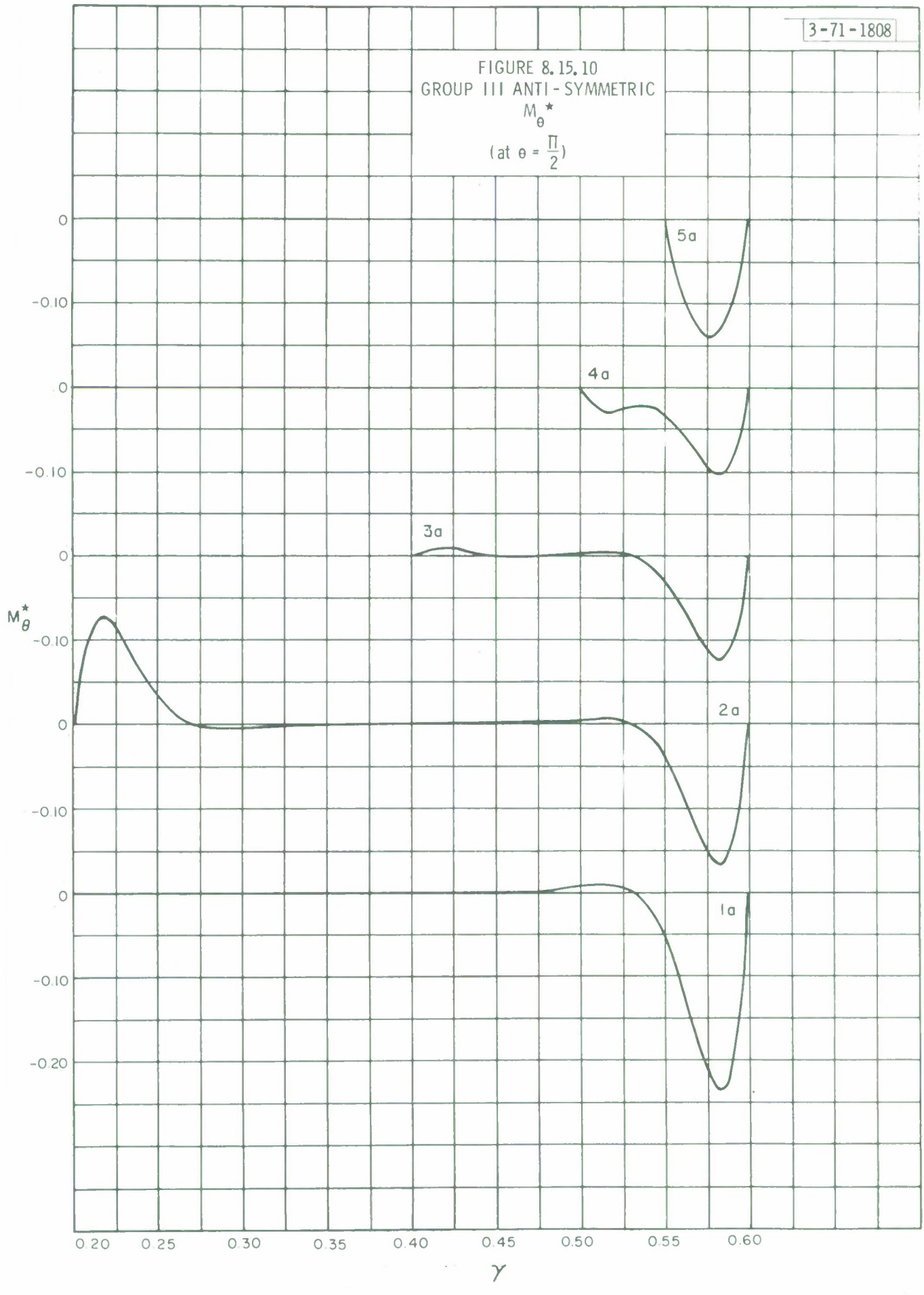
3-71-1808
FIGURE 8.15.10
GROUP III ANTI-SYMMETRIC
$M_\theta^\star$
(at $\theta = \frac{\Pi}{2}$)
5a
4a
3a
2a
1a
0
-0.10
0
-0.10
0
$M_\theta^\star$
-0.10
0
-0.10
0
-0.10
-0.20
0.20
0.25
0.30
0.35
0.40
0.45
0.50
0.55
0.60
γ

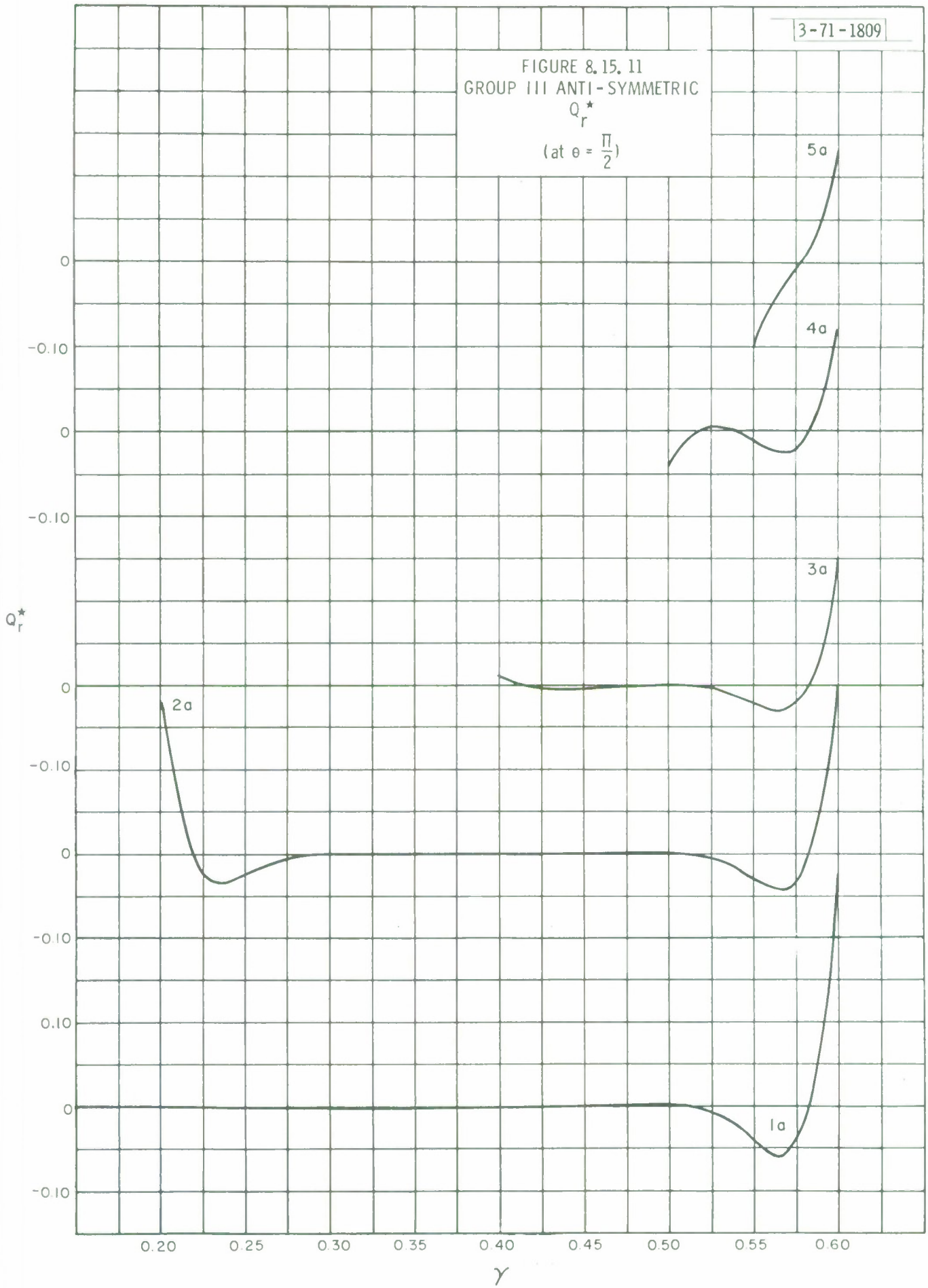
3-71-1809
FIGURE 8.15.11
GROUP III ANTI-SYMMETRIC
Q_r^*
(at $\theta = \frac{\pi}{2}$)
5a
4a
3a
2a
1a
0
-0.10
0
-0.10
0
-0.10
0
-0.10
0.10
0
-0.10
Q_r^*
0.20
0.25
0.30
0.35
0.40
0.45
0.50
0.55
0.60
γ

3-71-1810

FIGURE 8.15.12
GROUP III ANTI-SYMMETRIC
$-u_r^*$ (at $\theta = \frac{\pi}{2}$)
u_θ^* (at $\theta = 0$)

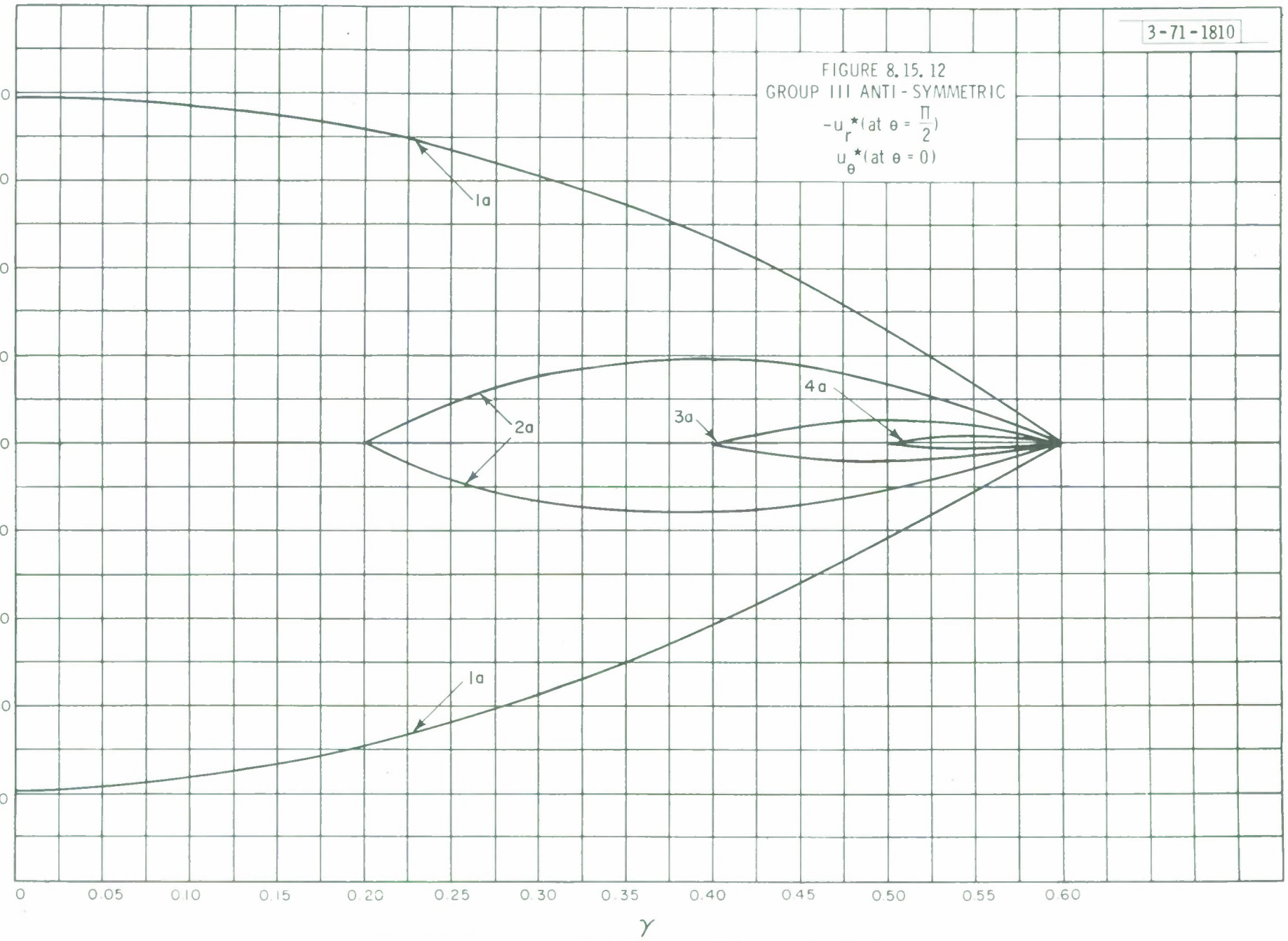

8.16 Group IV - Seven Shells with an Outer Radius of 921.6 Inches

The results in this section illustrate the behavior of seven shells with the same outer radius of 921.6 inches but terminating at various inner radii. Dimensions and other pertinent data are summarized in Table 8.16.1. The outer radius is equivalent to γ = .80 while the inner radii correspond to a shell closed at the apex and to slopes of γ = .32, .40, .50, .60, .66, and .75. Both the symmetric and anti-symmetric behavior under gravity loads are shown with the former corresponding to a pointing angle of ψ = 0° and the latter to ψ = 90°. The curves, in addition to the heading of three groups of numbers (e.g. 8.16.1), bear either the letter s, signifying symmetric behavior, or a, signifying anti-symmetric behavior. Results are all in normalized form (see page 43 of this report).

In general, the Group IV results are comparable to the Group II and III results for shells with smaller outer radii and to the Group V results for shells with a larger outer radii (read discussion in section 8.14). The deflections are larger for the Group IV shells than for the smaller Group II and III shells. Note, however, that the quantities associated with the bending behavior such as edge zone width, M_r^* , M_θ^* , Q_r^* , Q_θ^* , etc. have substantially the same magnitudes.

Table 8.16.1

Group IV Examples

Case	R_1 (inches)	R_2 (inches)	B.C. at R_1	B.C. at R_2	Loading
1s	368.64	921.6	Simple support	Simple support	Sym.-gravity
2s	460.8	"	"	"	"
3s	576	"	"	"	"
4s	691.2	"	"	"	"
5s	806.40	"	"	"	"
6s	864.00	"	"	"	"
7s	---	"	---	"	"
1a	368.64	"	Simple support	"	Anti Sym.-gravity
2a	560.8	"	"	"	"
3a	576	"	"	"	"
4a	691.2	"	"	"	"
5a	806.40	"	"	"	"
6a	864.00	"	"	"	"
7a	---	"	---	"	"

Note: Material properties are E = 10^7 p.s.i., ν = .3, ρ_0 = .10 lb. per cubic inch.

Focal length f = 576 inches, shell thickness h = 1 inch.

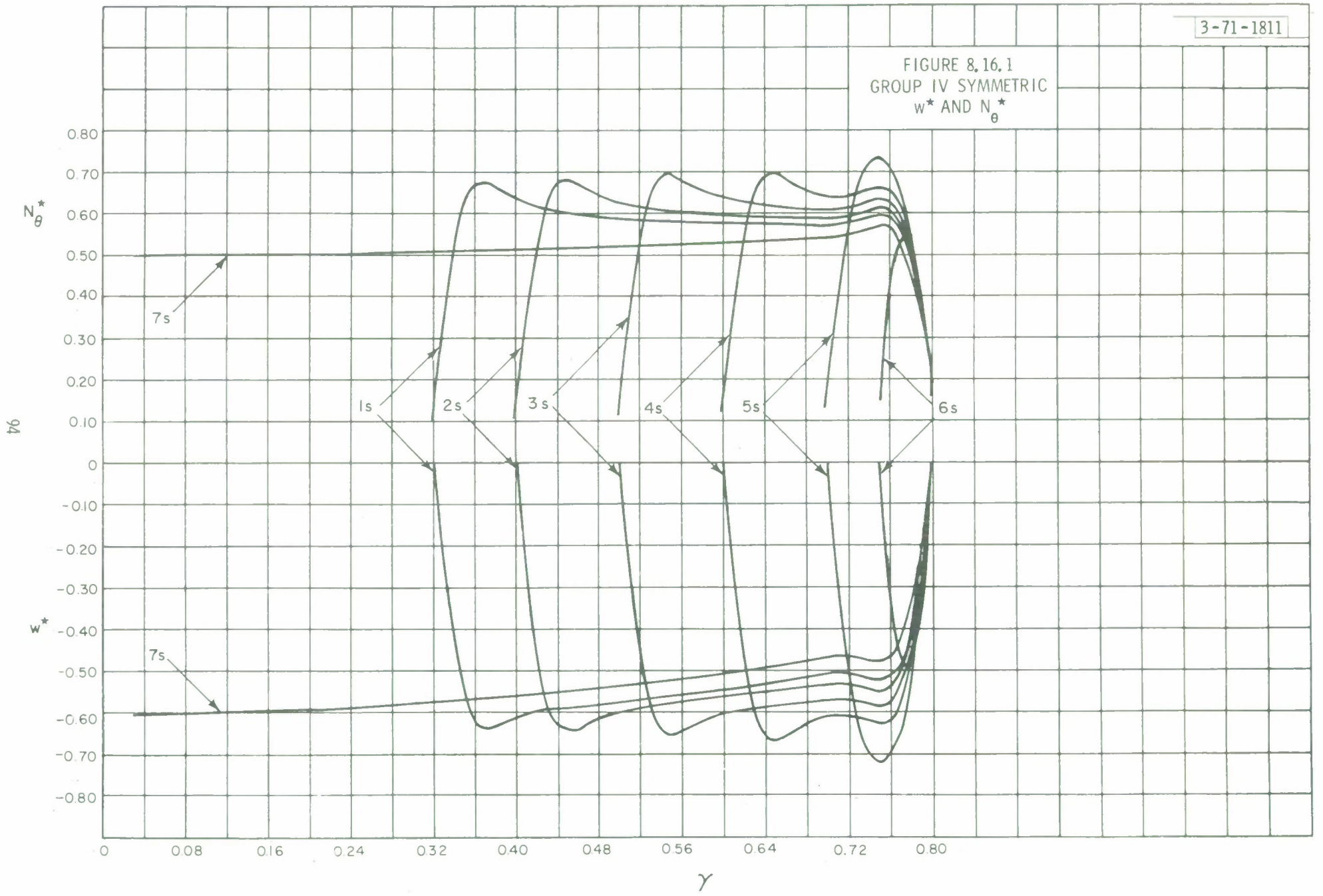
3-71-1811
FIGURE 8.16.1
GROUP IV SYMMETRIC
w* AND N_θ^*
N_θ^*
w*
0.80
0.70
0.60
0.50
0.40
0.30
0.20
0.10
0
-0.10
-0.20
-0.30
-0.40
-0.50
-0.60
-0.70
-0.80
0
0.08
0.16
0.24
0.32
0.40
0.48
0.56
0.64
0.72
0.80
γ
7s
1s
2s
3s
4s
5s
6s
7s

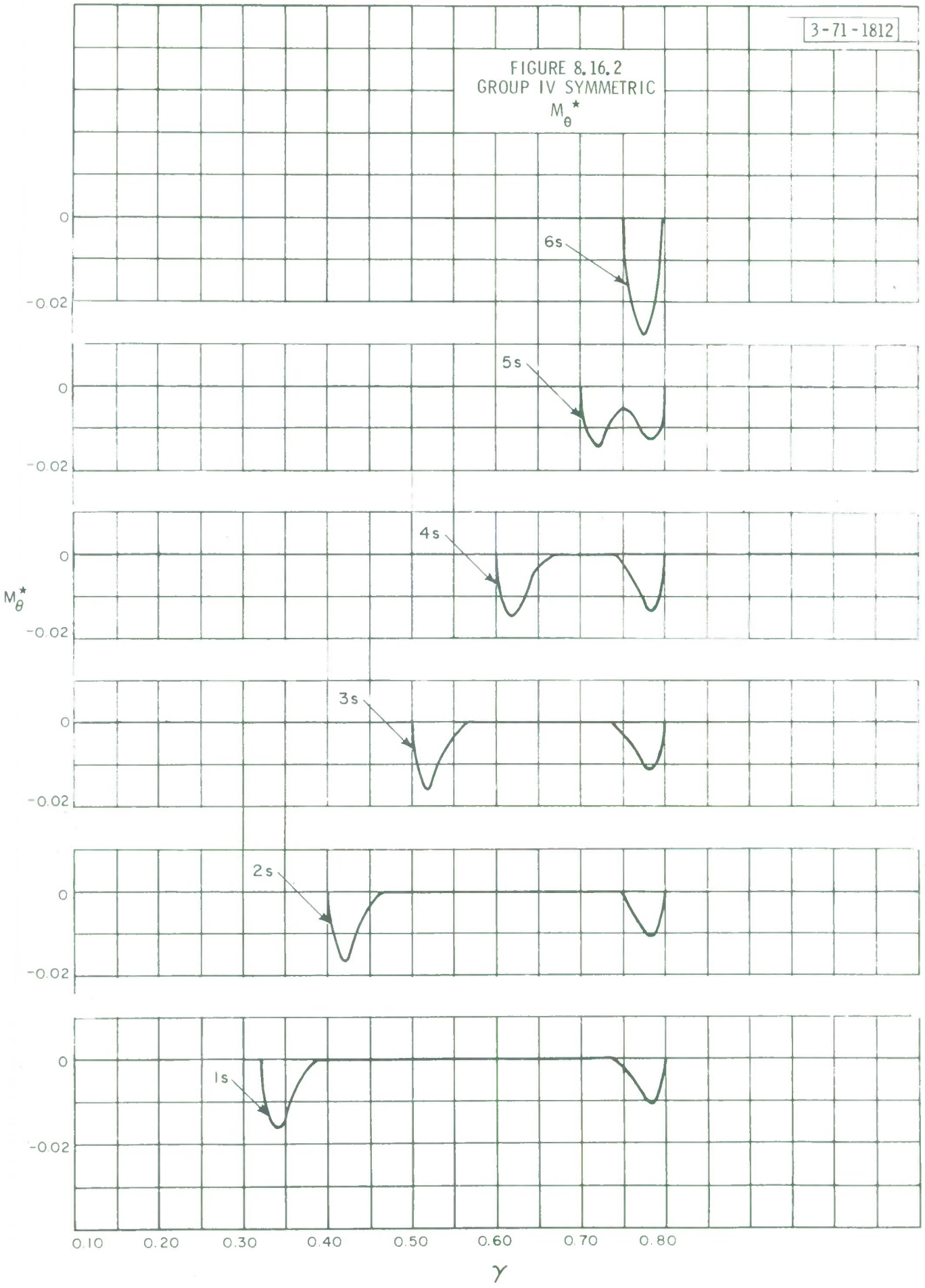
3-71-1812
FIGURE 8.16.2
GROUP IV SYMMETRIC
$M_\theta^\star$
6s
5s
4s
3s
2s
1s
0
-0.02
$M_\theta^\star$
0.10
0.20
0.30
0.40
0.50
0.60
0.70
0.80
γ

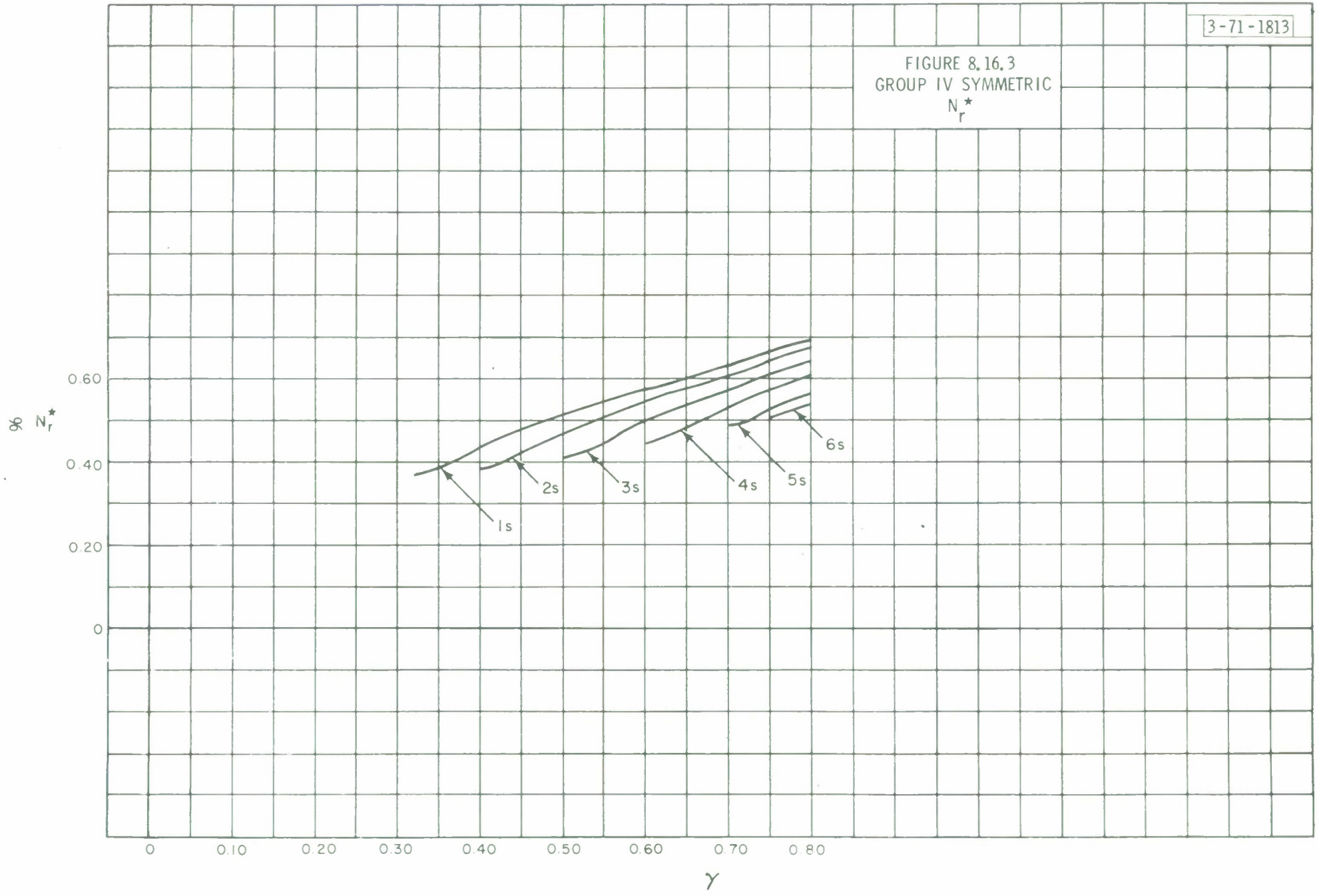
3-71-1813
FIGURE 8.16.3
GROUP IV SYMMETRIC
N_r^*
$\gamma_{N_r^*}$
0.60
0.40
0.20
0
0
0.10
0.20
0.30
0.40
0.50
0.60
0.70
0.80
γ
1s
2s
3s
4s
5s
6s

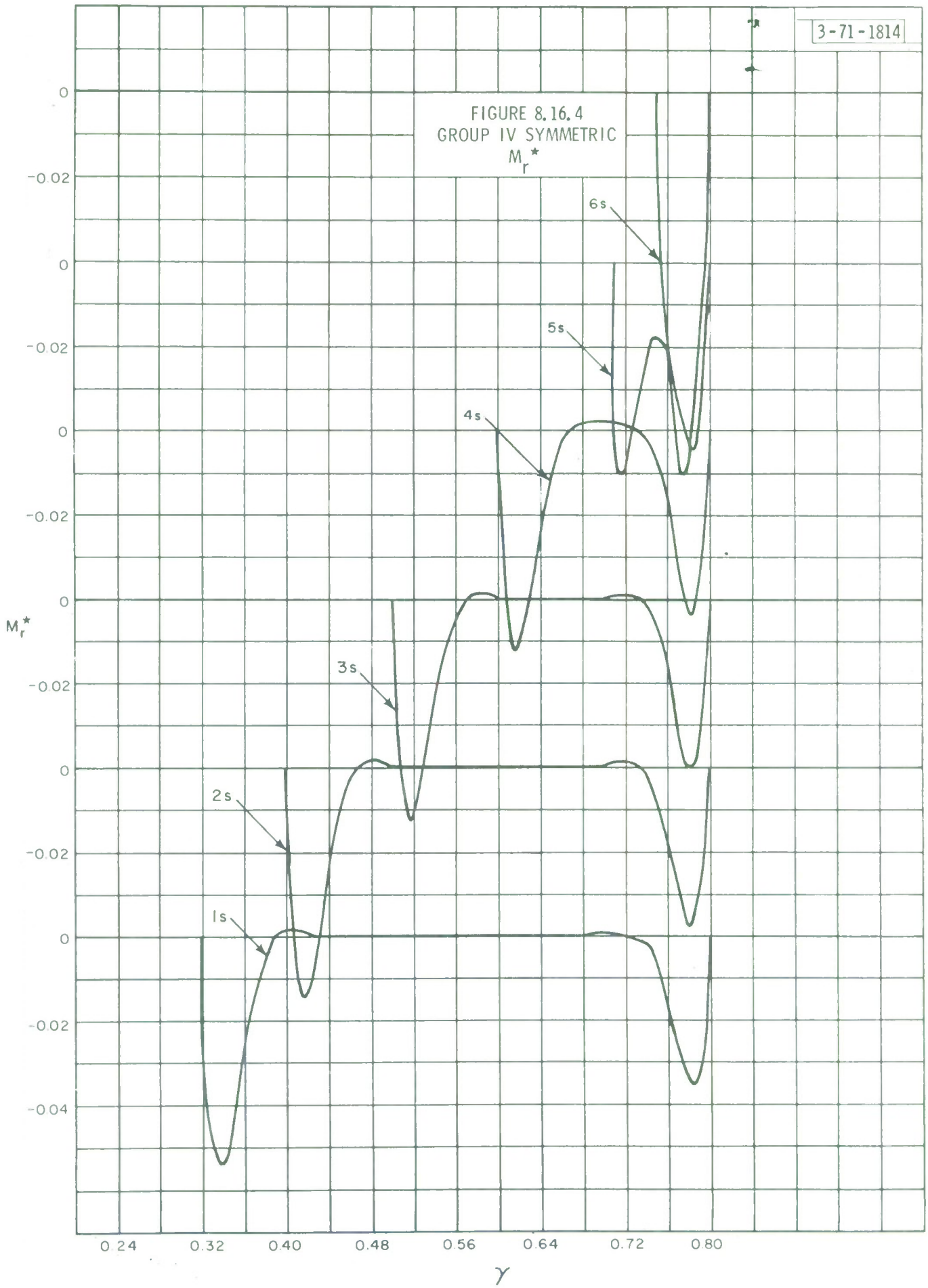
3-71-1814
FIGURE 8.16.4
GROUP IV SYMMETRIC
M_r^*
6s
5s
4s
3s
2s
1s
0
-0.02
0
-0.02
0
-0.02
0
-0.02
0
-0.02
0
-0.04
M_r^*
0.24
0.32
0.40
0.48
0.56
0.64
0.72
0.80
γ

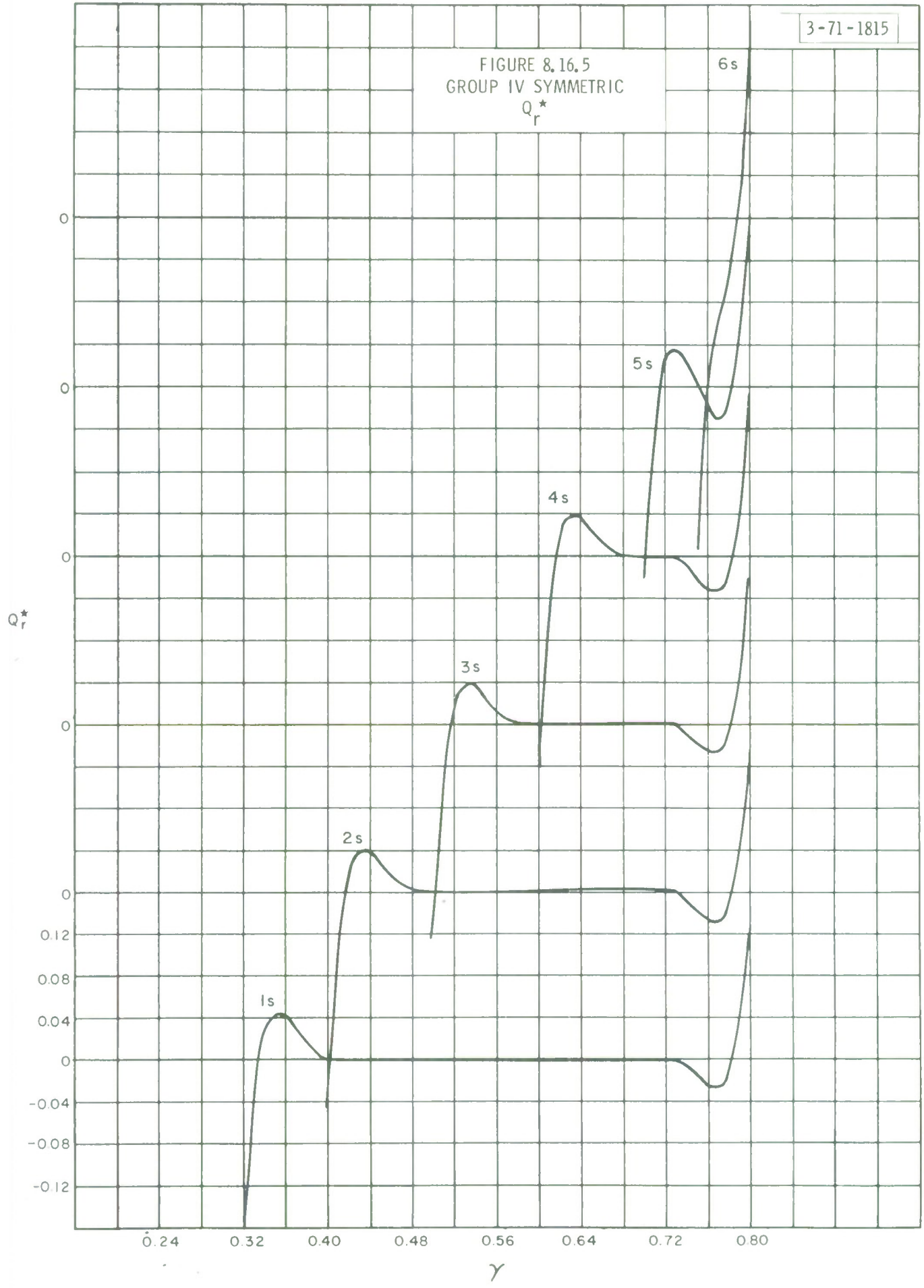
3-71-1815
FIGURE 8.16.5
GROUP IV SYMMETRIC
Q_r^*
6s
5s
4s
3s
2s
1s
Q_r^*
0
0
0
0
0
0.12
0.08
0.04
0
-0.04
-0.08
-0.12
0.24
0.32
0.40
0.48
0.56
0.64
0.72
0.80
γ

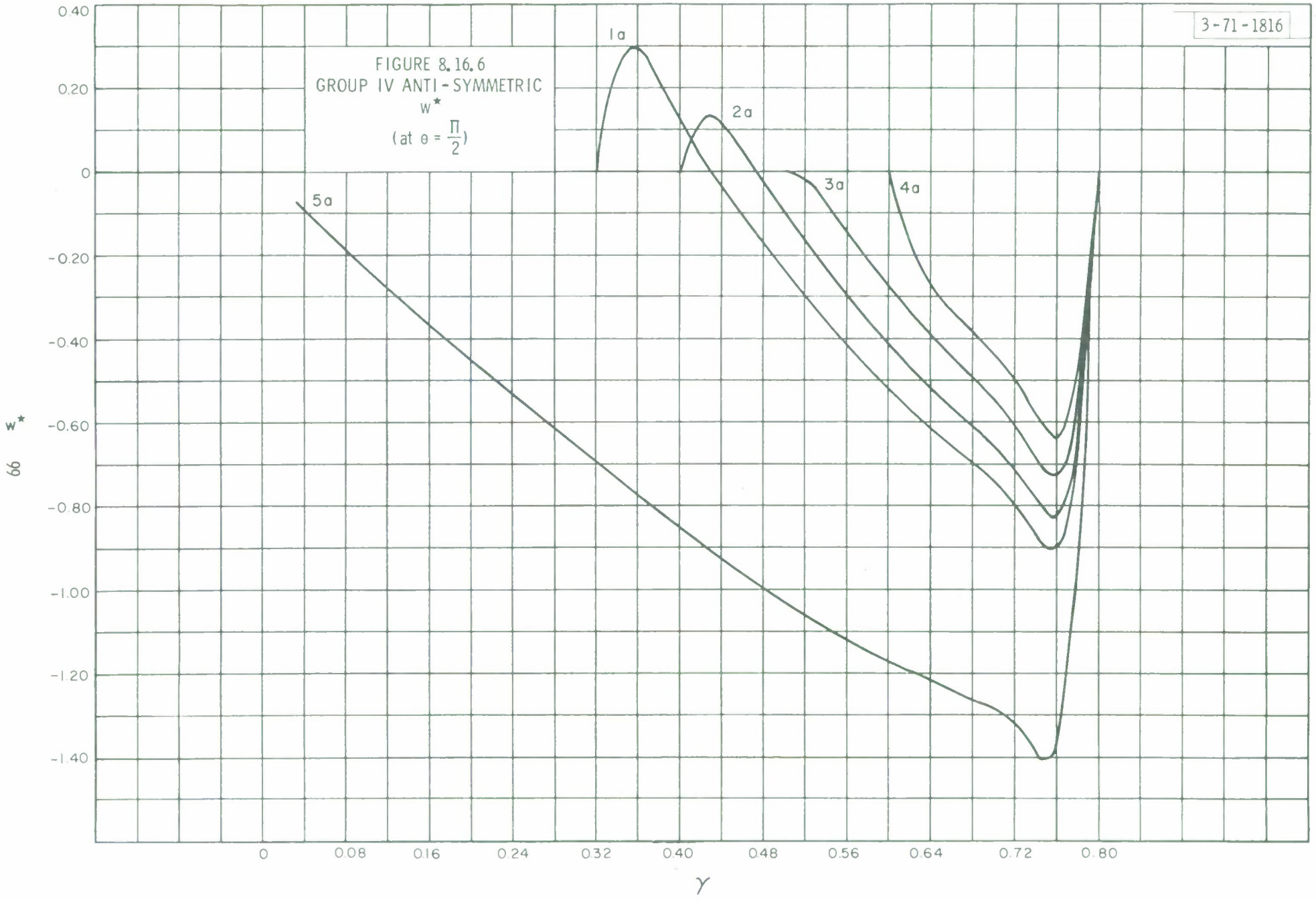
3-71-1816
FIGURE 8.16.6
GROUP IV ANTI-SYMMETRIC
w*
(at θ = Π/2)
1a
2a
3a
4a
5a
0.40
0.20
0
-0.20
-0.40
-0.60
-0.80
-1.00
-1.20
-1.40
w*
0
0.08
0.16
0.24
0.32
0.40
0.48
0.56
0.64
0.72
0.80
γ

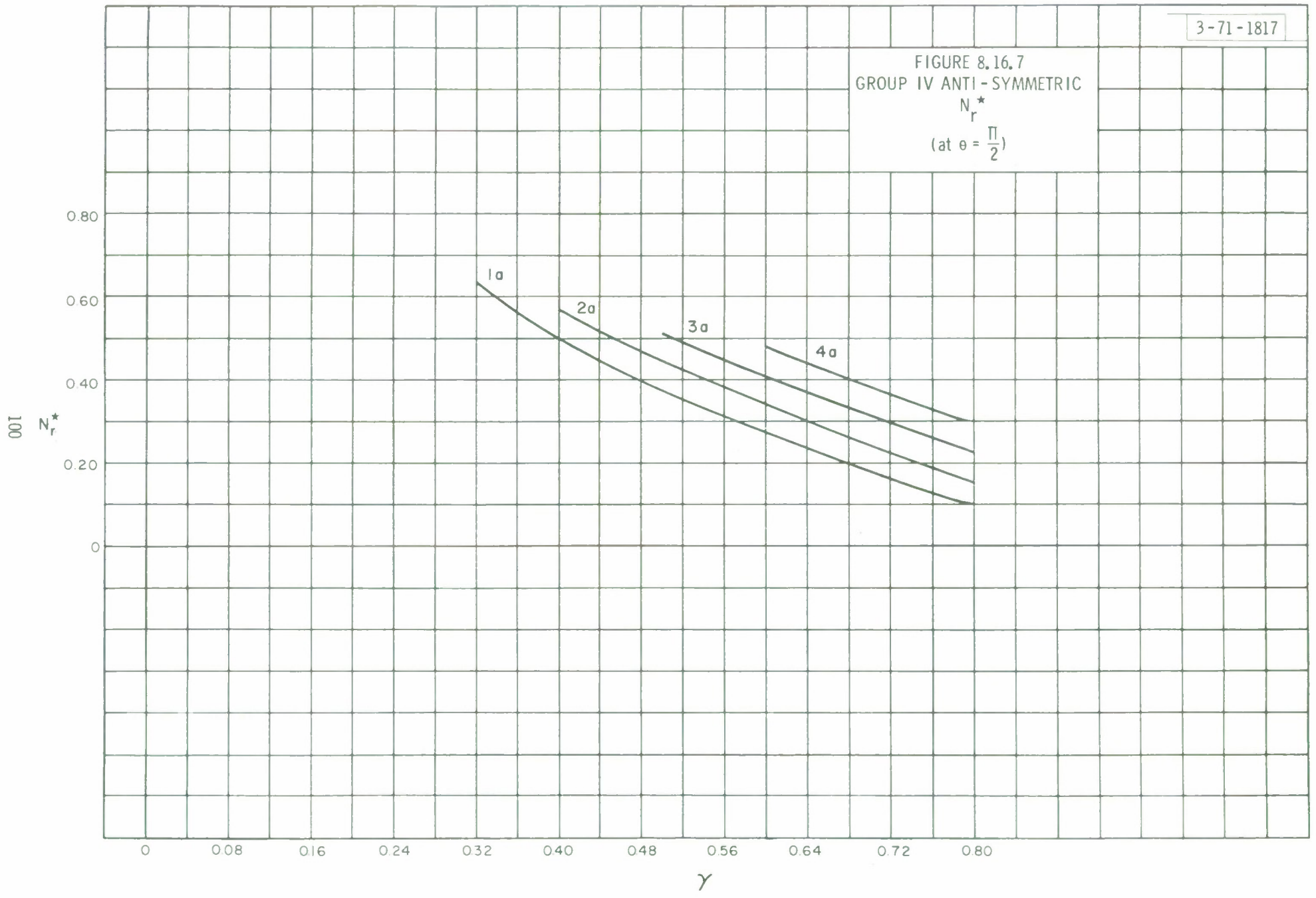
3-71-1817
FIGURE 8.16.7
GROUP IV ANTI-SYMMETRIC
N_r^*
(at $\theta = \frac{\pi}{2}$)
0.80
0.60
0.40
0.20
0
100
N_r^*
1a
2a
3a
4a
0
0.08
0.16
0.24
0.32
0.40
0.48
0.56
0.64
0.72
0.80
γ

3-71-1818

FIGURE 8.16.8
GROUP IV ANTI-SYMMETRIC
N_θ^*
(at $\theta = \frac{\pi}{2}$)

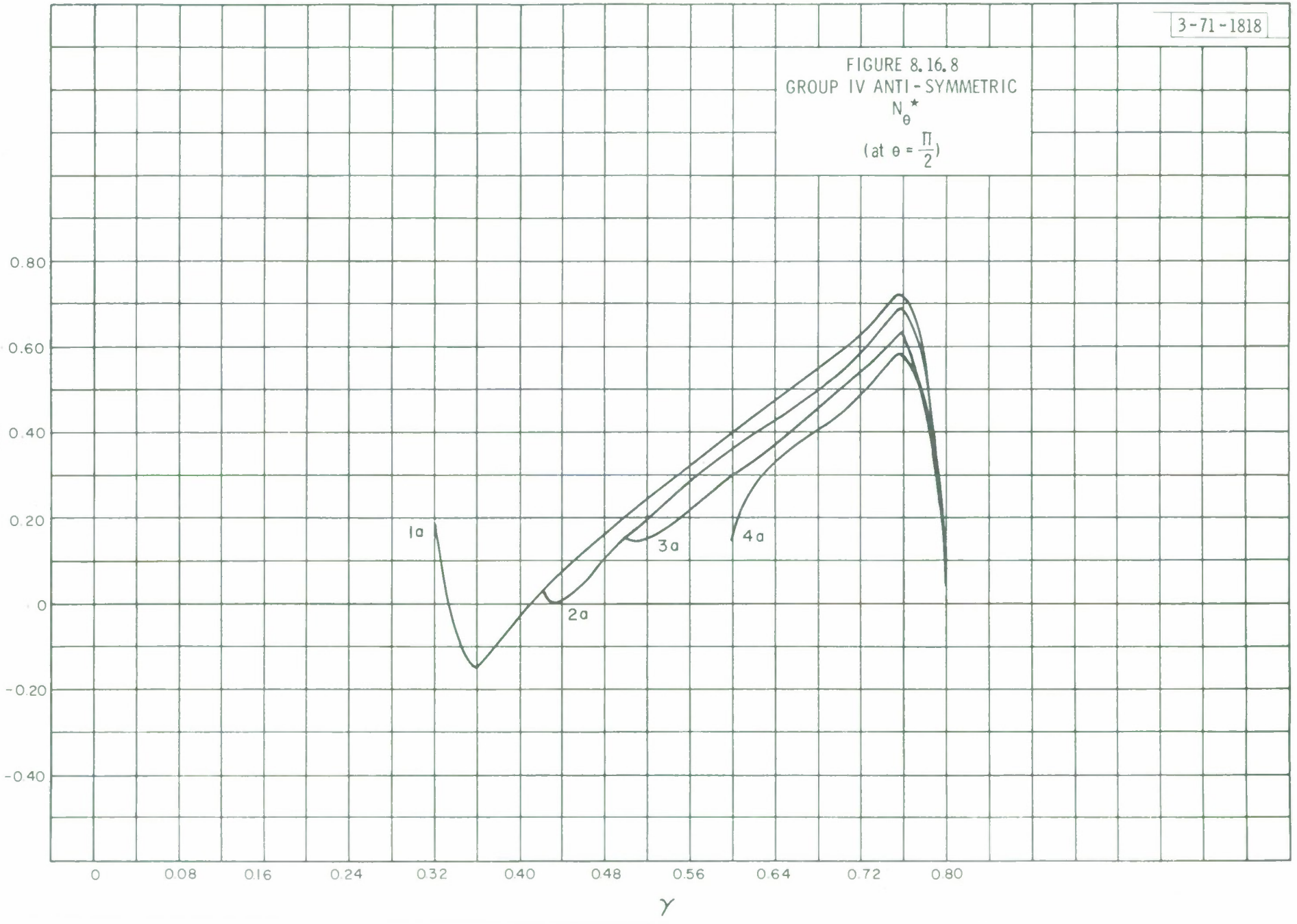

3-71-1819

FIGURE 8.16.9
GROUP IV ANTI-SYMMETRIC
$N_{r\theta}^{\star}$
(at $\theta = 0$)

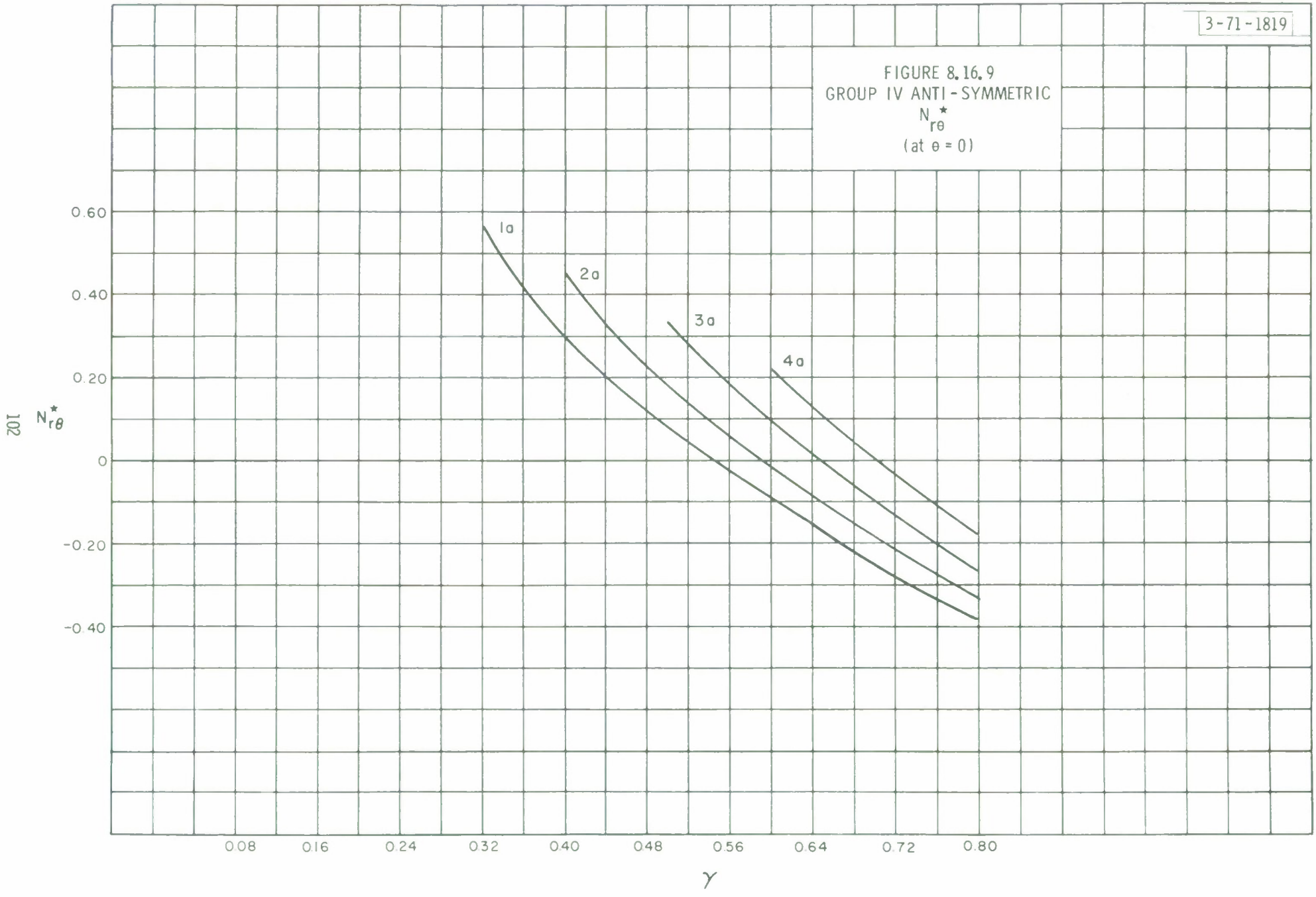

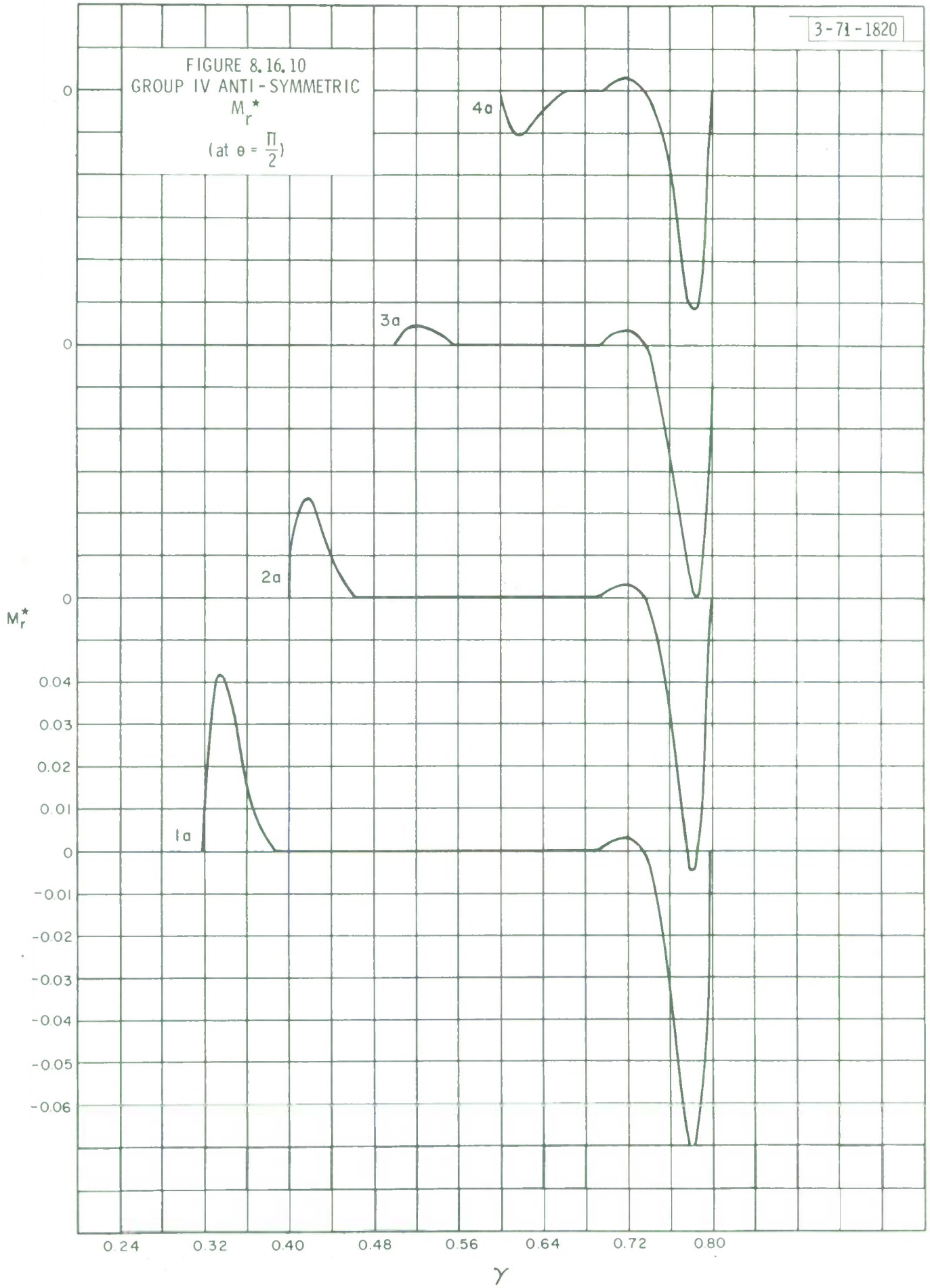
3-71-1820
FIGURE 8.16.10
GROUP IV ANTI-SYMMETRIC
M_r^*
(at $\theta = \frac{\pi}{2}$)
4a
3a
2a
1a
0
0
0
M_r^*
0.04
0.03
0.02
0.01
0
-0.01
-0.02
-0.03
-0.04
-0.05
-0.06
0.24
0.32
0.40
0.48
0.56
0.64
0.72
0.80
γ

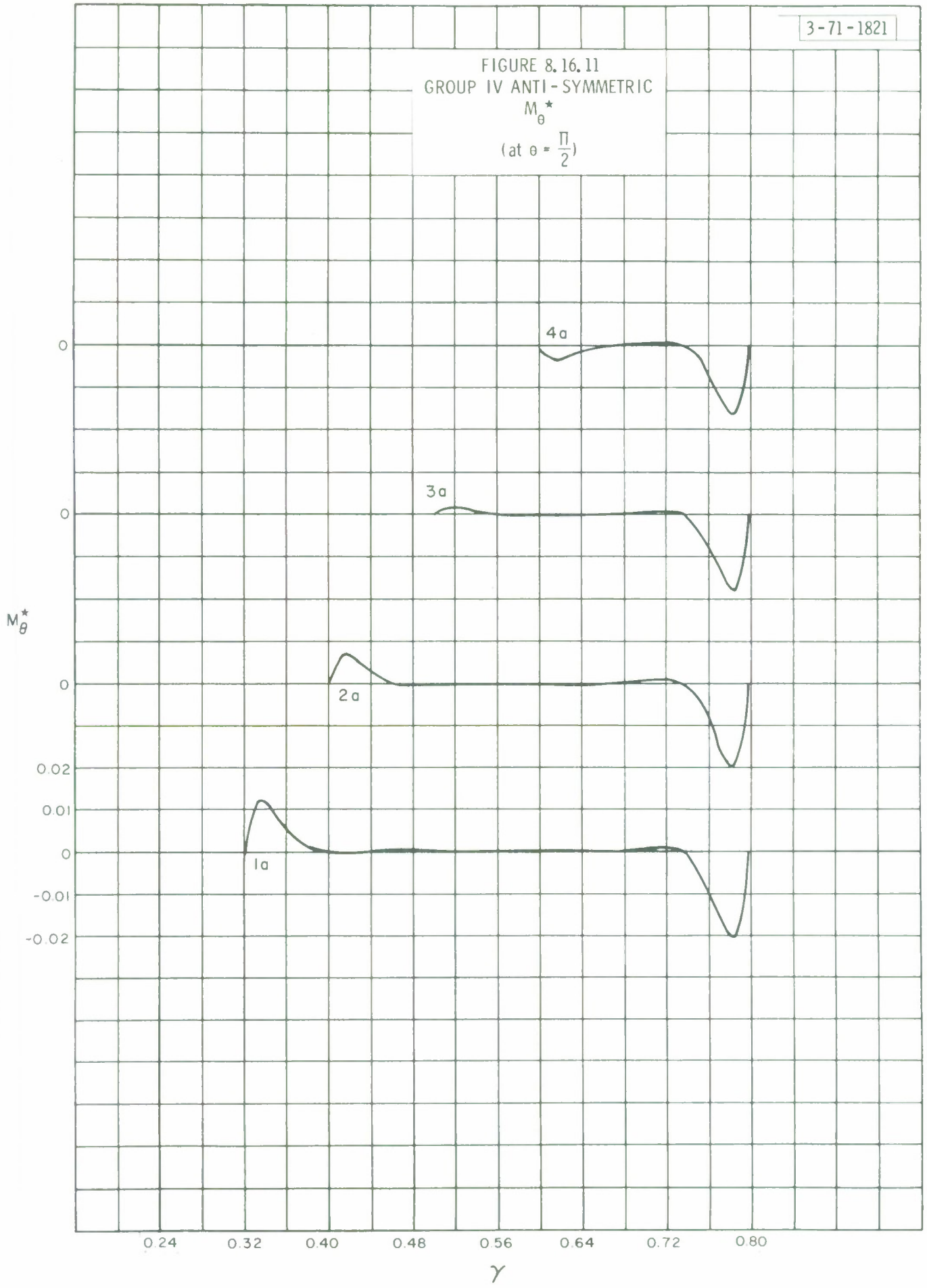
3-71-1821
FIGURE 8.16.11
GROUP IV ANTI-SYMMETRIC
M_θ^*
(at $\theta = \frac{\Pi}{2}$)
4a
3a
2a
1a
0
0
0
0.02
0.01
0
-0.01
-0.02
M_θ^*
0.24
0.32
0.40
0.48
0.56
0.64
0.72
0.80
γ

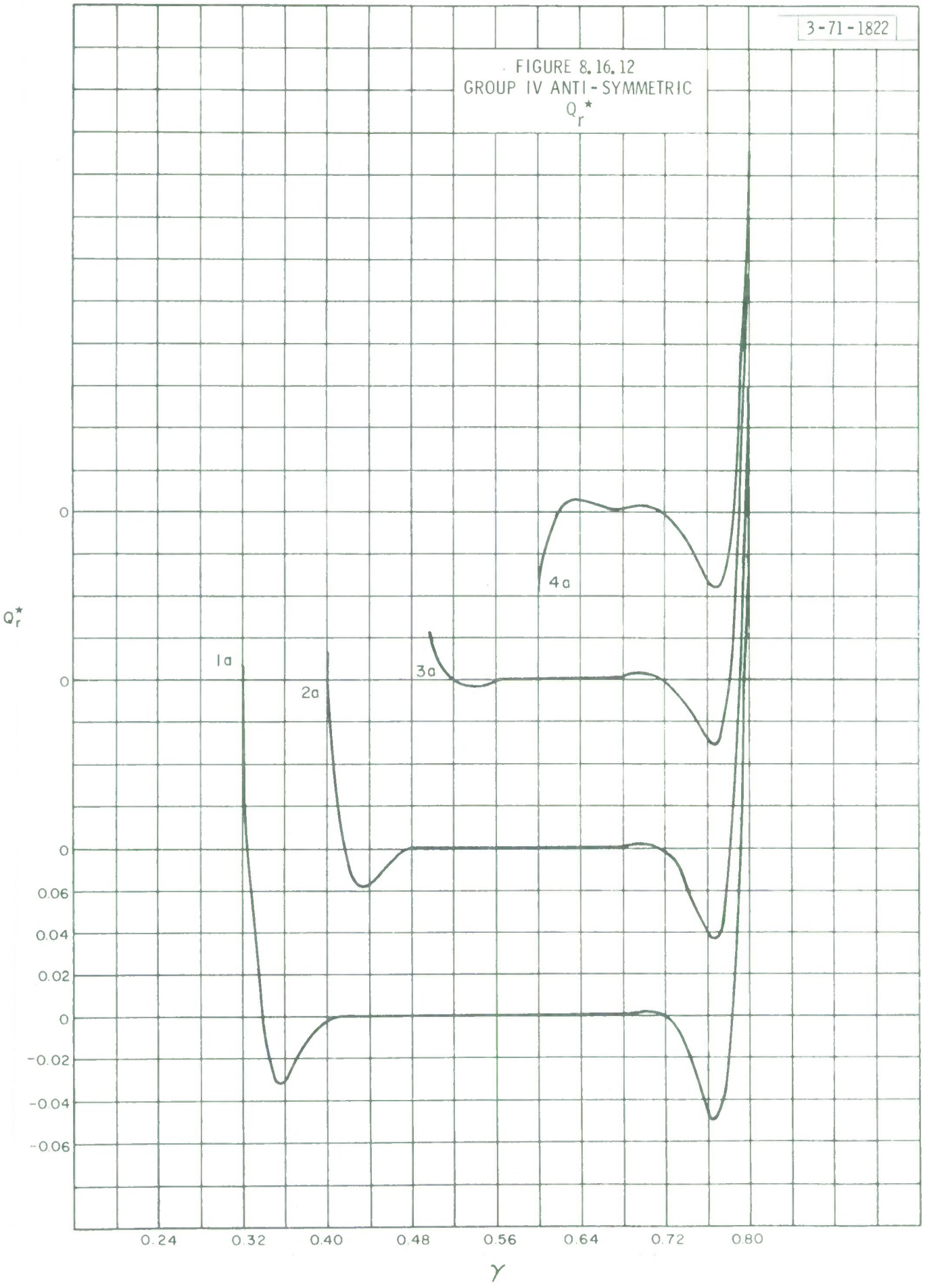
3-71-1822
FIGURE 8.16.12
GROUP IV ANTI-SYMMETRIC
Q_r^*
Q_r^*
0
0
0
0.06
0.04
0.02
0
-0.02
-0.04
-0.06
1a
2a
3a
4a
0.24
0.32
0.40
0.48
0.56
0.64
0.72
0.80
γ

FIGURE 8.16.13
GROUP IV ANTI-SYMMETRIC
u_r^* (at $\theta = \frac{\pi}{2}$)
u_θ^* (at $\theta = 0$)

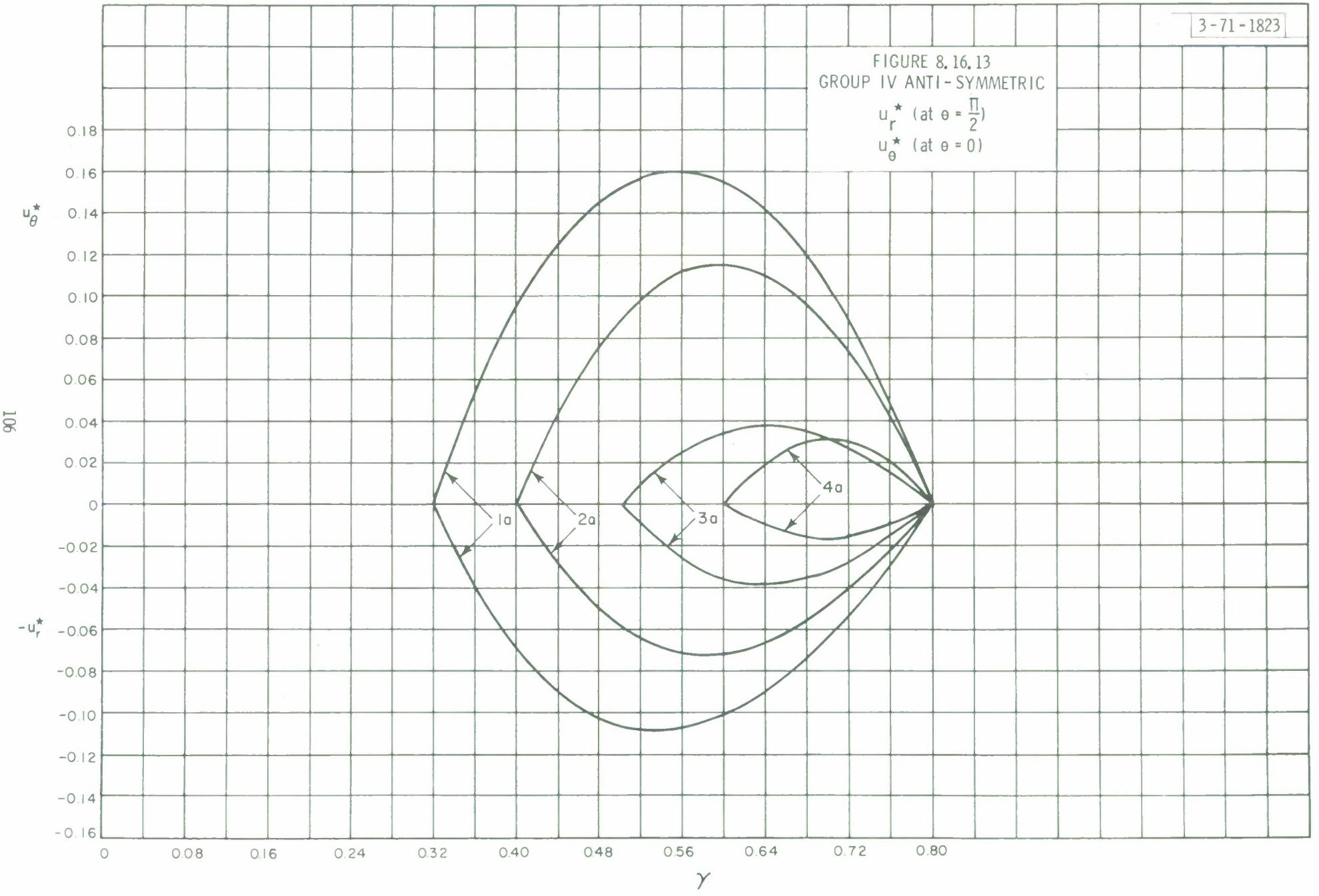

8.17 Group V - Ten Shells with an Outer Radius of 1382.4 Inches

The results in this section illustrate the behavior of seven shells with the same outer radius of 1382.4 inches but with different inner radii. Dimensions and other pertinent data are summarized in Table 8.17.1. The outer radius is equivalent to $\gamma = 1.20$ while the inner radii correspond to a shell closed at the apex and to slopes of $\gamma = .30, .40, .48, .60, .75, .90, 1.05, 1.075$ and 1.15. Both the symmetric and anti-symmetric behavior under gravity loads are shown with the former corresponding to a pointing angle of $\psi = 0°$ and the latter to $\psi = 90°$. The curves, in addition to the heading of three groups of numbers (e.g. 8.17.1), bear either the letter s, signifying symmetric behavior or a, signifying anti-symmetric behavior. Results are all in normalized form (see page 43 of this report).

In general, the Group V results exhibit the same trends as the results for Groups II, III, and IV which are shells with smaller outer radii. The deflections are larger for the Group V shells because the outer radius is the largest of all the groups. Note, however, that the quantities associated with bending behavior such as edge zone width, M_r^*, Q_r^*, etc. do not vary appreciably between the four groups.

Table 8.17.1

Group V Examples

Case	R_1 (inches)	R_2 (inches)	B.C. at R_1	B.C. at R_2	Loading
1s	552.96	1382.4	Simple support	Simple support	Sym.-gravity
2s	691.2	"	"	"	"
3s	864	"	"	"	"
4s	1036.8	"	"	"	"
5s	1209.6	"	"	"	"
6s	1296.0	"	"	"	"
7s	---	"	---	"	"
1a	552.96	"	Simple support	"	Anti-Sym.-gravity
2a	691.2	"	"	"	"
3a	864	"	"	"	"
4a	1036.8	"	"	"	"
5a	1209.6	"	"	"	"
6a	1296.0	"	"	"	"
7a	---	"	---	"	"
8a	345.6	"	Simple support	"	"
9a	460.8	"	"	"	"
10a	1324.8	"	"	"	"

Note: Material properties are $E = 10^7$ p.s.i., $\nu = .3$, $\rho_o = .10$ lb. per cubic inch.

Focal length $f = 576$ inches, shell thickness $h = 1$ inch.

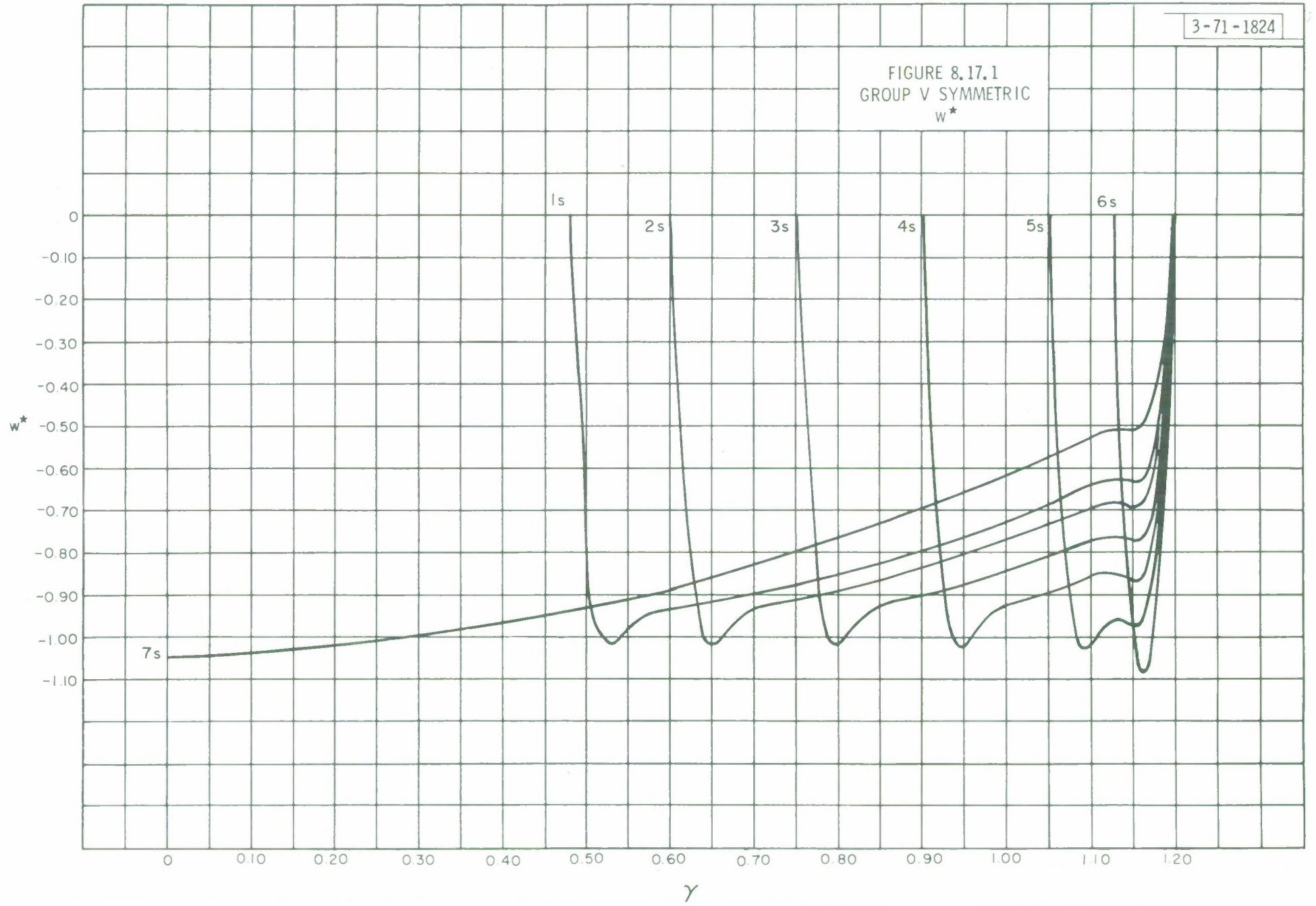
3-71-1824
FIGURE 8.17.1
GROUP V SYMMETRIC
w*
1s
2s
3s
4s
5s
6s
7s
0
-0.10
-0.20
-0.30
-0.40
-0.50
-0.60
-0.70
-0.80
-0.90
-1.00
-1.10
w*
0
0.10
0.20
0.30
0.40
0.50
0.60
0.70
0.80
0.90
1.00
1.10
1.20
γ

3-71-1825

FIGURE 8.17.2
GROUP V SYMMETRIC
$N_\theta^\star$

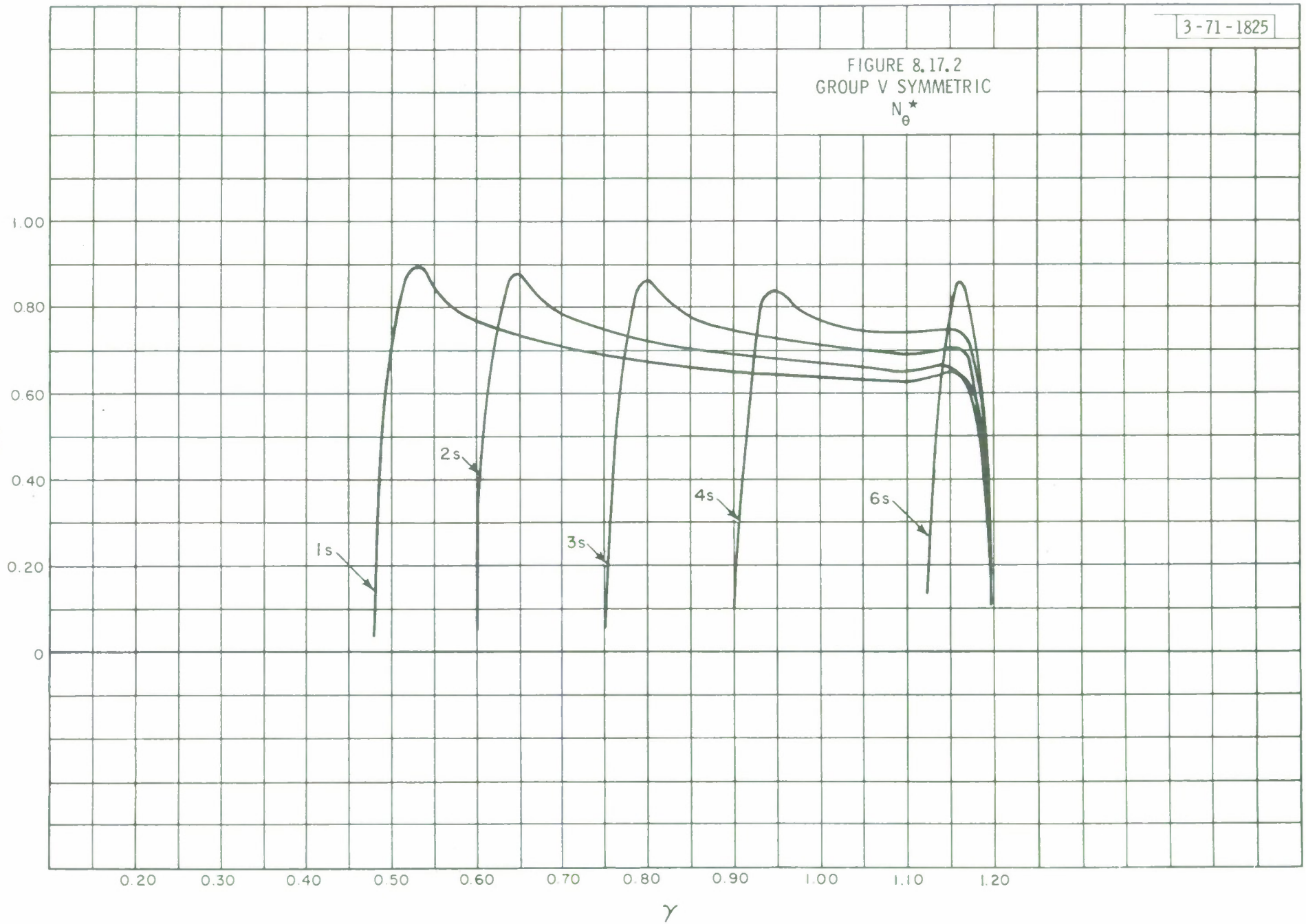

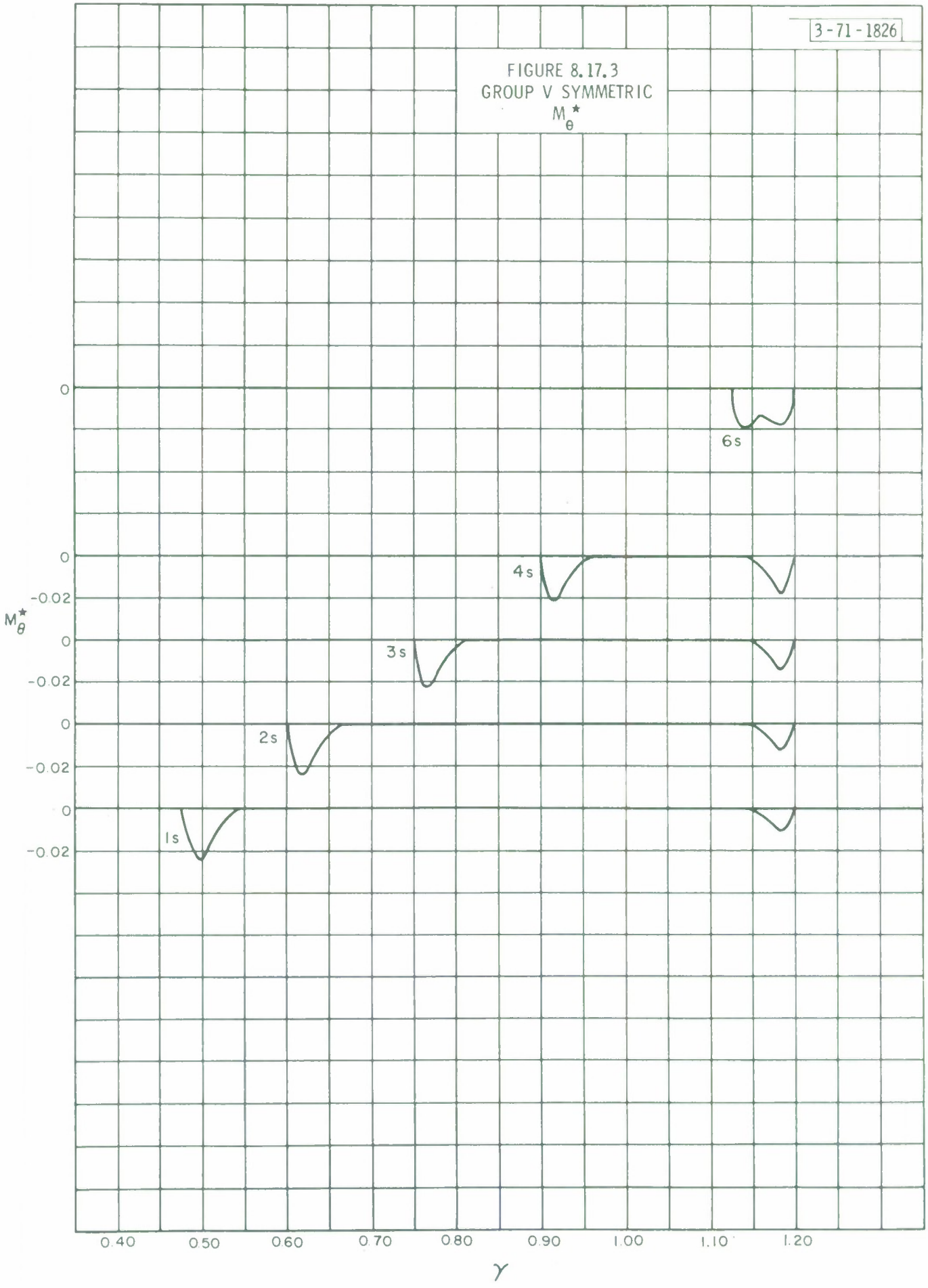
3-71-1826
FIGURE 8.17.3
GROUP V SYMMETRIC
$M_\theta^\star$
0
0
-0.02
0
-0.02
0
-0.02
0
-0.02
$M_\theta^\star$
1s
2s
3s
4s
6s
0.40
0.50
0.60
0.70
0.80
0.90
1.00
1.10
1.20
γ

3-71-1827

FIGURE 8.17.4
GROUP V SYMMETRIC
N_r^*

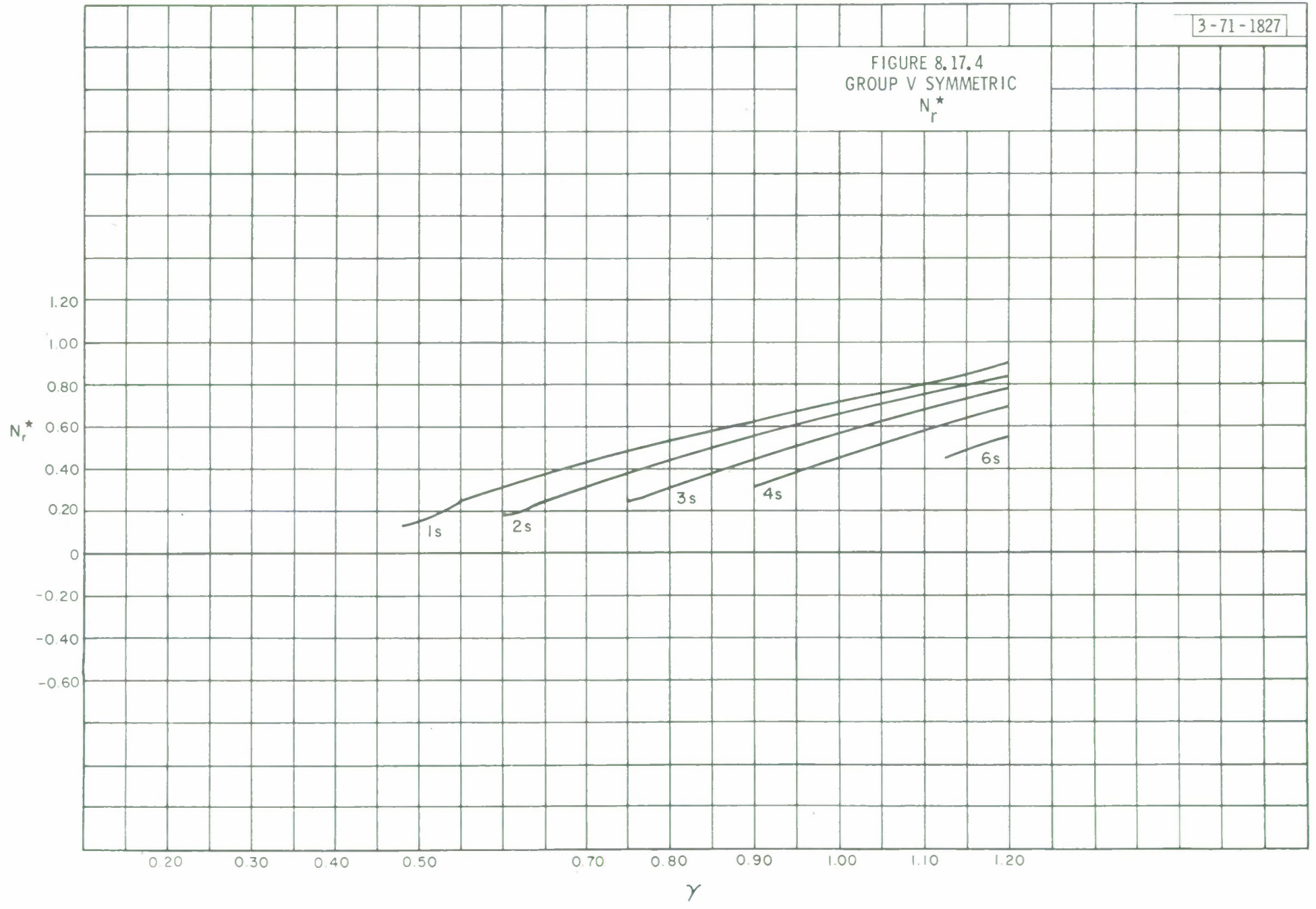

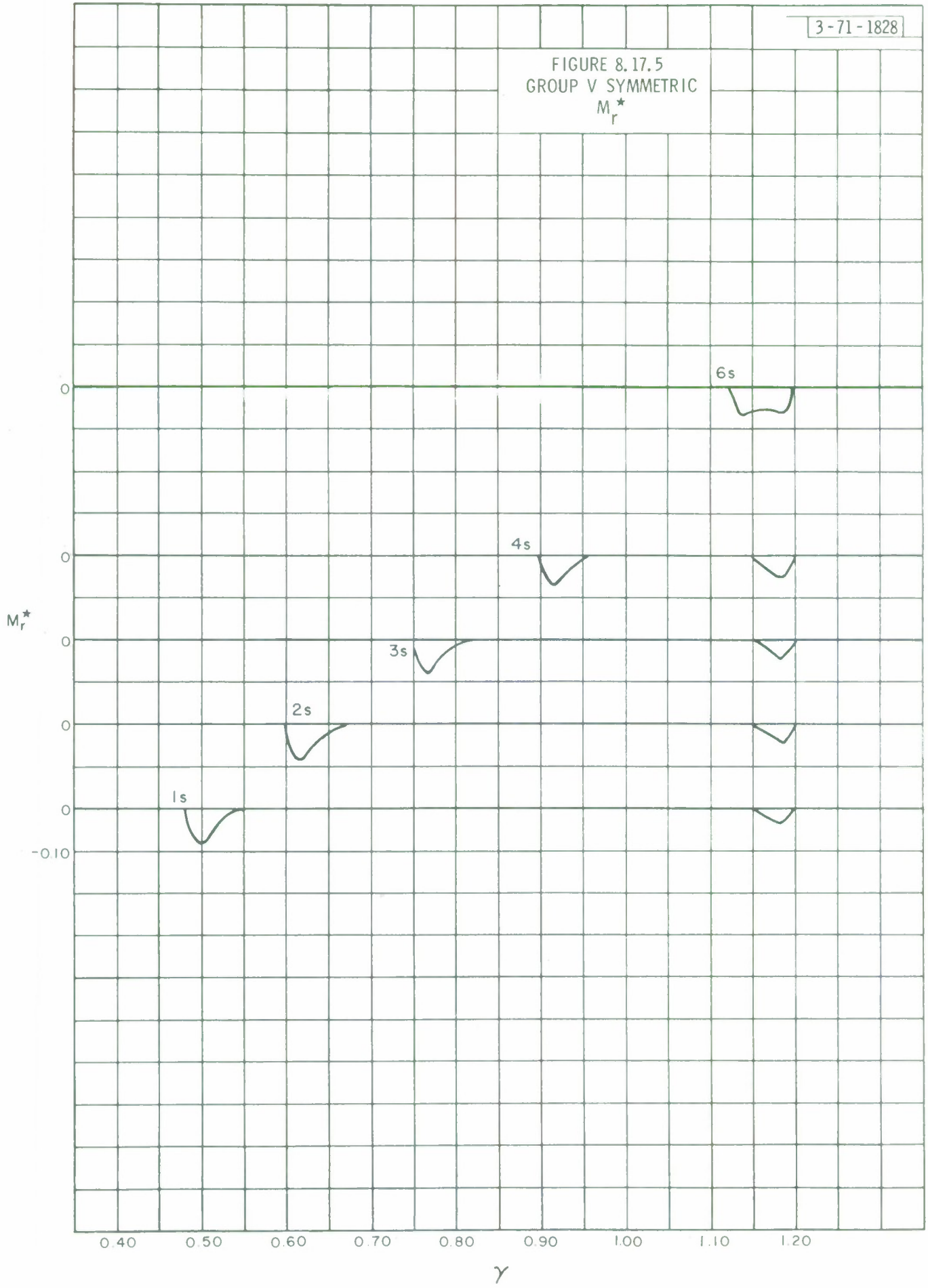
3-71-1828
FIGURE 8.17.5
GROUP V SYMMETRIC
M_r^*
6s
4s
3s
2s
1s
0
0
0
0
-0.10
M_r^*
0.40
0.50
0.60
0.70
0.80
0.90
1.00
1.10
1.20
γ

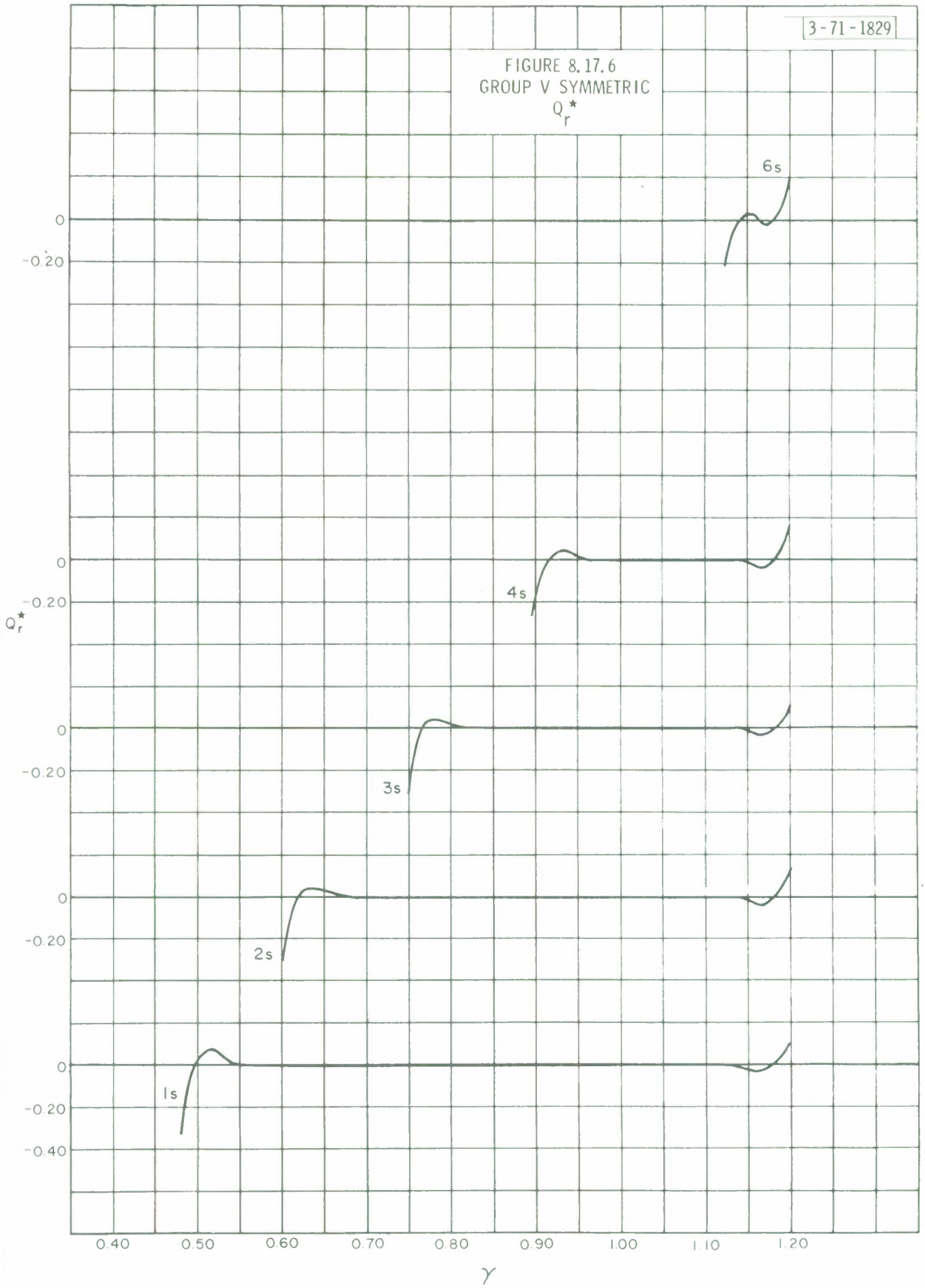
3-71-1829
FIGURE 8.17.6
GROUP V SYMMETRIC
Q_r^*
6s
4s
3s
2s
1s
0
-0.20
-0.40
Q_r^*
0.40
0.50
0.60
0.70
0.80
0.90
1.00
1.10
1.20
γ

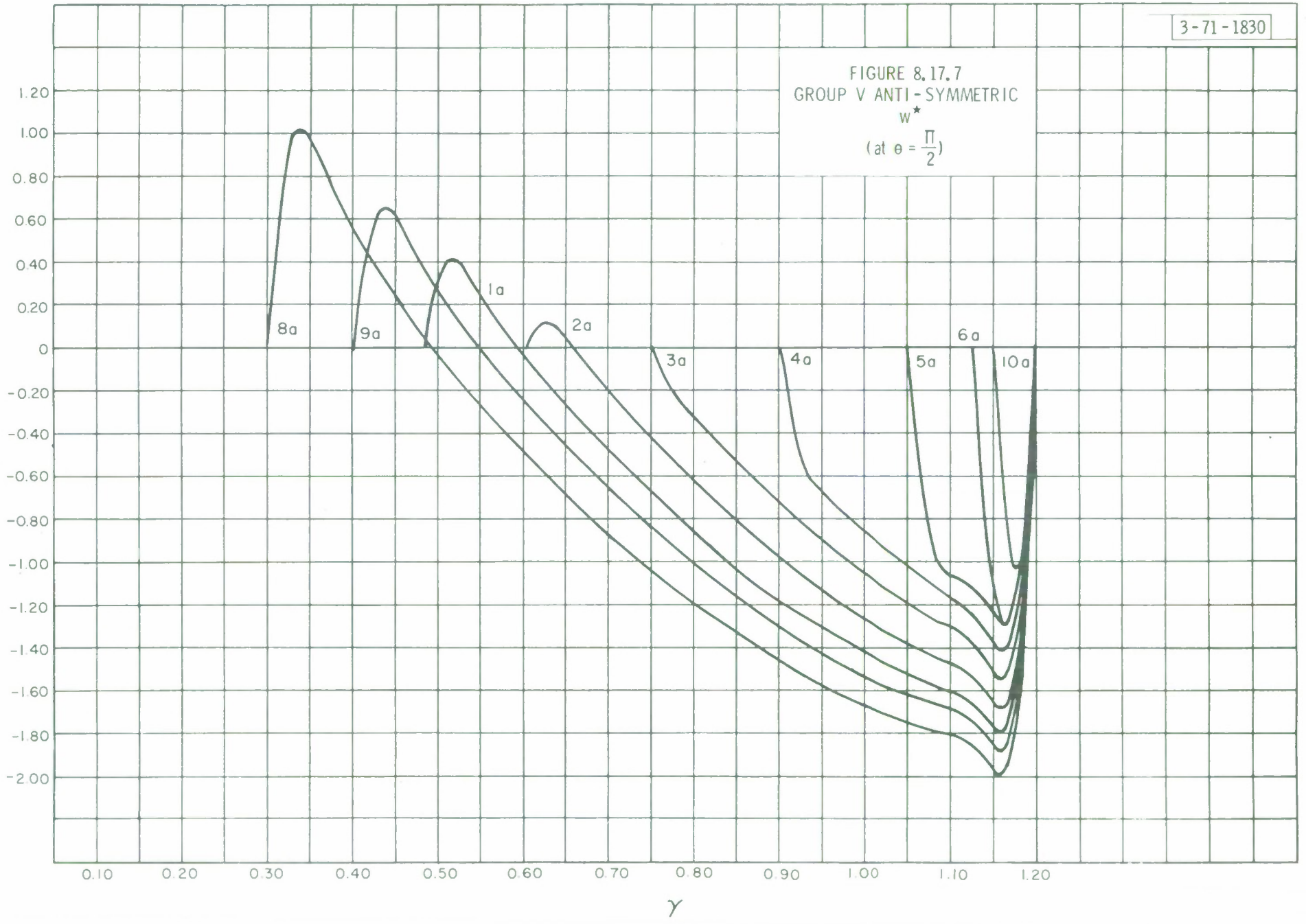
3-71-1830
FIGURE 8.17.7
GROUP V ANTI-SYMMETRIC
w*
(at θ = π/2)
1.20
1.00
0.80
0.60
0.40
0.20
0
-0.20
-0.40
-0.60
-0.80
-1.00
-1.20
-1.40
-1.60
-1.80
-2.00
w*
8a
9a
1a
2a
3a
4a
5a
6a
10a
0.10
0.20
0.30
0.40
0.50
0.60
0.70
0.80
0.90
1.00
1.10
1.20
γ

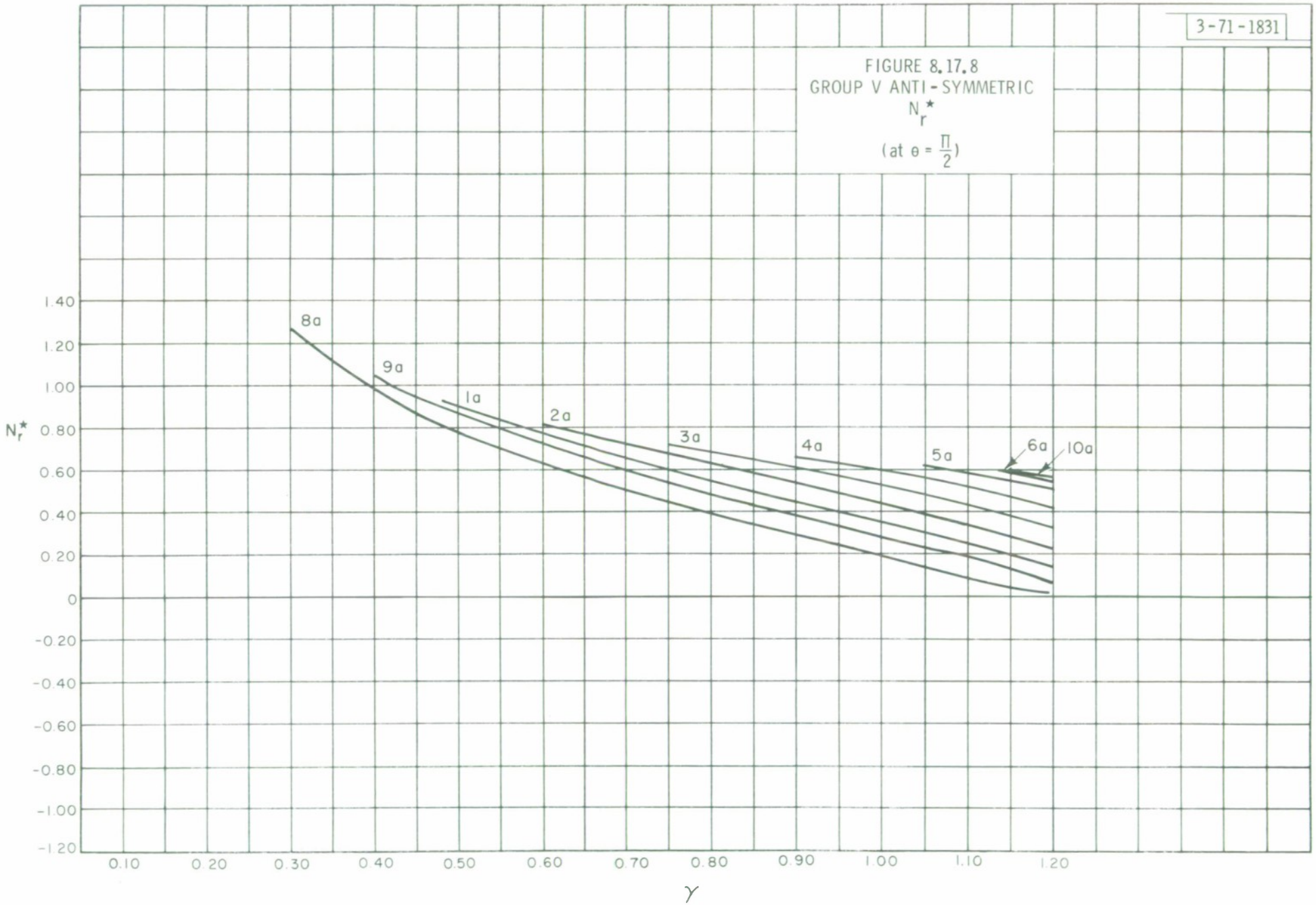
3-71-1831
FIGURE 8.17.8
GROUP V ANTI-SYMMETRIC
N_r^*
(at $\theta = \frac{\pi}{2}$)
N_r^*
1.40
1.20
1.00
0.80
0.60
0.40
0.20
0
-0.20
-0.40
-0.60
-0.80
-1.00
-1.20
8a
9a
1a
2a
3a
4a
5a
6a
10a
0.10
0.20
0.30
0.40
0.50
0.60
0.70
0.80
0.90
1.00
1.10
1.20
γ

3-71-1832

FIGURE 8.17.9
GROUP V ANTI-SYMMETRIC
$N_\theta^\star$
(at $\theta = \frac{\pi}{2}$)

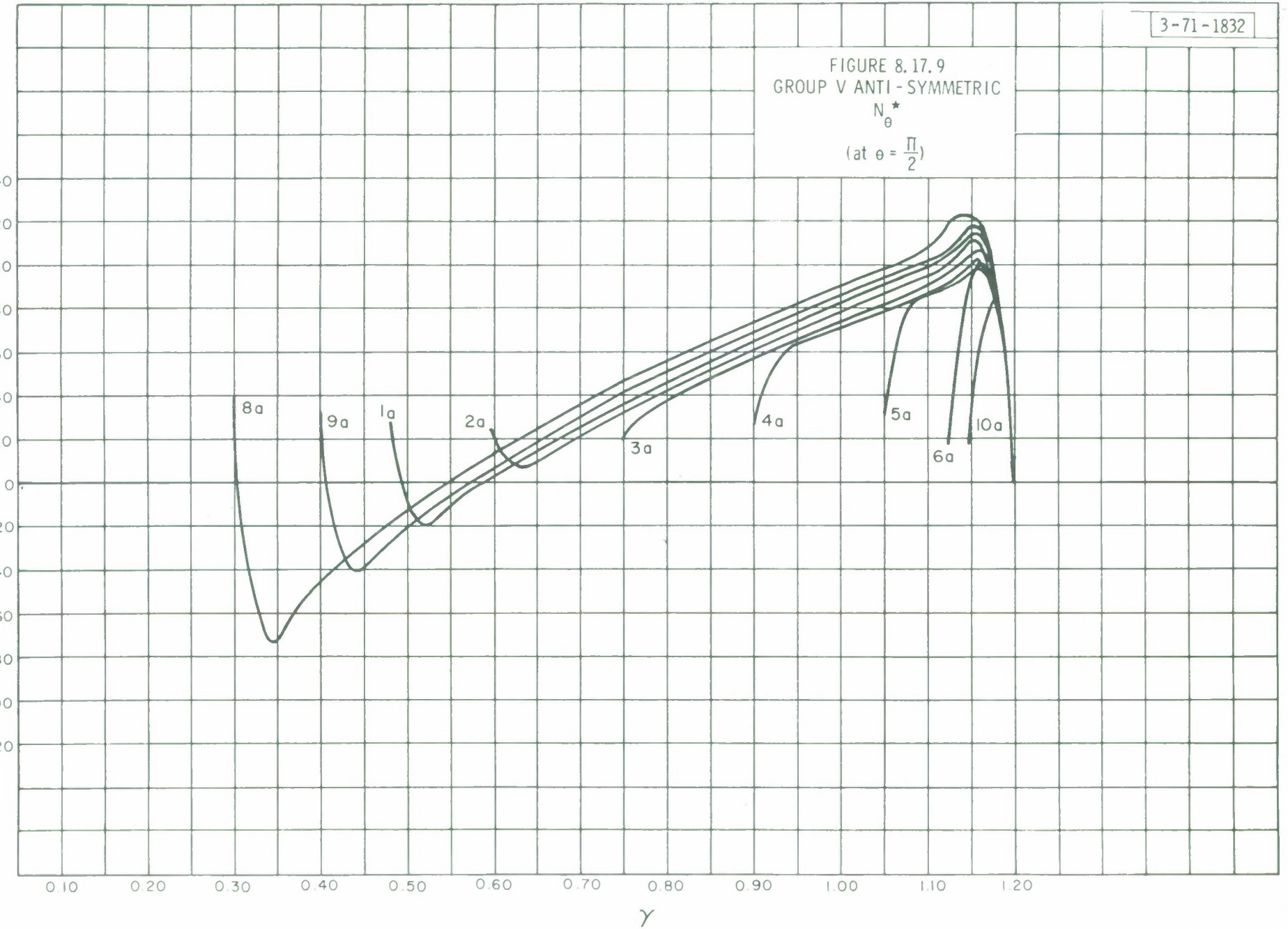

3-71-1833

FIGURE 8.17.10
GROUP V ANTI-SYMMETRIC
$N_{r\theta}^{\star}$
(at $\theta = 0$)

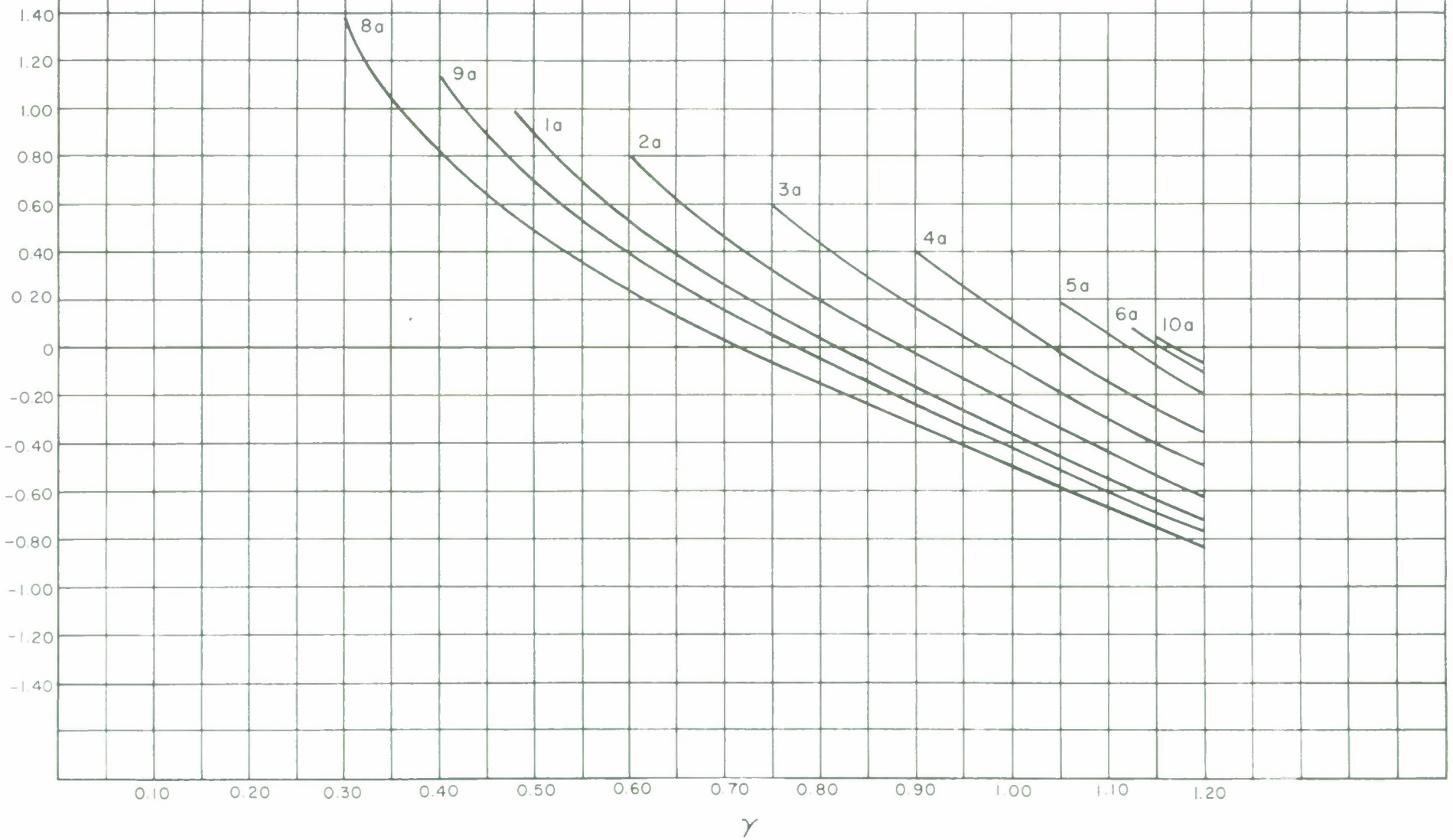

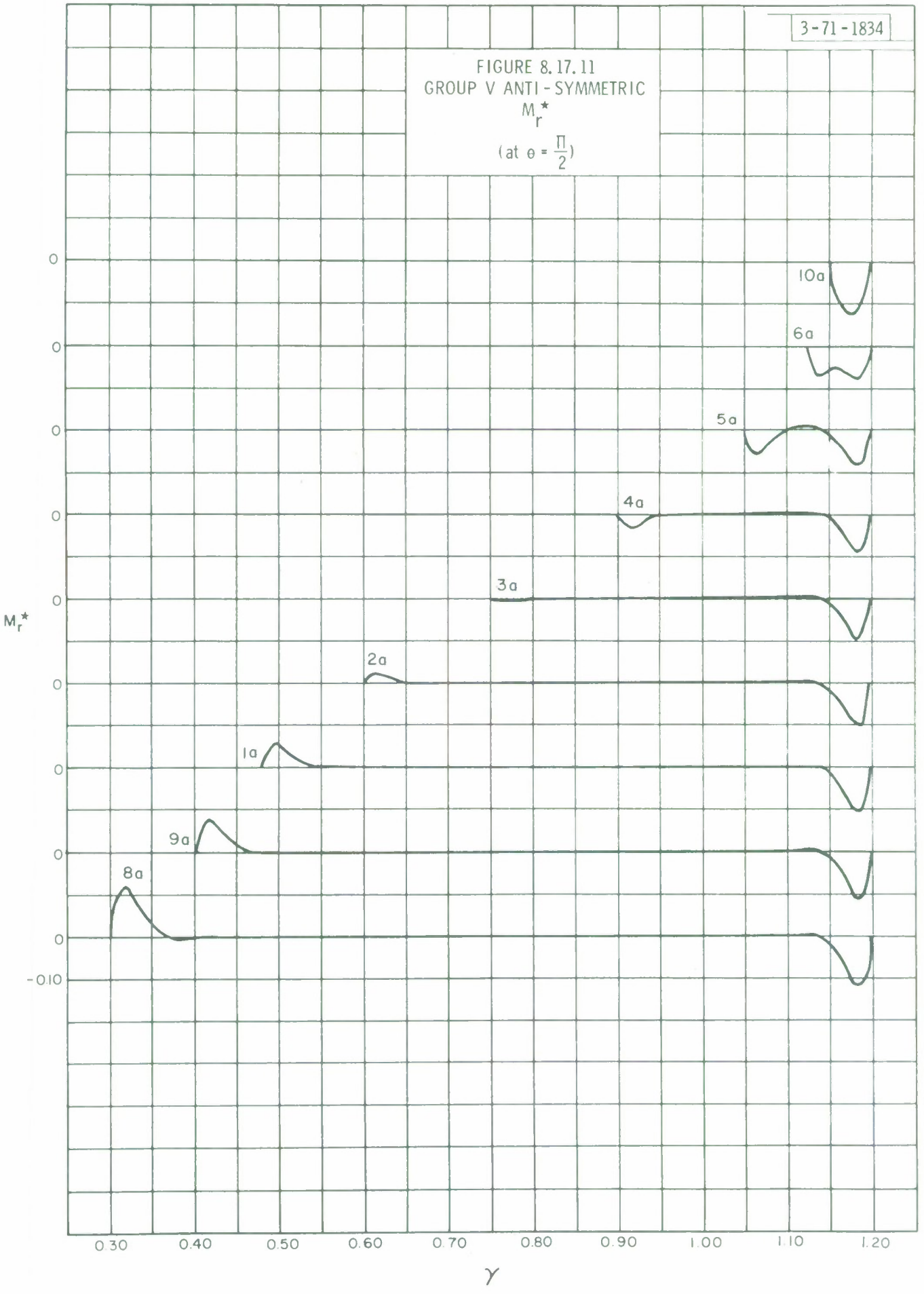
3-71-1834
FIGURE 8.17.11
GROUP V ANTI-SYMMETRIC
M_r^*
(at $\theta = \frac{\Pi}{2}$)
10a
6a
5a
4a
3a
2a
1a
9a
8a
M_r^*
0
0
0
0
0
0
0
0
0
-0.10
0.30
0.40
0.50
0.60
0.70
0.80
0.90
1.00
1.10
1.20
γ

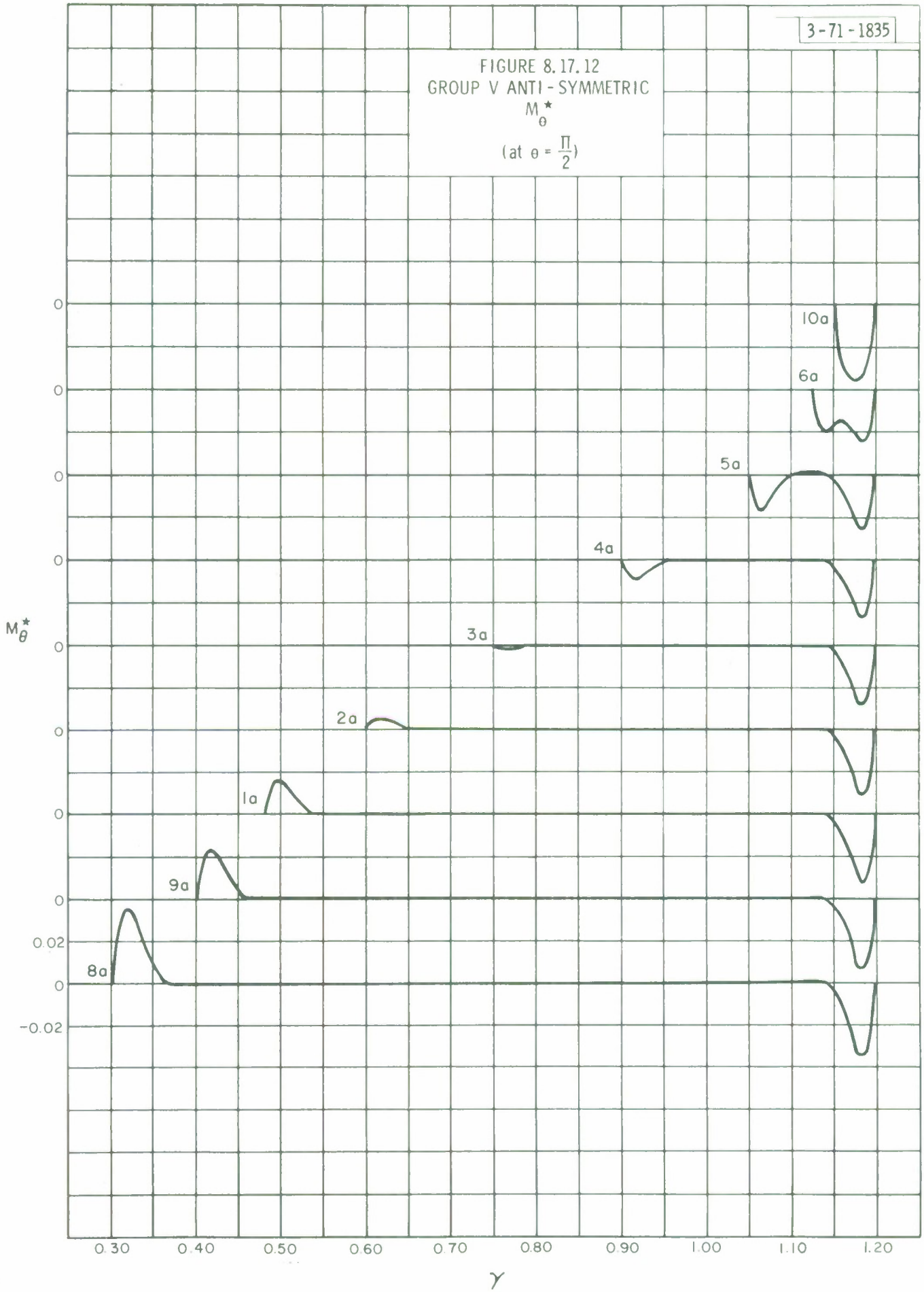
3-71-1835
FIGURE 8.17.12
GROUP V ANTI-SYMMETRIC
M_θ^*
(at $\theta = \frac{\Pi}{2}$)
10a
6a
5a
4a
3a
2a
1a
9a
8a
0
0
0
0
0
0
0
0
0.02
0
-0.02
M_θ^*
0.30
0.40
0.50
0.60
0.70
0.80
0.90
1.00
1.10
1.20
γ

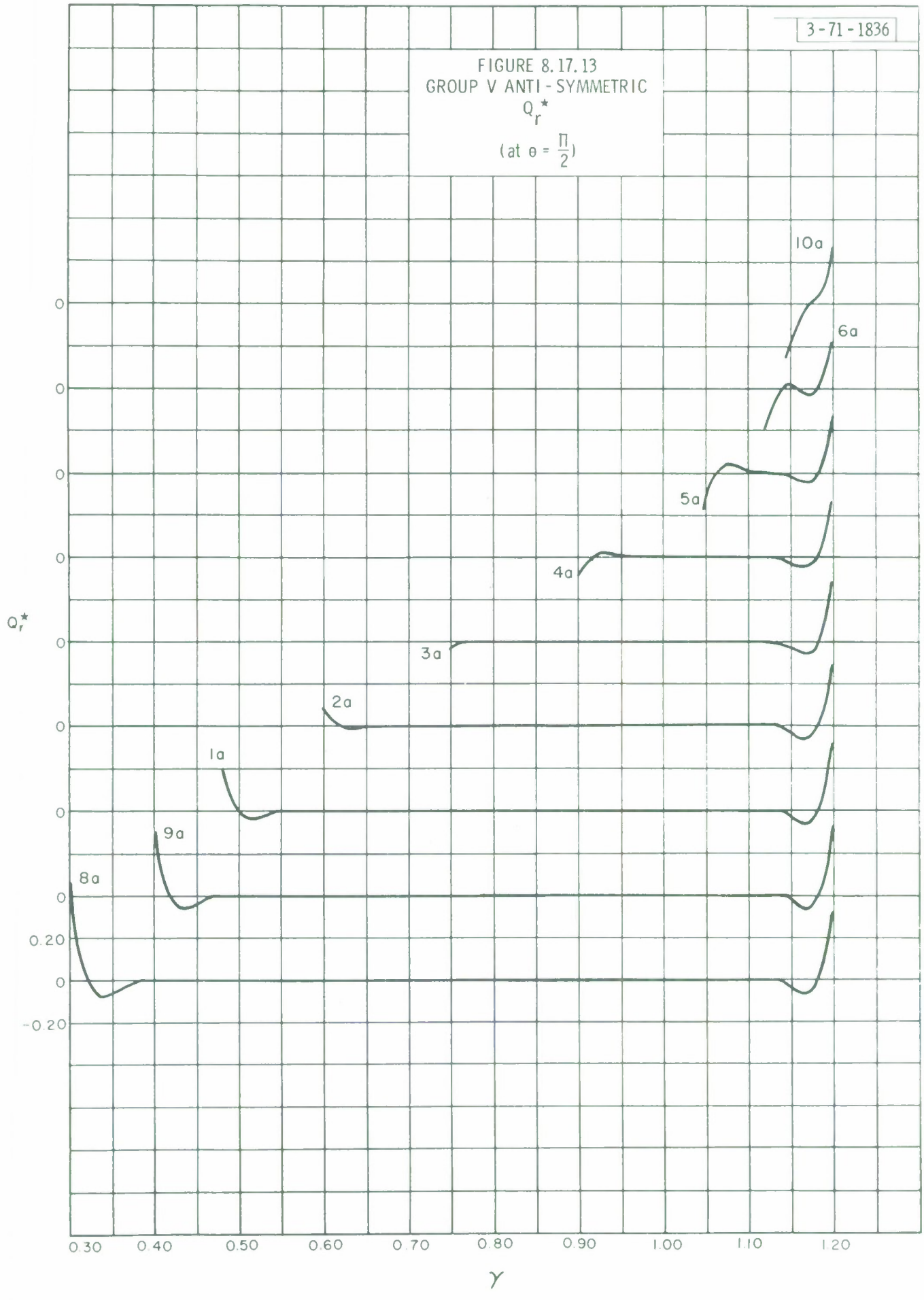
3-71-1836
FIGURE 8.17.13
GROUP V ANTI-SYMMETRIC
Q_r^*
(at $\theta = \frac{\Pi}{2}$)
10a
6a
5a
4a
3a
2a
1a
9a
8a
Q_r^*
0
0
0
0
0
0
0
0
0.20
0
-0.20
0.30
0.40
0.50
0.60
0.70
0.80
0.90
1.00
1.10
1.20
γ

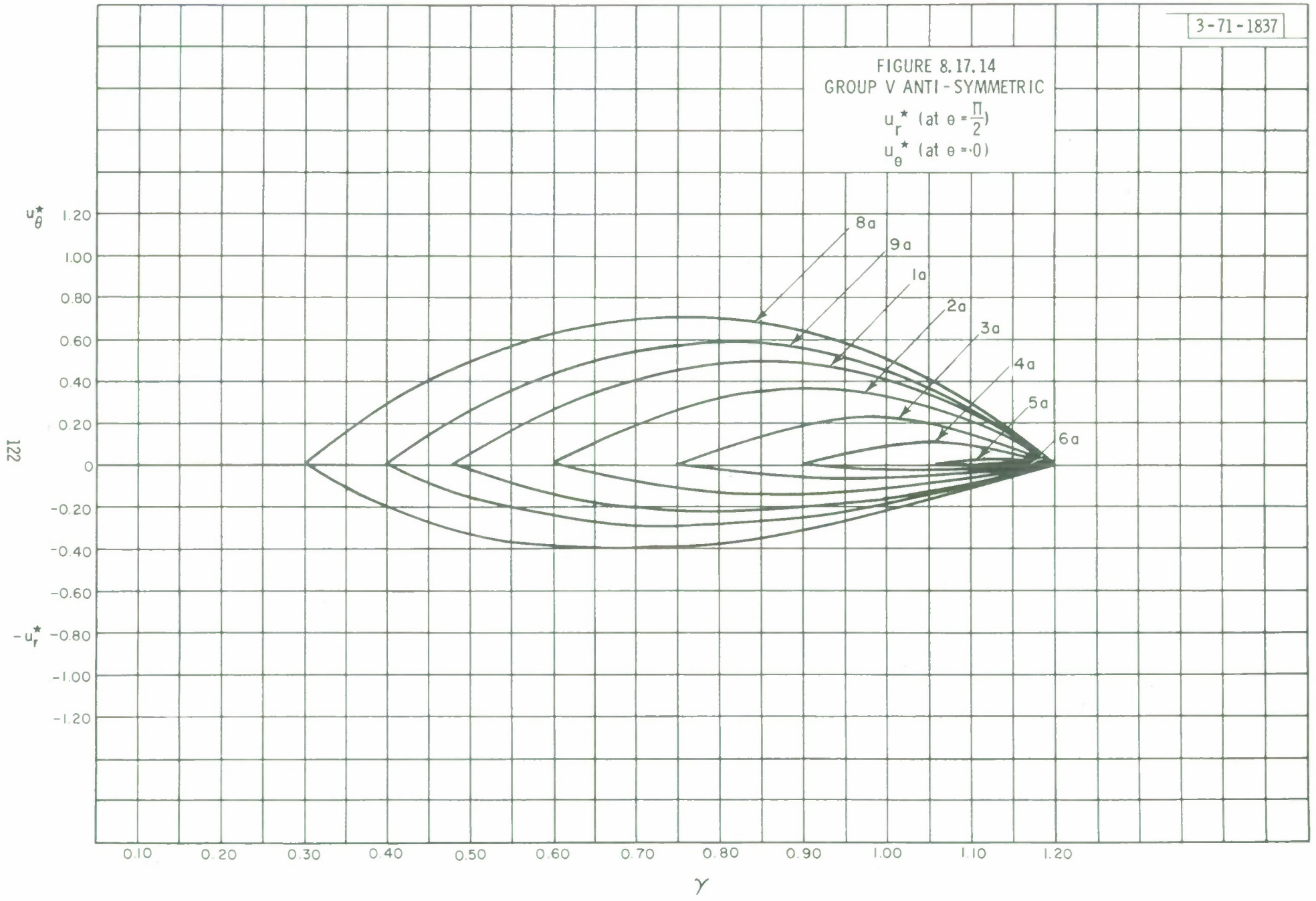
3-71-1837
FIGURE 8.17.14
GROUP V ANTI-SYMMETRIC
u_r^* (at $\theta = \frac{\Pi}{2}$)
u_θ^* (at $\theta = 0$)
8a
9a
1a
2a
3a
4a
5a
6a
u_θ^*
$-u_r^*$
1.20
1.00
0.80
0.60
0.40
0.20
0
-0.20
-0.40
-0.60
-0.80
-1.00
-1.20
0.10
0.20
0.30
0.40
0.50
0.60
0.70
0.80
0.90
1.00
1.10
1.20
γ

8.18 Group VI - Four Shells Which are Free at the Inner Boundary

The results in this section illustrate the behavior of four shells with the same outer radius of 460.8 inches but with different inner radii. In this section, each shell is simply supported along the outer edge and is free at the inner edge. Dimensions and other pertinent data are summarized in table 8.18.1. The outer radius is equivalent to $\gamma = .4$ while the inner radii correspond to slopes of $\gamma = .16, .20, .25,$ and $.30$. Only w^* and M_r^* have been shown.

It is observed that the deflections for the symmetric loading increase as the span of the shell decreases. This is contrary to the usual behavior of planar structures and dramatically illustrates the manner in which a shell derives its rigidity. The missing part of the shell (i.e., the part which was removed to make the hole) supplies support to the remainder of the shell. (One can visualize what would happen to a simple cable if a piece of it were removed.) Since the shell is a two dimensional structure, it will not collapse because the loss of the "cable action" is compensated by an increase in the hoop action. This mode of behavior is not as efficient as the "cable action" and hence, leads to larger displacements. The trend of increasing deflection with decreasing span does eventually reverse (as it must) but at a span which corresponds to a very narrow ring (see shallow shell results). Note that the bending moment M_r^* exhibits a rather slow variation with changing span.

In general, the results are the same as those previously shown for shallow shells (see sections 7.12.4 and 7.12.5).

The anti-symmetric case does not exhibit the same trend of increasing deflections with decreasing span. In the anti-symmetric case, the larger components of the gravity load vector are aligned along the tangent plane rather than along the surface normal. This means that there is less bending action in the anti-symmetric loading, and it is the bending action which leads to the results which have been discussed.

Table 8.18.1

Group VI Examples

Case	R_1 (inches)	R_2 (inches)	B.C. at R_1	B.C. at R_2	Loading
1s	184.32	460.8	free	Simple support	Sym.-gravity
2s	230.4	"	"	"	"
3s	288	"	"	"	"
4s	345.6	"	"	"	"
1a	184.32	460.8	"	"	Anti-Sym.-gravity
2a	230.4	"	"	"	"
3a	288	"	"	"	"
4a	345.6	"	"	"	"

Note: Material properties are $E = 10^7$ p.s.i., $\nu = .3$, $\rho_o = .10$ lb. per cubic inch.

Focal length $f = 576$ inches, shell thickness = 1 inch.

3-71-1838

FIGURE 8.18.1
GROUP VI SYMMETRIC
FREE AT INNER BOUNDARY
w*

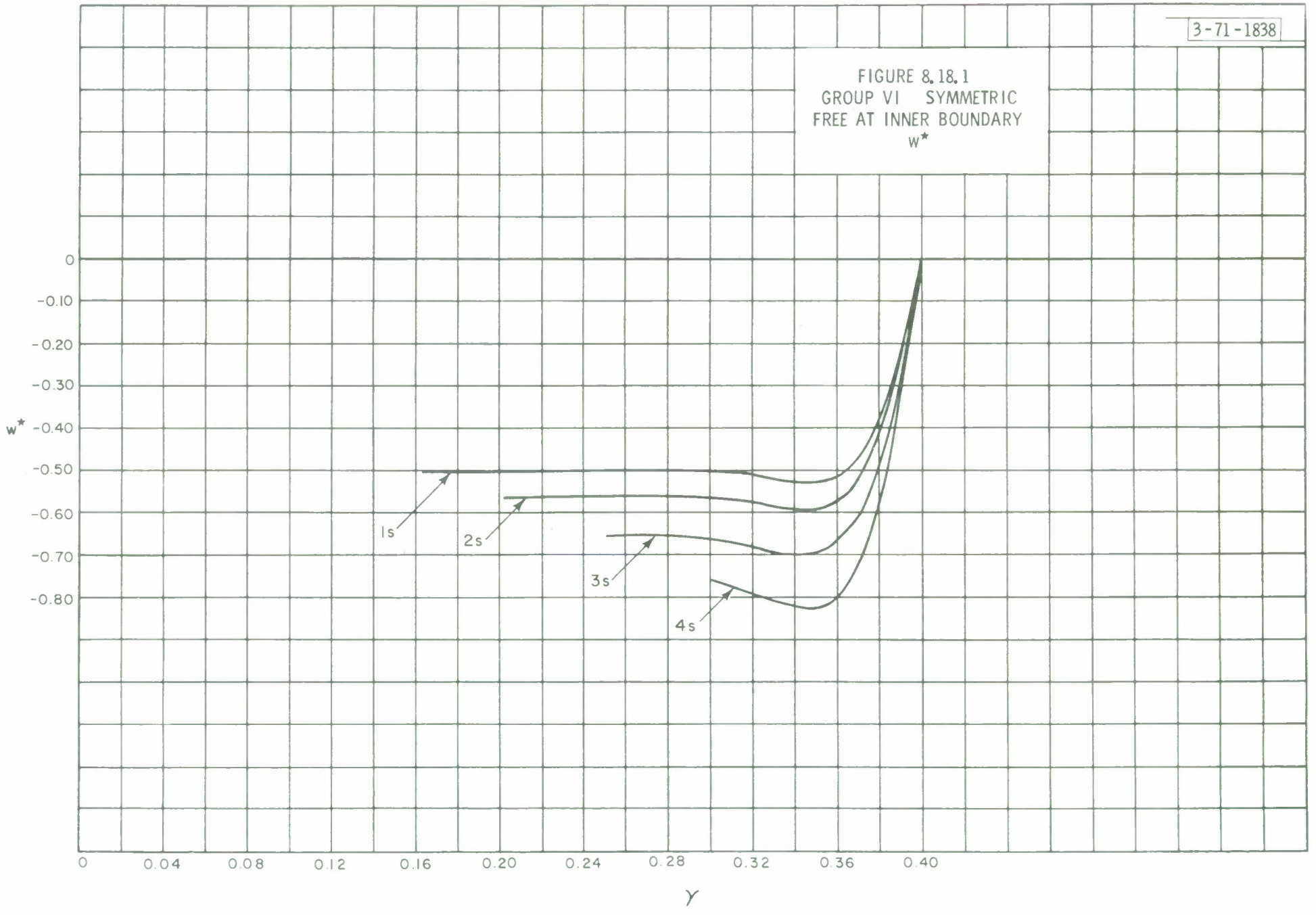

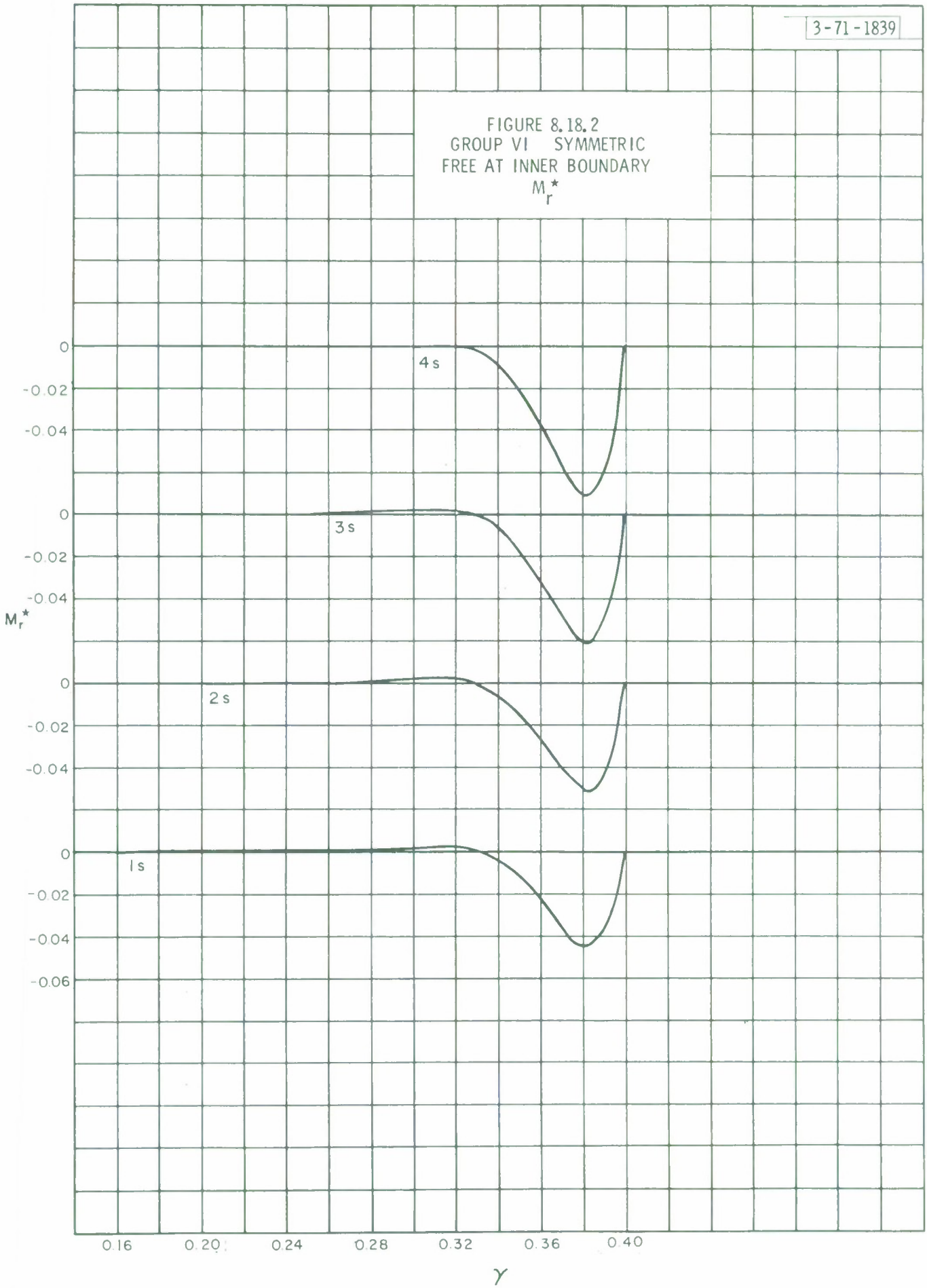
3-71-1839
FIGURE 8.18.2
GROUP VI SYMMETRIC
FREE AT INNER BOUNDARY
M_r^*
4s
3s
2s
1s
0
-0.02
-0.04
-0.06
M_r^*
0.16
0.20
0.24
0.28
0.32
0.36
0.40
γ

3-71-1860

FIGURE 8.18.3
GROUP VI ANTI-SYMMETRIC
FREE AT INNER BOUNDARY
w*

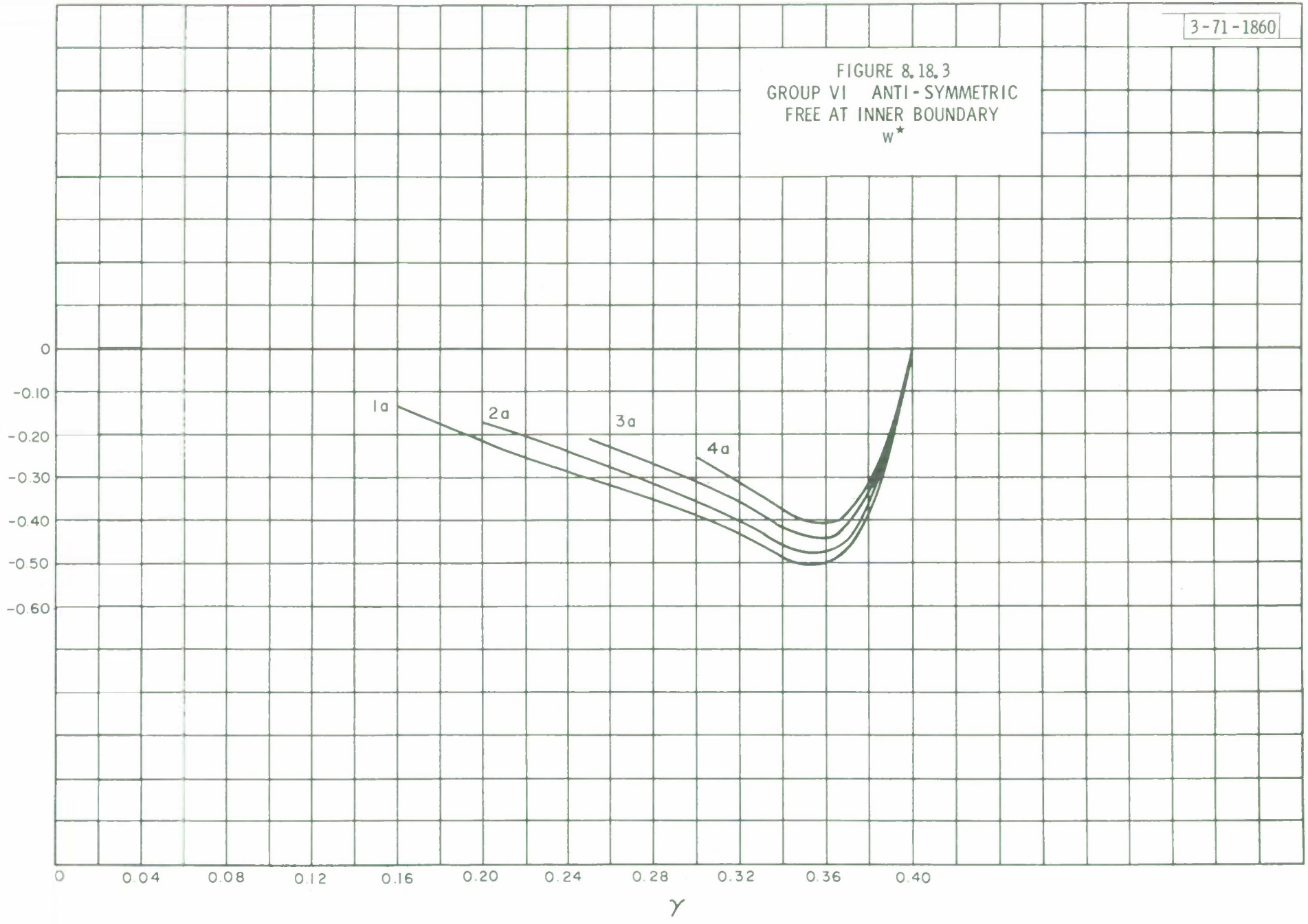

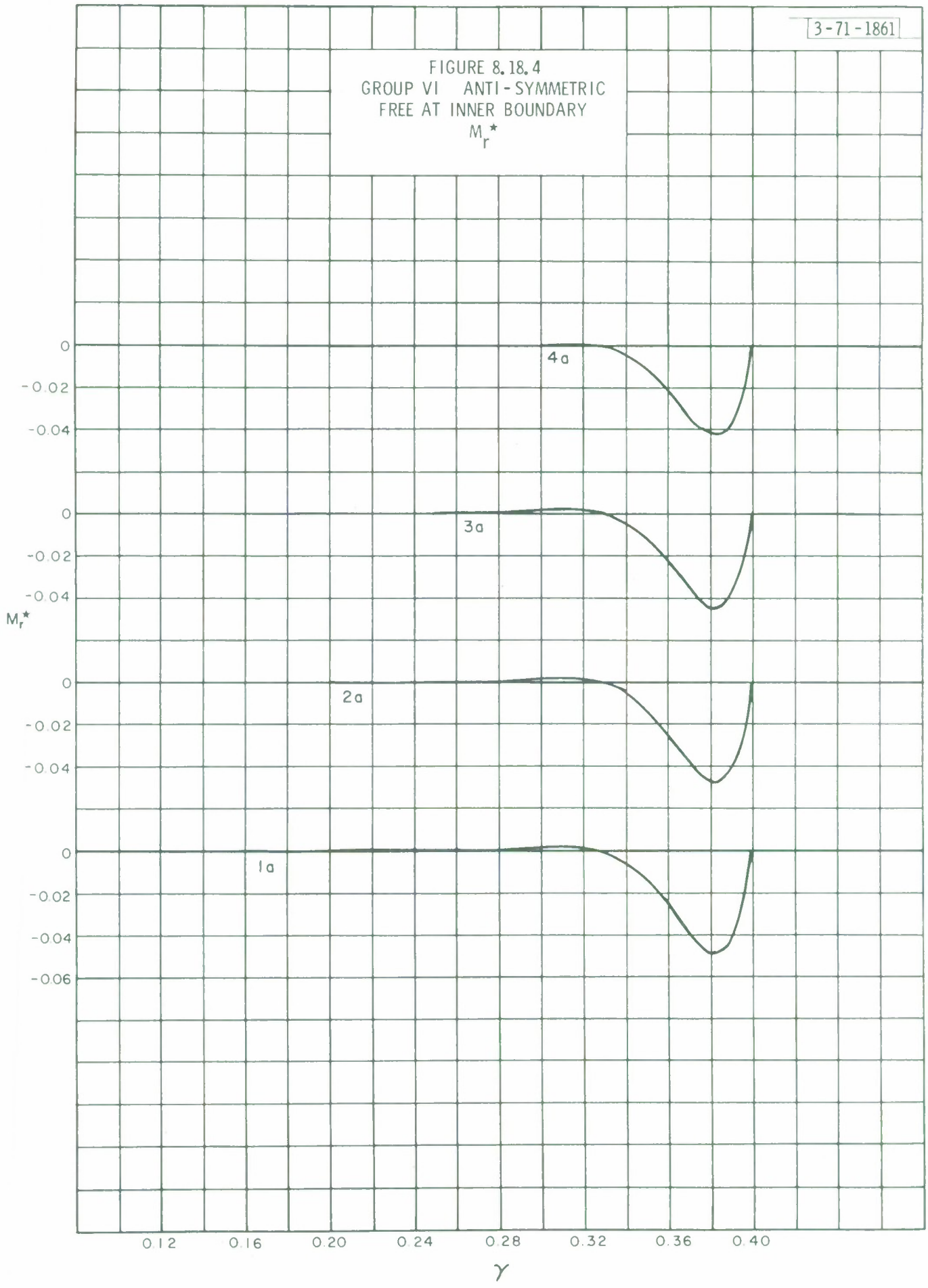
3-71-1861
FIGURE 8.18.4
GROUP VI ANTI-SYMMETRIC
FREE AT INNER BOUNDARY
M_r^*
0
-0.02
-0.04
4a
0
-0.02
-0.04
3a
M_r^*
0
-0.02
-0.04
2a
0
-0.02
-0.04
-0.06
1a
0.12
0.16
0.20
0.24
0.28
0.32
0.36
0.40
γ

8.19 Group VII - Five Shells which are Free at the Inner Boundary

The results in this section illustrate the behavior of four shells with the same outer radius of 921.6 inches but with different inner radii. As in section 8.18, each shell is simply supported at the outer radius and is free at the inner radius. Dimensions and other pertinent data are summarized in table 8.19.1. The outer radius is equivalent to $\gamma = .8$ while the inner radii correspond to slopes of $\gamma = .32, .40, .50, .60$, and $.70$. Only w^* and M_r^* have been shown. Results are presented in normalized form.

The Group VII results are similar to those of Group VI and the discussion in section 8.18 is applicable.

Table 8.19.1

Group VII Examples

Case	R_1 (inches)	R_2 (inches)	B.C. at R_1	B.C. at R_2	Loading
1s	368.64	921.6	free	Simple support	Sym.-gravity
2s	460.8	"	"	"	"
3s	576	"	"	"	"
4s	691.2	"	"	"	"
5s	806.4	"	"	"	"
1a	368.64	"	"	"	Anti-Sym.-gravity
2a	460.8	"	"	"	"
3a	576	"	"	"	"
4a	691.2	"	"	"	"
5a	806.4	"	"	"	"

Note: Material properties are $E = 10^7$ p.s.i., $\nu = .3$, $\rho_0 = .10$ lb. per cubic inch.

Focal length $f = 576$ inches, shell thickness $h = 1$ inch.

3-71-1840

FIGURE 8.19.1
GROUP VII SYMMETRIC
FREE AT INNER BOUNDARY
w^*

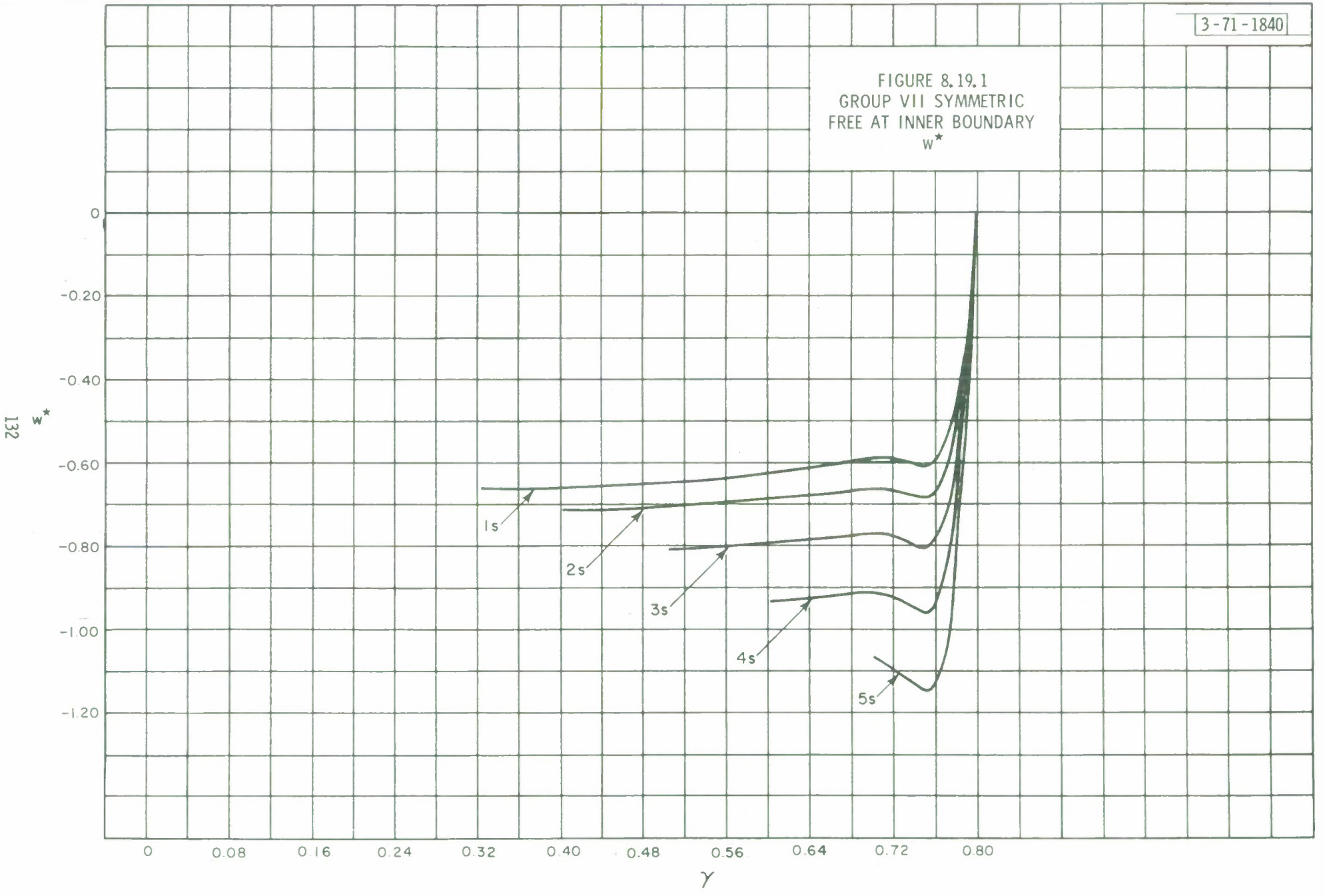

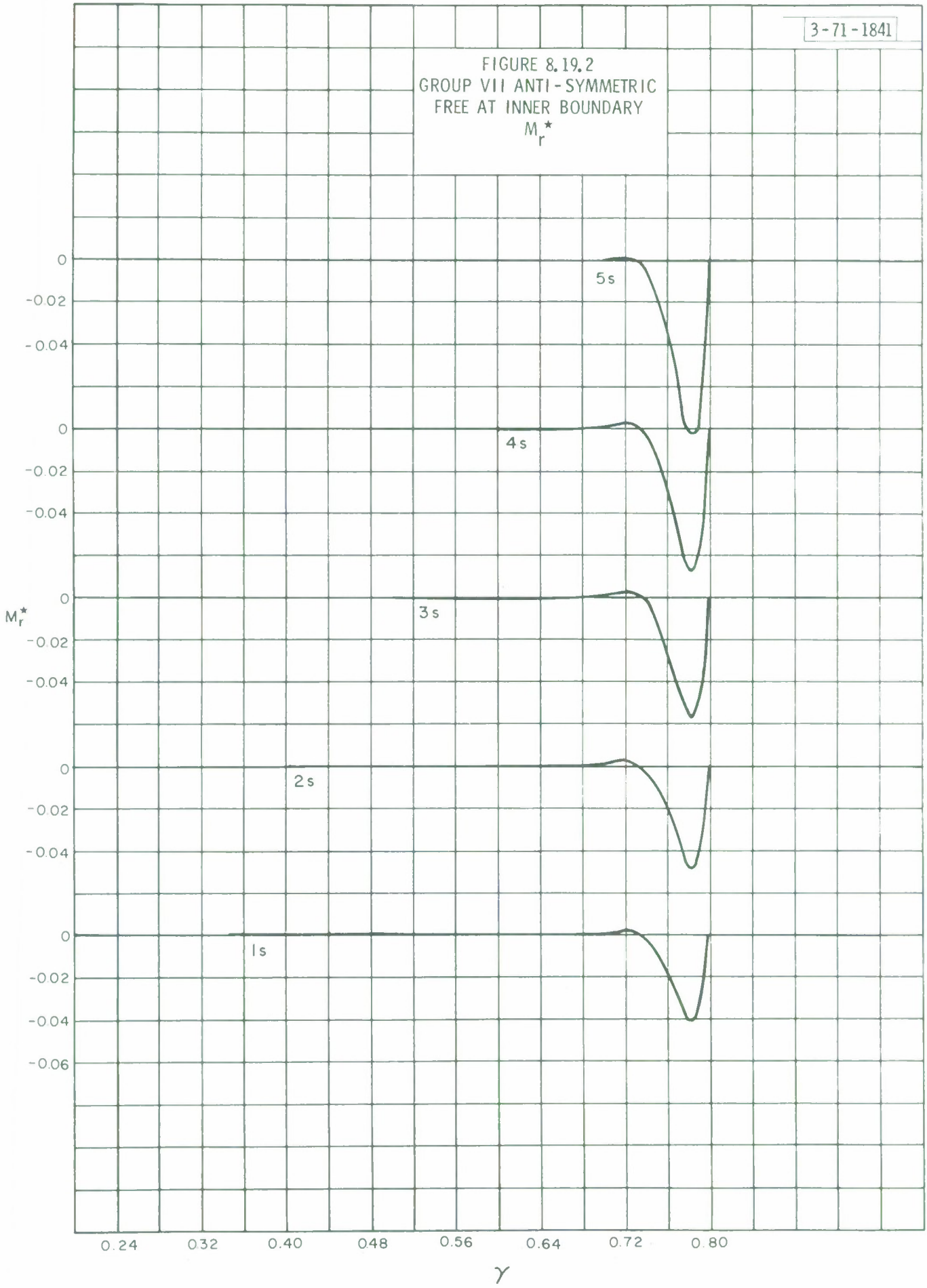
3-71-1841
FIGURE 8.19.2
GROUP VII ANTI-SYMMETRIC
FREE AT INNER BOUNDARY
M_r^*
0
-0.02
-0.04
5s
4s
3s
2s
1s
-0.06
M_r^*
0.24
0.32
0.40
0.48
0.56
0.64
0.72
0.80
γ

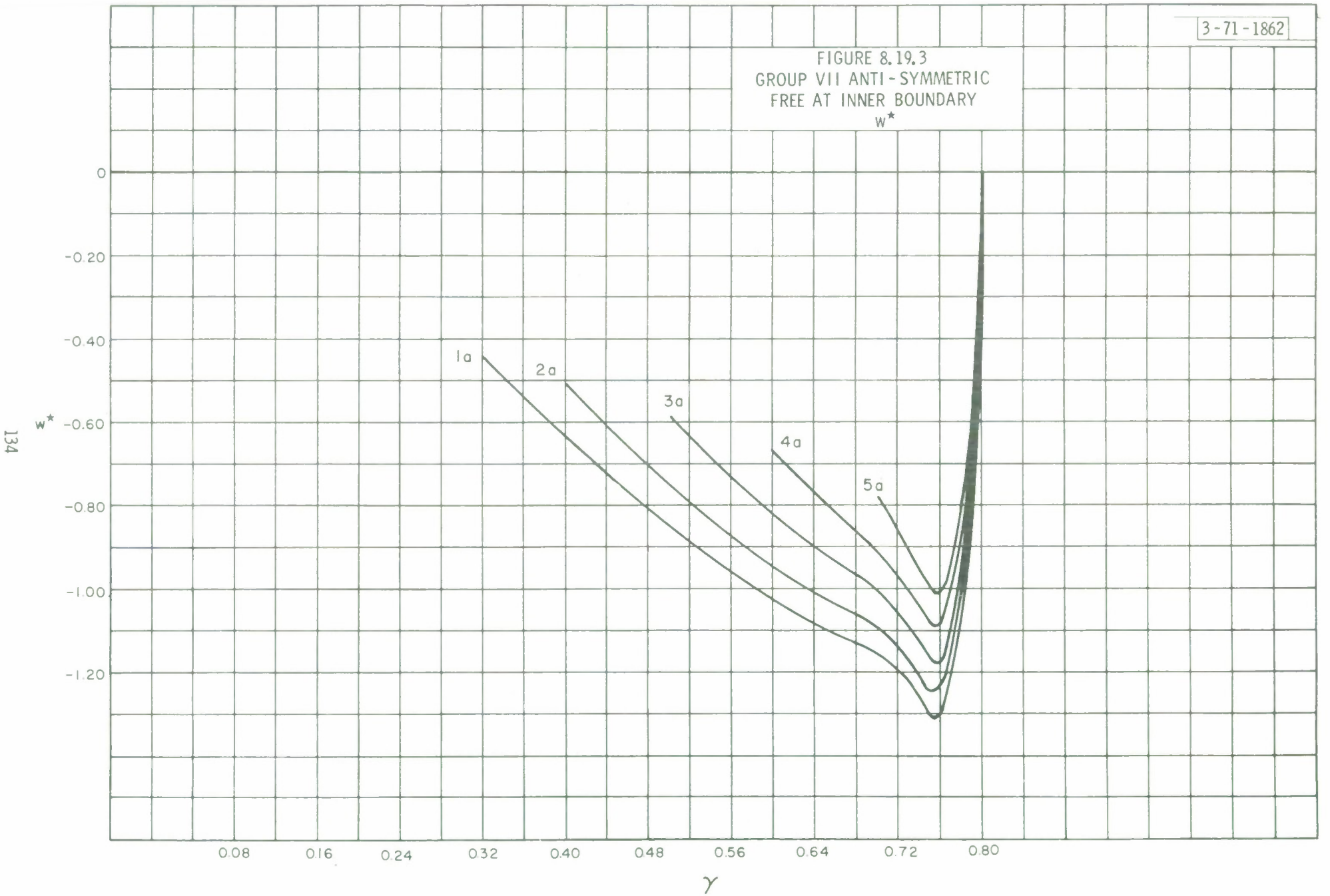
3-71-1862
FIGURE 8.19.3
GROUP VII ANTI-SYMMETRIC
FREE AT INNER BOUNDARY
w*
0
-0.20
-0.40
-0.60
-0.80
-1.00
-1.20
w*
1a
2a
3a
4a
5a
0.08
0.16
0.24
0.32
0.40
0.48
0.56
0.64
0.72
0.80
γ

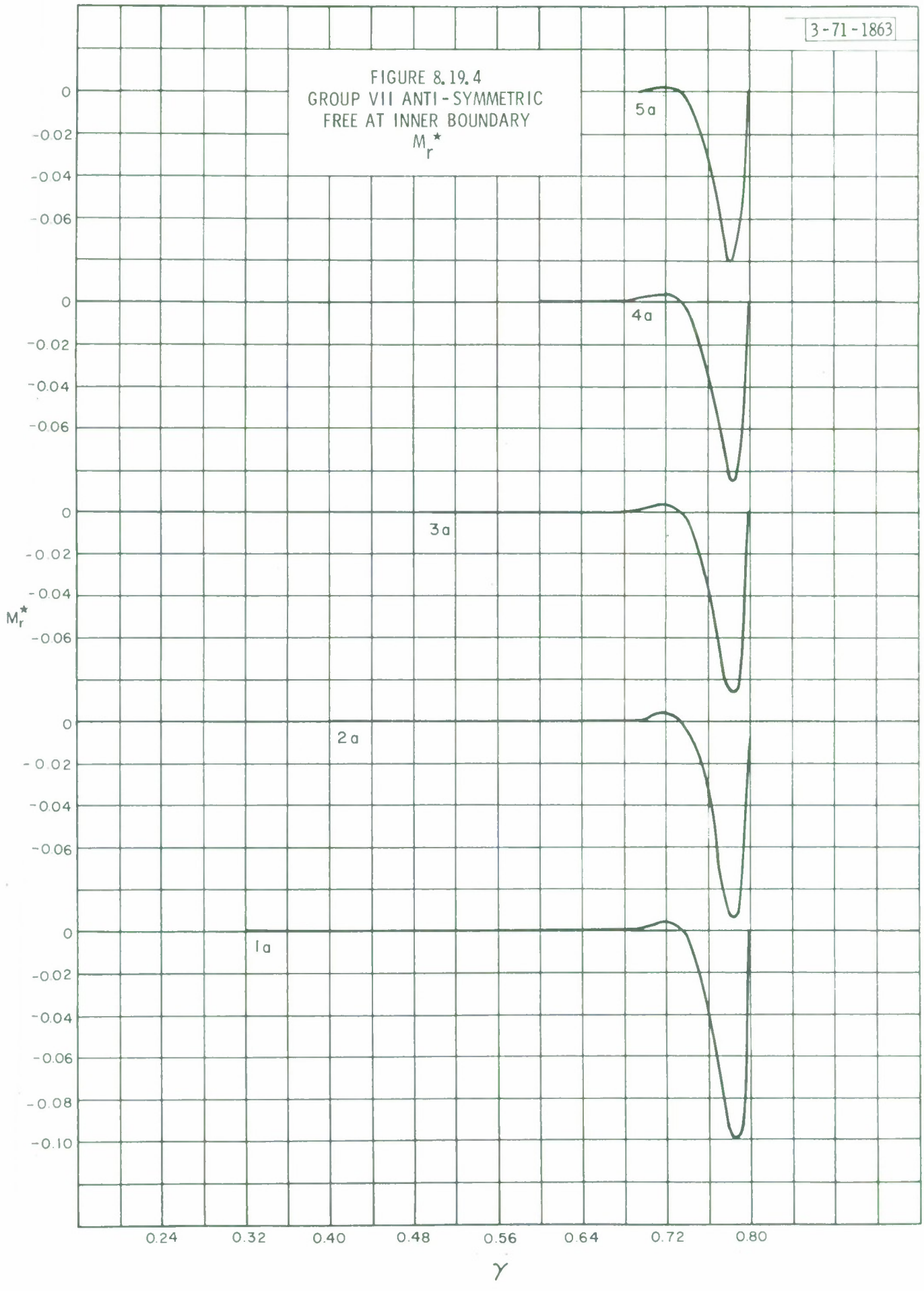
3-71-1863
FIGURE 8.19.4
GROUP VII ANTI-SYMMETRIC
FREE AT INNER BOUNDARY
M_r^*
5a
4a
3a
2a
1a
0
-0.02
-0.04
-0.06
-0.08
-0.10
M_r^*
0.24
0.32
0.40
0.48
0.56
0.64
0.72
0.80
γ

8.20, 8.21, 8.22 Group VIII - Asymmetric Behavior of Three Shells Simply Supported at the Outer Boundary

In previous sections, the symmetric behavior and anti-symmetric behavior which correspond to pointing angles ψ of 0° and 90° were presented. In this section, the deflection patterns for the shell at pointing angles of ψ = 15°, 30°, 45°, 60°, and 90° are shown in the form of polar plots.

As has already been discussed (see section 7.12.7 of part III) large antennae will generally be erected in the face-up position (ψ = 0°). Thus, it becomes of interest to determine the deflections of the antenna relative to the face-up position. The displacements normal to the middle surface for gravity loads are given by

$$w(\gamma, \theta) = w_s(\gamma) \cos \psi + w_a(\gamma) \sin \psi \sin \theta \qquad 8.20.1$$

where

$w_s(\gamma)$ = symmetric part of the solution

$w_a(\gamma)$ = anti-symmetric part of solution at $\theta = \frac{\pi}{2}$

The plots in the preceding sections are of w_s and w_a.

Let $\tilde{w}(\gamma, \theta)$ be the deflection relative to the antenna in its face-up position, i.e., relative to $\psi = 0$. Then

$$\tilde{w}(\gamma, \theta) = w(\gamma, \theta) - w_s(\gamma) \qquad 8.20.2$$

which leads to

$$\tilde{w}(\gamma, \theta) = w_s(\cos \psi - 1) + w_a \sin \psi \sin \theta \qquad 8.20.3$$

The three shells analyzed in this section have the same dimensions as shells previously considered. Dimensions and other

pertinent data are as follows:

$E = 10^7$ p.s.i.

$\nu = .3$

$\rho_o = .10$ lb. per cubic inch

focal length $f = 576$ inches

shell thickness $h = 1$ inch

All three shells are closed at the apex and the boundaries correspond to radii of 460.8 inches, 691.2 inches and 921.6 inches, respectively.

The results are presented in the form of contour plots wherein lines of constant $\tilde{w}^*$ are shown. A polar representation has been used in which the horizontal radius is the coordinate on the shell given by $\theta = 0$. Radii emanating from the origin are lines of negative θ below the horizontal and positive θ above the horizontal. Each plot constitutes the deflected shape of the shell in the normal direction relative to the face-up position, i.e., of $\tilde{w}^*$, for various pointing angles ψ. Since the behavior is symmetric about a vertical plane, only the region of the shell, $-\frac{\pi}{2} \leq \theta \leq \frac{\pi}{2}$ has been shown.

The curves are self-explanatory. Each contour is roughly in the shape of a U with the legs approximately horizontal. Positive values mean that the shell has deflected inward. Note that the largest values are positive and occur in the upper half of the shell.

FIGURES 8.20.1, 2, & 3
ASYMMETRIC - VARYING ψ
$\gamma_2 = 0.4$

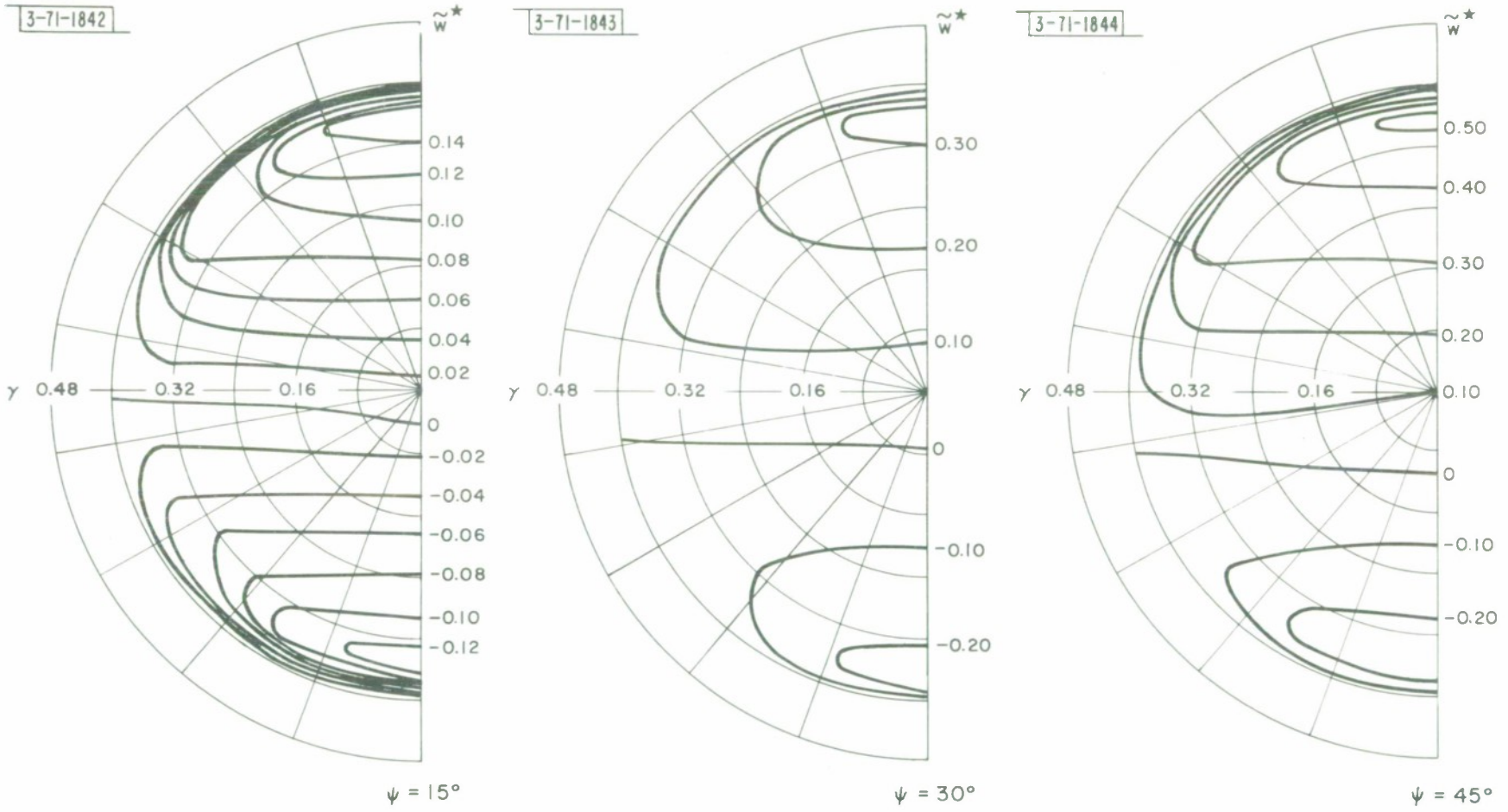

FIGURES 8.20.4, 5, & 6
ASYMMETRIC - VARYING ψ
$\gamma_2 = 0.4$

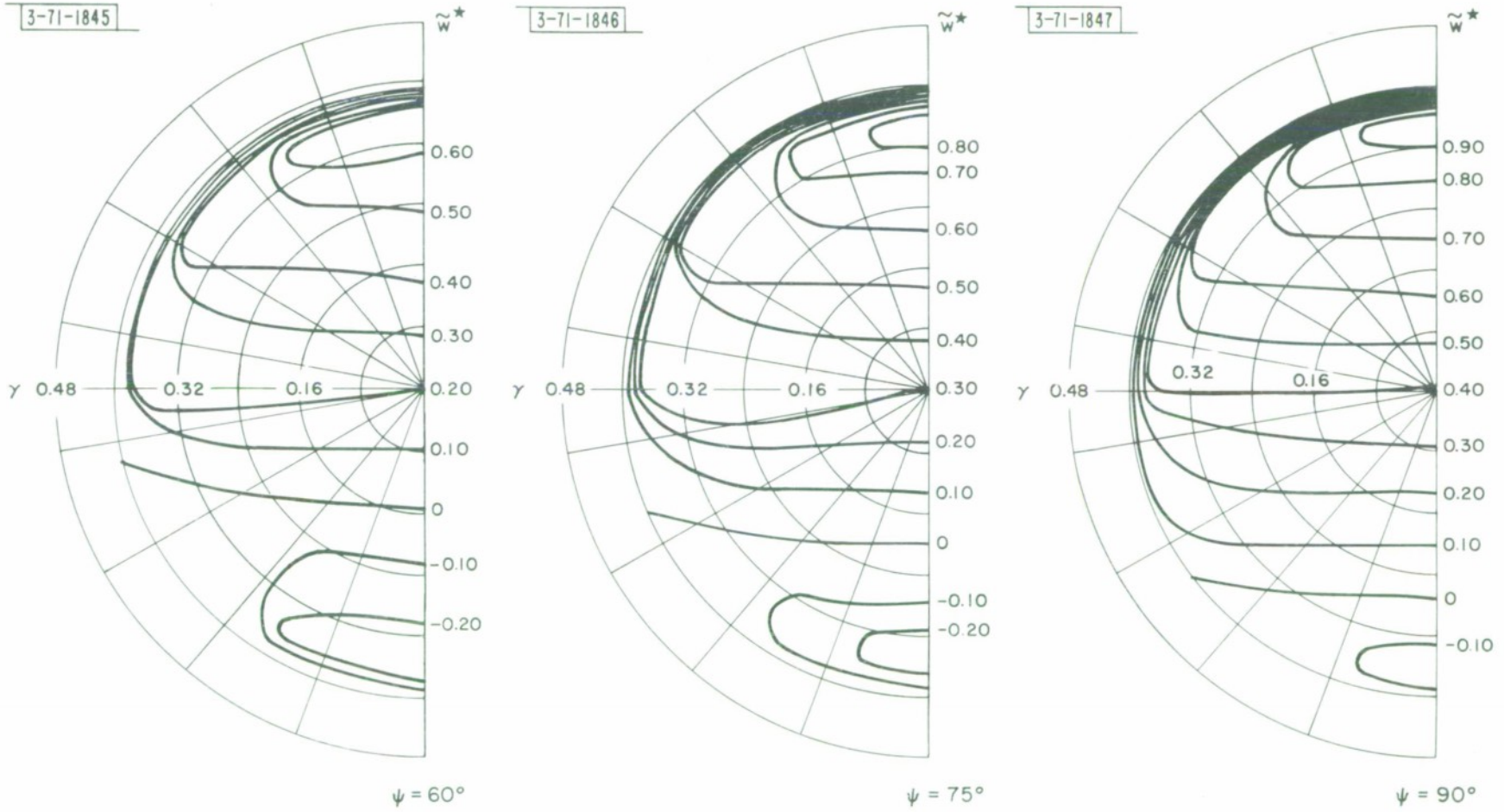

FIGURES 8.21.1, 2, & 3
ASYMMETRIC - VARYING ψ
$\gamma_2 = 0.60$

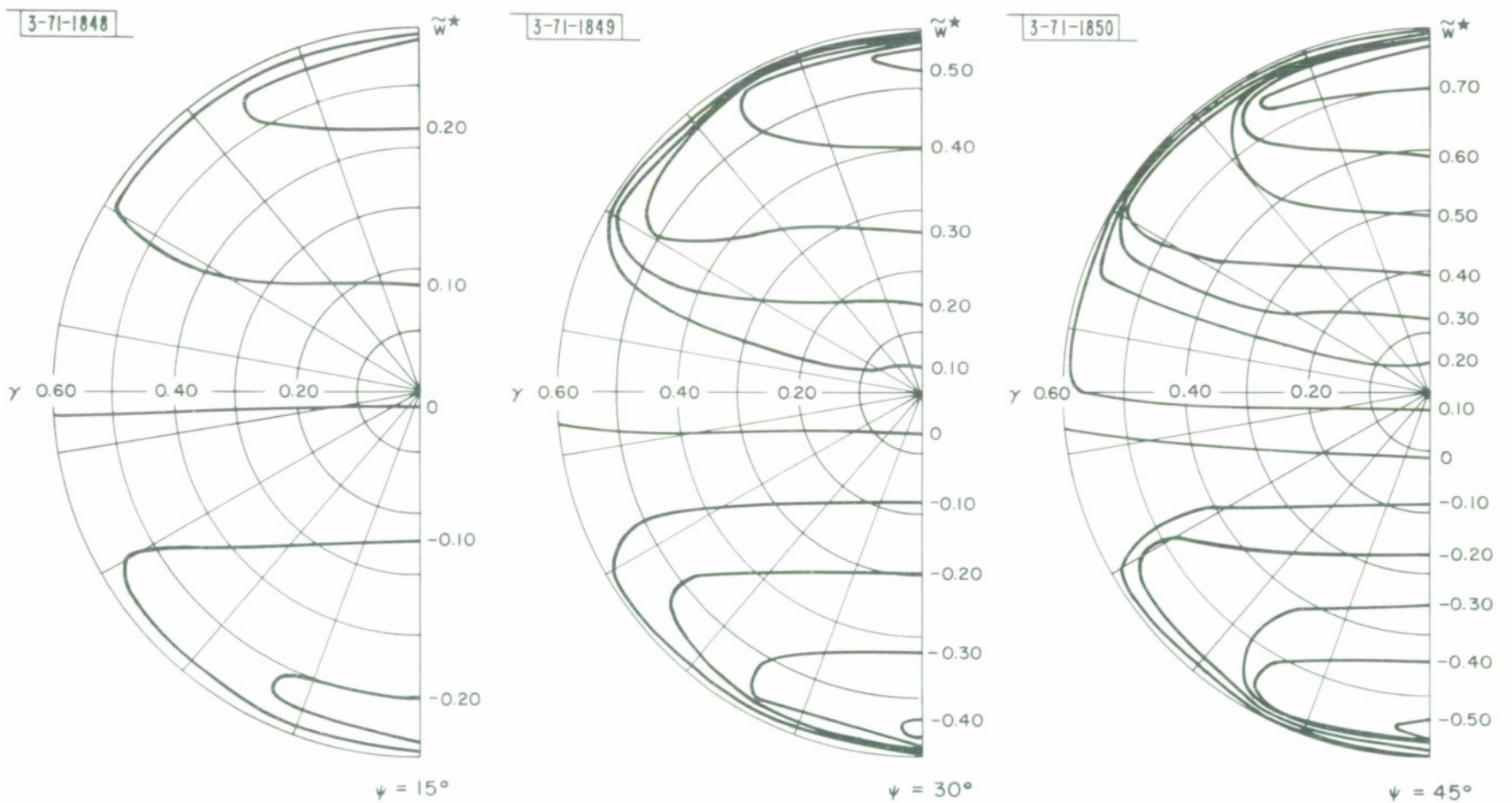

FIGURES 8.21.4, 5, & 6
ASYMMETRIC - VARYING ψ
$\gamma_2 = 0.60$

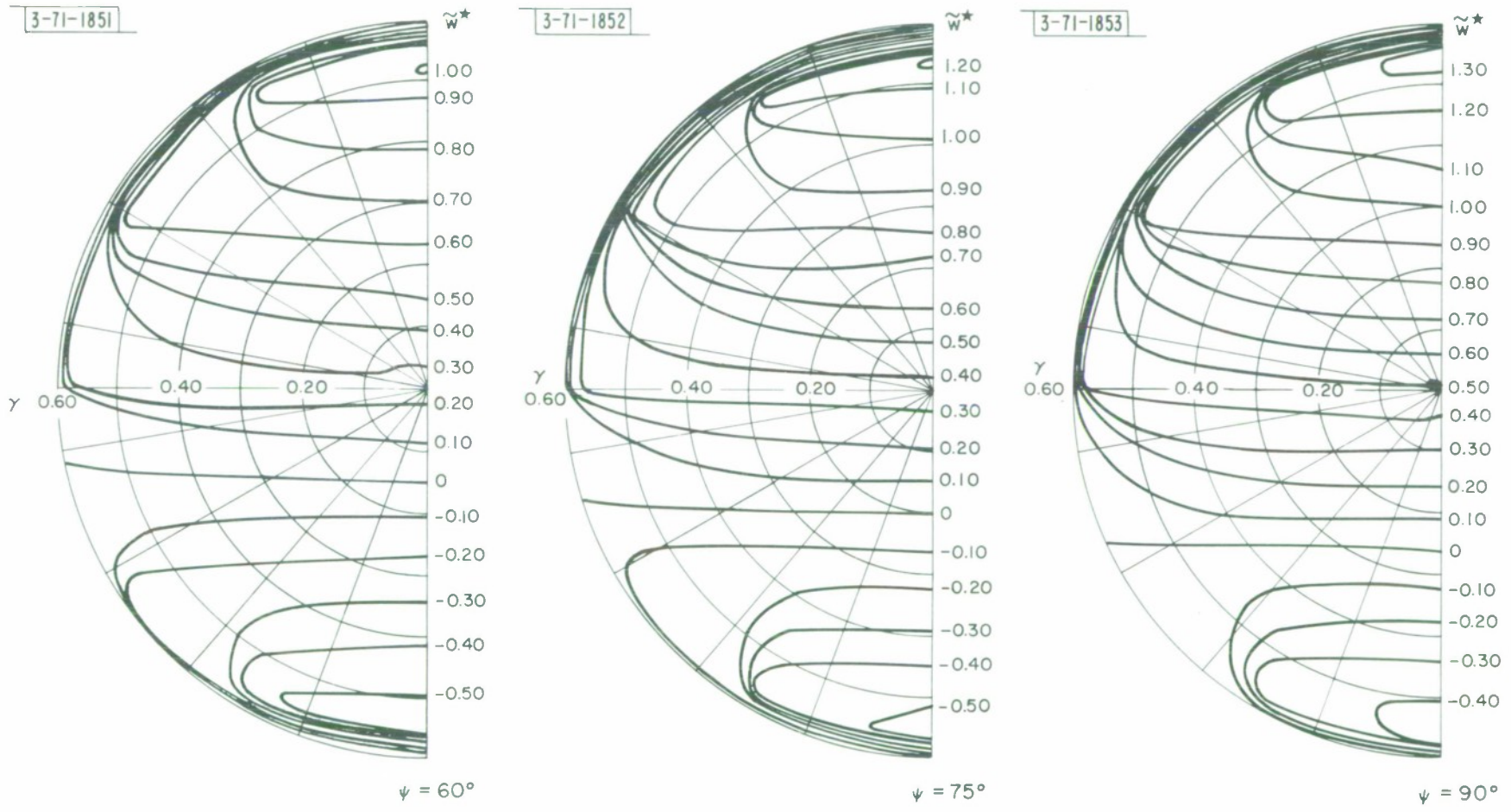

FIGURE 8.22.1, 2, & 3
ASYMMETRIC - VARYING ψ
$\gamma_2 = 0.80$

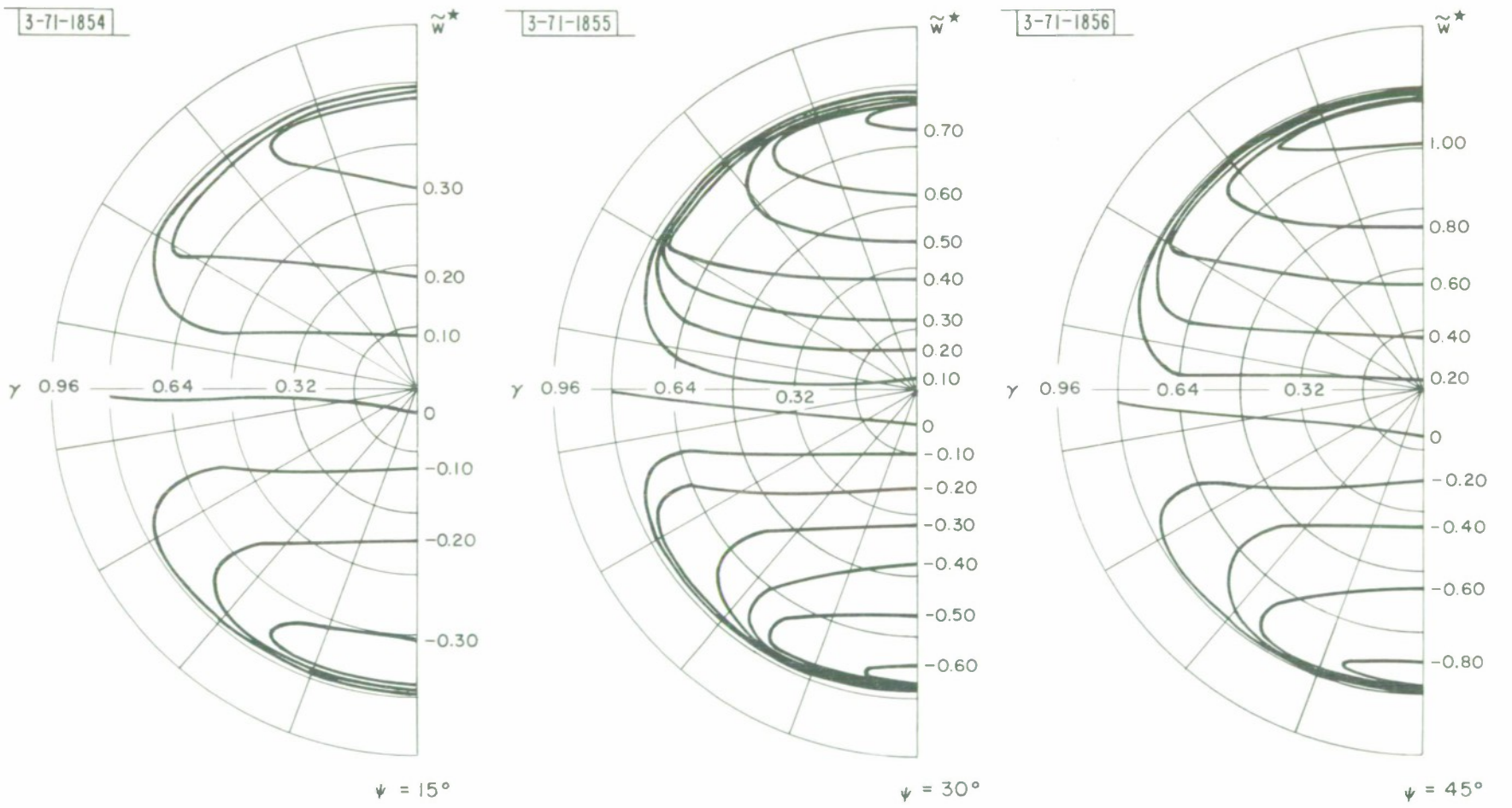

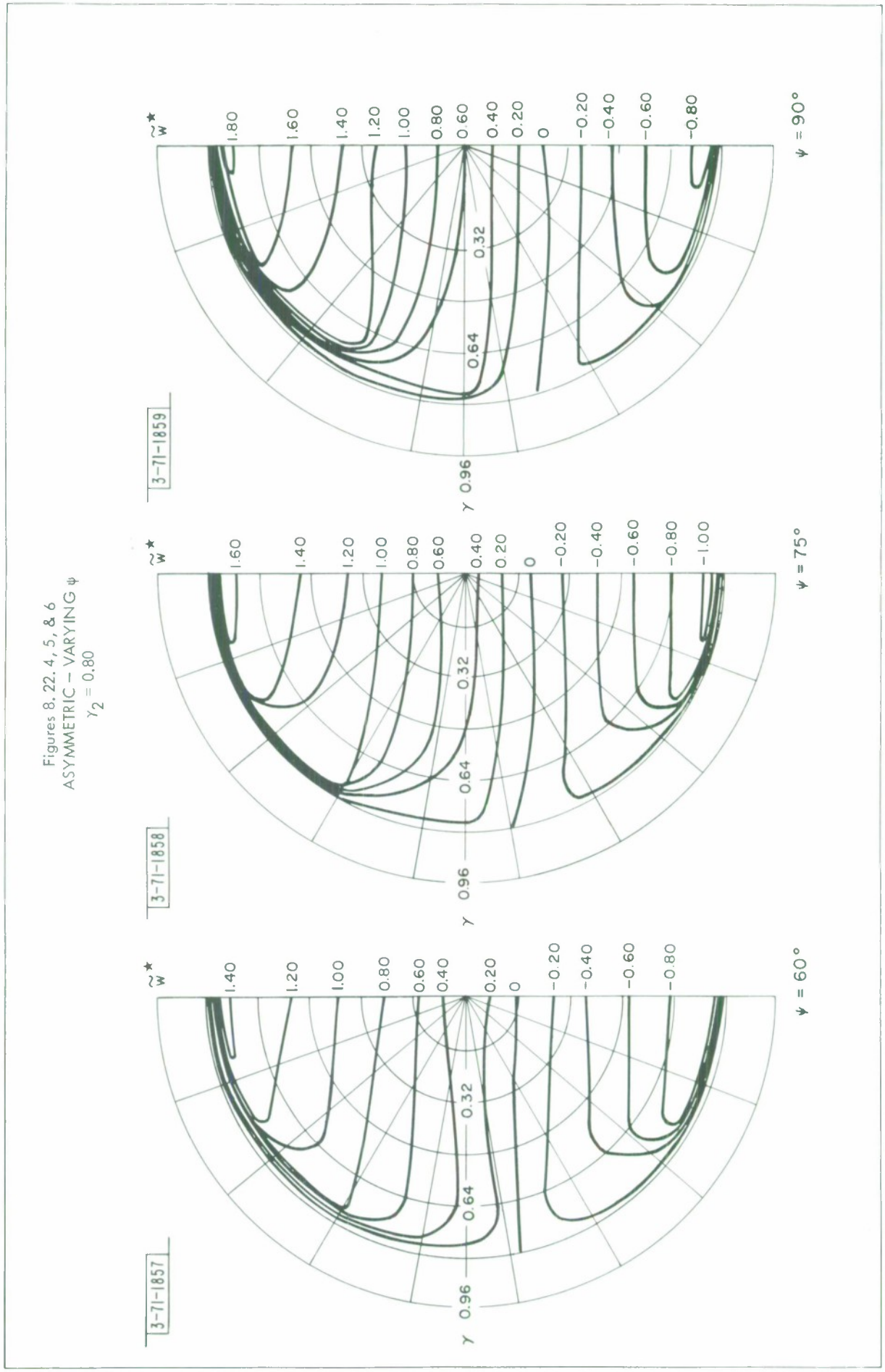

Figures 8.22.4, 5, & 6
ASYMMETRIC – VARYING ψ
$\gamma_2 = 0.80$

REFERENCES

1. Green, A. E. and W. Zerna, Theoretical Elasticity, Oxford University Press, London, 1960.

2. Novozhilov, V. V., The Theory of Thin Shells, (Translated by P. G. Lowe), P. Noordhoff Ltd., Groningen, 1959.

3. Flugge, W., Stresses in Shells, Springer-Verlag, Berlin, 1960.

4. Timoshenko, S., Theory of Plates and Shells, McGraw-Hill Book Co., New York, 1940.

5. Mar, J. W., "Class Notes for a Course in Shell Theory," M.I.T., 1960.

6. Wang, C. T., Applied Elasticity, McGraw-Hill Book Co., New York, 1953.

7. Reissner, E., "A New Derivation of the Equations for the Deformation of Elastic Shells," American Journal of Mathematics, Vol. LXIII, No. 1, January, 1941.

8. Knowles, J. K. and E. Reissner, "A Derivation of the Equations of Shell Theory for General Orthogonal Coordinates," Journal of Mathematics and Physics, Vol. XXXV, No. 4, January, 1957.

9. Reissner, E., "Note on the Membrane Theory of Shells of Revolution," Journal of Mathematics and Physics, Vol. XXVI, No. 4, January, 1948.

10. Truesdell, C., "The Membrane Theory of Shells of Revolution," Transactions of the American Mathematical Society, Vol. 58, 1945, pp. 96-166.

11. Truesdell, C., "On the Reliability of the Membrane Theory of Shells of Revolution," American Mathematical Society Bulletin, Vol. 54, 1948, pp. 994-1008.

12. Hildebrand, F. B., "On Asymptotic Integration in Shell Theory," Proceedings of Symposia in Applied Mathematics, Vol. III, McGraw-Hill Book Co., New York, 1950.

13. Wittrick, W. H., "Edge Stresses in Thin Shells of Revolution," Aeronautics Research Laboratories, Report S.M. 253, Melbourne, 1957.

14. Flugge, W., "Bending Theory for Shells of Revolution Subjected to Non-Symmetric Edge Loads," Division of Engineering Mechanics, Stanford University Technical Report 113, 1957.

15. McConnell, A. J., Applications of Tensor Analysis, Dover Publications, Inc., 1957.

16. Sokolnikoff, I. S., Tensor Analysis, John Wiley and Sons, Inc., New York, 1951.

17. Struik, D. J., Differential Geometry, Addison-Wesley Press, Inc., Reading, Massachusetts, 1950.

18. Ince, E. L., Ordinary Differential Equations, Dover Publications, Inc., New York, 1956.

19. Jeffreys, H. and B. S. Jeffreys, Methods of Mathematical Physics, Third Edition, Cambridge University Press, London, 1956.

20. Courant, R. and D. Hilbert, Methods of Mathematical Physics, Vol. 1, Interscience Publishers, Inc., New York, 1953.

21. Carslaw, H. S., Fourier Series and Integrals, Third Edition, MacMillan and Co., Ltd., London, 1930.

22. Reissner, E., "Stresses and Small Displacements of Shallow Spherical Shells," Part I, Journal of Mathematics and Physics, Vol. 25, 1946, pp. 80-85.

23. Reissner, E., "Stresses and Small Displacements of Shallow Spherical Shells, Part II, Journal of Mathematics and Physics, Vol. 25, 1946, pp. 229-300.

24. Reissner, E., "On the Determination of Stresses and Displacements for Unsymmetrical Deformations of Shallow Spherical Shells," Journal of Mathematics and Physics, Vol. 38, 1959, pp. 16-35.

25. McLachlan, N. W., Bessel Functions for Engineers, Oxford University Press, Second Edition, 1954.

26. Gray, A., G. B. Mathews and T. M. MacRoberts, A Treatise On Bessel Functions and Their Applications to Physics, MacMillan and Co., Ltd., 1952.

27. Prescott, J., Applied Elasticity, Longmans, Green and Co., 1924.

28. Wan, F. Y. M., "On the Assumptions of Shallow Shell Theory and Some Related Results," [U], Lincoln Laboratory Report 71G-6 (to be published).

29. Hildebrand, F. B., Advanced Calculus for Engineers, Prentice-Hall, Inc., 1948.

30. Reissner, E., "Variational Considerations for Elastic Beams and Shells," Journal of the Engineering Mechanics Division, Proceedings of the American Society of Civil Engineers, Vol. 88, No. EM1, February, 1962.

31. Reissner, E., "A Note on Membrane and Bending Stresses in Spherical Shells," Journal of the Society of Industrial and Applied Mathematics, Vol. 4, No. 4, December, 1956.

32. Mar, J. W. and F. Y. M. Wan, "Distortions and Stresses of Paraboloidal Surface Structures, Part I," [U], Group Report 71G-1, Lincoln Laboratory, M.I.T., 9 January 1962.

33. Mar, J. W. and F. Y. M. Wan, "Distortions and Stresses of Paraboloidal Surface Structures, Part II," [U], Group Report 71G-1, Lincoln Laboratory, M.I.T., 4 January 1963.

34. Mar, J. W. and F. Y. M. Wan, "Distortions and Stresses of Paraboloidal Surface Structures, Part III, " [U], Group Report 71G-1, Lincoln Laboratory, M.I.T., 15 August 1963.

35. Turrittin, H. L., "Asymptotic Expansions of Solutions of Systems of Ordinary Linear Differential Equations Containing a Parameter," Contributions to the Theory of Non-Linear Oscillations, Princeton University Press, Princeton, New Jersey, 1952, pp. 81-116.

36. Erdelyi, A., Asymptotic Expansions, Dover Publications, Inc., 1956.

37. deBruijn, N. G., Asymptotic Methods in Analysis, Amsterdam, North Holland Publication Company; New York, Interscience Publishers, 1958.

38. Horn, J., "Uber lineare differentialgleichungen mit einem veranderlichen parameter," Mathematische Amalen,Vol. 52, 1899, pp. 340-362.

39. Birchoff, G. D., "On the Asymptotic Character of the Solutions of Certain Linear Differential Equations Containing a Large Parameter," Trans. of American Math. Society, Vol. 9, 1908, pp. 219-231.

40. Langer, R. E., "On the Asymptotic Solution of Ordinary Differential Equations," Trans. of the American Math. Society, Vol. 33, 1931, pp. 23-64.

41. Langer, R. E., "On the Asymptotic Solution of Ordinary Differential Equations with Reference to the Stokes Phenomenon About a Singular Point," Trans. of American Math. Society, Vol. 37, 1935, pp. 397-416.

42. DeSilva, C. N., "Deformation of Elastic Paraboloidal Shells of Revolution," Journal of Applied Mechanics, Vol. 24, September, 1957, pp. 397-404.

43. Steele, C. R., "A Systematic Analysis for Shells of Revolution with Non-Symmetric Loads," Proceedings of the 4th U.S. National Congress of Applied Mechanics, 1962, (to be published).